First order phase transitions beyond the Standard Model

Fëanor Reuben Ares

Submitted for the degree of Doctor of Philosophy

University of Sussex

July 2022

Declaration

I hereby declare that this thesis has not been and will not be submitted in whole or in part to another University for the award of any other degree.

The work in this thesis has been completed in collaboration with Oscar Henriksson, Mark Hindmarsh, Carlos Hoyos, and Niko Jokela, and is comprised of the following papers:

- F. R. Ares, M. Hindmarsh, C. Hoyos, and N. Jokela, “Gravitational waves from a holographic phase transition”, *J. High Energ. Phys.* 2021, 100 (2021), DOI: 10.1007/JHEP04(2021)100, arXiv: 2011.12878 [hep-th]

  In this paper I developed the code to be able to solve the differential equations for the master function, and then used those solutions to create a code package which solves for all thermodynamic quantities. I then performed the numeric parameter scan for each of the quantities as well as calculated all the gravitational wave signals. All plots found in the paper were produced by me, and I wrote a significant portion of the paper.

- F. R. Ares, O. Henriksson, M. Hindmarsh, C. Hoyos, and N. Jokela, “Effective actions and bubble nucleation from holography”, *Phys. Rev. D* 105, 066020 (2022), DOI: 10.1103/PhysRevD.105.066020, arXiv: 2109.13784 [hep-th]

  In this paper I wrote parts of section 3 as well as the entirety of section 4. For this I calculated the domain of first-order transitions for each Λ_f branch, as well as where the second-order transition would occur. I determined the negligibility of the higher derivative terms through numerics, producing ratio comparisons for multiple different cases. I calculated and produced ratios of the $O(3)$ and $O(4)$ bubble actions, and went on to calculate the effect N-scaling would have on the various quantities we would need to consider. For the domain wall section I calculated all critical bubble profiles numerically and their energy densities and compared these to tanh solutions, then calculated and produced a scan of the surface tension for the entire parameter space. I produced all figures in the paper.

- F. R. Ares, O. Henriksson, M. Hindmarsh, C. Hoyos, and N. Jokela, "Gravitational Waves at Strong Coupling from an Effective Action", *Phys. Rev. Lett.* 128, 131101 (2022), DOI: 10.1103/PhysRevLett.128.131101, arXiv: 2110.14442 [hep-th]

  In this paper I took the black brane solutions for the fields and created the mathematica codes which solved for the scalar field profiles for every combination of Λ, f, and g. I then also created the code which located the nucleation temperature, produced the action curve, and found the transition strength for each parameter set, and produced similar codes for using the thermodynamic variables to find scans of the transition strength and u_w. I collated all of this together to produce a parameter scan on the gravitational wave signal. Once again I produced all figures in the work and wrote a significant portion of the paper.

Signature:

Fëanor Reuben Ares

UNIVERSITY OF SUSSEX

Fëanor Reuben Ares, Doctor of Philosophy

First order phase transitions beyond the Standard Model

Summary

Gravitational waves have had a long and interesting history, and recently have been experimentally confirmed. This and the fact that many areas of physics are beyond the reach of traditional observational prospects has been the catalyst to new space-based gravitational wave detectors such as LISA being proposed and confirmed for the near future. Cosmological phase transitions in the early Universe proceed through bubble nucleation and collision if they are first-order which is thought to produce gravitational waves which could be detected by these missions, and so a great effort is being expended to scrutinise how these transitions would proceed and what their controlling factors are. Aspects of these transitions are difficult to determine however due to most knowledge being limited to the perturbative regime where couplings are weak, a limitation which is not necessarily fulfilled by these scenarios.

In this thesis I study the nature of these phase transitions and the type of gravitational waves they could produce, and then take advantage of the nature of the AdS/CFT correspondence (also called the gauge/gravity duality or holographic principle) which translates strongly-coupled field theories to weakly-coupled higher dimensional gravitational theories to be able to reframe the difficult problems in these transitions into more easily tractable versions. Using this approach I find techniques to determine the most important parameters that control the phase transition, generally scanning across a broad range of parameter spaces to ascertain generic features, and then use these to establish whether detectable gravitational wave signals will be produced in the models I consider.

Acknowledgements

There are many people who deserve my wholehearted gratitude for getting me through these challenging and unusual few years.

Firstly, of course, I have to give a special thanks to my advisor Mark Hindmarsh. His mentorship has allowed me to flourish and really find my stride in research, as well as teaching me many valuable lessons. His willingness to give me freedom to explore the avenues which really interested me have made these last few years incredibly enjoyable and fulfilling; I think that has been integral to me being able to be successful in this degree and really prepared me for an academic career.

Along with Mark I also have to thank my other academic collaborators Oscar Henriksson, Carlos Hoyos, and Niko Jokela, who have been excellent companions on the journey of conducting research and writing articles. They have all given me invaluable insight and hands on experience into the paper writing process, as well as dispensed their deep knowledge in so many areas of physics.

Next I would like to thank Chloe Gowling (now Hopling) who joined as Mark's student at the same time as I and has been with me during this entire experience. Her constant presence during the highs and lows which are par for the course in a situation such as this has kept me sane, and I'm glad I was able to share this with her. Due to this I was also able to have the pleasure of meeting her boyfriend Michael and seeing their relationship blossom into what it is today, culminating into having the joy of attending their wedding in May 2022. They have provided me with so many fond memories.

My friends Danny, Jake, Kieran, Max, Megan, Tam, Tyler, as well as Charlie, Dan, *etc.* in Sussex and the whole Helsinki department have provided me with something which was indispensable for a project such as this, which was the fun and carefreeness that came along with spending time with them. Weekly evenings letting loose with Kieran in Brighton and numerous visits and long stays with the others in Manchester allowed me to blow off steam when things got tough, which was worth its weight in gold.

My family and the time I have been able to spend with them has been amazing these past few years and deserves thanks, and getting to enjoy extended time with my nieces and nephew whilst they were young as well as my sister and parents has been incredible.

Finally, and most deservedly, I have to thank my fiancée Phoenix. She has been with me the entire duration of my doctorate and has put up with all the strains that go along with it. Despite the difficulty of moving around frequently and often living in separate countries she has always been there for me, and I cannot thank her enough for that. We have managed to make this experience wonderful with the places we have visited and truly an adventure, one which would not have been the same without her and I will not forget.

Contents

List of Figures

Chapter 1

Introduction

The physical Universe, as much as we have attempted to quantify and describe it, is still a wild west in terms of how little we know. For years before the quantum revolution physicists thought we knew almost “all there was to know”, and that physics was almost finished as a field; how similar a position we are in now. In the century since quantum mechanics was initiated we have learned much about the minutia of the particle world, and our understanding of the peculiarities of gravity through general relativity has increased immensely. However, even with crowning achievements such as the Standard Model, we still recognise the incompleteness of our physical picture. How to reconcile gravity and the three other fundamental forces in our distinct regimes, why gravity is so much weaker comparatively, and whether the Universe realises all available symmetries or not are still cavernous holes in our knowledge. Nevertheless intriguing theories pop up every so often, and string theory presenting the AdS/CFT correspondence (or holography) is one of them which can be utilised from subjects as diverse as superconductors all the way to gravitational waves.

The study of gravitational waves is not a new one, but its ability to explore regions of the cosmos previously invisible is hard to ignore. The recent experimental confirmation of gravitational waves by the Laser-Interferometer Gravitational Wave Observatory (LIGO) in 2015 [4] produced by the merger of two black holes in a binary black hole (BBH) system has proven that gravitational wave astronomy is a worthwhile endeavour, and therefore exploring physics in the new paradigm of detection by gravitation as well as the previously unequalled detection by light is now a feasible goal. This has opened up new windows for research in previously obstructed areas where light detection could no longer be relied upon, such as in the early Universe which was opaque to light prior to recombination, or in black hole systems where light cannot escape the intense gravitational fields.

In this vein, the use of the AdS/CFT correspondence to study these areas is indeed a relatively new venture but has so far been exceedingly successful. Its ability to translate the problems of a strongly coupled regime in a field theoretic sense to a weakly coupled gravitational sense has been invaluable for exploring areas that have been inaccessible to conventional perturbation theory. From this, the area of strongly coupled field theories which dictate gravitational wave spectra has flourished through the dual study of gravitation in one higher dimension. Specifically, applying this technique to gravitational wave production from first-order cosmological phase transitions has been of particular interest due to the observational prospects of planned space-based detectors such as the Laser Interferometer Space Antenna (LISA) [5, 6], Taiji [7], and TianQin [8, 9]. As the Standard Model electroweak phase transition is predicted to be a crossover [10, 11, 12], we would not expect to observe gravitational waves due to a lack of a barrier separating the distinct phases. However, there are numerous motivations to believe that beyond the Standard Model effects would lead to the re-obtention of a first-order transition, and so a search for gravitational waves in this manner is a search for physics beyond the Standard Model.

To fully understand what these signals represent we must delve deep into the dynamics and energy content of the phase transitions, and this amounts to mastering the fundamental parameters which drive the transition; of which fortunately there turn out to be relatively few. The important parameters boil down to five main quantities: the transition strength α, the nucleation temperature T_{n}, the transition rate (in units of the Hubble parameter) β/H_{n}, the bubble wall velocity v_{w}, and the speed of sound c_s^2 (which has a separate value for each phase present). Calculating each requires in-depth treatments of a certain sector of phase transition physics; the transition strength and sound speed are calculable from just the thermodynamic parameters, whereas the nucleation temperature and nucleation rate require complicated field theory derivations to calculate the effective potential of a bubble. The wall velocity as an out-of-equilibrium quantity requires computation in terms of the microscopic theory, which can be challenging even for weakly coupled theories [13, 14]. The calculation of these parameters then (barring v_{w}) shall be the focus of my thesis. By using the holographic principle I will derive calculations to be able to determine the values of four out of the five, even in strongly coupled theories, and demonstrate the feasibility of detecting the signals they shall produce in the experiments mentioned above. The wall velocity, being resistive to yielding its computation even in weakly coupled theories, has not yet been fully ascertained. Due to this, in our work we make use of the state-of-the-art treatments which are the most convincing as yet known.

1.1 Thesis Structure

There are three main pillars necessary for understanding the work done in this thesis: phase transitions, gravitational waves, and the AdS/CFT correspondence through holography. All of these work in harmony with their techniques and nuances being critical to the thesis goal, and so we shall try and go as in-depth with the details as is necessary to have a good understanding of their place in the research results.

In chapter 2 I go through some very basic concepts in general relativity and cosmology which will be necessary such as the definitions of curvature tensors and density evolution to understand the more complex ideas in later sections. I also briefly touch on black holes and their properties including short derivations for the Hawking temperature T_H and the Bekenstein-Hawking entropy S_{BH}.

In chapter 3 I discuss the formulation of the Standard Model and its content including the Higgs particle. I then proceed to discuss the Higgs' interactions with other particles, how mass can be acquired in the Universe through spontaneous symmetry breaking at zero temperature, and how this sort of process is part of a larger set of unifications of the fundamental forces. After this, a brief review of thermal field theory is given so as to be able to explain how effective actions and potential can be derived at finite temperature, and we show that the Higgs potential can be broken through thermal effects. I then motivate beyond the standard model reasons as to why the electroweak phase transition could be first-order, and describe the dynamics of the transition.

In chapter 4 I move on to gravitational waves and how to derive them from general relativity as perturbations upon a flat background metric. I discuss the usual gauges which reduce these equations to manageable levels, and then promote these arguments to curved background spaces. I then go through the derivation of the gravitational wave spectrum, detailing all factors which are generally accepted to influence the shape and intensity of the spectrum and also how this relates to the signal-to-noise ratio. Finally I discuss the main points of and how to calculate the quantities which characterise the spectrum: α, $\beta/H_{\rm n}$, $T_{\rm n}$, $v_{\rm w}$, and c_s^2.

In chapter 5 I now shift gears and begin a whirlwind tour of string theory and related concepts. I start off giving some base properties for conformal field theories and then anti-de Sitter spacetimes which are useful to keep in mind. I quickly speak a little about supersymmetry as it plays an important role in constructing string theory. After this I move on to describing the different types of string theories: bosonic and superstring, the latter of which is divided up into five equally valid types. I detail that actually there is a web of dualities (formed of S-dualities and T-dualities) which relate all of these theories together under one umbrella named M-theory. From this discussion of dualities I springboard into one major type in chapter 6, namely the AdS/CFT correspondence. I relate how this can be built up from a string picture and show this in the concrete case of $\mathcal{N}=4$ supersymmetric Yang-Mills theory. Using this case I motivate how strongly coupled field theories in d-dimensions can be translated into a weakly coupled gravitational theory in $d+1$-dimensions, then give a "holographic dictionary" which relates the main quantities on both sides. Lastly I detail how there is a special treatment to renormalise these theories to make them well-behaved, and then extend these arguments to finite temperature for use in our papers.

That concludes the background theory, and the rest of the thesis is concerned with the articles I published during my doctorate.

Chapter 7 is the first paper produced during my research. Using a master function method and a potential built from a superpotential comprised of two variable quantities, ϕ_M and ϕ_Q, a holographic model is explored. Using this holographic duality with a black hole in the bulk, the thermodynamic properties of the system are found. Deforming the potential by changing ϕ_M, ϕ_Q, the parameter space of important quantities is explored such as latent heat, critical temperature, transition strength, and sound speed. Collating all this information it is shown where gravitational wave signals could perhaps be detected with the correct transition rate.

In chapter 8 we follow up on the work in the first paper by attempting to expand upon what it was lacking. We derive a new method of calculating the effective potential from holographic considerations, utilising "multi-trace deformations" to ensure that our model has a first-order phase transition. We demonstrate how the effect of the number of colours N will act on quantities important for gravitational wave signals, and produce a parameter scan of the domain wall solutions.

Finally, chapter 9 is our latest paper. In this we use the newly detailed method of calculating the effective action from the previous paper to explore a holographic model in a more in-depth way. We numerically produce solutions to the holographic equations and map out the parameter space by varying the multi-trace operator couplings. Effective action found, we now fully calculate holographically both the transition rate and nucleation temperature as well as the transition strength, and so we scan over all these quantities to demonstrate whether gravitational waves will be able to be detected in this model.

Chapter 2

Cosmology and General Relativity

In this chapter we shall review some of the machinery which powers the later discussions. General relativity is an integral part to all concepts in this thesis due to its ability to describe the effects of gravity through spacetime curvature in much more extreme circumstances than the flat space that Newtonian gravity is formulated in. Many weird and wonderful predictions have emerged out of general relativity such as the prediction of black holes and gravitational waves, both of which have now been observed in nature. As these concepts are of central importance to this thesis, we shall explore the very basics of General Relativity here which is necessary for the gravitational wave analysis in chapter 4 as well as some basics of cosmology and black holes, which is necessary for chapters 4, 5, and 6.

2.1 General Relativity Preamble

General Relativity (GR) is built around the equivalence of reference frames. This is a statement which at its heart describes that there are no "special observers" in the Universe, and so the fundamental laws act equivalently no matter how the observer is moving in relation to a reference point, or no matter how spacetime is curved around them. This idea leads to the invariant quantity of the spacetime interval

$$ds^2 = g_{\mu\nu} dx^\mu dx^\nu \ , \tag{2.1}$$

which details how two points are related when they are separated by infinitesimal changes in time ($(dt)^2$) and space ($(dx)^2$). How these points are related is dictated by the metric tensor $g_{\mu\nu}$, which describes the underlying curvature of the spacetime in question. In flat space this general metric simplifies to the flat space metric known as the "Minkowski metric", labelled by $\eta_{\mu\nu}$[1]. From this metric, curvature tensors can be constructed which describe properties of the spacetime curvature such as the Christoffel symbols $\Gamma^{\rho}_{\mu\nu}$, the Riemann tensor $R^{\tau}_{\mu\nu\rho}$, the Ricci tensor $R_{\mu\nu}$, and the Ricci scalar R. The Christoffel symbol is comprised of the metric and its derivatives as

$$\Gamma^{\rho}_{\mu\nu} = \frac{1}{2} g^{\rho\tau} \left(\partial_\nu g_{\tau\mu} + \partial_\mu g_{\tau\nu} - \partial_\tau g_{\mu\nu}\right) \ , \tag{2.2}$$

and essentially measures the corrections needed when considering curved space (and so for $\eta_{\mu\nu}$ this gives $\Gamma^{\rho}_{\mu\nu} = 0$). Using the definition for the connection, the Riemann curvature tensor can be defined through

$$R^{\tau}_{\mu\nu\rho} = \partial_\nu \Gamma^{\tau}_{\rho\mu} - \partial_\rho \Gamma^{\tau}_{\nu\mu} + \Gamma^{\tau}_{\nu\sigma}\Gamma^{\sigma}_{\rho\mu} - \Gamma^{\tau}_{\rho\sigma}\Gamma^{\sigma}_{\nu\mu} \ . \tag{2.3}$$

From this we can construct other curvature quantities such as the Ricci tensor

$$R_{\mu\nu} = R^{\rho}_{\mu\rho\nu} = \partial_\rho \Gamma^{\rho}_{\mu\nu} - \partial_\mu \Gamma^{\rho}_{\nu\rho} + \Gamma^{\rho}_{\rho\tau}\Gamma^{\tau}_{\mu\nu} - \Gamma^{\rho}_{\mu\tau}\Gamma^{\tau}_{\rho\nu} \ , \tag{2.4}$$

and contracting this with the metric we get the curvature invariant of the Ricci scalar

$$R = g^{\mu\nu} R_{\mu\nu} \ . \tag{2.5}$$

With those definitions in place we now have everything necessary to describe curvature in a vacuum. The real power of general relativity however comes from the fact that we can go beyond the vacuum, and we can equate this curvature to energy and mass distributions in the form of the stress-energy (or equally named energy-momentum) tensor $T_{\mu\nu}$. This allows us to explore the connection between spacetime and matter in the form of the Einstein equation,

$$R_{\mu\nu} - \frac{1}{2} R g_{\mu\nu} + \Lambda g_{\mu\nu} = \kappa^2 T_{\mu\nu} \ , \tag{2.6}$$

where κ^2 is Einstein gravitational constant, related to the gravitational constant G through $\kappa^2 = 8\pi G$, and Λ is the cosmological constant. Often we will make use of the Hilbert stress-energy tensor when considering gravity coupled to matter. In this way, the stress-energy tensor is found through a functional derivative of the matter part of the action $S_{\text{matter}} = \int d^d x \sqrt{-g} \mathcal{L}_{\text{matter}}$ with respect to the metric. This produces the tensor

$$T_{\mu\nu} = \frac{-2}{\sqrt{-g}} \frac{\delta S_{\text{matter}}}{\delta g^{\mu\nu}} = -2 \frac{\partial \mathcal{L}_{\text{matter}}}{\partial g^{\mu\nu}} + g_{\mu\nu} \mathcal{L}_{\text{matter}} \ . \tag{2.7}$$

[1]see appendix G

2.2 FLRW Cosmology

Shortly after the introduction of general relativity as a theory of gravitation, efforts were made to explore exact solutions corresponding to physically interesting situations. In an attempt to model the Universe, Friedmann [15, 16], Lemaître [17, 18], Robertson [19, 20, 21], and Walker [22] devised a set of solutions based on the homogeneous, isotropic, and expanding metric

$$ds^2 = -dt^2 + a(t)^2\left(\frac{dr^2}{1-kr^2} + r^2(d\theta^2 + \sin^2\theta d\phi^2)\right) , \tag{2.8}$$

where $a(t)$ is the scale factor which describes the expansion (or contraction) of the Universe, and k is a constant representing the curvature of the space. This metric permits three types of interesting solutions. If we first study a slight transformation of

$$k \to \frac{k}{|k|}, \quad r \to \sqrt{|k|}r, \quad a \to \frac{a}{\sqrt{k}} , \tag{2.9}$$

we can see that the metric remains the same. As k is now just a quantity divided by its magnitude it can take only one of three values, namely -1, 0, and +1. The most familiar scenario is when we set $k = 0$, which just reduces the metric to flat Euclidean space in spherical coordinates. With $k = 1$ we have constant positive curvature which after a transformation of $r = \sin\chi$ can only be the metric of a closed 3-sphere. Finally, with $k = -1$ we have constant negative curvature and after the transformation r $= \sinh\chi$ has a metric of the open 3-hyperboloid.

Working through the curvature equations 2.4 and 2.5 produces

$$R_{00} = 3\frac{\ddot{a}}{a} , \qquad R_{ij} = \frac{1}{a^2}(a\ddot{a} + 2\dot{a}^2 + 2k)g_{ij} , \tag{2.10}$$

and

$$R = \frac{6}{a^2}(a\ddot{a} + \dot{a}^2 + k) . \tag{2.11}$$

It is normal to treat the constituents of the Universe as perfect fluids, which is described by the energy-momentum tensor

$$T_{\mu\nu} = (p+\rho)u_\mu u_\nu + pg_{\mu\nu} \tag{2.12}$$

where u^μ is the four-velocity of the perfect fluid, ρ is the energy density, and p is the pressure. If we trace over this quantity, we see that we produce a combination of the pressure and energy density alone as

$$T^\mu_\mu = g^{\mu\nu}T_{\mu\nu} = -\rho + 3p . \tag{2.13}$$

From these and equation 2.6, we find conditions on the scale factor using the temporal components:

$$\left(\frac{\dot{a}}{a}\right)^2 = \frac{\kappa^2}{3}\rho - \frac{k}{a^2} \ , \tag{2.14}$$

and the spatial components:

$$\frac{\ddot{a}}{a} = -\frac{\kappa^2}{6}\left(\rho + 3p\right) \ . \tag{2.15}$$

We will mostly just be interested in the temporal equation and so define the Hubble parameter which dictates how the Universe is expanding or contracting as

$$H \equiv \frac{\dot{a}}{a} \ . \tag{2.16}$$

It will be useful for later to categorise the ratio of the energy density to the "critical" energy density in the Universe, ρ_{crit}, which is simply defined as the energy density found from equation 2.14 when $k = 0$. Labelling this Ω, it appears as

$$\Omega \equiv \frac{\rho}{\rho_{\text{crit}}} = \frac{\kappa^2\rho}{3H^2} \ . \tag{2.17}$$

The equations can also be used to inform us how the quantities depend upon time or temperature. If we utilise the necessity of conservation of energy, $\partial^\mu T_{\mu\nu} = 0$, we see

$$\dot{\rho} = -3H(\rho + p) \ . \tag{2.18}$$

It is conventional to define a quantity known as the equation of state which relates the pressure and energy density directly as $p = w\rho$, so the previous equation becomes (written in a more useful form)

$$\frac{d\text{log}\rho}{dt} = -3(1+w)\frac{d\text{log}a}{dt} \ , \tag{2.19}$$

where we have used that $\frac{1}{a}\frac{da}{dt} = \frac{d\text{log}a}{dt}$. A simple integration shows us that (if the equation of state is constant) the energy density and scale factor can be related through

$$\rho \propto a^{-3(1+w)} \ , \tag{2.20}$$

which for instance in the radiation dominated case with $w = 1/3$ tells us the energy density is diluted as $\rho \propto a^{-4}$.

As the expansion of the Universe will possibly have a large impact on physical quantities we will be using, we want to understand how quantities will change in time during this expansion. The cosmological redshift z (which determines expansion through wavelength shift due to expanding space) can be related to the scale factor a through the relation

$$a(z) = a_0(1+z)^{-1} \ , \tag{2.21}$$

where a_0 is the scale now (generally taken to be 1). As we know that the scale factor has a time dependence, we can manipulate the redshift to determine its relation to time through

$$dz = d(1+z) = d\left(\frac{a_0}{a}\right) = -\frac{a_0}{a^2}da = -\frac{a_0}{a}Hdt = -(1+z)H(z)dt \ . \tag{2.22}$$

We can also find a scaling of the temperature from the Universe expansion, which will be useful later. Under this expansion the blackbody spectral shape is preserved, however the total energy density and characteristic temperature decrease with the expansion. Thus the temperature of the CMB as a function of redshift is:

$$T(z) = T_0(1+z) \ , \tag{2.23}$$

where T_0 is the temperature observed today. Taking the derivative with respect to z is simply

$$\frac{dT}{dz} = T_0 \ , \tag{2.24}$$

which can then be converted to a differential with respect to time through the formula we just found in eq. 2.22 as

$$\frac{dT}{dt} = -\frac{T_0}{(1+z)}H \ . \tag{2.25}$$

Finally we can re-enter the definition of temperature in eq. 2.23 to remove the constant and find

$$\frac{dT}{dt} = -H(T)T \ . \tag{2.26}$$

These relations can also now translate other quantities into the more useful temperature dependent form. For instance, eq. 2.20 with $w = 1/3$ (radiation dominated) can now be written as $\rho \propto T^4$ by noting that $H \propto a^{-2}$ is this case from eq. 2.14, which leads to the relation $a(T) \propto T^{-1}$.

2.3 Black Holes

A hugely important facet that drops out of the study of general relativity is the discovery of objects in the equations of zero size and infinite density (but finite mass), dubbed "black holes" for their property of being so gravitationally intense that past a certain limit no light-cone leads out of the object. The singularities appearing in general relativity come about due to curvature invariants diverging, and black holes by definition have at least one event horizon (however in some recent papers the possibility of a naked singularity has been postulated [23, 24]). The event horizon shields the singularity of a black hole,

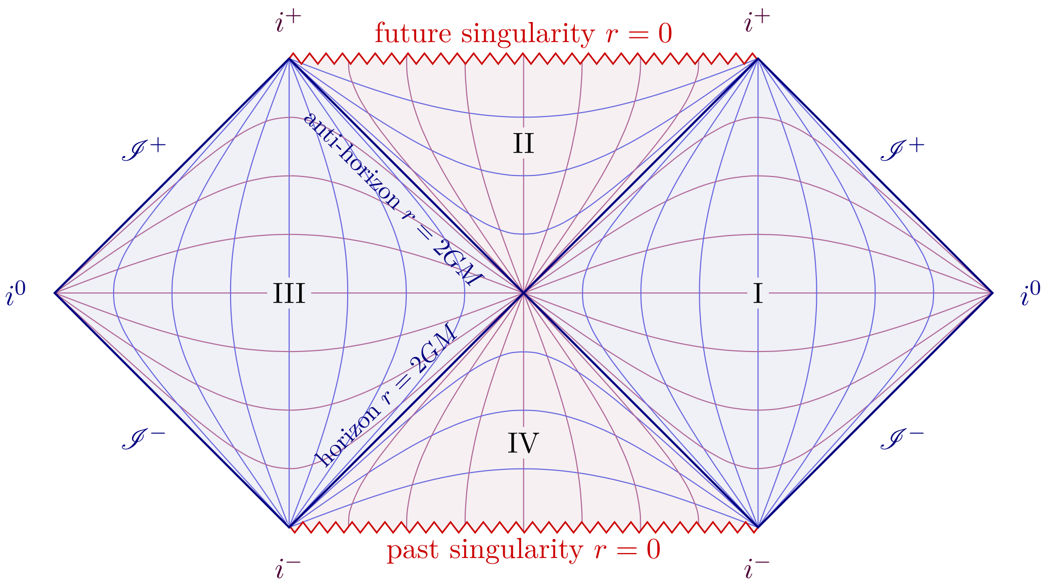

Figure 2.1: Penrose diagram of a black hole showing the causal connections between regions of spacetime. The label i^0 is spacelike infinity ($r = \infty$), whereas i^+ and i^- are future and past timelike infinity ($t = \pm\infty$), respectively. $\mathscr{I}^+, \mathscr{I}^-$ are lightlike infinities.

and is a hypersurface separating spacetime points connected to infinity by a timelike path from those which are not [25].

The Schwarzschild black hole is the simplest and first non-trivial solution found, devised by Karl Schwarzschild in 1916 [26], and is a spherically symmetric vacuum solution to the Einstein equation 2.6 surrounding a mass M, which in the usual four dimensions is

$$ds^2 = -h(r)dt^2 + \frac{1}{h(r)}dr^2 + r^2 d\Omega_2^2 \ , \tag{2.27}$$

where $h(r)$ is known as a blackening factor and in four dimensions is parameterised by the radius and horizon radius r_h as

$$h(r) = 1 - \frac{r}{r_h} \ . \tag{2.28}$$

The horizon radius may also be described in terms of the mass and the gravitational constant G through the relation

$$r_h = 2GM \ . \tag{2.29}$$

The Penrose diagram (which captures the causal relations between different points in spacetime [27]) for this sort of object in shown in fig. 2.1, with region I corresponding to normal spacetime, with lines of constant time (red) or space (blue). The black hole is region II with horizon at $r_h = 2GM$ past which nothing can escape, and the true singularity is the future singularity at $r = 0$. Region IV is a white hole, and region III is a causally disconnected spacetime. As I will be considering higher-dimensional theories, it will be useful to see how this solution extends in D-dimensions. The metric now becomes

$$ds^2 = -h(r)dt^2 + \frac{1}{h(r)}dr^2 + r^2 d\Omega_{D-2}^2, \tag{2.30}$$

where the blackening factor is

$$h(r) = 1 - \left(\frac{r_h}{r}\right)^{D-3} , \tag{2.31}$$

with the horizon radius in D-dimensions taking the form

$$r_h^{D-3} = \frac{16\pi M G_D}{(D-2)\Omega_{D-2}} . \tag{2.32}$$

The quantity Ω_n is the volume of a unit-n-sphere,

$$\Omega_n = \frac{2\pi^{(n+1)/2}}{\Gamma(\frac{n+1}{2})} , \tag{2.33}$$

where $\Gamma(n)$ is the Euler gamma function [28]

$$\Gamma(z) = \int_0^\infty x^{z-1}e^{-x}dx . \tag{2.34}$$

2.3.1 Hawking Temperature T_H

For years black holes baffled physicists with their seeming ability to be the one object in the Universe to disobey normal rules of thermodynamics, specifically that once an object passed the event horizon it was lost forever along with the information it carried and the entropy in the Universe decreased, fundamentally opposing the second law of thermodynamics that $dS \geq 0$. The reason for this was that classical black holes as were known at the time were subject to the “no-hair theorem” [29, 30, 31], meaning that these types of black holes could be categorised by only three quantities: the mass of the black hole M, its angular momentum (whether it was rotating or not) J, and its electric charge Q. As the black hole’s properties did not include anything else such as entropy (no “hairy” attributes with which to distinguish one black hole with the same M, J, and Q from another), when an object was absorbed these three quantities were changed but the entropy S of the object and the information contained with that quantity vanished, decreasing the entropy of the Universe. In 1972 however, Bekenstein showed relations between black hole entropies and area [32] and in 1974 Hawking showed in landmark papers that black holes do in fact radiate away [33, 34] which in doing so provide the system with a mensurable temperature known as the Hawking temperature T_H. In proving that black holes do indeed have usual thermodynamic quantities (beginning from either the entropy or the temperature) then other normal thermodynamic quantities can follow, and the temperature being quantifiable as a change in entropy against internal energy shows that the black hole must have an entropy associated with it or vice versa. We will begin with the temperature, then move on to the entropy.

The derivation of this temperature is as follows: to begin, extend the metric to a more general form in which the time coordinate is compactified (known as Eucilidean signature)

$$ds^2 = f(r)d\tau^2 + \frac{1}{g(r)}dr^2 + r^2 d\Omega_{D-2}^2 \ . \tag{2.35}$$

For the quantities $f(r)$ and $g(r)$, we assume that at the horizon they go to zero at first order, *i.e.* $f(r_h) = g(r_h) = 0$. Using this information, we can Taylor expand expand around the horizon as

$$f(r) = f'(r_h)(r - r_h) + \mathcal{O}((r - r_h)^2), \qquad g(r) = g'(r_h)(r - r_h) + \mathcal{O}((r - r_h)^2) \ . \tag{2.36}$$

Noting that we have periodicity in τ as well as the constraints of vanishing functions f and g at the horizon r_h, we see that this ensures regularity of Euclidean space. Entering the forms of the expansion into the metric equation 2.35 we find

$$ds^2 = f'(r_h)(r - r_h)d\tau^2 + \frac{1}{g'(r_h)(r - r_h)}dr^2 + r^2 d\Omega_{D-2}^2 + \dots \ . \tag{2.37}$$

If we now perform a change of variables of

$$\rho = 2\sqrt{\frac{r - r_h}{g'(r_h)}} \ , \tag{2.38}$$

the metric can be rewritten as

$$ds^2 = \frac{f'(r_h)g'(r_h)}{4}\rho^2 d\tau^2 + d\rho^2 + \dots \ , \tag{2.39}$$

and further, we can identify that setting the time coordinate to

$$d\phi = \sqrt{\frac{f'(r_h)g'(r_h)}{4}}d\tau \tag{2.40}$$

will take us to cylindrical coordinates. We can therefore integrate equation 2.40 remembering that the time direction is compactified on a circle and periodic in the temperature to give

$$\int_0^{2\pi} d\phi = \int_0^{1/T} \sqrt{\frac{f'(r_h)g'(r_h)}{4}}d\tau \ . \tag{2.41}$$

When integrated and rearranged, we arrive at the relation for the temperature of a black hole,

$$T_H = \left. \frac{\sqrt{f'(r)g'(r)}}{4\pi} \right|_{r_h} \ . \tag{2.42}$$

2.3.2 Bekenstein-Hawking Entropy S_{BH}

If black holes have a temperature, we expect them to display properties common to other thermodynamic systems also. We can see an analogy to the first law of thermodynamics in the result that two neighbouring black hole equilibrium states are related by [35]

$$dM = \frac{\kappa}{8\pi} dA + \Omega dJ \ , \tag{2.43}$$

where M is the mass (or equally Energy in these units), κ is the surface gravity (a quantity related to the local proper acceleration defined through Killing vectors), Ω is the angular velocity, and J is the angular momentum of the black hole. We can compare this to a more familiar thermodynamic relation

$$dU = TdS + pdV \ , \tag{2.44}$$

where U is the internal energy, T is the temperature, S is the entropy, p is the pressure, and V is the volume. The thermodynamic analogy proposed in Bekenstein [36] and later Hawking's [34] papers were then that by analogy one could relate this as (for a non-rotating black hole)

$$dM = TdS \ , \tag{2.45}$$

and so through eq. 2.43 the temperature is directly related to the surface gravity and the entropy is directly related to the area. This makes sense so far for the temperature we calculated in the previous section, as the result we found is indeed simply related to the surface gravity through $T_H = \kappa/2\pi$. For the Schwarzschild black hole, the temperature is given by eq. 2.42 with $f(r) = g(r) = (1 - r/r_h)$ and from this we find a Hawking temperature of $T_H = (4\pi r_h)^{-1}$. We can translate this into a mass dependence through eq. 2.29 as

$$T_H = \frac{1}{8\pi MG} \ , \tag{2.46}$$

and so requiring $S \to 0$ as $M \to 0$ we can integrate and find

$$S = 4\pi M^2 G \ . \tag{2.47}$$

Finally we can relate this to the area of the black hole through the relations

$$A = 4\pi r_h^2 = 16\pi (MG)^2 \ , \tag{2.48}$$

and so this leads to the entropy of a black hole in terms of its horizon surface area A and the gravitational constant G as the famous Bekenstein-Hawking entropy

$$S_{BH} = \frac{A}{4G} \ . \tag{2.49}$$

This result is not limited to just Schwarzschild black holes, nor is it limited to just four dimensions. We can promote this relation to a general relation for a black hole in any dimension (which are the consequence of studying GR in different dimensions [37]) by modifying it to

$$S_{BH} = \frac{A}{4G_D} \ , \tag{2.50}$$

where G_D is just the gravitational constant in D-dimensions.

Chapter 3

The Standard Model, Phase Transitions, and Beyond

3.1 The Standard Model

The Standard Model, being the most complete model we have so far of the content of our Universe, is a non-Abelian gauge theory comprised of the symmetries [38, 39, 40, 41, 42]

$$\mathrm{SU}(3)_c \times \mathrm{SU}(2)_\mathrm{L} \times \mathrm{U}(1)_\mathrm{Y} \;, \tag{3.1}$$

with the subscript c referring to the colour symmetry of SU(3), the subscript L referring to how only the left-handed fermions transform under the $\mathrm{SU}(2)_\mathrm{L}$ group, and the subscript Y referring to the weak hypercharge. Each segment of the group symmetries corresponds to a section of the standard model: $\mathrm{SU}(3)_c$ corresponds to the strong interaction of the coloured particles (in the form of quarks and gluons) through quantum chromodynamics (QCD), whilst $\mathrm{SU}(2)_\mathrm{L} \times \mathrm{U}(1)_\mathrm{Y}$ corresponds to the electroweak (EW) sector formed by both electromagnetism and weak interactions. That both strong and electroweak forces are introduced as gauge interactions is an essential feature of the Standard Model [43], but as of yet the final force, gravity, is unable to be reconciled in this hugely successful theoretical framework. The two main constituents which comprise the Standard Model are bosons and fermions, distinct in their type of spin quantum number: integer spin for bosons and half-integer spin for fermions. Due to this, these classes of particles obey entirely different statistics and therefore have very different properties. Bosons obey Bose-Einstein statistics while fermions obey Fermi-Dirac statistics, determining the possibility of multiple occupancy of states. Further to these classifications, the Standard Model is split up as such:

- Bosons:
  - Gauge Bosons - Vector Bosons $\mathrm{W}^{\pm}$ and Z^0, photon γ, gluons g
  - Scalar Bosons - Higgs Boson ϕ
- Fermions:
  - Quarks and their antiparticles - Three generations of quarks: up, down (u,d); charm, strange (c,s); top/truth, bottom/beauty (t,b)
  - Leptons and their antiparticles - Three generations of leptons $(\mathrm{e}^-, \mu^-, \tau^-)$ and lepton neutrinos $(\nu_e, \nu_\mu, \nu_\tau)$.

Let us first examine the fermionic section. The fermionic matter fields are chiral, allowing for projection into components based on whether they are "left-handed" or "right-handed". The projection operators for this chirality are defined as

$$P_L = \frac{1-\gamma^5}{2} \ , \quad P_R = \frac{1+\gamma^5}{2} \tag{3.2}$$

where γ^5 is the product of the four other gamma matrices as $\gamma^5 = i\gamma^0\gamma^1\gamma^2\gamma^3$ which are in turn formed through the Pauli matrices σ^i as $\gamma^0 = \sigma^3 \otimes I$, $\gamma^i = i\sigma^2 \otimes \sigma^i$. With our projection operators, if we act upon a fermionic field we retrieve the projected fields as

$$\psi_L = P_L\psi \ , \quad \psi_R = P_R\psi \ . \tag{3.3}$$

As the weak force only displays interaction with left-handed chiral fermions (a right-handed fermion is neutral under the weak force) we see that the left-handed particles transform as SU(2) doublets under weak isospin SU(2) transformations but the right-handed particles are SU(2) singlets. Due to this distinction then, we shall denote our particle specifies as follows: the quarks will be formed into the quantity

$$q_L^a = \left(\begin{pmatrix} \mathrm{u} \\ \mathrm{d} \end{pmatrix}_L , \begin{pmatrix} \mathrm{c} \\ \mathrm{s} \end{pmatrix}_L , \begin{pmatrix} \mathrm{t} \\ \mathrm{b} \end{pmatrix}_L \right) \ , \tag{3.4}$$

where a is the generation index, which will later be used as the SU(2) index. We will therefore define a quantity with the up quark and quarks with similar properties as

$$u_R^a = (\mathrm{u}_R, \mathrm{c}_R, \mathrm{t}_R) \ , \tag{3.5}$$

and a quantity with the down quark and quarks with similar properties as

$$d_R^a = (\mathrm{d}_R, \mathrm{s}_R, \mathrm{b}_R) \ . \tag{3.6}$$

Similarly, the leptons will be formed into

$$l_L^a = \left(\begin{pmatrix} \mathrm{e} \\ \nu_e \end{pmatrix}_L , \begin{pmatrix} \mu \\ \nu_\mu \end{pmatrix}_L , \begin{pmatrix} \tau \\ \nu_\tau \end{pmatrix}_L \right) , \tag{3.7}$$

which have related right-handed quantities, with the leptons as

$$\mathrm{e}_R^a = (\mathrm{e}_R, \mu_R, \tau_R) \ , \tag{3.8}$$

and the lepton neutrinos as

$$\nu_L^R = (\nu_{e,R}, \nu_{\mu,R}, \nu_{\tau,R}) \ . \tag{3.9}$$

Now let us turn to the bosonic section. Looking back to the symmetry group of the standard model we can identify the gauge fields related to the generators of the group algebra as

$$\begin{array}{ccccc} \mathrm{SU}(3)_c & \times & \mathrm{SU(2)_L} & \times & \mathrm{U(1)_Y} \ , \\ \downarrow & & \downarrow & & \downarrow \\ 8G_\mu^\alpha & & 3W_\mu^a & & B_\mu \end{array}$$

where G_μ^α are the gluons which mediate the strong force and provide "colour" charge to any particle which interact with them, of which there are eight spin-1 types; W_μ^a are the vector bosons which mediate the weak force, of which there are three spin-1 types; and B_μ which is a singular spin-1 particle that is related to the mediation of the hypercharge interactions. From this then, we can write the Lagrangian of the Yang-Mills section of the Standard Model with the interactions of the matter section as

$$\begin{aligned} \mathcal{L}_{\mathrm{SM}} \supset \mathcal{L}_{\mathrm{YM}} = &-\frac{1}{4} G_{\mu\nu}^\alpha G^{\alpha\mu\nu} - \frac{1}{4} W_{\mu\nu}^a W^{a\mu\nu} - \frac{1}{4} B_{\mu\nu} B^{\mu\nu} \\ &- i\bar{q}\gamma^\mu D_\mu q - i\bar{u}\gamma^\mu D_\mu u - i\bar{d}\gamma^\mu D_\mu d - i\bar{l}\gamma^\mu D_\mu l - i\bar{e}\gamma^\mu D_\mu e \ , \end{aligned} \tag{3.10}$$

where

$$\begin{aligned} B_{\mu\nu} &= \partial_\mu B_\nu - \partial_\nu B_\mu \ , \\ W_{\mu\nu}^a &= \partial W_\mu^a - \partial W_\nu^a + g_2 \epsilon_{abc} W_\mu^b W_\nu^c \ , \quad a = 1, 2, 3 \\ G_{\mu\nu}^\alpha &= \partial_\mu G_\nu^\alpha - \partial_\nu G_\mu^\alpha + g_3 f_{\alpha\beta\gamma} G_\mu^\beta G_\nu^\gamma , \quad \alpha = 1, \ldots, N_c^2 - 1 \ ; \end{aligned} \tag{3.11}$$

here N_c is the number of colours which in the Standard Model is 3, ϵ_{abc} is the Levi-Civita symbol (structure constant for SU(2)) and $f_{\alpha\beta\gamma}$ is the structure constant for SU(3) which satisfy

$$[\sigma_a, \sigma_b] = 2i\epsilon_{abc}\sigma_c \quad \text{and} \quad [T^a, T^b] = if_{abc}T^c \ , \tag{3.12}$$

where σ_a and T^a are the generators of the groups. It is useful to remember that the positioning of these labels is arbitrary and can be changed with no change to the quantity *i.e.* $f^{abc} = f_{abc}$. Also present are g_2 and g_3 which are the coupling constants of the strong and weak force respectively; the coupling constant to U(1) will relatedly be labelled g_1. The covariant derivatives contained in equation 3.10 act in various ways depending upon the quantity they act on, so for completeness these are found by:

$$\begin{aligned} D_\mu q^a &= \left(\partial_\mu + \frac{ig_1}{6}B_\mu - \frac{i}{2}g_2\sigma_a W_\mu^a - \frac{i}{2}g_3\lambda_\alpha G_\mu^\alpha\right) q^a \ , \\ D_\mu u^a &= \left(\partial_\mu + \frac{2ig_1}{3}B_\mu - \frac{ig_3}{2}\lambda_\alpha G_\mu^\alpha\right) u^a \ , \\ D_\mu d^a &= \left(\partial_\mu + \frac{ig_1}{3}B_\mu - \frac{ig_3}{2}\lambda_\alpha G_\mu^\alpha\right) d^a \ , \end{aligned} \tag{3.13}$$

for the quarks, and:

$$\begin{aligned} D_\mu l^a &= \left(\partial_\mu + \frac{ig_1}{2}B_\mu - \frac{ig_2}{2}\sigma_a W_\mu^a\right) l^a \ , \\ D_\mu e^a &= \left(\partial_\mu + \frac{ig_1}{2}B_\mu\right) e^a \ , \\ D_\mu \nu^a &= (\partial_\mu)\, \nu^a \ , \end{aligned} \tag{3.14}$$

for the leptons. The varying factors in front of the B_μ terms simply arise from the different hypercharges Y which is the generator of the $\mathrm{U(1)_Y}$ group.

As we can see, in equation 3.10 there are no mass terms. For our symmetry group of $\mathrm{SU(3)_c \times SU(2)_L \times U(1)_Y}$ to be satisfied the Lagrangian we have formed must respect gauge invariance. This requires that only singlet terms can be included in the SM Lagrangian, precluding the ability for massive fermionic and gauge fields in this group initially.

The only other piece to now discuss is the final boson present in our previous discussion, a scalar named the Higgs boson. Long theorised, the Higgs particle was finally truly discovered in 2012 at CERN [44]. This scalar is hugely important to the Standard Model for providing masses to the other particles and in the mechanism of spontaneous electroweak symmetry breaking (EWSB), which will be discussed further in the next section. The Higgs Lagrangian is given by

$$\mathcal{L}_{\mathrm{SM}} \supset \mathcal{L}_{\mathrm{Higgs}} = -(D_\mu\phi)^\dagger(D^\mu\phi) - V(\phi^\dagger\phi) \ , \tag{3.15}$$

where V is the most general renormalisable potential invariant under $\mathrm{SU(2)_L \times U(1)_Y}$ which can be shown to be at tree level (up to constant redefinitions)

$$V(\phi) = \mu^2\phi^\dagger\phi + \lambda(\phi^\dagger\phi)^2 \ , \tag{3.16}$$

and the covariant derivative acting upon the Higgs is given by

$$D_\mu\phi = (\partial_\mu - \frac{ig_1}{2}B_\mu - \frac{ig_2}{2}\sigma_a W_\mu^a)\phi \ . \tag{3.17}$$

The masses therefore come through the interaction of the gauge fields and fermions with the Higgs particle by spontaneous symmetry breaking (SSB), known as Yukawa interactions, in which they acquire mass proportional to the vacuum expectation value (v.e.v.) of the Higgs field. The Lagrangian piece produced from these interactions is

$$\mathcal{L}_{\mathrm{SM}} \supset \mathcal{L}_{\mathrm{Yukawa}} = \overline{q}^a h_u u^b \tilde{\phi} + \overline{q}^a h_d d^b \phi + \bar{l} h_e e \phi + \bar{l} h_\nu \nu \tilde{\phi} + \text{h.c.} \ , \tag{3.18}$$

where h_u, h_d, h_e, and h_ν are the 3×3 Yukawa coupling matrices and h.c. indicates the inclusion of the hermitian conjugates of the terms. The Yukawa couplings reduce the global symmetries of the gauged kinetic terms to four phase symmetries, baryon number and the three lepton numbers [45].

Altogether then, we can write the Lagrangian of the Standard Model as

$$\begin{aligned}\mathcal{L}_{\mathrm{SM}} = & -\frac{1}{4} G^{\alpha}_{\mu\nu} G^{\alpha\mu\nu} - \frac{1}{4} W^{a}_{\mu\nu} W^{a\mu\nu} - \frac{1}{4} B_{\mu\nu} B^{\mu\nu} \\ & - i\overline{q}_a \gamma^\mu D_\mu q_a - i\overline{u}_a \gamma^\mu D_\mu u_a - i\overline{d}_a \gamma^\mu D_\mu d_a - i\bar{l} \gamma^\mu D_\mu l - i\overline{e} \gamma^\mu D_\mu e \\ & - (D_\mu \phi)^\dagger (D^\mu \phi) - V(\phi^\dagger \phi) + \overline{q}^a h_u u^b \tilde{\phi} + \overline{q}^a h_d d^b \phi + \overline{l}^a h_e e^b \phi + \overline{l}^a h_\nu \nu^b \tilde{\phi} + \text{h.c.}\end{aligned} \tag{3.19}$$

3.2 Symmetries and Breaking

We now wish to understand exactly how the symmetry is spontaneously broken and mass is acquired in the Standard Model. Finding the minimum of the Higgs potential in equation 3.16 using $\partial V(\phi)/\partial \phi = 0$ gives the condition

$$|\phi|^2 = \phi^\dagger \phi = -\frac{\mu^2}{2\lambda} \ . \tag{3.20}$$

For $\mu^2 > 0$ the potential is constantly positive, and so the minimum and therefore vacuum expectation value will be zero. With the coefficient μ^2 having a negative value instead the minimum will be located wherever equation 3.20 is satisfied. As seen in figure 3.1 there is in fact a continuous ring of degenerate minima which satisfy this condition, and the choice of one of the infinite states breaks the $\mathrm{SU}(2)_{\mathrm{L}}$ symmetry by the mechanism

$$\mathrm{SU}(2)_{\mathrm{L}} \times \mathrm{U}(1)_{\mathrm{Y}} \to \mathrm{U}(1)_{\mathrm{em}} \ , \tag{3.21}$$

where $\mathrm{U}(1)_{\mathrm{em}}$ is the symmetry group of electromagnetism.

The Higgs doublet may be parameterised as

$$\phi = \frac{1}{\sqrt{2}} \begin{pmatrix} \phi^+ \\ \phi^0 \end{pmatrix} = \frac{1}{\sqrt{2}} \begin{pmatrix} \phi_2 + i\phi_3 \\ \phi_0 + i\phi_1 \end{pmatrix} \ , \tag{3.22}$$

which leads to

$$(\phi_0^2 + \phi_1^2 + \phi_2^2 + \phi_3^2) = -\frac{\mu^2}{\lambda} \ . \tag{3.23}$$

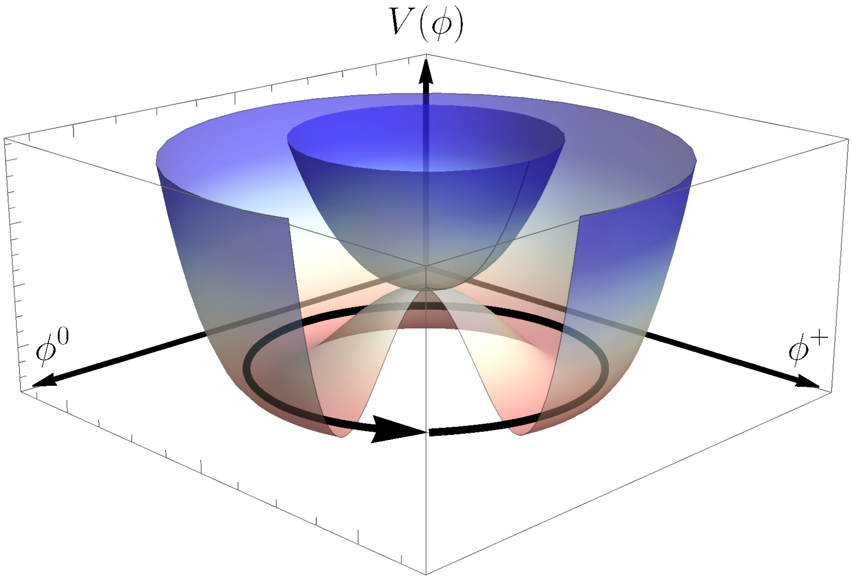

Figure 3.1: A schematic representation of the spontaneous symmetry breaking of the Higgs mechanism. Before SSB, there is a single minimum of the potential with zero expectation value, after SSB a new ring of minima (actually a 3-sphere for the Standard Model) appear which have non-zero vacuum expectation values, shown by the black circular arrow.

We can label the real constant that minimises the scalar potential

$$v \equiv \sqrt{\phi^\dagger \phi} = \sqrt{-\frac{\mu^2}{2\lambda}} \tag{3.24}$$

and our U(1) rotational symmetry allows us to choose therefore the real uncharged part of the doublet ϕ_0 so we may write the doublet as

$$\phi = \frac{1}{\sqrt{2}} \begin{pmatrix} 0 \\ h(x) + v \end{pmatrix} , \tag{3.25}$$

where h is the scalar field with $\langle h \rangle = 0$. Finally we can see that we acquire a non-zero vacuum expectation value as

$$\langle \phi \rangle = \frac{1}{\sqrt{2}} \begin{pmatrix} 0 \\ v \end{pmatrix} . \tag{3.26}$$

How do the gauge fields we introduced previously correspond to the physical bosons? We find that the electric charge $Q = Y + T^3$ actually couples to the combination of

$$A_\mu = \frac{g_1 W^3_\mu + g_2 B_\mu}{\sqrt{g_1^2 + g_2^2}} , \tag{3.27}$$

which is the boson mediating the electromagnetic group $\mathrm{U}(1)_{\mathrm{em}}$ called the photon. Similarly, the combination

$$\mathrm{Z}_\mu = \frac{g_2 W^3_\mu - g_1 B_\mu}{\sqrt{g_1^2 + g_2^2}} \tag{3.28}$$

can be used to define the Z boson. Defining the "Weinberg angle" θ_W through $\tan\theta_W = g_1/g_2$ [46], these relations can be written as

$$\begin{aligned} A_\mu &= \sin\theta_W W^3_\mu + \cos\theta_W B_\mu \ , \\ \mathrm{Z}_\mu &= \cos\theta_W W^3_\mu - \sin\theta_W B_\mu \ . \end{aligned} \tag{3.29}$$

Through the commutation relations $[Q, T^3] = [Q, Y] = 0$ we recognise that this implies both the photon and Z boson have neutral electric charge, and so we label the Z boson Z^0. Considering the other W gauge fields generated by T^1 and T^2 the commutation relations now give $[Q, T^1 \pm iT^2] = \mp(T^1 \pm iT^2)$, showing they hold electric charge. The W bosons are then

$$\mathrm{W}^\pm_\mu = \frac{1}{\sqrt{2}}(W^1_\mu \mp W^2_\mu) \ . \tag{3.30}$$

Looking at our Higgs covariant derivative in equation 3.17 we see that from interactions with this Higgs particle the gauge bosons acquire mass through (truncating to terms quadratic in the fields)

$$|D_\mu\phi|^2 = \frac{v^2}{8}\left(g_2^2 W^-_\mu W^{+\mu} + (g_1^2 + g_2^2) Z_\mu Z^\mu\right) + \dots \ , \tag{3.31}$$

where we can read off the masses as (using the definitions for the γ, Z, and W fields in equations 3.27, 3.28, and 3.30 respectively)

$$m_{\mathrm{W}} = \frac{1}{2} v g_2 \ , \quad m_{\mathrm{Z}} = \frac{1}{2} v \sqrt{g_1^2 + g_2^2} \ , \quad m_\gamma = 0 \ , \tag{3.32}$$

giving three massive gauge bosons and a massless photon exactly as expected.

Let us now consider these symmetries and concepts in a more realistic matter, where temperature dependence plays a role. Temperature dependence clearly plays a fundamental part in modelling the properties of the Universe, and the symmetries held by the Standard Model are obviously not exempt from that. Symmetry restoration at increasing temperature takes multiple forms, not least of which includes the Higgs mechanism breaking the electroweak $\mathrm{SU(2)_L \times U(1)_Y}$ to only the electromagnetic symmetry $\mathrm{U(1)_{em}}$ which was just discussed. Previously thought of as completely separate forces, the electromagnetic and weak force were shown to unify past the unification energy scale of 246 GeV (a temperature of about 10^{15} K) into a single force in the Standard Model by Glashow, Salam, and Weinberg. Indeed we could expect this sort of behaviour for all of the known forces of the Standard Model as the temperature rises further. Georgi and Glashow showed that for an SU(5) gauge group past about 10^{14} GeV (around 10^{27} K) [47], there could be the the unification of strong, weak, and electromagnetic forces known as the Grand Unified Theory (G.U.T.); obtention of such a theory being prized as a main objective of modern physics.

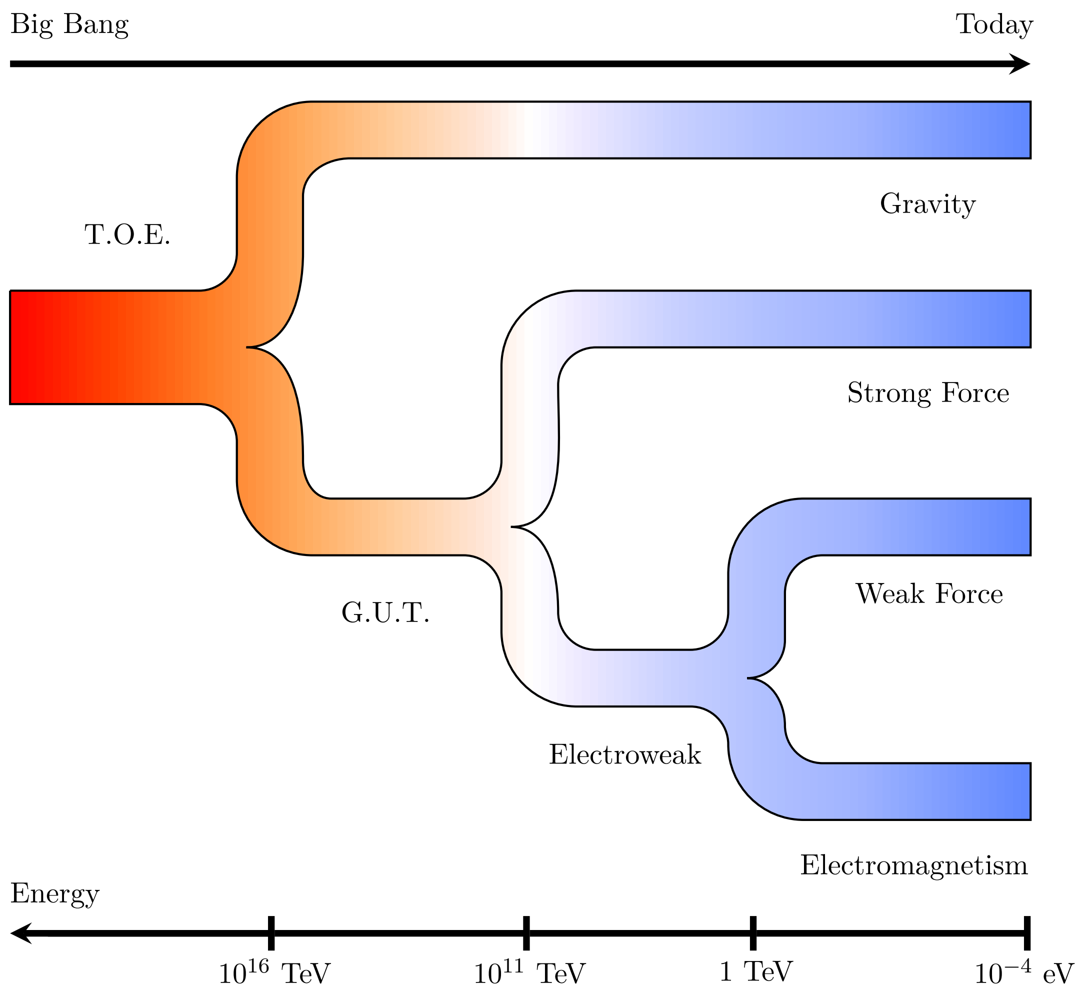

Figure 3.2: Energy scales and evolution of the fundamental forces, showing their possible unifications in the early Universe.

Moving past even that is the possibility of an all-encompassing "Theory of Everything" (T.O.E.) at extremely high temperatures which unifies all four forces into one fundamental force from which everything can be derived. These unifications and approximate energy scales are represented pictorially in figure 3.2.

We would like to look at what this temperature dependence could mean for the Higgs mechanism we explored previously then. To do so we shall have to branch out into quantum field theories at finite temperature known as thermal field theories, and so for full understanding we shall now take a look at the basics of these TFTs.

3.2.1 Thermal Field Theory

For field theories at finite temperature, everything is derived from the partition function $\mathcal{Z}$. The partition function is a quantity which effectively describes the probability of finding a system in a given state or the number of ways you can partition microstates, and in quantum field theory it is the generating functional of all correlation functions. In considering these types of field theories we must take into account not only the usual quantum fluctuations but also thermal fluctuations from interactions with the thermal "bath". The canonical partition function where the system can exchange heat with the thermal bath and is therefore a function of temperature is defined as

$$\mathcal{Z}(T) \equiv \mathrm{Tr}[e^{-\beta \hat{H}}] \; , \tag{3.33}$$

where $\beta = 1/T$ is the inverse temperature and $\hat{H}$ is the Hamiltonian of the system; the trace is taken over the full Hilbert space. We can therefore calculate expectation values of operators through

$$\langle \mathcal{O} \rangle = \frac{1}{\mathcal{Z}} \mathrm{Tr}[\mathcal{O} e^{-\beta \hat{H}}] \; , \tag{3.34}$$

with $\mathcal{Z}$ normalising the operator. If we think about the form for the partition function displayed in equation 3.33 we recognise that is appears very similarly to the form of the unitary operator $U = e^{-i\hat{H}t}$ in quantum field theory which describes how a system evolves in time. If we therefore consider this operator between two points in time $U(t_1, t_2) = e^{-i\hat{H}(t_1 - t_2)}$ and perform a Wick rotation (the process of transforming from Minkowski to Euclidean space by analytically continuing through $t \to -i\tau$) we see

$$U(\tau_1, \tau_2) = e^{-\hat{H}(\tau_1 - \tau_2)} = e^{-\beta \hat{H}} \; , \tag{3.35}$$

where β has been identified with the imaginary time difference. We can also explore what effects this sort of continuation would have on functions of interest such as the two-point correlator. Looking at the correlation between two operators at different spacetime points and inserting a complete set of states we find (using the cyclical nature of traces)

$$\begin{aligned} \langle \mathcal{O}(t_1, \mathbf{x}) \mathcal{O}(t_2, \mathbf{y}) \rangle &= \frac{1}{\mathcal{Z}} \mathrm{Tr}[\mathcal{O}(t_1, \mathbf{x}) e^{-\beta \hat{H}} e^{\beta \hat{H}} \mathcal{O}(t_2, \mathbf{y}) e^{-\beta \hat{H}}] \\ &= \frac{1}{\mathcal{Z}} \mathrm{Tr}[\mathcal{O}(t_1, \mathbf{x}) e^{-\beta \hat{H}} e^{i(-i\beta \hat{H})} \mathcal{O}(t_2, \mathbf{y}) e^{-i(-i\beta \hat{H})}] \\ &= \frac{1}{\mathcal{Z}} \mathrm{Tr}[\mathcal{O}(t_1, \mathbf{x}) e^{-\beta \hat{H}} \mathcal{O}(t_2 - i\beta, \mathbf{y})] \\ &= \langle \mathcal{O}(t_2 - i\beta, \mathbf{y}) \mathcal{O}(t_1, \mathbf{x}) \rangle \; , \end{aligned} \tag{3.36}$$

which demonstrates that the thermal field theory has temporal dimension compactified on a circle with circumference $\beta = 1/T$ due to the periodic boundary conditions in t_2 necessitated by equation 3.36. If we consider what this does to a Lagrangian, and taking the example of a real scalar field, we find when Wick rotating:

$$\mathcal{L} = \int d^4x \left(-\frac{1}{2}(\partial_t \phi)^2 + \frac{1}{2}(\partial_i \phi)^2 - V(\phi) \right) \tag{3.37}$$

$$\overset{t \to -i\tau}{=} i \int_0^\beta d\tau \int d^3x \left(\frac{1}{2}(\partial_\tau \phi)^2 + \frac{1}{2}(\partial_i \phi)^2 - V(\phi) \right) \tag{3.38}$$

$$= i \int d^4x \mathcal{L}_{\mathrm{E}} \ . \tag{3.39}$$

What we see therefore is that the implication of Wick rotating to obtain a thermal field theory is that we always go from a Minkowskian theory to a Euclidean theory, and the formalism of this technique is known as imaginary time formalism. Converting this then to the quantum field theory description, the generating functional as we previously called it can be written in Wick rotated imaginary time form as

$$\mathcal{Z} = \int \mathcal{D}\phi e^{-S_{\mathrm{E}}} = \int \mathcal{D}\phi \exp \left(-\int_0^\beta d\tau \int d^3x \mathcal{L}_{\mathrm{E}} \right) \tag{3.40}$$

where we have described it in path integral form. From this quantity then we may obtain the desired thermodynamic observables of the free energy F, the average energy E, and the entropy S through the standard relations of

$$\begin{aligned} F &= -T \log \mathcal{Z} \ , \\ E &= \frac{1}{\mathcal{Z}} \mathrm{Tr}[\hat{H} e^{-\beta \hat{H}}] \ , \\ S &= -\frac{\partial F}{\partial T} = \log \mathcal{Z} + \frac{1}{T\mathcal{Z}} \mathrm{Tr}[\hat{H} e^{-\beta \hat{H}}] = -\frac{F}{T} + \frac{E}{T} \ . \end{aligned} \tag{3.41}$$

In this work we will always use these quantities per unit volume through

$$f = \frac{F}{V} \ , \quad \rho = \frac{E}{V} \ , \quad s = \frac{S}{V} \ , \tag{3.42}$$

and so we can multiply the final relation in equations 3.41 by temperature and write the relation

$$w \equiv sT = \rho + p \ . \tag{3.43}$$

3.2.2 Effective Actions and Potentials

With some idea of how to extend quantum field theories to finite temperature, let us see if we can now calculate how higher orders in loops and thermal effects would alter the Higgs mechanism in the Standard Model, which was first studied in [48, 49, 50, 51]. First we will have to explore normal quantum one-loop corrections to get a feel of the machinery of calculating these intricate processes, and then we will move on to the thermal analogues.

To do this we shall need to look at the effective potential of the thermal situation, and so need to understand some details about quantum generating functionals. In a quantum field theory the generating functional determines correlation functions. There are multiple types of generating functional, with $Z[J]$ being the most fundamental type determining all correlation functions which is most closely related to the partition function; here $J(x)$ is the source to the dual operator $\phi(x)$. The other two we shall consider are $W[J]$ and $\Gamma[\phi]$. We can define $W[J]$ through its relation to $Z[J]$, and so is defined by

$$Z[J] \equiv e^{iW[J]} \ . \tag{3.44}$$

This functional contains the information of and generates the connected Green's functions, a subset of which that are important to us are the one-particle irreducible (1PI) Feynman diagrams which can have an internal line cut and still stay connected. Specifically, these 1PI diagrams are generated by the "effective action" $\Gamma[\phi]$ which takes into account quantum corrections to the classical action and is defined through a Legendre transform of the connected generating functional as [52]

$$\Gamma[\phi] \equiv W[J] - \int d^d x J(x)\phi(x) \ . \tag{3.45}$$

From this, the classical field or expectation value is found as

$$\langle \phi(x) \rangle_J = \frac{1}{Z[J=0]} \int \mathcal{D}\phi e^{iS + \int J(x)\phi(x) d^4 x} \phi(x) = \frac{\delta W[J]}{\delta J(x)} \ . \tag{3.46}$$

We start from the Green's functions which can be written in the suggestive form of the n-point correlation functions as

$$G^{(n)}(x_1, \ldots, x_n) = \frac{(-i)^n}{Z[0]} \frac{\delta}{\delta J(x_1) \ldots \delta J(x_n)} Z[J] \ . \tag{3.47}$$

From this we see that we can now expand the generating functional $Z[J]$ in a power series of J, to obtain its representation in terms of these n-point correlation functions (Green functions) as

$$Z[J] = Z[0] \sum_{n=0}^{\infty} \frac{i^n}{n!} \int dx_1 \ldots dx_n G^{(n)}(x_1, \ldots, x_n) J(x_1) \ldots J(x_n) \ ; \tag{3.48}$$

a similar thing can be done for $W[J]$ if we modify the correlation function to the connected Green's functions $G_c^{(n)}(x_1, \ldots, x_n)$ to give

$$iW[J] = \sum_{n=0}^{\infty} \frac{i^n}{n!} \int dx_1 \ldots dx_n G_c^{(n)}(x_1, \ldots, x_n) J(x_1) \ldots J(x_n) \ . \tag{3.49}$$

Finally we can extend this perturbative expansion to the effective action by now expanding in powers of $\bar{\phi}$ and considering the one-particle irreducible (1PI) Green's functions $\Gamma^{(n)}(x_1, \ldots, x_n)$ which are defined through

$$\Gamma^{(n)}(x_1, \ldots, x_n) = \frac{\delta}{\delta\bar{\phi}(x_1)} \cdots \frac{\delta}{\delta\bar{\phi}(x_n)} \Gamma[\phi] \tag{3.50}$$

to give

$$\Gamma[\bar{\phi}] = \sum_{n=0}^{\infty} \frac{1}{n!} \int dx_1 \ldots dx_n \Gamma^{(n)}(x_1, \ldots, x_n) \bar{\phi}(x_1) \ldots \bar{\phi}(x_n) \ . \tag{3.51}$$

Specifically, these Green's functions encode the 1PI n-point correlation functions due to

$$\langle \phi(x_1) \ldots \phi(x_n) \rangle_{\text{1PI}} = \Gamma^{(n)}(x_1, \ldots, x_n) \Big|_{J=0} \ . \tag{3.52}$$

To define the effective potential we will need the effective action in terms of momentum, so we will Fourier transform $\Gamma^{(n)}(x_1, \ldots, x_n)$ as

$$\Gamma^{(n)}(x_1, \ldots, x_n) = \int \prod_{i=1}^{n} \left(\frac{d^4 p_i}{(2\pi)^4} e^{i p_i x_i} \right) \Gamma^{(n)}(p_1, \ldots, p_n) (2\pi)^4 \delta^{(4)} \left(p_1 + \ldots + p_n \right) \ . \tag{3.53}$$

Combining this with equation 3.51 allows us to find the effective action in terms of momenta as

$$\Gamma[\bar{\phi}] = \sum_{n=0}^{\infty} \frac{1}{n!} \int \prod_{j=1}^{n} \left(d^4 x_j \bar{\phi}(x_j) \right) \int \prod_{i=1}^{n} \left(\frac{d^4 p_i}{(2\pi)^4} e^{i p_i x_i} \right) \Gamma^{(n)}(p_1, \ldots, p_n) (2\pi)^4 \delta^{(4)} \left(p_1 + \ldots + p_n \right) \ . \tag{3.54}$$

Using the definition of the delta function in momentum space

$$\delta^{(4)} \left(p_1 + \ldots + p_n \right) = \int \frac{d^4 x}{(2\pi)^4} e^{-i(p_1 + \ldots + p_n) x} \tag{3.55}$$

instead gives

$$\Gamma[\bar{\phi}] = \sum_{n=0}^{\infty} \frac{1}{n!} \int d^4 x \int \prod_{j=1}^{n} \left(d^4 x_j \bar{\phi}(x_j) \right) \int \prod_{i=1}^{n} \left(\frac{d^4 p_i}{(2\pi)^4} e^{i p_i (x_i - x)} \right) \Gamma^{(n)}(p_1, \ldots, p_n) \ , \tag{3.56}$$

and then using a similar definition for the delta function in position space

$$\delta^{(4)} \left(x_i - x \right) = \int \frac{d^4 p_i}{(2\pi)^4} e^{i(x_i - x) p_i} \tag{3.57}$$

collapses all integrals except one to leave

$$\Gamma[\bar{\phi}] = \sum_{n=0}^{\infty} \frac{1}{n!} \int d^4 x \bar{\phi}^n(x) \Gamma^{(n)}(p_1, \ldots, p_n) \ . \tag{3.58}$$

The effective action may also be expanded in a derivative expansion in powers of the external momenta around where all external momenta are zero [53] (which will be useful later) as

$$\Gamma[\bar{\phi}] = \int d^4 x \left(-V_{\text{eff}}(\bar{\phi}) + \frac{1}{2} Z(\bar{\phi}) \partial_\mu \phi \partial^\mu \phi + \ldots \right) \ , \tag{3.59}$$

where $Z(\bar{\phi})$ is the kinetic term field renormalisation function which only takes the classical value of one in the tree-level approximation (for perturbative calculations of this quantity see [54, 55, 56]); this is defined in Minkowski signature. From these definitions then we can immediately see that the effective potential V_{eff} for a constant field $\bar{\phi}$ is

$$\Gamma[\bar{\phi}] = -\int d^4x V_{\text{eff}}(\bar{\phi}) \ . \tag{3.60}$$

Now we make the recognition that since equation 3.59 is expanded where the external momentum is zero if we consider a similar setup for equation 3.58 we may be able to perform term-by-term matching to obtain an expression for the effective potential. Expanding equation 3.58 around zero momentum then gives (showing first term only)

$$\Gamma[\bar{\phi}] = \sum_{n=0}^{\infty} \frac{1}{n!} \int d^4x \{\Gamma^{(n)}(0, \ldots, 0)\bar{\phi}^n(x) + \ldots\} \ , \tag{3.61}$$

and so we can easily see match the effective potential with this initial term by comparing 3.59 and 3.61 to give

$$V_{\text{eff}} = -\sum_{n=0}^{\infty} \frac{1}{n!} \Gamma^{(n)}(0, \ldots, 0)\bar{\phi}^n \ . \tag{3.62}$$

With this in hand, we can now look into loop corrections. We stress here that we perform these calculations in a perturbative setting as it is necessary for conventional quantum field theory, however this is not the only way. Indeed, later on we shall examine the effective potential in a non-perturbative sense using holography. We can also briefly mention the $1/N$ expansion which is present for perturbation theory, and will have a role in our holographic discussions later. For theories with internal symmetry groups such as $\mathrm{O}(N)$ and $\mathrm{SU}(N)$ (with rank N) we may explicitly introduce the factor $1/N$ into the self interaction term and consider the large-N limit, in which we have treated N as a free parameter. Perturbatively, we will find Feynman diagrams which generate factors of N to cancel these appearances of $1/N$ as well as diagrams which retain overall factors of $1/N$ and higher orders in this parameter; in the limit $N \to \infty$ however only the $\mathcal{O}(N^0)$ contributions will remain. More realistically, for a physical theory such as QCD where the number of colours is known and finite these terms in increasing orders of $1/N$ will not disappear, and will instead act as the perturbation series around which the quantum field theory can be expanded.

The zero-loop effective potential is simply the tree-level potential we already have for the Higgs, which we shall modify slightly for nicer results to

$$V(\phi) = \frac{1}{2}\mu^2\phi^2 + \frac{\lambda}{4!}\phi^4 \ , \tag{3.63}$$

$$\sum_{n=1}^{\infty}\Gamma^{(2n)}(0,\ldots,0) = \Gamma^{(2)}(0,0) + \Gamma^{(4)}(0,\ldots,0) + \Gamma^{(6)}(0,\ldots,0) + \Gamma^{(8)}(0,\ldots,0) + \ldots$$

$=$ 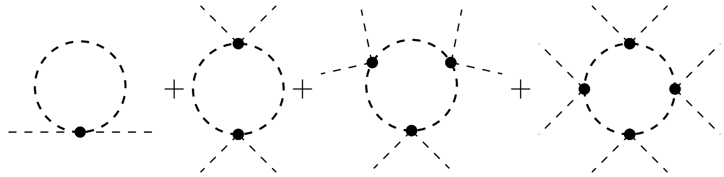 $+\ldots$

Figure 3.3: Summation of all contributing 1PI Feynman diagrams, where dashed lines correspond to scalar propagators and dots correspond to ϕ^4 interaction vertices.

so for more insight into the effects of V_{eff} we need to go to higher loop orders. The one loop correction to the potential will be all contributions from one-particle irreducible Feynman diagrams which we need to sum, and specifically as this theory has $\mathbb{Z}_2$ symmetry we need only consider diagrams with an even number of external legs, as depicted in figure 3.3.

Scalar Feynman Rules			
	Zero Temperature	Finite Temperature	
Scalar Propagator	$\frac{i}{p^2-m^2+i\epsilon}$, $p^\mu = (p^0, \vec{p})$	$\frac{i}{p^2-m^2+i\epsilon}$, $p^\mu = (\omega_n, \vec{p})$	
Vertex Function	$(2\pi)^4\delta^{(4)}(p_i)$	$-i\beta(2\pi)^3\delta^{(3)}(\vec{p}_i)\delta(\omega_i)$	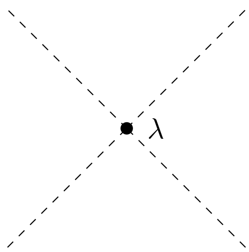
Loop Integral	$\int \frac{d^4p}{(2\pi)^4}$	$iT\sum_{n=-\infty}^{\infty}\int\frac{d^3p}{(2\pi)^3}$	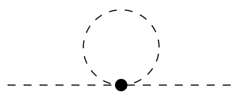

Figure 3.4: Feynman rules for a scalar particle with ϕ^4 interaction.

This can be represented formulaically as

$$\Gamma^{(2n)}(0,\ldots,0) = \frac{(2n)!}{2n}\int\frac{d^4p}{(2\pi)^4}\left[\left(\frac{-i\lambda}{2}\right)\frac{i}{p^2-m^2+i\epsilon}\right]^n , \tag{3.64}$$

where each part comes from the Feynman rules at zero-temperature laid out in figure 3.4. Specifically, the factor of $(2n)!$ comes from the combinatorics of distributing $2n$ particles in $2n$ external lines; the factor of $1/2n$ is a symmetry condition accounting for indistinguishable rotations and reflections; the integral is a consequence of having to account for loop momentum; each vertex contributes a factor of $-i\lambda/2$ (accounting for symmetry of exchanging two external lines); and finally each propagator contributes a factor of $(i/(p^2 - m^2 + i\epsilon))$. Inserting this expression in to the form for the effective potential we found before in equation 3.62 we see that to one loop this is

$$\begin{aligned} V_{\text{one-loop}} &= i\sum_{n=1}^{\infty}\int \frac{d^4p}{(2\pi)^4}\frac{1}{2n}\left[\frac{\lambda\bar{\phi}^2/2}{p^2 - m^2 + i\epsilon}\right]^n \\ &= -\frac{i}{2}\int \frac{d^4p}{(2\pi)^4}\log\left[1 - \frac{\lambda\bar{\phi}^2/2}{p^2 - m^2 + i\epsilon}\right] , \end{aligned} \tag{3.65}$$

where in the second line we have used the relation $\log(1-x) = -\sum_{n=0}^{\infty}\frac{x^n}{n}$. We now note that the field-dependent effective mass can be defined through the second derivative of the tree-level potential eq. 3.63, which gives

$$m_{\text{eff}}^2 = \mu^2 + \frac{\lambda\bar{\phi}^2}{2} . \tag{3.66}$$

We can insert this (recognising that $\mu^2 = -m^2$ here) and Wick rotate for the one-loop Coleman-Weinberg potential of

$$V_{\text{CW}} = \frac{1}{2}\int \frac{d^4p_E}{(2\pi)^4}\log(p_E^2 + m_{\text{eff}}^2(\bar{\phi})) - \frac{1}{2}\int \frac{d^4p_E}{(2\pi)^4}\log(p_E^2 + m^2) , \tag{3.67}$$

where only the first term has any dependence upon the field.

These tools we have learned lead us nicely into promoting these arguments to thermal considerations. We will simplify to considering just the neutral component of the Higgs doublet (now labelled ϕ) with the same dynamics and potential as before and see if we can calculate the effective potential in this case. For the thermal case new Feynman rules can be calculated, now for Euclidean QFT in periodic imaginary time (which has a relation to temperature as previously discussed). In this formalism (known as the Matsubara formalism [57]) instead of continuous values for the momenta there will be a discrete spectrum. The Feynman rules generated from this approach are shown in fig. 3.4, and applying these translates eq. 3.65 into

$$V_{\text{one-loop}}^{\beta} = \frac{T}{2}\int \frac{d^3p}{(2\pi)^3}\sum_{n=-\infty}^{\infty}\log(\omega_n^2 + \omega^2) \tag{3.68}$$

with $\omega^2 = \vec{p}^2 + m_{\text{eff}}^2(\bar{\phi})$. If we just instead consider a function and its derivative

$$f(\omega) = \sum_{n=-\infty}^{\infty}\log(\omega_n^2 + \omega^2) , \quad \frac{\partial f(\omega)}{\partial\omega} = \sum_{n=-\infty}^{\infty}\frac{2\omega}{\omega_n^2 + \omega^2} , \tag{3.69}$$

we can use the definition for Bosonic Matsubara modes $\omega_n = 2\pi n\beta^{-1}$ (which describe the poles of the Bose-Einstein distribution) to write

$$\frac{\partial f(\omega)}{\partial\omega} = \frac{2\beta}{\pi}\left(\frac{1}{2} + \sum_{n=1}^{\infty}\frac{\tilde{\omega}}{n^2 + \tilde{\omega}^2}\right) , \tag{3.70}$$

where $\tilde{\omega} = \beta\omega/2\pi$. The sum is well-defined and has a closed form representation as

$$\sum_{n=1}^{\infty} \frac{a}{a^2+n^2} = -\frac{1}{2a} + \frac{\pi}{2} + \frac{\pi e^{-2\pi a}}{1-e^{-2\pi a}} \ , \tag{3.71}$$

which we can plug-in to our expression 3.70 along with the definition for $\tilde{\omega}$ to find

$$\frac{\partial f(\omega)}{\partial \omega} = 2\beta \left(\frac{1}{2} + \frac{e^{-\beta\omega}}{1-e^{-\beta\omega}} \right) \ . \tag{3.72}$$

An integration of this gives us the relation (replacing $\beta = 1/T$ sporadically and ignoring the ω independent constant)

$$\sum_{n=-\infty}^{\infty} \log(\omega_n^2 + \omega^2) = \frac{2}{T} \left[\frac{\omega}{2} + T \log(1 - e^{-\beta\omega}) \right] \ , \tag{3.73}$$

which we can enter into equation 3.68 to find the one-loop thermal effective potential as

$$V(\bar{\phi})_T = \int \frac{d^3p}{(2\pi)^3} \left[\frac{E_p}{2} + T \log(1 - e^{-\beta E_p}) \right]_{E_p = \sqrt{\vec{p}^2 + m_{\text{eff}}^2} = \left|\sqrt{\omega^2}\right|} \ . \tag{3.74}$$

This thermal one-loop part can be split up into two sections then, the temperature independent vacuum energy density which we define as $J_0(m_{\text{eff}}) = \int E_p/2$ and the thermal part $J_T(m_{\text{eff}}) = \int T \log(1 - e^{-\beta E_p})$ so the thermal corrections to the effective potential are

$$V(\bar{\phi})_T = J_0(m_{\text{eff}}) + J_T(m_{\text{eff}}) \ , \tag{3.75}$$

where it can be readily identified that the temperature independent part is precisely what we found for the zero-temperature one-loop corrections. The integral for the temperature dependent part can be recast in spherical form with the substitution $x = p/T$ and angular dependence integrated out as

$$J_T(m_{\text{eff}}) = \frac{T^4}{2\pi^2} \int_0^{\infty} dx\, x^2 \log\left[1 - e^{-\sqrt{x^2+y^2}}\right]_{y = \frac{m_{\text{eff}}}{T}} \ , \tag{3.76}$$

which has the large temperature (with respect to mass) expansion of

$$J_T(m_{\text{eff}}) = -\frac{\pi^2 T^4}{90} + \frac{m_{\text{eff}}^2 T^2}{24} - \frac{m_{\text{eff}}^3 T}{12\pi} - \frac{m_{\text{eff}}^4}{2(4\pi)^2} \left[\log\left(\frac{m_{\text{eff}} e^{\gamma_E}}{4\pi T} \right) - \frac{3}{4} \right] + \dots \ . \tag{3.77}$$

Inputting the equivalence of effective mass $m_{\text{eff}}^2 = \mu^2 + \lambda\bar{\phi}^2/2$ we therefore see that the finite temperature one-loop thermal corrections to the effective potential can be written with the tree-level potential as

$$V_{\text{eff}} = V_{\text{tree}}(T=0) + V_T = \frac{1}{2} \left(\mu^2 + \frac{\lambda T^2}{4!} \right) \bar{\phi}^2 + \lambda\bar{\phi}^4 + \dots \ , \tag{3.78}$$

and so we can see that at high temperatures the thermal contributions to the effective potential will dominate and the expectation value will be zero, but as the temperature decreases the symmetry will be spontaneously broken past the critical temperature T_c which is defined through

$$T_\mathrm{c}^2 = -\frac{4!\mu^2}{\lambda} \ , \tag{3.79}$$

and past this point the system will develop an expectation value of v.

We also know that the effective potential is intimately linked to the free energy of the system. In fact, the equation of state can be found through

$$f = -g_\mathrm{eff}\frac{\pi^2}{90}T^4 + V_T(\phi) \tag{3.80}$$

$$\rho = g_\mathrm{eff}\frac{3\pi^2}{90}T^4 + V_T(\phi) - T\frac{\partial V(\phi, T)}{\partial T} \ , \tag{3.81}$$

where g_eff is the effective number of relativistic degrees of freedom present in the Universe at the temperature T; this is an important quantity, as it can change greatly as the temperature drops due to expansion. For the Standard Model, this quantity is given through

$$g_\mathrm{eff}(T) = \sum_\mathrm{bosons} g_b \left(\frac{T_b}{T}\right)^4 + \frac{7}{8}\sum_\mathrm{fermions} g_f \left(\frac{T_f}{T}\right)^4 \ , \tag{3.82}$$

which is separated into two parts to represent the contributions of degrees of freedom from bosons and fermions. In both terms we see a temperature dependence (T_b for each boson and T_f for each fermion), which takes into account whether particles are relativistic or not compared to the thermal bath of photons in which they are submerged.

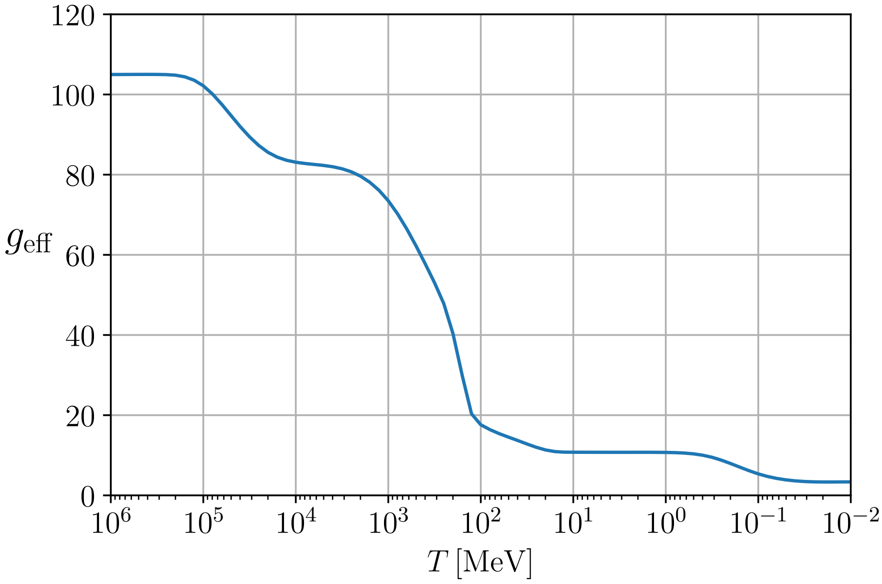

Figure 3.5: The evolution of the Standard Model degrees of freedom as temperature decreases in the Universe, produced by a cubic spine of the data provided in Ref. [1] found through lattice methods.

In figure 3.5 we plot this dependency upon temperature, showing how the degrees of freedom decrease as temperature drops in the early Universe towards times closer to present day. We see for instance that above the value of the top quark mass ($m_t = 173$ GeV) all particles are relativistic and therefore we have the maximum degrees of freedom (for known particles).

So now we see that indeed in the early Universe when temperatures were high the electroweak symmetry would be restored, and subsequently as the Universe expanded and cooled this would be broken through a phase transition from symmetric to broken phase. This leaves one very large question though: what type of transition would the Universe undergo from this process? Depending on the shape of our potential the transition would fall into one of two categories: in second-order transitions the phase transits continuously from one state to another as the temperature decreases maintaining the $\mathbb{Z}_2$ symmetry throughout, whereas for first-order phase transitions the phase jumps abruptly and discontinuously from one state to the other with the potential retaining $\mathbb{Z}_2$ symmetry only for $T = 0$ and $T \gg T_\mathrm{c}$.

To explore this we need to include higher order terms from 3.77. Going to the next order, we have a cubic in m_eff. If we momentarily consider the limit in which the tree-level Higgs potential has zero mass (*i.e.* $\mu^2 \to 0$) we see that this gives an effective potential of

$$V_\mathrm{eff} = \frac{1}{2}\left(\frac{\lambda T^2}{4!}\right)\bar{\phi}^2 - \frac{T}{12\pi}\left(\frac{\lambda}{2}\right)^{3/2}|\bar{\phi}|^3 + \lambda\bar{\phi}^4 + \ldots\ , \tag{3.83}$$

and we recognise that the appearance of a cubic term with an opposite sign may indeed be able to cause the potential barrier necessary to facilitate a first-order phase transition. This would have far-reaching consequences.

In figure 3.6 we see the differences in the potential for a first- and second-order transition. At the critical temperature T_c the minimum is still just at $\phi = 0$ for the second-order transition, and below that temperature a new minimum develops which is further from the origin that the field rolls to, generating an expectation value and providing mass. For the first-order transition however at the critical temperature there are two degenerate minima separated by a potential barrier. Lowering the temperature further, the minimum not located at the origin becomes the “true” minimum of the potential which would be most energetically stable. For the field stuck at the “false” minimum at the origin blocked by the hurdle there are but two options: thermally fluctuate over or quantum mechanically tunnel through the potential barrier.

Let us examine what this would mean in practice for the physical situation of the Higgs scalar undergoing a first-order phase transition. At high temperatures the Higgs field will

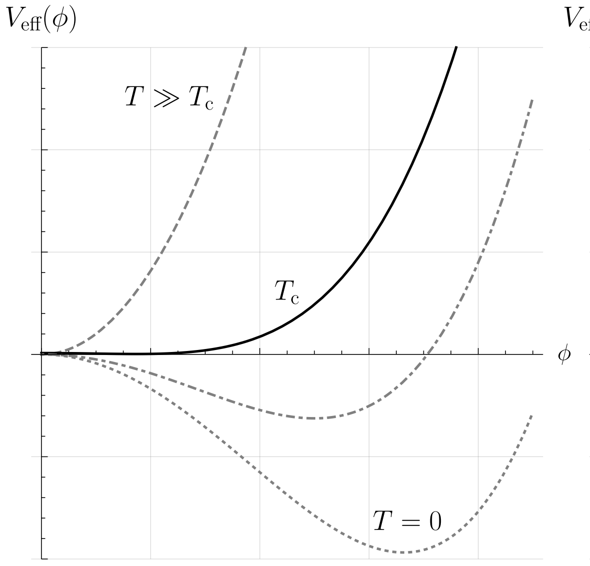

(a) Second-Order Transition

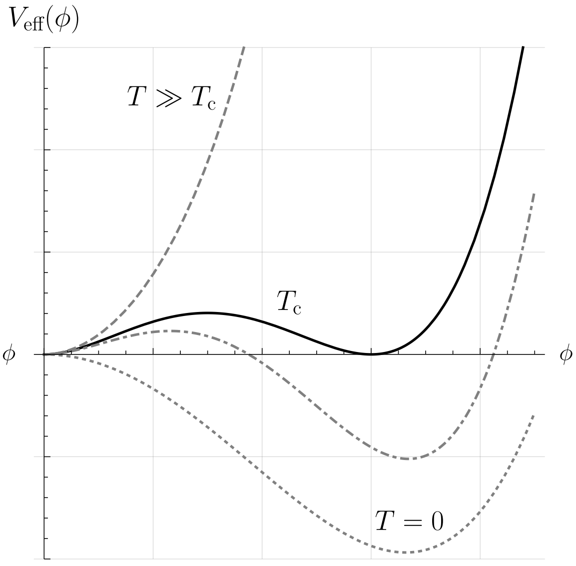

(b) First-Order Transition

Figure 3.6: The progression of the effective potential as the temperature is lowered for a first and second order phase transition. The second-order transition can be compared to figure 3.1 as taking a 2D "slice" of the 3D potential plot, with the $T = 0$ curve corresponding to the spontaneously broken case with $m^2 > 0$ and the $T \gg T_{\rm c}$ corresponding to the symmetric $m^2 < 0$ case, exemplified by the dominance of each term in the $\bar{\phi}^2$ coefficient in equation 3.78 for the respective regimes.

be in a symmetric potential with only one minimum at $\phi = 0$, producing an expectation value of $\langle\phi\rangle = 0$ as $v = 0$. Due to this, we see from equation 3.32 that no other particle will gain mass and it is only the Higgs boson which will be massive. As the temperature lowers a new "meta-stable" minimum appears, which is a false vacuum state compared to the true ground state. At the critical temperature this minimum becomes equally as energetically stable as at $\phi = 0$; both states are now true vacuum states. Below $T_{\rm c}$ the minimum at $\phi = 0$ is now the metastable vacuum with the other minimum being the true vacuum. In this configuration it is possible for the field to overcome the barrier, and so eventually a phase transition will occur as the field jumps from the symmetric minimum to broken minimum. The presence of a potential barrier dictates that when this process transpires a bubble of the new, true vacuum state phase will form which will be enveloped by the false vacuum state; a bubble domain wall will emerge as an interface between the two phases. For the Higgs scalar transitioning to the broken phase an expectation value is now obtained exactly as previously discussed, and so inside these bubbles particles acquire mass from the Higgs field. The nucleation, growth, and collision of these bubbles would therefore convert the Universe from a massless state to a massive one in a hugely energetic process.

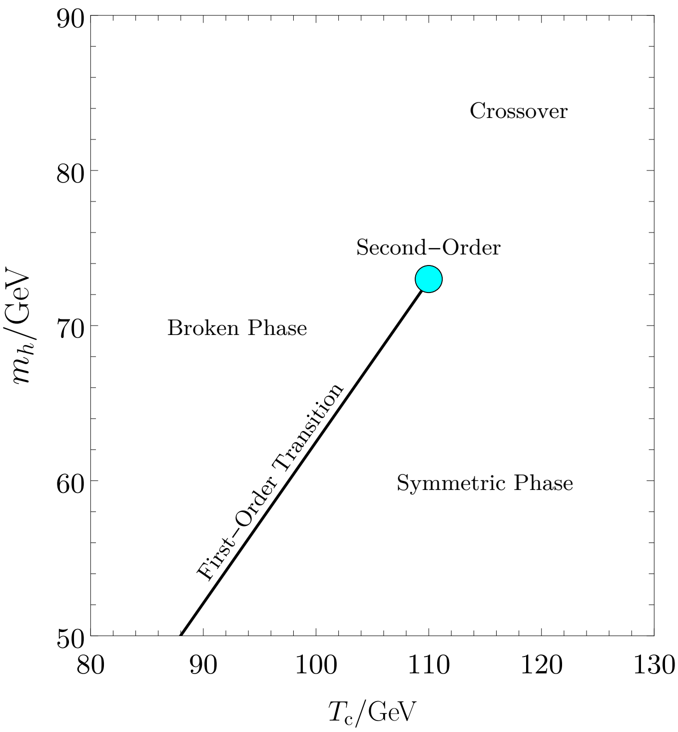

Figure 3.7: The phase diagram of the Standard Model Higgs showing the regions of symmetric phase, broken phase, and the regions where different transitions will occur.

Here we must be careful then; does the cubic term in equation 3.83 dictate that there *must* be a first-order phase transition? The quick answer is no. Although a cubic term may indeed allow for a first-order transition, it does not necessitate it; the interplay between coefficients in the effective potential will instead determine what type of transition the electroweak symmetry breaking process will go through and so needs more detailed analysis. We can frame this analysis instead as a consideration of the ratio of Higgs mass to the W-boson mass (which we consider as $m_{\mathrm{W}} \simeq 80$ GeV) at various temperatures. If the ratio of the two is small ($\lesssim \mathcal{O}(1)$), then the perturbative evaluation of the thermal potential we just carried out is reasonably accurate and we find that there is indeed a first-order phase transition. If we try to extend this perturbative analysis further (*i.e.* for heavier Higgs masses which push the ratio past $\mathcal{O}(1)$) we find that the perturbative analysis breaks down due to Linde's problem [58] which occurs as the gauge bosons that are light near the EW symmetric phase cause the high temperature expansion parameter becomes of the order of unity. However from lattice simulations we know [10, 59, 60, 61, 62] that as the ratio increases past $\mathcal{O}(1)$ the strength of the transition will decrease eventually to zero at a critical point, after which the transition is second-order and then a crossover. For the Higgs mass at zero-temperature the critical point will be at around 80 GeV, and so the experimentally determined Higgs mass value of 125 GeV would mean that the Standard Model electroweak phase transition would fall firmly into the crossover region and no first-order transition would occur. In figure 3.7 we have plotted the phase diagram detailing where transitions would be first-order, second-order, or crossovers depending on the mass of the Higgs and the critical temperature.

3.2.3 Beyond the Standard Model Theories and Their Necessity

As we have seen, in the formulation of the Standard Model the electroweak phase transition will undoubtedly be a crossover, no bubbles will be formed, and mass in the Universe will be switched on smoothly and continuously. In many ways this would be a disappointing conclusion for observational prospects; the energy release in bubble nucleation and collision which would be present in first-order transitions and could leave a lasting observational signature would be absent in this crossover case.

All is not lost in hoping these processes may still occur though, in fact we have numerous reasons as to why we believe we would recover first-order electroweak transitions in the physical Universe. To understand these, let us quickly re-examine some points of the Standard Model. As we stated when we started this chapter, the Standard Model in its current formulation is a marvel of theoretical ideas from large swathes of physical understanding which have been masterfully pieced together, and the level of experimental scrutiny it has stood up to is virtually unparalleled. But it is incomplete. First and foremost the Standard Model is fundamentally incompatible with General Relativity, a theory which shares a similar level of prestige in its ability to stand up to scrutiny; any attempt to renormalise General Relativity in a quantum field theoretic way inexorably leads to infinites which dictate the conclusion that it is a non-renormalisable [63, 64] (however the SM can be made into a theory with the symmetries of GR). In addition to this, the inability for the Standard Model to supply any realistic particle candidate for dark matter (except for the neutrinos, which still could only account for a fraction [65] and whose masses the Standard Model fails to account for as well) or provide any explanation for dark energy (the unknown form of energy that affects the expansion of the Universe) which together constitute 95% of the total energy content leaves our knowledge of the majority of the Universe severely lacking (see Ref. [66] for a succinct review with a large list of references). Yet another large hole in the particle content of the Standard Model is the lack of significant amounts of antimatter. The Standard Model predicts that matter and antimatter should be produced at relatively similar rates and yet we observe a huge dominance of matter over antimatter with no mechanism of explaining this asymmetry [67, 68, 69]. These are but a few of the shortcomings of the Standard Model; a more comprehensive study can be found in Ref. [70].

This long list of unexplained phenomena strongly motivates exploring Beyond the Standard Model (BSM) theories which come in various classes and extend the Standard Model in one particular way or another. They can appear as simple extensions to the scalar sector, in which either new singlets [71, 72, 73, 74, 75] or doublets [76, 77, 78, 79] are added which allow for strongly first-order transitions, or through strongly coupled sectors leading to areas such as composite Higgs (see [80] for an overview). For example in the well-known Minimally Supersymmetric Standard Model (MSSM) the cubic term in the finite temperature effective potential is modified to be much larger through the thermal loops of new bosonic modes of the light scalar supersymmetric top quark (stop) [81, 82].

A further class of extensions are the effective field theory models. In these cases, new physics and degrees of freedom can be added at a scale not in the region of the electroweak transition, and the effects studied through means of effective field theories. Higher orders in powers of the Higgs field can be added such as in the Standard Model Effective Field Theory [83, 84, 85] where these operators will be suppressed by the scale at which the new physics is at. For instance, a dimension-6 operator (introduced by a ϕ^6 term in the potential) could be sourced by strongly coupled gravity [86].

A final set of extensions that we shall mention are ones arising from non-standard numbers of spatial dimensions *i.e.* warped extra-dimensional models such as in Refs. [87, 88, 89, 90, 91, 92]. These can provide well-motivated reasons for exploring theories with higher dimensions such as the ability to produce strongly first-order transitions and also solve other large discrepancies such as the hierarchy problem [93]. In these the radion (a scalar produced from the five-dimensional part of the metric) undergoes a phase transition which can trigger electroweak symmetry breaking in a first-order way.

What we can take from all these ways that there could realistically be a first-order phase transition in the early Universe is that it is indeed well-motivated to continue on probing what the Universe would look like if one had occurred; not only is it conceivable but the possible relics left over from their existence would be tantalisingly rich in new ways to explore physics. This seems like an avenue that should not be ignored, and so we continue under the assumption that a first-order phase transition will occur for the electroweak symmetry from an unspecified mechanism.

3.3 Phase Transition Dynamics

As previously stated, in a finite temperature setup of a first-order transition past the critical temperature the most energetically stable minimum will be the one separated from the field by a potential barrier. This will in turn precipitate either a thermal fluctuation [94, 95] or quantum tunnelling [96, 97] to the more favourable state; the choice of which will have an effect on the dynamics of the situation and so therefore this needs to be understood. To study the dynamics of this sort of electroweak phase transition then we will consider a situation with a single scalar field which provides contributions to energy-momentum through

$$T_{\mu\nu} = \partial_\mu \phi \partial_\nu \phi - g_{\mu\nu} \left(g^{\alpha\beta} \partial_\alpha \phi \partial_\beta \phi + V(\phi) \right) \ . \tag{3.84}$$

From our previous section we know we can construct the effective action in the Euclidean metric for our situation, which in 4-dimensions and to first-order in derivatives is

$$\Gamma(\psi, T) = N^2 \int_0^\beta d\tau \int_0^\infty d^3x \left(\frac{1}{2} Z(\psi) \partial_\mu \psi \partial^\mu \psi + V(\psi) \right) \ , \tag{3.85}$$

where $V(\psi)$ and $Z(\psi)$ are the (as before) effective potential and non-canonical kinetic function respectively. As we are considering field solutions which exist at the critical points of the potential (specifically the minima) we are therefore searching for semiclassical Euclidean instanton solutions which solve the quantum equations of motion from the effective action, with different bubble type solutions coming from high and low temperature limits influencing the boundary conditions in the imaginary time dimension.

When the temperature is identically zero we have exact O(4) symmetry; this is due to $\beta = \frac{1}{T} \xrightarrow{T \to 0^+} \infty$ causing the infinite Euclidean time direction to act exactly the same as the spatial directions. Tunnelling through the barrier in this case will be solely by quantum fluctuations. We can write the coordinates as a single quantity through $\rho = \sqrt{\tau^2 + x^i x_i}$ and integrate as a three-sphere S^3 to find the effective action of an O(4) bubble as

$$\Gamma_{\mathrm{O}(4)} = 2\pi^2 N^2 \int_0^\infty d\rho \, \rho^3 \left(\frac{1}{2} Z(\psi) \left(\frac{d\psi}{d\rho} \right)^2 + V(\psi) \right) \ , \tag{3.86}$$

with the field obeying the equations of motion of the form

$$\frac{d^2\psi}{d\rho^2} + \frac{3}{\rho} \frac{d\psi}{d\rho} + \frac{1}{2} \frac{\partial_\psi Z(\psi)}{Z(\psi)} \left(\frac{d\psi}{d\rho} \right)^2 - \frac{\partial_\psi V(\psi)}{Z(\psi)} = 0 \ . \tag{3.87}$$

Very low but non-zero temperatures will also obey solutions of this form to a good approximation.

Conversely for very large temperatures our Euclidean time direction is compactified on a circle and we lose the inherent 4d rotational symmetry, reducing to only O(3) rotational symmetry. The tunnelling present in this case will instead be overwhelmingly dominated by thermal fluctuations, producing a much more classical effect. This allows us to integrate over our imaginary time coordinate, define the field dependence now as $\rho = \sqrt{x^i x_i}$ and integrate as a two-sphere S^2 to write the action as

$$\Gamma_{\mathrm{O}(3)} = \frac{4\pi N^2}{T} \int_0^\infty d\rho \, \rho^2 \left(\frac{1}{2} Z(\psi) \left(\frac{d\psi}{d\rho} \right)^2 + V(\psi, T) \right) \,, \tag{3.88}$$

which minimising now gives the equation of motion for the bubble solution as

$$\frac{d^2\psi}{d\rho^2} + \frac{2}{\rho}\frac{d\psi}{d\rho} + \frac{1}{2}\frac{\partial_\psi Z(\psi)}{Z(\psi)} \left(\frac{d\psi}{d\rho} \right)^2 - \frac{\partial_\psi V(\psi)}{Z(\psi)} = 0 \,. \tag{3.89}$$

The final possible configuration is at finite but not "very large" temperatures, which will be the majority of interesting solutions. Here the instanton solution interpolates between the two limiting cases mentioned previously and enjoys the symmetry of neither.

When solving for the field profile of these cases the necessary boundary conditions are

$$\left. \frac{d\psi(\rho)}{d\rho} \right|_{\rho=0} = 0 \quad \text{and} \quad \lim_{\rho \to \infty} \psi(\rho) = \psi_0 \,, \tag{3.90}$$

where ψ_0 is the value of the field in the symmetric phase. In practice we will always normalise the location of this minimum to be at the origin and so $\psi_0 = 0$.

As the majority of cases will be of the last type mentioned ("hybrid" solutions with both quantum and thermal methods for the field to overcome the barrier) we must decide which will be the dominant contribution to the vacuum decay. This is found through which method has the largest probability of occurring, *i.e.*

$$p(t) = \max \left[p_{\mathrm{O}(4)}, p_{\mathrm{O}(3)} \right] \,, \tag{3.91}$$

where $p_{\mathrm{O}(4)}$ is the probability for an O(4) bubble to nucleate through quantum tunnelling and $p_{\mathrm{O}(3)}$ is the probability for an O(3) bubble to nucleate through thermal fluctuation. As these probabilities can be expressed as

$$p_{\mathrm{O}(4)} \propto e^{-\Gamma_{\mathrm{O}(4)}} \quad \text{and} \quad p_{\mathrm{O}(3)} \propto e^{-\Gamma_{\mathrm{O}(3)}} \tag{3.92}$$

this translates to the condition

$$\Gamma(t) = \min \left[\Gamma_{\mathrm{O}(4)}, \Gamma_{\mathrm{O}(3)} \right] \,, \tag{3.93}$$

and so this must always be checked and taken into consideration when calculating quantities derived from $\Gamma(t)$.

With our knowledge about the phase transitions we will be encountering complete we now want to see how these could be observed in the form of the gravitational waves they would produce and their dependence upon the particularities of the transition.

Chapter 4

Gravitational Waves

Gravitational waves were first predicted by Poincaré in 1905 [98], and then by Einstein as a consequence of his theory of general relativity in 1916 [99]. These are caused by the disturbances of spacetime, and although all massive accelerating bodies produce them, the signals from all but the most energetic processes are very weak. This extreme energy needed to distort spacetime means they are produced by either large masses interacting or during intensely energetic processes. The possibilities to produce gravitational waves are therefore quite large, and although we are mainly concerned with the nucleation and collision of Higgs bubbles other interesting processes can be explored such as their production from preheating at the end of inflation (see *e.g.* [100, 101, 102, 103] for inflation and *e.g.* [104, 105, 106, 107, 108, 109, 110, 111] for phase transitions with bubbles).

4.1 The Applications of General Relativity for Gravitational Waves

In the absence of a gravitational source, we consider usual spacetime to be flat and described by the Minkowski metric

$$\eta_{\mu\nu} = \mathrm{diag}(-1, 1, 1, 1) \ . \tag{4.1}$$

Due to the weak nature of the gravitational field that describes a gravitational wave, the metric which describes a gravitational wave can be well described as a flat Minkowski background with small linearised perturbations from the wave (as a simplified case to explore the basic details of gravitational waves; one can also perform this analysis in a cosmological background as we shall see later). This is expressed as

$$g_{\mu\nu} = \eta_{\mu\nu} + h_{\mu\nu} \ , \tag{4.2}$$

where $h_{\mu\nu}$ is the tensor describing the perturbations with value $|h_{\mu\nu}| \ll 1$. Using this choice of metric, we can explore how these perturbations would appear and how they would interact with matter through the Einstein equations defined in equation 2.6. To do so we must first calculate our curvature quantities using the definitions given in equations 2.4 and 2.5. From these, we calculate the Ricci tensor as being

$$R_{\mu\nu} = \frac{1}{2}\left(\partial_\rho\partial_\mu h^\rho_\nu + \partial_\rho\partial_\nu h^\rho_\mu - \partial_\mu\partial_\nu\eta^{\rho\tau}h_{\rho\tau} - \eta^{\rho\tau}\partial_\rho\partial_\tau h_{\mu\nu}\right) \ , \tag{4.3}$$

where the (1,1)-tensors are just raised with the Minkowski metric, *i.e.* $h^\alpha_\beta = \eta^{\alpha\gamma}h_{\gamma\beta}$. Conventionally, the trace of the perturbation is labelled as $h \equiv h^\mu_\mu = h_{\mu\nu}\eta^{\mu\nu}$. The Ricci scalar follows simply from this quantity as

$$R = \partial^\mu\partial^\nu h_{\mu\nu} - \eta^{\mu\nu}\partial_\mu\partial_\nu h \ . \tag{4.4}$$

These quantities can be combined to the final form of

$$G_{\mu\nu} = \frac{1}{2}\left(\partial_\rho\partial_\mu h^\rho_\nu + \partial_\rho\partial_\nu h^\rho_\mu - \partial_\mu\partial_\nu h - \Box h_{\mu\nu} - \eta_{\mu\nu}\partial^\rho\partial^\tau h_{\rho\tau} + \eta_{\mu\nu}\Box h\right) = \kappa^2 T_{\mu\nu} \ , \tag{4.5}$$

where we have used the "box" notation for the d'Alembertian operator of $\Box = \eta^{\mu\nu}\partial_\mu\partial_\nu$. With a complete expression for the field equations now found, we may consider ways to simplify further. As general relativity is fundamentally a diffeomorphism invariant theory, we can exploit picking certain "gauges" to reduce the number of terms. Specifically in this situation, the metric that we chose of small perturbations around a flat background does not completely specify the spacetime coordinate system as the metric being composed of a flat background with a perturbation is not unique; the perturbation will be different in other coordinate systems. Before we begin thinking about gauge choices, we will first employ an often used quantity of

$$\bar{h}_{\mu\nu} = h_{\mu\nu} - \frac{1}{2}\eta_{\mu\nu}h \ , \tag{4.6}$$

known as the "trace-reversed" perturbation. Replacing all appearances of $h_{\mu\nu}$ in equation 4.5 using the trace-reversed perturbation this will now reduce our Einstein equation to

$$\frac{1}{2}(-\Box\bar{h}_{\mu\nu} + \eta_{\nu\tau}\partial_\rho\partial_\mu\bar{h}^{\rho\tau} + \eta_{\mu\tau}\partial_\rho\partial_\nu\bar{h}^{\rho\tau} - \eta_{\mu\nu}\partial_\rho\partial_\tau\bar{h}^{\rho\tau}) = \kappa^2 T_{\mu\nu} \ , \tag{4.7}$$

and now with a simplified expression we move on to gauge-fixing.

4.1.1 Transverse-Traceless Gauge

As our intention is to analyse gravitational waves, it seems only natural to consider simplifications that mimic conventional waves and therefore satisfy the wave equation, or d'Alembert's equation. In scalar form, this is expressed as the condition $\Box u = 0$ where u is a scalar function $u(t, x, y, z, \ldots)$. For general relativity, this is replaced by the "harmonic coordinate" condition

$$g^{\mu\nu}\nabla_\mu\nabla_\nu x^\rho = 0 \ , \tag{4.8}$$

which simplifies to the condition

$$\Gamma^\rho_{\mu\nu} g^{\mu\nu} = 0 \tag{4.9}$$

due to the covariant derivative acting upon a coordinate (*i.e.* $\nabla_\mu x^\nu = \partial_\mu x^\nu$, $\nabla_\nu \partial_\mu = \partial_\nu\partial_\mu - \Gamma^\tau_{\mu\nu}\partial_\tau$). Recalling the definition of the Christoffel symbol in equation 2.2 this can be written as

$$\partial_\mu g^{\rho\mu} - \frac{1}{2} g^{\mu\nu}\partial^\rho g_{\mu\nu} = 0 \ , \tag{4.10}$$

and specifying this to our linearised perturbations (utilising that $\partial_\mu \eta_{\alpha\beta} = 0$) produces

$$\partial_\mu h^{\rho\mu} - \frac{1}{2}\partial^\rho h = 0 \ . \tag{4.11}$$

More succinctly, this gives the condition on the trace-reversed perturbation of

$$\partial^\mu \overline{h}_{\mu\nu} = 0 \ , \tag{4.12}$$

which instantly greatly reduces the form of our Einstein equation for this perturbative metric 4.7 to

$$-\frac{1}{2}\Box \overline{h}_{\mu\nu} = \kappa^2 T_{\mu\nu} \ . \tag{4.13}$$

We immediately see that this is simply a wave equation for the trace-reversed perturbation sourced by the energy-momentum tensor, which could be compared directly to d'Alembert's equation $\Box u = 0$ when in vacuum. The solution to equation 4.13 in vacuum is simple to find, with the form of a plane wave as

$$\overline{h}_{\mu\nu} = \varepsilon_{\mu\nu} e^{ik_\rho x^\rho} \ , \tag{4.14}$$

where k_μ is the wavevector $k_\mu = (-\omega, \vec{k})$ and $\varepsilon_{\mu\nu}$ is the gravitational wave polarisation tensor. This tensor is symmetric ($\varepsilon_{\mu\nu} = \varepsilon_{\nu\mu}$), meaning that there are only ten independent constituents. If we also consider our condition given in equation 4.12, we see that

$$k^\mu \varepsilon_{\mu\nu} = 0 \ , \tag{4.15}$$

imposing four more conditions on our polarisation tensor, reducing the number of independent constituents to six. A further thing we can glean from this solution is that when inserting the solution 4.14 into the vacuum version of equation 4.13, it produces

$$k_\rho k^\rho \overline{h}_{\mu\nu} = 0 \ . \tag{4.16}$$

The only non-trivial solution to this is that (momentarily restoring constants for clarity) $k_\rho k^\rho = -\frac{\omega^2}{c^2} + \vec{k}^2 = 0$, which tells us that gravitational waves must travel at the speed of light in a vacuum.

We still also have a residual gauge freedom under the infinitesimal diffeomorphisms $x^\mu \to x^\mu + \xi^\mu$ and $h_{\mu\nu} \to h_{\mu\nu} - \partial_\mu \xi_\nu - \partial_\nu \xi_\mu$ with which we can reduce things. Consider first that we are still operating under the harmonic condition of $\Box x^\mu = 0$. For the diffeomorphism $x^\mu \to x^\mu + \xi^\mu$, this is true iff. $\Box \xi^\mu = 0$, dictating another plane wave solution for this quantity. We write the solution to this as

$$\xi^\mu = \zeta^\mu e^{ik_\rho x^\rho} \ , \tag{4.17}$$

where ζ^μ is a 4-vector of constants. Let us now apply our diffeomorphisms to the trace-reversed perturbation.

$$\begin{aligned} \overline{h}_{\mu\nu} &= h_{\mu\nu} - \frac{1}{2}\eta_{\mu\nu} h \\ &\to (h_{\mu\nu} - \partial_\mu \xi_\nu - \partial_\nu \xi_\mu) - \frac{1}{2}\eta_{\mu\nu}\eta^{\rho\tau}(h_{\rho\tau} - \partial_\rho \xi_\tau - \partial_\tau \xi_\rho) \\ &\to \overline{h}_{\mu\nu} - ik_\mu \zeta_\nu e^{ik_\rho x^\rho} - ik_\nu \zeta_\mu e^{ik_\rho x^\rho} + i\eta_{\mu\nu} k^\tau \zeta_\tau e^{ik_\rho x^\rho} \ . \end{aligned} \tag{4.18}$$

Inserting the form of $\overline{h}_{\mu\nu}$ from equation 4.14 and dividing through by $e^{ik_\rho x^\rho}$ allows this to be cast as

$$\varepsilon_{\mu\nu} \to \varepsilon_{\mu\nu} - ik_\mu \zeta_\nu - ik_\nu \zeta_\mu + i\eta_{\mu\nu} k^\tau \zeta_\tau \ . \tag{4.19}$$

Taking the trace of the expression as $\varepsilon^\mu_\mu = \eta^{\mu\nu}\varepsilon_{\mu\nu}$ this now becomes

$$\varepsilon^\mu_\mu \to \varepsilon^\mu_\mu + 2ik^\mu \zeta_\mu \ , \tag{4.20}$$

and we can choose to set $k^\mu \zeta_\mu = \frac{i}{2}\varepsilon^\mu_\mu$ which causes both the polarisation tensor and $\overline{h}_{\mu\nu}$ to be traceless, reducing our independent components by another four down to just two. There are no more freedoms left to gauge away these two components, so these two are what fully carry the physical information about the gravitational waves with the gauge choices we have made. What does the tracelessness of the trace-reversed perturbation imply? Tracing over equation 4.6 we can see that this must imply that $h = 0$, and so with our gauge choices $\overline{h}_{\mu\nu}$ and $h_{\mu\nu}$ coincide.

Solutions to equation 4.13 are well known to take the form of Green's functions

$$h_{\mu\nu}(x^\rho) = -2\kappa^2 \int d^4y \ G(x^\rho - y^\rho) T_{\mu\nu}(y^\rho) \ , \tag{4.21}$$

where the Green's function satisfies the relation

$$\partial_\mu \partial^\mu G(x^\rho - y^\rho) = \delta^{(4)}(x^\rho - y^\rho) \ . \tag{4.22}$$

The Green's function which suffices for this condition is

$$G(x^\rho - y^\rho) = -\frac{1}{4\pi|\vec{x}-\vec{y}|}\delta(|\vec{x}-\vec{y}| - (x^0 - y^0))\theta(x^0 - y^0) \ , \tag{4.23}$$

where $\theta(x)$ is the Heaviside step function. This gives the expression for the perturbations

$$h_{\mu\nu} = \frac{\kappa^2}{2\pi}\int d^3y \ \frac{1}{t-t_r}T_{\mu\nu}(t_r, \vec{y}) \ , \tag{4.24}$$

where we have defined the retarded time as $t_r = t - |\vec{x}-\vec{y}|$. This is very informative, as it shows to us that the perturbations are generated from all energy-momentum sources in the retarded time past light-cone.

4.2 Gravitational Wave Spectrum

As we will be working with transverse-traceless quantities we also need to figure out how to easily convert other important quantities such as the energy-momentum tensor into this form, which requires the generation of a projection tensor to project these quantities out. We construct

$$P_{ij}(\mathbf{n}) = \delta_{ij} - \hat{n}_i\hat{n}_j \ , \tag{4.25}$$

which is transverse in that $n^iP_{ij} = 0$ but not traceless, with $P^i_i = 2$. It is also manifestly symmetric under the exchange of $i \leftrightarrow j$. We can however use this to construct

$$\Lambda_{ij,kl}(\mathbf{n}) = P_{il}(\mathbf{n})P_{jk}(\mathbf{n}) - \frac{1}{2}P_{ij}(\mathbf{n})P_{kl}(\mathbf{n}), \tag{4.26}$$

which is traceless when contracting over either the first or last pair of indices *i.e.* ${\Lambda^i}_{i,kl} = {\Lambda_{ij,}}^k{}_k = 0$, transverse for any index, and symmetric under $(i,j) \leftrightarrow (k,l)$. For projection operators we would also expect that when projection operators are contracted they form another projection operator, which can be verified for both of these as

$$P^i{}_j(\mathbf{n})P_{ik}(\mathbf{n}) = P_{jk}(\mathbf{n}) \quad \text{and} \quad \Lambda^{ij}{}_{,kl}(\mathbf{n})\Lambda_{ij,mn}(\mathbf{n}) = \Lambda_{kl,mn}(\mathbf{n}) \ . \tag{4.27}$$

Therefore we can always project out our gravitational wave perturbation into the transverse-traceless gauge through

$$h^{\mathrm{TT}}_{ij}(\mathbf{k}) = \Lambda^{ab}{}_{,ij}(\mathbf{k})h_{ab}(\mathbf{k}) \ . \tag{4.28}$$

4.2.1 Non-linear Considerations and the GW Stress-Energy Tensor

All calculations done in the previous section were a simplified version of the true picture. The Universe is not always well described by a flat Minkowski metric, and because the energy-momentum tensors in other theories such as scalar field theory or electromagnetism arise from quadratic terms of the fields (which we have ignored) we have implicitly assumed that the gravitational waves do not carry energy that curves the spacetime. Now we have a better grasp on the foundations of gravitational waves, we need to rectify these oversights. We begin this treatment to promoting the metric to one in which the background can vary with x^μ,

$$g_{\mu\nu}(x) = \overline{g}_{\mu\nu}(x) + h_{\mu\nu}(x) \tag{4.29}$$

If we contract equation 2.6 with the metric and input the relation we get of $R = -\kappa^2 T_{\mu\nu} g^{\mu\nu}$ back into the same equation we can write the Einstein equations in the form of

$$R_{\mu\nu} = \kappa^2 \left(T_{\mu\nu} - \frac{1}{2} g_{\mu\nu} T \right) \ , \tag{4.30}$$

where we have defined the quantity $T = T_{\mu\nu} g^{\mu\nu}$. The Ricci tensor due to its construction can be split up into pieces with increasing order in the perturbations as

$$R_{\mu\nu} = \overline{R}_{\mu\nu} + R^{(1)}_{\mu\nu} + R^{(2)}_{\mu\nu} + \dots \ , \tag{4.31}$$

where $\overline{R}_{\mu\nu}$ contains the Ricci tensor arising just due to the background curvature, $R^{(1)}_{\mu\nu}$ is from the terms linear in $h_{\mu\nu}$, and $R^{(2)}_{\mu\nu}$ is from the previously ignored terms quadratic in $h_{\mu\nu}$. The reason for this choice of splitting is due to how it distributes the types of modes present in the curvature. The background is expected to be varying slowly, and therefore can be categorised as containing frequency modes in the lower end of the spectrum up to some particular maximum f_b^{max}. The gravitational wave perturbations however should be high frequency modes characterised by frequency f_{gw}, and as long as they obey the condition

$$f_b^{\mathrm{max}} \ll f_{\mathrm{gw}} \tag{4.32}$$

the two sets of modes should be distinguishable. For a more intuitive understanding, consider a container of water. If you picked up one side of the container and then dropped it, you would generate waves which propagated from one side to the other and then back again. After a short while, these waves would have decreased in intensity to the point of appearing as just slight undulations on the liquid surface; this represents the slowly varying, low frequency background. If you then trickled some droplets of water into the container from above you would see sharply defined ripples which are easily discernible even with the liquid as a whole having a moving background; these are the high frequency perturbations. If we push this metaphor even further, where the droplet ripples are present there is a slight pushback on the varying background which will alter how this background propagates further. This can be likened to how the presence of gravitational waves inherently curves spacetime also.

We can so far separate $\overline{R}_{\mu\nu}$ and $R^{(1)}_{\mu\nu}$ into two distinct frequency regimes then, the low frequency background and the high frequency perturbations respectively, the latter of which is of most import to us. What about $R^{(2)}_{\mu\nu}$? Comprised of terms including two factors of $h_{\mu\nu}$ means it will certainly have high frequency modes. However, there may also be combinations where two high frequency modes have opposite magnitude wavevectors, leading to the possibility of low frequency modes in this term as well. To deal with this, we split up the Einstein equation 4.30 into

$$\overline{R}_{\mu\nu} = -[R^{(2)}_{\mu\nu}]_{\text{low}} + \kappa^2 \left(T_{\mu\nu} - \frac{1}{2} g_{\mu\nu} T \right)_{\text{low}} \tag{4.33}$$

and

$$R^{(1)}_{\mu\nu} = -[R^{(2)}_{\mu\nu}]_{\text{high}} + \kappa^2 \left(T_{\mu\nu} - \frac{1}{2} g_{\mu\nu} T \right)_{\text{high}} \quad , \tag{4.34}$$

where we have truncated $R_{\mu\nu}$ to second-order in perturbations. To explore these equations in more detail we will have to calculate the actual forms of these curvature quantities. Obviously, without specifying the form of $\overline{g}_{\mu\nu}$ then all we can say for the form of $\overline{R}_{\mu\nu}$ is that it is equation 2.4 with the replacement $\Gamma(g_{\mu\nu}) \to \overline{\Gamma}(\overline{g}_{\mu\nu})$. Working through in orders of the perturbation however gives

$$R^{(1)}_{\mu\nu} = \frac{1}{2} \left(\overline{\nabla}^{\rho} \overline{\nabla}_{\mu} h_{\nu\rho} + \overline{\nabla}^{\rho} \overline{\nabla}_{\nu} h_{\mu\rho} - \overline{\nabla}^{\rho} \overline{\nabla}_{\rho} h_{\mu\nu} - \overline{\nabla}_{\mu} \overline{\nabla}_{\nu} h \right) \quad , \tag{4.35}$$

where $\overline{\nabla}_{\mu}$ is the covariant derivative with definition $\overline{\nabla}_{\rho} h_{\mu\nu} = \partial_{\rho} h_{\mu\nu} - \overline{\Gamma}^{\tau}_{\rho\mu} h_{\tau\nu} - \overline{\Gamma}^{\tau}_{\rho\nu} h_{\mu\tau}$, and

$$\begin{aligned} R^{(2)}_{\mu\nu} = \frac{1}{2} \overline{g}^{\rho\tau} \overline{g}^{\alpha\beta} \Big\{ & \frac{1}{2} \overline{\nabla}_{\mu} h_{\rho\alpha} \overline{\nabla}_{\nu} h_{\tau\beta} + h_{\rho\alpha} (\overline{\nabla}_{\nu} \overline{\nabla}_{\mu} h_{\tau\beta} + \overline{\nabla}_{\beta} \overline{\nabla}_{\tau} h_{\mu\nu} - \overline{\nabla}_{\beta} \overline{\nabla}_{\nu} h_{\mu\tau} - \overline{\nabla}_{\beta} \overline{\nabla}_{\mu} h_{\nu\tau}) \\ & + \overline{\nabla}_{\rho} h_{\nu\alpha} \overline{\nabla}_{\tau} h_{\mu\beta} - \overline{\nabla}_{\rho} h_{\nu\alpha} \overline{\nabla}_{\beta} h_{\mu\tau} - \overline{\nabla}_{\rho} h_{\alpha\tau} \overline{\nabla}_{\nu} h_{\mu\beta} + \overline{\nabla}_{\rho} h_{\alpha\tau} \overline{\nabla}_{\beta} h_{\mu\nu} - \overline{\nabla}_{\rho} h_{\alpha\tau} \overline{\nabla}_{\mu} h_{\nu\beta} \\ & - \frac{1}{2} \overline{\nabla}_{\alpha} h_{\rho\tau} \overline{\nabla}_{\beta} h_{\mu\nu} + \frac{1}{2} \overline{\nabla}_{\alpha} h_{\rho\tau} \overline{\nabla}_{\nu} h_{\mu\beta} + \frac{1}{2} \overline{\nabla}_{\alpha} h_{\rho\tau} \overline{\nabla}_{\mu} h_{\nu\beta} \Big\} \end{aligned} \tag{4.36}$$

to second order in the perturbations. With the knowledge of how we have two main regimes, we may introduce an intermediate scale $\hat{f}$, which satisfies the inequality relation

$$f_b^{\max} \ll \hat{f} \ll f_{\text{gw}} \ . \tag{4.37}$$

The meaning of this scale is that it categorises a wave which would have completed many periods by the time the background had completed one but only a very small fraction of a period in the time of one full gravitational wave period. Due to this, if we consider averaging over the scale of this intermediate frequency $\hat{f}$ then we notice that the low frequency background will have barely changed and so will be approximately constant, however the gravitational wave will have completed many cycles and so will average to zero. This allows equation 4.33 to be expressed as

$$\overline{R}_{\mu\nu} = -\langle R^{(2)}_{\mu\nu} \rangle + \kappa^2 \langle T_{\mu\nu} - \frac{1}{2} g_{\mu\nu} T \rangle \ , \tag{4.38}$$

where we have used the notation $\langle x \rangle$ to indicate that we are now averaging the quantity x over many periods of the gravitational waves. If we apply a similar treatment to equation 4.34 we will instead find the condition

$$\langle R^{(1)}_{\mu\nu} \rangle = 0 \tag{4.39}$$

due to it being composed only of high frequency modes which will average to zero. The averaged energy-momentum tensor can be defined in terms of an effective tensor $\overline{T}_{\mu\nu}$ with its related trace $\overline{T} = \overline{T}_{\mu\nu} \overline{g}^{\mu\nu}$ as

$$\langle T_{\mu\nu} - \frac{1}{2} g_{\mu\nu} T \rangle = \overline{T}_{\mu\nu} - \frac{1}{2} \langle g_{\mu\nu} \rangle \overline{T} \ , \tag{4.40}$$

and we can then recognise that $\langle g_{\mu\nu} \rangle = \langle \overline{g}_{\mu\nu} + h_{\mu\nu} \rangle$ will project out only the low-frequency modes so $\langle g_{\mu\nu} \rangle = \overline{g}_{\mu\nu}$. Taking the trace over equation 4.38 against the background $\overline{g}_{\mu\nu}$ and using equation 4.40 gives

$$\overline{R} = \overline{g}^{\mu\nu} \overline{R}_{\mu\nu} = -\overline{g}^{\mu\nu} \langle R^{(2)}_{\mu\nu} \rangle - \kappa^2 \overline{T} \ , \tag{4.41}$$

which can be rewritten as

$$\overline{R} = -\langle R^{(2)} \rangle - \kappa^2 \overline{T} \tag{4.42}$$

using the definition $\overline{g}^{\mu\nu} \langle R^{(2)}_{\mu\nu} \rangle = \langle \overline{g}^{\mu\nu} R^{(2)}_{\mu\nu} \rangle = \langle R^{(2)} \rangle$. Combining equations 4.38, 4.40, and 4.42 into the Einstein equations in the background we finally arrive at

$$\overline{R}_{\mu\nu} - \frac{1}{2} \overline{g}_{\mu\nu} \overline{R} = \kappa^2 \overline{T}_{\mu\nu} - [\langle R^{(2)}_{\mu\nu} \rangle - \frac{1}{2} \overline{g}_{\mu\nu} \langle R^{(2)} \rangle] \ . \tag{4.43}$$

What we can see from this equation is that the curvature of the background is formed by two separate contributions: curvature from the matter present in the spacetime in the low-frequency regime and also a completely matter non-dependent component which arises due to the gravitational wave perturbations. We can make this even more obvious by allowing the definition of a new tensor $t_{\mu\nu}$ through

$$t_{\mu\nu} = -\frac{1}{\kappa^2} \langle R^{(2)}_{\mu\nu} - \frac{1}{2} \overline{g}_{\mu\nu} R^{(2)} \rangle \ , \tag{4.44}$$

which when inserted into equation 4.43 now allows the right-hand side to appear like a conventional curvature-matter equivalence with two sources as

$$\overline{R}_{\mu\nu} - \frac{1}{2} \overline{g}_{\mu\nu} \overline{R} = \kappa^2 (\overline{T}_{\mu\nu} + t_{\mu\nu}) \ . \tag{4.45}$$

The main takeaway from this analysis is that by including terms up to quadratic order in the gravitational wave perturbation, just like including quadratic orders in other theories such as scalar field theory or electromagnetism, we generate an effect on the curvature in the background which acts exactly like an energy momentum tensor. This allows us to explicitly define the energy-momentum tensor of the gravitational waves through the tensor labelled $t_{\mu\nu}$, and will be used as such from now on.

Now with a relation for what the energy-momentum tensor of the gravitational waves is, we want to try and compute it fully. We have already derived an expression for $R^{(2)}_{\mu\nu}$ (equation 4.36), but the covariant derivatives mean that utilising this will be very unwieldy in our calculations. Fortunately, for all purposes in which we will be required to calculate $t_{\mu\nu}$ we will be considering the gravitational wave as being greatly removed from its source, and so it will be well approximated by the background curvature instead being flat space. This approximation amounts to the substitution $\overline{\nabla}_\mu \to \partial_\mu$ as $\Gamma[\eta_{\mu\nu}] = 0$, and so equation 4.36 simplifies to

$$
\begin{aligned}
R^{(2)}_{\mu\nu} = \frac{1}{2}\bigg[&\frac{1}{2}\partial_\mu h_{\rho\tau}\partial_\nu h^{\rho\tau} + h^{\rho\tau}\partial_\mu\partial_\nu h_{\rho\tau} + h^{\rho\tau}\partial_\rho\partial_\tau h_{\mu\nu} - h^{\rho\tau}\partial_\nu\partial_\tau h_{\rho\mu} - h^{\rho\tau}\partial_\mu\partial_\tau h_{\rho\nu} \\
&+ \partial^\tau h^\rho_\nu\partial_\rho h_{\tau\mu} - \partial^\tau h^\rho_\nu\partial_\rho h_{\tau\mu} - \partial_\tau h^{\rho\tau}\partial_\nu h_{\rho\mu} + \partial_\tau h^{\rho\tau}\partial_\rho h_{\mu\nu} - \partial_\tau h^{\rho\tau}\partial_\mu h_{\rho\nu} \\
&- \frac{1}{2}\partial^\rho h\partial_\rho h_{\mu\nu} + \frac{1}{2}\partial^\rho h\partial_\nu h_{\rho\mu} + \frac{1}{2}\partial^\rho h\partial_\mu h_{\rho\nu}\bigg] \ .
\end{aligned} \tag{4.46}
$$

This is still obviously a very complicated expression to be able to use, but we have already explored methods to reduce the complexity of equations involving the perturbation $h_{\mu\nu}$ through making the right gauge choices. Either by projecting out or simply considering our gauge restrictions of $\partial^\mu h_{\mu\nu} = 0$ and $h = 0$ this leaves (leaving off the TT superscript on $h^{\rm TT}_{\mu\nu}$ for now)

$$
\begin{aligned}
R^{(2)}_{\mu\nu} = \frac{1}{2}\bigg[&\frac{1}{2}\partial_\mu h_{\rho\tau}\partial_\nu h^{\rho\tau} + h^{\rho\tau}\partial_\mu\partial_\nu h_{\rho\tau} + h^{\rho\tau}\partial_\rho\partial_\tau h_{\mu\nu} - h^{\rho\tau}\partial_\nu\partial_\tau h_{\rho\mu} \\
&- h^{\rho\tau}\partial_\mu\partial_\tau h_{\rho\nu} + \partial^\tau h^\rho_\nu\partial_\rho h_{\tau\mu} - \partial^\tau h^\rho_\nu\partial_\rho h_{\tau\mu}\bigg]
\end{aligned} \tag{4.47}
$$

and

$$
R^{(2)} = \frac{1}{4}\partial_\mu h_{\rho\tau}\partial^\mu h^{\rho\tau} \ . \tag{4.48}
$$

A further simplification can be implemented through noticing that we can reframe the notion of our taking the average over many period intervals in the sense of an integration. Due to this, we may perform integration by parts and reuse the gauge conditions along with the wave equation $\partial_\rho\partial^\rho h_{\mu\nu} = 0$ to write the averaged quantities as

$$
\langle R^{(2)}_{\mu\nu}\rangle = -\frac{1}{4}\langle\partial_\mu h_{\rho\tau}\partial_\nu h^{\rho\tau}\rangle \tag{4.49}
$$

and

$$\langle R^{(2)} \rangle = 0 \ . \tag{4.50}$$

Entering these into equation 4.44, the energy-momentum tensor for the gravitational waves is now simply

$$t_{\mu\nu} = \frac{1}{4\kappa^2} \langle \partial_\mu h_{\rho\tau} \partial_\nu h^{\rho\tau} \rangle \ . \tag{4.51}$$

For detection of gravitational waves we will be concerned with the energy produced found through the energy density ρ, the temporal component of the energy-momentum tensor

$$\rho = t^{00} = \frac{1}{4\kappa^2} \langle \dot{h}_{\rho\tau} \dot{h}^{\rho\tau} \rangle \ . \tag{4.52}$$

Because of our gauge condition $\partial^\mu h_{\mu\nu} = 0$ and projecting into the transverse-traceless gauge using equation 4.28 we see that $t_{\mu\nu}$ is only dependent upon the modes h_{ij}^{TT}, and so this reduces to the important result (restoring TT superscript)

$$\rho_{\mathrm{gw}} = \frac{1}{4\kappa^2} \langle \dot{h}_{ij}^{\mathrm{TT}}(t, \mathbf{x}) \dot{h}_{ij}^{\mathrm{TT}}(t, \mathbf{x}) \rangle \ . \tag{4.53}$$

Due to the assumed stochastic nature of the generation of gravitational waves, we may write the averaged quantity as

$$\langle \dot{h}_{ij}^{\mathrm{TT}}(t, \mathbf{k}) \dot{h}_{ij}^{\mathrm{TT}}(t, \mathbf{k}') \rangle = P_{\dot{h}}(t, \mathbf{k}) (2\pi)^3 \delta(\mathbf{k} + \mathbf{k}') \ , \tag{4.54}$$

where $P_{\dot{h}}(t, \mathbf{k})$ is the spectral density of the time derivative of the perturbations in the metric. Taking the Fourier transform of 4.54 to get an expression in position space, we now find that the gravitational wave energy density is

$$\rho_{\mathrm{gw}} = \frac{1}{4\kappa^2} \int \frac{dk k^2}{2\pi^2} P_{\dot{h}}(k, t), \tag{4.55}$$

which we can put into the more useful (for our purposes) frequency dependent quantity through $k = 2\pi f$ as

$$\rho_{\mathrm{gw}} = \frac{\pi}{\kappa^2} \int df \, f^2 P_{\dot{h}}(f). \tag{4.56}$$

Finally we obtain the power spectrum of the gravitational wave energy density parameter which is conventionally defined as the energy density per logarithmic frequency interval scaled by the critical density ρ_{crit} through

$$\Omega_{\mathrm{gw}}(f) = \frac{1}{\rho_{\mathrm{crit}}} \frac{d\rho_{\mathrm{gw}}}{d \log f} = \frac{\pi}{\kappa^2 \rho_{\mathrm{crit}}} f^3 P_{\dot{h}}(f) \ . \tag{4.57}$$

All that is left to for the gravitational wave part of the analysis now is to categorise the spectral density of the perturbations in the situation of bubble nucleations and collisions.

4.2.2 Characterising the Spectrum

The aim of this work is to study cosmological first-order phase transitions, which will have a scalar field stuck in a metastable state which will undergo thermal and quantum phase transitions to the new stable state, which is separated by a potential barrier. These transitions will nucleate bubbles, which are surrounded by a hot relativistic plasma composed of early Universe particles. Therefore, the energy-momentum tensor of the model we are considering contains a classical scalar field ϕ which is coupled to ideal fluid. This allows us to write the tensor as just a combination of the EM tensors defined previously in 2.12 and 3.84 as

$$T^{\mu\nu} = T^{\mu\nu}_{\phi} + T^{\mu\nu}_{f} = \partial^\mu\phi\partial^\nu\phi - \frac{1}{2}g^{\mu\nu}\partial_\alpha\phi\partial^\alpha\phi + (p+\rho)u^\mu u^\nu + pg^{\mu\nu} \ . \tag{4.58}$$

As the gravitational waves are sourced only through the spatial components of the EM tensor in transverse-traceless gauge, we can instead consider a simplified tensor which sources our model as

$$\tau_{ij} = \tau^{\phi}_{ij} + \tau^{\mathrm{f}}_{ij} \ . \tag{4.59}$$

The field and fluid components respectively are

$$\tau^{\phi}_{ij} = \partial_i\phi\partial_j\phi \ , \qquad \tau^{\mathrm{f}}_{ij} = (p+\rho)u_i u_j = \gamma^2(p+\rho)v_i v_j \ , \tag{4.60}$$

where we have used the definition that $u_i = \gamma v_i$ with γ being the Lorentz factor and v_i being the 3D velocity vector. To recover the physical perturbations when using this simplification we must project out using our operator in equation 4.26, and so we can write our metric perturbations for this model as

$$h_{ij}(t,\mathbf{k}) = 2\kappa^2\Lambda_{ij,kl}(\mathbf{k})\int_0^t dt'\frac{\sin[k(t-t')]}{k}\tau^{kl}(\mathbf{k},t') \ , \tag{4.61}$$

with the $\sin[k(t-t')]/k$ coming from the Green function. This can then be differentiated with respect to time and averaged over to give the necessary quantity for the power spectrum as

$$\langle\dot{h}^{\mathrm{TT}}_{ij}(t,\mathbf{k})\dot{h}^{\mathrm{TT}}_{ij}(t,\mathbf{k}')\rangle = 4\kappa^4\int_0^t dt_1 dt_2 \cos[k(t-t_1)]\cos[k(t-t_2)]\Lambda_{ij,kl}(\mathbf{k})\langle\tau^{ij}_{\mathrm{f}}(\mathbf{k},t)\tau^{kl}_{\mathrm{f}}(\mathbf{k}',t)\rangle \ . \tag{4.62}$$

In this last equation we have used the simplification that unless the transition undergoes strong supercooling the scalar contribution is negligible due to the vast majority of the energy going into the fluid, and so $\tau^{kl} \simeq \tau^{kl}_{\mathrm{f}}$. We now introduce what is known as the unequal time correlator (UETC) for the shear stress of the fluid denoted Π^2, which is defined through the relation

$$\Lambda_{ij,kl}(\mathbf{k}) \left\langle \tau_{\mathrm{f}}^{ij}\left(\mathbf{k},t_1\right)\tau_{\mathrm{f}}^{kl}\left(\mathbf{k}',t_2\right)\right\rangle = \Pi^2\left(k,t_1,t_2\right)(2\pi)^3\delta\left(\mathbf{k}+\mathbf{k}'\right) \ . \tag{4.63}$$

If we enter this definition into equation 4.62 and compare that to 4.54, we see that the quantity we desire of $P_{\dot{h}}(k,t)$ is found through

$$P_{\dot{h}}(k,t) = 4\kappa^4 \int_0^t dt_1 dt_2 \cos[k(t-t_1)]\cos[k(t-t_2)]\Pi^2\left(k,t_1,t_2\right) \ , \tag{4.64}$$

which for the large periods that we are averaging over can instead be reduced to

$$P_{\dot{h}}(k,t) = 2\kappa^4 \int_0^t dt_1 dt_2 \cos\left[k\left(t_1-t_2\right)\right]\Pi^2\left(k,t_1,t_2\right) \ . \tag{4.65}$$

We can now define the overall amplitude of the fluid shear stress by the root mean square (RMS) four-velocity $\overline{U}_{\mathrm{f}}$ as

$$\overline{U}_{\mathrm{f}}^2 = \frac{1}{\overline{w}\mathcal{V}}\int_{\mathcal{V}} d^3x\tau_{ii}^{\mathrm{f}} \ , \tag{4.66}$$

where $\overline{w}$ is the averaged enthalpy density and $\mathcal{V}$ is the volume being averaged over (with an analogous quantity for the field, $\overline{U}_{\phi}$, being constructed with τ_{ii}^{ϕ} instead). Using this definition and that $\overline{\rho}$ is the average energy density and $\overline{p}$ is the average pressure, the amplitude of the source of gravitational waves is expected to be approximately $\left[(\bar{\rho}+\bar{p})\overline{U}_{\mathrm{f}}^2\right]^2$, with its length scale being the size of the bubble R_*. From this then, the unequal time correlator can be estimated as

$$\Pi^2\left(k,t_1,t_2\right) \simeq \left[(\bar{\rho}+\bar{p})\overline{U}_{\mathrm{f}}^2\right]^2 R_*^3\tilde{\Pi}^2\left(kR_*,z\right) \ , \tag{4.67}$$

where $\tilde{\Pi}^2$ is a dimensionless function of k, t_1, and t_2 and we have made the substitution $z = k(t_1-t_2)$. Using this estimation for the unequal time correlator as well as the same z substitution in equation 4.65 leaves the spectral density as

$$P_{\dot{h}}(k,t) = 2\kappa^4\left[(\bar{\rho}+\bar{p})\bar{U}_{\mathrm{f}}^2\right]^2 tk^{-1}R_*^3\int dz\cos(z)\tilde{\Pi}^2\left(kR_*,z\right) \ . \tag{4.68}$$

If we introduce a dimensionless "spectral density" for the gravitational waves $\tilde{P}_{\mathrm{gw}}(kR_*)$ which is defined through

$$\tilde{P}_{\mathrm{gw}}(kR_*) = \frac{1}{kR_*}\int dz\frac{\cos(z)}{2}\tilde{\Pi}^2\left(kR_*,z\right) \tag{4.69}$$

we can instead write the spectral density as

$$P_{\dot{h}}(k,t) = 4\kappa^4\left[(\bar{\rho}+\bar{p})\bar{U}_{\mathrm{f}}^2\right]^2 tR_*^4\tilde{P}_{\mathrm{gw}}(kR_*) \ . \tag{4.70}$$

Noting that the adiabatic index is given by the relation $\Gamma = 1+\overline{p}/\overline{\rho}$ and that the quantity $\overline{\rho} = \rho_{\mathrm{crit}}$ is related to the Hubble rate we may recast the spectral density in terms of the frequency as

$$P_{\dot{h}}(f) = 36H_{\mathrm{n}}^4\left[\Gamma\bar{U}_{\mathrm{f}}^2\right]^2 tR_*^4\tilde{P}_{\mathrm{gw}}(fR_*) \ . \tag{4.71}$$

With many simplifications achieved we remember that our full gravitational wave spectrum is equation 4.57, and making use of the relation between critical energy density and Hubble rate again this gives

$$\Omega_{\rm gw}(f) = 12\pi[\Gamma\bar{U}_{\rm f}^2]^2(H_{\rm n}t)(H_{\rm n}R_*)(fR_*)^3\tilde{P}_{\rm gw}(fR_*) \ , \tag{4.72}$$

which we can integrate to find

$$\Omega_{\rm gw}^{\int} \equiv \int \Omega_{\rm gw}(f) d\log f = 3[\Gamma\bar{U}_{\rm f}^2]^2(H_{\rm n}t)(H_{\rm n}R_*)\tilde{\Omega}_{\rm gw}^{\int} \tag{4.73}$$

where $\tilde{\Omega}_{\rm gw}^{\int}$ is defined as (with substitution $x = fR_*$)

$$\tilde{\Omega}_{\rm gw}^{\int} = 4\pi\int_0^\infty dx\, x^2\tilde{P}_{\rm gw}(x) \ . \tag{4.74}$$

What other contributions can we elucidate? If we now consider the timescales for these gravitational waves, we can label the approximate lifetime of the gravitational wave source as $t = \tau_{\rm v}$. It was demonstrated in [112] that the suppression due to this finite lifetime can be well-modelled in an expanding radiation-dominated Universe in which the source is constant and shuts off after time $\tau_{\rm sw}$ by taking this lifetime as (to a first approximation)

$$\tau_{\rm v} = H_{\rm n}^{-1}\left(1 - \frac{1}{\sqrt{1+2\tau_{\rm sw}H_{\rm n}}}\right) \ , \tag{4.75}$$

where $\tau_{\rm sw}$ is the non-linear soundwave timescale which can be described through $\tau_{\rm sw} \simeq R_*/\sqrt{K}$ from the non-linear terms in the fluid equations. This modifies the power spectrum form to

$$\Omega_{\rm gw}^{\int} = 3[\Gamma\bar{U}_{\rm f}^2]^2(H_{\rm n}R_*)\left(1 - \frac{K^{1/4}}{\sqrt{K^{1/2}+2H_{\rm n}R_*}}\right)\tilde{\Omega}_{\rm gw}^{\int} \ . \tag{4.76}$$

To obtain the amplitude of the gravitational wave power spectra today, the power spectrum must be modified by including a factor to normalise $\Omega_{\rm gw}$ of

$$F_{\rm gw,0} = \frac{1}{2}\Omega_{\gamma,0}g_0\left(\frac{g_0}{g_*}\right)^{1/3} \tag{4.77}$$

where $\Omega_{\gamma,0}$ is the current density of photons, g_0 is the current degrees of freedom, and g_* is the effective degrees of freedom. Inputting the value for g_0 and $\Omega_{\gamma,0}$ this gives us a numerical form with related uncertainty (mostly from value of H_0 used to calculate $\Omega_{\gamma,0}$) in terms of g_* of

$$F_{\rm gw,0} = (3.57 \pm 0.05)\times 10^{-5}\left(\frac{100}{g_*}\right)^{1/3} \ . \tag{4.78}$$

Including this modification we can write the integrated power spectrum as

$$\Omega_{\rm gw,0}^{\int} = 3F_{\rm gw,0}K^2(H_{\rm n}R_*)\left(1 - \frac{K^{1/4}}{\sqrt{K^{1/2}+2H_{\rm n}R_*}}\right)\tilde{\Omega}_{\rm gw}^{\int} \ , \tag{4.79}$$

where we have also used the definition that $K = \Gamma \bar{U}_{\rm f}^2$, which is known as the kinetic energy fraction. As $\bar{U}_{\rm f}^2$ is dependent upon the fluid velocity and enthalpy, both of which are dependent upon the wall speed and transition strength, the kinetic energy fraction will also be controlled by these. Taking the derivative of $\Omega^{\int}_{\rm gw,0}$ takes us back to $\Omega_{\rm gw,0}$, but as we can see from equation 4.74 the frequency dependence is now isolated in the term $\tilde{\Omega}^{\int}_{\rm gw}$. We may therefore write that the derivative of this quantity is formed of a numerical constant and a factor which is dependent on the frequency. This is frequently modelled as

$$\frac{d\tilde{\Omega}^{\int}_{\rm gw}}{d\log f} = \tilde{\Omega}_{\rm gw} C(fR_*) \ , \tag{4.80}$$

where $C(s)$ is the spectral shape function which describes the acoustic gravitational wave power spectrum using broken power laws. Numerous studies have been dedicated to modelling this shape function in great detail, however a simpler case which is used for the basis of the LISA group spectrum shape [113] is found as

$$C(s) = s^3 \left(\frac{7}{4 + 3s^2} \right)^{7/2} \ . \tag{4.81}$$

The other quantity $\tilde{\Omega}_{\rm gw}$ is found to have numerical value of $\tilde{\Omega}_{\rm gw} = 1.2 \times 10^{-2}$ from numerical simulations [114], where it reproduces the peak amplitude for an intermediate strength transition at high wall speed; this leaves

$$\Omega_{\rm gw,0} = 3F_{\rm gw,0} K^2 (H_{\rm n} R_*) \left(1 - \frac{K^{1/4}}{\sqrt{K^{1/2} + 2H_{\rm n} R_*}} \right) \tilde{\Omega}_{\rm gw} C(fR_*) \ . \tag{4.82}$$

We would also like to incorporate the peak frequency into the formula due to its ubiquity across models. To calculate the peak frequency today we begin with the frequency scale of when the spectrum was produced, which is $f = R_*^{-1}$. This relationship allows us to translate the dependency of the spectral shape into a ratio of the frequency over the peak frequency. Frequencies emerging from cosmological spectra will be subjected to large redshifting, which is taken into account through

$$f_{p,0} = \frac{1}{1+z} f_p = a f_p \ . \tag{4.83}$$

Due to the conservation of the entropy with comoving volume $\frac{d}{dt}(a^3 g(T) T^3) = 0$, we may then rewrite this as

$$f_{p,0} = \left(\frac{g_0}{g(T_{\rm n})} \right)^{1/3} \frac{T_{\gamma,0}}{T_{\rm n}} f_p \ , \tag{4.84}$$

where $T_{\gamma,0}$ is the photon temperature today and we have used the definition that $a(t_0) = 1$. Inserting a factor of H_n in the numerator and denominator and using the definition of f_p,

$$f_{p,0} = \left(\frac{g_0}{g(T_{\rm n})} \right)^{1/3} \frac{T_{\gamma,0}}{T_{\rm n}} \left(\frac{1}{H_{\rm n} R_*} \right) H_{\rm n} \ . \tag{4.85}$$

Using eq. 2.14 at the nucleation temperature with $k = 0$, $\kappa^2 = 8\pi M_p^{-2}$, and $\rho = \frac{4\pi^3}{45}T^4$ from the explanation at the end of sec. 2.2 we find (in a conventional form)

$$f_{p,0} = \frac{40\sqrt{5}\sqrt[3]{10}}{3}\pi^3 \left(\frac{1}{H_\mathrm{n}R_*}\right)\left(\frac{T_\mathrm{n}}{100\mathrm{GeV}}\right)\left(\frac{g_*}{100}\right)^{1/6}\frac{T_{\gamma,0}(g_0)^{1/3}}{M_P}\mathrm{GeV}\ , \tag{4.86}$$

and we can finally use the values $T_{\gamma,0} = 2.725$ K [115], $g_0 \simeq 3.36$, and $M_P = 1.22 \times 10^{19}$ GeV as well as the conversion from GeV to Hz as 1 GeV $= 2.418 \times 10^{23}$ Hz to leave

$$f_{p,0} \simeq 26\left(\frac{1}{H_\mathrm{n}R_*}\right)\left(\frac{T_\mathrm{n}}{100\mathrm{GeV}}\right)\left(\frac{g_*}{100}\right)^{1/6}\mu\mathrm{Hz}\ . \tag{4.87}$$

The most recent modifications to Ω_gw come through the recent findings that the value of the sound speed and reheating of the metastable phase will also have a significant effect on the gravitational wave signal.

In Refs. [116, 117] it was shown that the efficiency factor κ_eff (a quantity related to the kinetic energy fraction), which was determined from solving the hydrodynamic equations of the gravitational wave system is parameterised by only four variables: the transition strength, the wall velocity, and the speed of sound in both the symmetric and broken phases. Taking into consideration the dependency on sound speed departure from $c_s^2 = 1/3$ means substituting the kinetic energy fraction in equation 4.82 by

$$K \to K_\mathrm{GKSV} = \frac{3}{4}\left(1 + \frac{p_+}{\rho_+}\right)\alpha_{\overline{\theta}}\kappa_{\overline{\theta}}(c_s, \alpha_{\overline{\theta}}, v_\mathrm{w})\ , \tag{4.88}$$

where p_+ and ρ_+ are the pressure and energy density in the symmetric phase respectively, $\alpha_{\overline{\theta}}$ is the strength parameter found through the "pseudotrace" $\overline{\theta} = \rho - p/c_s^2$, and $\kappa_{\overline{\theta}}$ is the efficiency factor in this sound-speed dependent model also found through the pseudotrace.

In Ref. [118] it was found that a deficit in the kinetic energy was produced due to "droplets" of the metastable phase being reheated by energy transfer from the scalar field to the fluid. This has the effect of slowing the bubble walls, causing the gravitational wave signal to be suppressed. In our models we introduce this through the suppression function defined as

$$\Sigma(v_\mathrm{w}, \alpha) = \frac{\Omega_\mathrm{gw}}{\Omega_\mathrm{gw,exp}}\ , \tag{4.89}$$

where Ω_gw is the power spectrum found through the simulations in Ref. [118] and $\Omega_\mathrm{gw,exp}$ is the expected power spectrum found by the LISA Cosmology Working Group in Ref. [119]. It is customary to present the power spectrum with a factor of the observed Hubble parameter today h squared, and so multiplying by that on both sides we find the complete form of the power spectrum as

$$h^2\Omega_\mathrm{gw} = 2.061h^2F_\mathrm{gw,0}K^2_\mathrm{GKSV}(H_\mathrm{n}R_*)\left(1 - \frac{K^{1/4}_\mathrm{GKSV}}{\sqrt{K^{1/2}_\mathrm{GKSV} + 2H_\mathrm{n}R_*}}\right)\tilde{\Omega}_\mathrm{gw}C\left(\frac{f}{f_\mathrm{p,0}}\right)\Sigma(v_\mathrm{w}, \alpha)\ . \tag{4.90}$$

4.2.3 Signal to Noise Ratio (SNR)

Other than characterising the actual signal that will be received by the gravitational wave detector, the other consideration for practical experiments will be whether the detector itself is able to discern the signal from background noise due to its inherent sensitivity. The quantity used to measure this sensitivity is $\Omega_{\rm sens}$, which corresponds to the expected experiment sensitivity for a given configuration. This sensitivity is dependent upon noise based considerations such as the noise in the optical metrology system (or position noise) and the acceleration noise of a single test mass [120]. Obviously this varies from detector to detector, and so each experiment produces an in-depth determination of their apparatus' sensitivity. Specifically, in this thesis we consider the detection possibilities of three missions: LISA, Taiji, and TianQin. The LISA experiment and Taiji share very similar sensitivity thresholds (found in [121] and [7]), but TianQin will be focussed on a different parameter space, so its sensitivity calculation can be found in ref. [122]. Once the sensitivity is known, the signal-to-noise ratio can be calculated through the relation

$$\mathrm{SNR} = \sqrt{\mathcal{T} \int_{f_{\rm min}}^{f_{\rm max}} df \left[\frac{h^2 \Omega_{\rm gw}(f)}{h^2 \Omega_{\rm sens}(f)} \right]^2} \ , \tag{4.91}$$

where the ratio is squared and integrated over the frequency range in question. This is combined with the total duration time of the experiment mission $\mathcal{T}$.

4.3 Parameters of the Gravitational Wave Generating Phase Transition

4.3.1 Transition Strength α

The first parameter that we shall explore is the transition strength, broadly denoted by α. It is useful to quantify the strength of the transition as we can broadly classify types of transition by the value of this quantity, and we do this by considering the ratio of the difference in potential energy of the scalar field (trace anomaly) in both phases versus the enthalpy in the symmetric phase. The trace anomaly is defined as proportional to the trace of the energy-momentum tensor through the relation

$$\theta = -\frac{1}{4} g_{\mu\nu} T^{\mu\nu} = \frac{1}{4}\left(\rho - 3p\right) \ , \tag{4.92}$$

and so we define our transition strength from this as

$$\alpha_\theta = \frac{4}{3}\frac{\Delta\theta}{w_s} = \frac{4}{3}\frac{\theta_s - \theta_b}{w_s} \tag{4.93}$$

which also serves as a definition for Δ. An ultra-relativistic plasma for example which has equation of state $p/\rho = 1/3$ will therefore have no trace anomaly and zero transition strength in all cases. We can also rephrase this in terms of the effective potential, which can be more useful in situations where the potential is known directly. If we remember that the effective potential evaluated at the minima is simply the free energy, then $f = -p = V_T$. Recalling the definition of the enthalpy in terms of the entropy and temperature and also that the entropy can be written as a derivative of the pressure,

$$w = sT = T\frac{\partial p}{\partial T} = -T\frac{\partial V_T}{\partial T} \ . \tag{4.94}$$

Using the other definition for the enthalpy now in terms of the energy density and pressure (equation 3.43) we can write the energy density as

$$\rho = w - p = -T\frac{\partial V_T}{\partial T} + V_T \ , \tag{4.95}$$

and so combining these together gives the trace anomaly in terms of the effective potential as

$$\theta = \frac{1}{4}\left(4V_T(\phi) - T\frac{\partial V_T}{\partial T}\right) \ , \tag{4.96}$$

with the transition strength now being able to be written as

$$\alpha = -\frac{1}{3}\frac{\Delta\left(4V_T(\phi) - T\frac{\partial V_T}{\partial T}\right)}{T\frac{\partial V_T}{\partial T}\big|_s} \ . \tag{4.97}$$

Other definitions of the transition strength exist which are instead in terms of the latent heat

$$L = \rho_s(T_c) - \rho_b(T_c) \tag{4.98}$$

labelled as α_L or in terms of just the free energy or energy density in the numerator. As a quantity describing the strength at nucleation, the transition strength will always be evaluated at the nucleation temperature T_n unless otherwise stated. As mentioned previously, the value we calculate for the transition strength categorises the type of transition that is undergone. The transition labels are not rigidly set and flow continuously from one type to the next, but if we split the spectrum up into "weak", "intermediate", "strong", and "very strong" then we can roughly define them as

$$\begin{aligned} \text{weak: } & \alpha \lesssim 0.01 \ , \\ \text{intermediate: } & \alpha \sim 0.1 \ , \\ \text{strong: } & \alpha \sim 1 \ , \\ \text{very strong: } & \alpha \gg 1 \ . \end{aligned}$$

4.3.2 Transition Rate β

We also wish to know how quickly bubbles will appear in our system, as this will affect how quickly our space will fill up and how quickly we shall see collisions. The probability of nucleation per unit time per unit volume is [123]

$$p(t) = A(t)e^{-\Gamma_b(t)} \ , \tag{4.99}$$

whose time dependence is related to the non-zero cooling rate in the expanding Universe, meaning the expression can equally be cast into a form dependent upon temperature also. The pre-exponential factor is a non-trivial quantity and requires special treatments to understand in depth, first being derived in [97]. As we know from section 3.3 there will be two types of bubble depending on the temperature, which alters the symmetries: O(3) symmetric and O(4) symmetric bubbles. We therefore need to study both cases. For an O(3) symmetric bubble this pre-factor will take the form (in the static case)

$$A = T\left(\frac{\Gamma_{\mathrm{O}(3)}}{2\pi}\right)^{3/2}\left(\frac{\det'[-\partial_i\partial^i + V''(\phi,T)]}{\det[-\partial_i\partial^i + V''(0,T)]}\right)^{-1/2} \ , \tag{4.100}$$

where the notation $\det'$ indicates that zero eigenvalues are not considered when taking the determinant of the quantity. Correspondingly, for an O(4) symmetric bubble this pre-factor will be

$$A = \left(\frac{\Gamma_{\mathrm{O}(4)}}{2\pi}\right)^{2}\left(\frac{\det'[-\partial_i\partial^i + V''(\phi)]}{\det[-\partial_i\partial^i + V''(0)]}\right)^{-1/2} \ . \tag{4.101}$$

The difference in powers of action between these two is due to the zero modes of the operator $-\partial_\mu\partial^\mu + V''(\phi)$. Each zero mode produces a factor of $\left(\Gamma_{\mathrm{O(n)}}/2\pi\right)^{1/2}$, with the O(3) bubble containing three zero modes and the O(4) four zero modes. The transition rate is then defined through the relation

$$\beta \equiv \frac{d}{dt}\log\left(p(t)\right) \ , \tag{4.102}$$

and considering that as previously mentioned for an expanding Universe the temperature decreases as (from eq. 2.26)

$$\frac{dT}{dt} = -H(T)T \tag{4.103}$$

we can therefore translate this definition into a transition rate dependent upon temperature in units of the Hubble rate of

$$\frac{\beta}{H(T)} = T\frac{d}{dT}\Gamma_b(T) \ . \tag{4.104}$$

4.3.3 Nucleation Temperature $T_\mathbf{n}$

The temperature at which bubbles are defined to nucleate T_n requires a strict definition for how this quantity is determined, and so to state it plainly the definition I will use is that

> *The phase transition, and therefore when a bubble is nucleated, occurs when the probability of nucleation per unit volume $p(t)$ reaches one bubble per Hubble volume per Hubble time.*

In equation form, this translates to stating that nucleation happens when $p = H^4$. Remembering from the previous section on cosmology that for the early Universe when temperatures are high and the energy density is dominated by a relativistic plasma which goes as $\rho = \frac{\pi^2}{30} g_* T^4$, we can write the Hubble rate as [124]

$$H^2 = \frac{8\pi}{3M_P^2}\rho - \frac{k}{a^2} = \frac{4\pi^3 g_*}{45}\frac{T^4}{M_P^2} \ , \tag{4.105}$$

where M_P is the Planck mass, k is the Gaussian curvature of the Universe which we set to zero in the second equality, and a is the scale factor. Setting Eq. 4.99 equal to the square of Eq. 4.105 to satisfy our definition for nucleation, we have

$$\left(\frac{4\pi^3 g_*}{45}\right)^2 \frac{T^8}{M_P^4} = A(T) e^{-\Gamma_b} \ . \tag{4.106}$$

For the O(3) bubble, this is

$$\left(\frac{4\pi^3 g_*}{45}\right)^2 \frac{T^8}{M_P^4} = T^4 \left(\frac{\Gamma_{\mathrm{O}(3)}}{2\pi}\right)^{3/2} e^{-\Gamma_{\mathrm{O}(3)}} \ , \tag{4.107}$$

which we can rearrange to

$$2\log\left(\frac{4\pi^3 g_*}{45}\right) + 4\log\left(\frac{T}{M_P}\right) = \frac{3}{2}\log\left(\frac{\Gamma_{\mathrm{O}(3)}}{2\pi}\right) - \Gamma_{\mathrm{O}(3)}(T) \ . \tag{4.108}$$

The first and third term in Eq. 4.108 are both small compared to the second and fourth term so can be discarded, leaving the relevant equation at the nucleation temperature of

$$\Gamma_{\mathrm{O}(3)}(T_\mathrm{n}) = 4\log\left(\frac{M_P}{T_\mathrm{n}}\right) \ . \tag{4.109}$$

Due to the logarithmic nature of the result, for any temperature around the range of the electroweak phase transition range of about 100 GeV - 1 TeV we gain the same result that the action at the nucleation temperature is about 150. Due to this then, we specify that the nucleation temperature is defined as the temperature at which the bubble action reaches 150.

4.3.4 Wall Velocity v_{w}

To attempt a calculation of the wall velocity, we begin with the energy-momentum tensor of the model as before. The energy-momentum tensor of the fluid is given by

$$T_{\mathrm{f}}^{\mu\nu} = \int \frac{\mathrm{d}^3 p}{(2\pi)^3} \frac{p^\mu p^\nu}{p^0} f(p,x) \ , \tag{4.110}$$

where p^μ is the four-momentum and $f(p,x)$ is the distribution of the particles which make up the fluid. This is for a more generalised fluid, but for a perfect fluid in local equilibrium with a distribution

$$f^{\mathrm{eq}} = \frac{1}{e^{\beta u^\mu p_\mu} \pm 1} \ , \tag{4.111}$$

this simply reduces to the form used before in equation 2.12. The measure used in equation 4.110 can always be recast as

$$\int \frac{\mathrm{d}^3 p}{(2\pi)^3} \frac{1}{p^0} = \int \frac{\mathrm{d}^4 p}{(2\pi)^4} \delta\left(p^2 + m^2\right) \theta\left(p^0\right) \ , \tag{4.112}$$

which is often useful as it demonstrates that it transforms as a scalar under Lorentz transformations.

If we consider how the particle distribution will evolve in time, we make the substitutions:

$$\begin{aligned} x^\mu(\tau) &\to x^\mu(\tau) + \frac{dx^\mu(\tau)}{d\tau} d\tau = x^\mu(\tau) + \frac{p^\mu(\tau)}{m} d\tau \ , \\ p^\mu(\tau) &\to p^\mu(\tau) + \frac{dp^\mu(\tau)}{d\tau} d\tau = p^\mu(\tau) + F^\mu(\tau) d\tau \ , \end{aligned} \tag{4.113}$$

where F^μ is the four-force. Particle distributions without collisions must be constant when considering infinitesimal changes in time due to the conservation of particle number in infinitesimal phase space volume, and therefore we can write

$$f\left(p^\mu(\tau) + F^\mu(\tau) d\tau, x^\mu(\tau) + \frac{p^\mu(\tau)}{m} d\tau\right) = f(p^\mu, x^\mu) \ . \tag{4.114}$$

If, however, there are collisions, we must include the "collision function" $C[f]$ into this which describes the possibility of scattering removing and adding particles to the phase space volume element as

$$f\left(p^\mu(\tau) + F^\mu(\tau) d\tau, x^\mu(\tau) + \frac{p^\mu(\tau)}{m} d\tau\right) = f(p^\mu, x^\mu) + C[f] \ . \tag{4.115}$$

Taylor expanding the left-hand side to linear order in $d\tau = 0$, this gives the relation

$$f\left(p^\mu + F^\mu d\tau, x^\mu + \frac{p^\mu}{m} d\tau\right) = f(p,x) + F^\mu \frac{\partial f(p,x)}{\partial p^\mu} + \frac{p^\mu}{m} \frac{\partial f(p,x)}{\partial x^\mu} \ , \tag{4.116}$$

which we can insert in to equation 4.115 and rearrange to give

$$\left(m F^\mu \frac{\partial}{\partial p^\mu} + p^\mu \partial_\mu\right) \theta(p^0) \delta(p^2 + m^2) f(p,x) = C[f] \ . \tag{4.117}$$

Here we have inserted the factor $\theta(p^0)\delta(p^2+m^2)$ which is the on-shell condition which ensures that the differential equation is consistent. A further condition we impose is that particle number and momentum are conserved which is enforced through

$$\int \frac{d^3p}{(2\pi)^3}\frac{1}{2p^0}\Xi(p,x)C[f] = 0 \ , \tag{4.118}$$

where $\Xi(p,x)$ is any function constructed out of arbitrary sub-functions as $\Xi(p,x) = \zeta(x) + \varpi_\mu(x)p^\mu$. If we multiply both sides by the momentum and integrate, we find

$$0 = \int \frac{d^4p}{(2\pi)^4}p^\nu C[f] = \int \frac{d^4p}{(2\pi)^4}p^\nu \left(mF^\mu \frac{\partial}{\partial p^\mu} + p^\mu\partial_\mu\right)\theta(p^0)\delta(p^2+m^2)f(p,x) \ , \tag{4.119}$$

with both sides equalling zero due to the condition 4.118. Manipulating just the rightmost equation then, we can write this as

$$-mF^\nu \int \frac{d^3p}{(2\pi)^3}\frac{1}{2E}f(p,x) + \partial_\mu \int \frac{d^3p}{(2\pi)^3}\frac{p^\mu p^\nu}{2E}f(p,x) = 0 \ , \tag{4.120}$$

where we have used integration by parts on the first term with the relation $\partial p^\mu/\partial p^\nu = \delta^\nu_\mu$ and pulled the derivative out of the front of the second term then used equation 4.112 on both. Our definition for the fluid energy-momentum tensor in equation 4.110 can be inserted for

$$-mF^\nu \int \frac{d^3p}{(2\pi)^3}\frac{1}{2E}f(p,x) + \frac{1}{2}\partial_\mu T^{\mu\nu}_{\mathrm{f}} = 0 \ , \tag{4.121}$$

and finally, using the definition for the force and the substitution $dm/dm^2 = (2m)^{-1}$ this leaves

$$\partial_\mu T^{\mu\nu}_{\mathrm{f}} = -\partial^\nu\phi\frac{dm^2}{d\phi}\int \frac{d^3p}{(2\pi)^3}\frac{1}{2E}f(p,x) \ . \tag{4.122}$$

The overall energy-momentum must be conserved, so

$$\partial_\mu T^{\mu\nu} = \partial_\mu T^{\mu\nu}_\phi + \partial_\mu T^{\mu\nu}_{\mathrm{f}} = 0 \ . \tag{4.123}$$

As we have just found out what the second term in that equals, we now work through the derivative of the field EM tensor. Using 3.84,

$$\begin{aligned}\partial_\mu T^{\mu\nu}_\phi &= \partial_\mu\partial^\mu\phi\partial^\nu\phi + \partial^\mu\phi\partial_\mu\partial^\nu\phi - \partial^\nu\left(g^{\alpha\beta}\partial_\alpha\phi\partial_\beta\phi + V(\phi)\right)\\ &= \partial^\nu\phi\left(\partial^\mu\partial_\mu\phi - \partial_\phi V(\phi)\right) \ .\end{aligned} \tag{4.124}$$

From the conservation equation 4.123 then and the result of the derivative of the fluid EM tensor equation 4.122, this implies a relation of (after dividing through by a common factor)

$$\partial^\mu\partial_\mu\phi - \partial_\phi V(\phi) = -\frac{dm^2}{d\phi}\int \frac{d^3p}{(2\pi)^3 2E}f(p,x) \ , \tag{4.125}$$

i.e. that the non-conservation of the fluid energy-momentum much be compensated for through a term in the conservation of the scalar field. The distribution can be decomposed into

$$f(p,x) = f^{\mathrm{eq}}(p,x) + \delta f(p,x) \ , \tag{4.126}$$

where $f^{\mathrm{eq}}(p,x)$ is the equilibrium distribution function and $\delta f(p)$ is the departure from equilibrium. This allows equation 4.125 to be rewritten as

$$\partial^\mu \partial_\mu \phi - \partial_\phi V(\phi) = -\frac{dm^2}{d\phi} \int \frac{d^3p}{(2\pi)^3 2E} \delta f(p,x) + \partial_\phi V(\phi, T) \ , \tag{4.127}$$

and we can combine the components of the potential into the "thermal potential" $V_T(\phi, T) = V(\phi) + V(\phi, T)$ to leave

$$\partial^\mu \partial_\mu \phi - \partial_\phi V_T(\phi) = -\frac{dm^2}{d\phi} \int \frac{d^3p}{(2\pi)^3 2E} \delta f(p,x) \ . \tag{4.128}$$

Linear response theory gives us an indication of what the right-hand side should analogously act like, with the integral behaving proportionally to the gradient of the scalar field as

$$\int \frac{d^3p}{(2\pi)^3 2E} \delta f(p,x) = \eta u^\mu \partial_\mu \phi \ . \tag{4.129}$$

This quantity can be thought of as a "friction" term; as the particle distributions deviate from equilibrium, this term will in effect slow the wall as it attempts to expand. If we use this ansatz, we can explore what this will mean for the wall speed then. Our equation of motion is

$$\partial^\mu \partial_\mu \phi - \partial_\phi V_T(\phi) = -\eta \frac{dm^2}{d\phi} u^\mu \partial_\mu \phi \ , \tag{4.130}$$

and we can consider the wall moving in just the z-direction to simplify this to

$$\partial_z^2 \phi - \partial_\phi V_T(\phi) = -\tilde{\eta} \gamma v \partial_z \phi \tag{4.131}$$

where we have absorbed the dependence on mass as $\tilde{\eta} = \eta dm^2/d\phi$. As we can see, we now have an equation in terms of the velocity for the situation. In practical terms though, many things are still unknown and exceedingly difficult to calculate effectively. The ansatz in equation 4.129 is phenomenologically motivated, and the exact details of the relation are elusive. Further to this, the calculation would require solving a coupled system involving Boltzmann equations for particle species with a large coupling to the Higgs field [119]. Whilst this has indeed been done somewhat for the standard model [125] and minimally supersymmetric standard model (MSSM) [126], these analyses are valid only for small deviations from equilibrium, $\delta f(p,x) \ll f^{\mathrm{eq}}(p,x)$, which correspond to weakly first-order phase transitions. In our work we will consider far beyond just weak transitions, so there is effectively no realistic and accurate method as of yet for calculating the wall speed generally.

4.3.5 Sound Speed c_s^2

Finally, let us turn to the sound speed. The quantity itself is important in phase transitions of this sort as it will determine the hydrodynamics associated with the motion of the bubble walls [127] and which type of situation our fluid is in; deflagration, hybrid, or detonation. The conformal value of the speed of sound is $c_s^2 = 1/3$ which corresponds to a relativistic plasma and is the value most often used to approximate. Whilst useful for estimations, this value cannot account for any models with more realistic particle physics. For general equations of state for example the sound speed is temperature dependent and differs depending on whether you are in the symmetric or broken phase. We define the speed of sound as

$$c_s^2 \equiv \frac{\partial p/\partial T}{\partial \rho/\partial T} \ , \tag{4.132}$$

noting that this can take two forms of $c_{s,b}^2$ and $c_{s,s}^2$ for the value in the broken and symmetric phases respectively.

How does this quantity actually affect the hydrodynamics then? Let us consider once again the energy-momentum tensor of the fluid from equation 2.12 and take the quantity $u_\nu \partial_\mu T^{\mu\nu}$. Projecting along the flow direction of the fluid with $u_\mu \partial_\nu u^\mu = 0$ gives

$$\partial_\mu (u^\mu w) - u_\mu \partial^\mu p = 0 \ , \tag{4.133}$$

and projecting perpendicular to the flow direction gives

$$\overline{u}^\nu u^\mu w \partial_\mu u_\nu - \overline{u}_\mu \partial^\mu p = 0 \ . \tag{4.134}$$

For bubble solutions we may reformulate the situation into a spherically symmetric bubble, which can be well described by the parameter $\xi = r/t$ (where r is the bubble centre distance and t is the time since the nucleation of the bubble) due to the system being "self-similar", *i.e.* the system appears the appears constant in the reference of this parameter ξ. We may therefore express the gradients as

$$u_\mu \partial^\mu = -\frac{\gamma}{t}(\xi - v)\partial_\xi \ , \quad \overline{u}_\mu \partial^\mu = \frac{\gamma}{t}(1 - \xi v)\partial_\xi \ , \tag{4.135}$$

which when used in equations 4.133 and 4.134 give us

$$\begin{aligned} (\xi - v)\frac{\partial_\xi \rho}{w} &= 2\frac{v}{\xi} + [1 - \gamma^2 v(\xi - v)]\partial_\xi v \ , \\ (1 - v\xi)\frac{\partial_\xi p}{w} &= \gamma^2 (\xi - v)\partial_\xi v \ . \end{aligned} \tag{4.136}$$

Using our definition we presented for the speed of sound in equation 4.132 we find that one combination of these two formulae gives

$$\frac{\partial v}{\partial \xi} = \frac{2v}{\xi\gamma^2(1-v\xi)}\frac{c_s^2}{\mu^2 - c_s^2} \ , \tag{4.137}$$

where

$$\mu(v,\xi) = \frac{\xi - v}{1-\xi v} \ , \tag{4.138}$$

which is the fluid-velocity when Lorentz transformed. The other combination of the two formulae along with what was just found in equation 4.137 gives

$$\frac{\partial w}{\partial \xi} = w\left(1 + \frac{1}{c_s^2}\right)\gamma^2\mu\frac{\partial v}{\partial \xi} \ . \tag{4.139}$$

As we can see, the sound speed heavily influences the profiles of the velocity and the enthalpy, and it is usual to define the type of transition that is undergone in reference to the speed of sound. There are three types of solutions which are allowed by the hydrodynamic equations as mentioned previously: deflagration, hybrid, or detonation.

Deflagration - In this type, the wall is subsonic ($v_{\rm w} < c_{s,b}^2$). The fluid forms a "shock" in front of the wall pulling the bubble outwards, while the fluid behind the wall is at rest.

Detonation - In this type, the wall is explosive in nature. The bubble wall velocity is supersonic ($v_{\rm w} > c_{s,b}^2$), and is being pushed out from behind through a rarefaction wave whilst the fluid in front is at rest.

Hybrid - A combination of both as the name suggests, the hybrid solution has elements of a detonation and deflagration by containing a shockwave and a rarefaction wave. The dependence on the sound speed is more complicated, and the wall velocity falls in the range larger than the broken phase sound speed but smaller than the Jouguet velocity defined through [117]

$$\xi_J = \frac{1+\sqrt{3\alpha_\theta(1-c_s^2+3c_s^2\alpha_\theta)}}{1/c_s + 3c_s\alpha_\theta} \ . \tag{4.140}$$

Chapter 5

String Theory, Anti-de Sitter Spacetimes, and Conformal Theories

5.1 Conformal Field Theories

Conformal Field Theories (CFTs) are an integral part to exploring the dualities of string theory. These are a class of quantum field theories which retain their symmetry under conformal transformations, *i.e.* those transformations that respect

$$g_{\mu\nu}(x) \to g'_{\mu\nu}(x') = \Omega(x) g_{\mu\nu}(x) \tag{5.1}$$

by leaving the metric invariant up to a scale change (where $\Omega(x)$ is the scale transformation). This scaling symmetry preserves angles and the causal structure as well as inherently preserves the Poincaré group symmetries (briefly described in appendix H) as the metric transforms like $g'_{\mu\nu}(x') = g_{\mu\nu}(x)$ such that the symmetry of the full group of transformations is $\mathrm{SO}(2, d)$.

By taking the infinitesimal coordinate transformation $x^\mu \to x^\mu + \epsilon^\mu(x)$ we see that the metric will transform as

$$\begin{aligned} ds^2 = \eta_{\mu\nu} dx^\mu dx^\nu &\to (\eta_{\mu\nu} + \partial_\mu \epsilon_\nu + \partial_\nu \epsilon_\mu) dx^\mu dx^\nu \\ &= ds^2 + (\partial_\mu \epsilon_\nu + \partial_\nu \epsilon_\mu) dx^\mu dx^\nu \ , \end{aligned} \tag{5.2}$$

and to satisfy the the condition in equation 5.1 that this transformation appears as an overall multiplicative factor to the metric we require

$$\partial_\mu \epsilon_\nu + \partial_\nu \epsilon_\mu = a \eta_{\mu\nu}, \tag{5.3}$$

where a is the constant of proportionality. Tracing over both sides then fixes the constant as $a = \frac{2}{d}\partial^\mu \epsilon_\mu$ and taking a double derivative of eq. 5.3 then gives the condition (known as the Killing equation)

$$(\eta_{\mu\nu}\Box + (d-2)\partial_\mu\partial_\nu)\partial_\rho\epsilon^\rho = 0 \ . \tag{5.4}$$

As can be seen there is a special case for this condition at $d = 2$, however we shall limit our discussion to the cases of $d > 2$. From equation 5.4 we recognise that for $d > 2$ the quantity ϵ_μ can be at maximum second-order in x (due to the requirement that $\partial^3\epsilon = 0$) and so this determines the possibilities for transformations. The most general form that ϵ_μ can take is

$$\epsilon_\mu(x) = a_\mu + \omega^\nu{}_\mu x_\nu + \lambda x_\mu + b_\mu x_\rho x^\rho - 2x_\mu b_\rho x^\rho \ , \tag{5.5}$$

with each term representing a set of specific transformations as follows:

- a_μ: These represent usual translations.
- $\omega^\nu{}_\mu x_\nu$: These represent Lorentz transformations.
- λx_μ: These represent scale transformations (also known as dilatations).
- $b_\mu x_\rho x^\rho - 2x_\mu b_\rho x^\rho$: These are the "special conformal transformations", where b_μ is an arbitrary constant 4-vector.

We can associate generators with each of these, and so we find that the generators of the translations are P_μ, the generators of the rotations are $M_{\mu\nu}$, the generator of dilatations is the operator D, and the generators of the special coordinate transformations is the operator K_μ.

Together these transformations form the "conformal transformations" and satisfy the conformal algebra which is comprised of the Poincaré algebra along with the commutation relations

$$\begin{aligned}
[M_{\mu\nu}, K_\rho] &= i(\eta_{\mu\rho}K_\nu - \eta_{\nu\rho}K_\mu) \ , \\
[D, P_\mu] &= iP_\mu \ , \\
[D, K_\mu] &= -iK_\mu \ , \\
[D, M_{\mu\nu}] &= 0 \ , \\
[K_\mu, K_\nu] &= 0 \ , \\
[K_\mu, P_\nu] &= -2i(\eta_{\mu\nu}D - J_{\mu\nu}) \ .
\end{aligned} \tag{5.6}$$

What does a quantum field theory with these properties look like then? The fields in these CFTs will transform in irreducible representations of the conformal algebra. Under dilatations $x \to \lambda x$ the fields would transform as

$$\phi(x) \to \lambda^{-\Delta}\phi(x) \ , \tag{5.7}$$

where Δ is the scaling dimension of the field. In a simple theory with for example just a scalar field and quartic interaction these dilatation transformations would indeed leave the action invariant then, but the inclusion of a mass term would break the invariance. If we explore the symmetries we see that the translations and Lorentz transformations will give conserved currents as usual of the energy-momentum (EM) tensor $T_{\mu\nu}$ and the current $N_{\mu\nu\rho} = x_\nu T_{\mu\rho} - x_\rho T_{\mu\nu}$ respectively through Noether's theorem. The new symmetries of the dilatations and special conformal transformations will also be associated with conserved currents, given by

$$J^D_\mu = T_{\mu\nu}x^\nu \quad \text{and} \quad J^K_{\mu\nu} = x^2 T_{\mu\nu} - 2x_\nu x^\rho T_{\mu\rho} \ . \tag{5.8}$$

If we work through these currents we see that conservation of the energy momentum tensor $\partial^\mu T_{\mu\nu} = 0$ automatically conserves $N_{\mu\nu\rho}$ if the EM tensor is symmetric. The conservation equations for the new currents with these conditions are

$$\partial^\mu J^D_\mu = T^\mu_\mu \quad \text{and} \quad \partial^\mu J^K_{\mu\nu} = -2T^\mu_\mu x_\nu \ , \tag{5.9}$$

and so we see that the requirement for conformal invariance in a field theory is that the energy-momentum tensor is traceless, *i.e.* $T^\mu_\mu = 0$.

When is this condition satisfied in a quantum field theory? Through renormalisation we discover that the couplings can run, that is that they have a dependence upon some energy scale μ through the beta function

$$\beta(g) = \mu\frac{\partial g}{\partial \mu} \ , \tag{5.10}$$

where g is the set of couplings of a theory; this necessitates the presence of the renormalisation group (RG) and its ability to flow in a quantum field theory. When considering renormalisation, we renormalise our fields as $\phi_r = Z_\phi^{-1/2}\phi_0$, where Z_ϕ is the field renormalisation factor and ϕ_0 is the bare field (*i.e.* the one which appears in a Lagrangian). Our previous scaling dimension of the field in equation 5.7 will subsequently be modified to the form

$$\Delta = \Delta_0 + \gamma(g) \ , \tag{5.11}$$

where Δ_0 is the original classical scaling dimension and $\gamma(g)$ is the anomalous dimension given by

$$\gamma(g) = \frac{1}{2}\frac{\mu}{Z_\phi}\frac{\partial Z_\phi}{\partial \mu} \ . \tag{5.12}$$

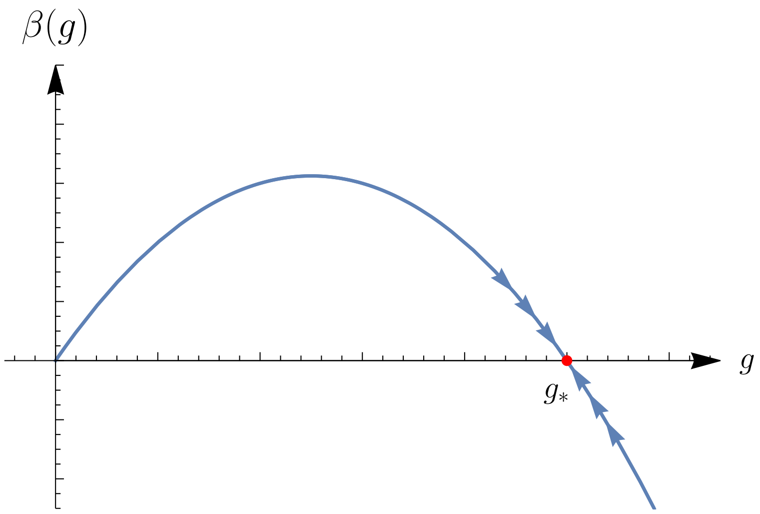

Figure 5.1: A sketch of an RG flow with a UV fixed point (shown as a red dot). The shape of the flow indicates that the coupling grows with energy scale up to a certain point at which the flow reverses and the coupling shrinks. The arrows indicate the flow towards the fixed point.

Due to this, some theories with classical conformal invariance do not maintain their conformal invariance when promoted to a quantum mechanical setting. Theories which are classically scale invariant but lose this property under quantum mechanics are said to acquire a trace anomaly when[1]

$$T^{\mu}_{\mu} \neq 0 \ . \tag{5.13}$$

If in quantum field theories classical scale invariance is broken by these quantum considerations at different energy scales, is it ever possible to obtain a conformal field theory? By examining equation 5.10 we see that the field theory continues to be conformal (scale invariant) only when $\beta(g) = 0$, *i.e.* when the coupling has no dependence upon μ. These are known as fixed points of the renormalisation group flow, and it is where we will locate our CFTs. From this condition then we can find quantum field theories which are conformal in two ways:

- The theory has value $\beta(g) = 0$ for all couplings, and are known as finite theories. These theories do not "flow", and so are conformal even at the quantum level, with the coupling tracing out a line (or manifold) of fixed points. A theory of particular importance in this class is that of $\mathcal{N} = 4$ SYM (Supersymmetric Yang-Mills) theory, where the contributions to the beta-function from scalars and fermions precisely balances out the contribution of the gauge fields to at least third-order in loops

[1] however this property alone does not imply that the theory was originally classically scale invariant.

[128, 129, 130, 131]. We shall explore this in more details later.

- The theory has particular points g_* which satisfy $\beta(g_*) = 0$, known as the "fixed points" of the renormalisation group. Here the theory can flow at different energy scales and therefore will contain a trace anomaly, but at these fixed points we will recover the CFT with $T^\mu_\mu = 0$ and the RG equation reduces to the Ward identity for dilatations. An example of such a theory is shown in figure 5.1.

The restriction to a CFT imposes quite stringent limitations on the correlation functions for this type of quantum field theory. Enforcing invariance of the action leads to the dilatation Ward identity as just mentioned which takes the form

$$\sum_{i=1}^{n}\left(x_i^\mu \frac{\partial}{\partial x_i^\mu} + \Delta_i\right)\langle\phi_1(x_1)\phi_2(x_2)\ldots\phi_i(x_I)\ldots\phi_n(x_n)\rangle = 0 \ , \tag{5.14}$$

where Δ_i is the scaling dimension for each particular field ϕ_i. The invariances present in conformal transformations therefore restrict the forms of the two- and three-point functions, which can be found as [132]

$$\langle\mathcal{O}(x_1)\mathcal{O}(x_2)\rangle = \frac{1}{(x_1 - x_2)^{2\Delta}} \tag{5.15}$$

and

$$\langle\mathcal{O}(x_1)\mathcal{O}(x_2)\mathcal{O}(x_3)\rangle = \frac{C_{123}}{(x_1 - x_2)^{\Delta_1+\Delta_2-\Delta_3}(x_2 - x_3)^{-\Delta_1+\Delta_2+\Delta_3}(x_1 - x_3)^{\Delta_1-\Delta_2+\Delta_3}} \ , \tag{5.16}$$

where $\mathcal{O}_i$ are the operators and Δ_i are their scaling dimensions as mentioned previously; higher point functions are determined entirely in terms of these.

5.2 Anti-de Sitter Spacetimes

Due to the vital role that anti-de Sitter spacetimes play in the correspondence which we utilise in this work, we need to understand some of its basic properties. The de Sitter (and the related Anti-de Sitter) spacetimes are maximally symmetric manifolds with either positive or negative constant curvature respectively (in the form of a positive or negative cosmological constant); in this work we will focus on anti-de Sitter spacetimes. The action which anti-de Sitter space corresponds to is the Einstein-Hilbert action of

$$S = \frac{1}{16\pi G_{d+1}}\left(\int_{\mathcal{M}} d^{d+1}x\sqrt{-g}\,(R - 2\Lambda) - 2\int_{\partial\mathcal{M}} d^d x\sqrt{-\gamma}K\right) \ , \tag{5.17}$$

where G_{d+1} is the $(d+1)$-dimensional gravitational constant, Λ is the cosmological constant, $\mathcal{M}$ is the manifold and $\partial\mathcal{M}$ is the boundary of the manifold. The second term is the Gibbons-Hawking-York (GHY) term for bounded surfaces where $\gamma_{\mu\nu}$ is the induced metric of the surface and $K = K^{\mu\nu}\gamma_{\mu\nu}$ is the trace of the extrinsic curvature. This action will give vacuum field equations of

$$R_{\mu\nu} - \frac{1}{2}Rg_{\mu\nu} + \Lambda g_{\mu\nu} = 0 \ , \tag{5.18}$$

which can be contracted to find the Ricci scalar of

$$R = 2\frac{d+1}{d-1}\Lambda \ . \tag{5.19}$$

Replacing this in the field equations now gives the Ricci tensor

$$R_{\mu\nu} = \frac{2}{d-1}\Lambda g_{\mu\nu} \ . \tag{5.20}$$

To understand the meaning of this sort of geometry we must embed it. To do so we consider embedding in $\mathbb{R}^n$, specifically we embed $(n+1)$-dimensional AdS_{n+1} as a submanifold in the flat space $(n+2)$-dimensional flat space manifold $\mathbb{R}^{n+2}$ with metric

$$ds^2 = \eta_{MN}dX^M dX^N = -dX_0^2 + \sum_{i=1}^{d} dX_i^2 - dX_{d+1}^2 \ . \tag{5.21}$$

This means that the AdS can be defined as the hyperboloid in this space with equation

$$-L^2 = \eta_{MN}X^M X^N = -X_0^2 + \sum_{i=1}^{d} X_i^2 - X_{d+1}^2 \ , \tag{5.22}$$

where L^2 is a quantity defined as the radius of the AdS space. With some basic definitions now complete we can explore some properties of this type of space. We may transform the space into the type originally considered by Maldacena [133] and follow his work by taking the parametrisation

$$\begin{aligned} X_0 &= \frac{L^2}{2r}\left(1 + \frac{r^2}{L^4}(-t^2 + \vec{x}^2 + L^2)\right) \ , \\ X_i &= \frac{rx_i}{L} \ , \quad i \in \{1, \ldots, d-1\} \ , \\ X_d &= \frac{L^2}{2r}\left(1 + \frac{r^2}{L^4}(-t^2 + \vec{x}^2 - L^2)\right) \ , \\ X_{d+1} &= \frac{rt}{L} \ , \end{aligned} \tag{5.23}$$

where we note now that we only cover half of the spacetime due to the restriction of $r > 0$ leading to "local coordinates". These local coordinates are presented in the form of a Poincaré patch, and from this we see that we can write the metric as

$$ds^2 = \frac{L^2}{r^2}dr^2 + \frac{r^2}{L^2}\eta_{\mu\nu}dx^\mu dx^\nu \ , \tag{5.24}$$

with the usual definition for the d-dimensional flat metric $\eta_{\mu\nu}$. Finally we can make another substitution, this time of $z = L^2/r$, to transform the metric into

$$ds^2 = g_{MN}dx^M dx^N \equiv \frac{L^2}{z^2}(dz^2 + \eta_{\mu\nu}dx^\mu dx^\nu) \ . \tag{5.25}$$

If we construct the curvature tensors through the usual methods using this metric we find that the Ricci tensor is

$$R_{\mu\nu} = -\frac{d}{L^2}g_{\mu\nu} \ , \tag{5.26}$$

and therefore comparing this form with the form from the field equations in 5.20 we can see that the cosmological constant is simply

$$\Lambda = -\frac{d(d-1)}{2L^2} \ . \tag{5.27}$$

Finally for completeness we recognise that this definition for the cosmological constant would transform the Ricci scalar into

$$R = -\frac{d(d+1)}{L^2} \ . \tag{5.28}$$

How can we view these descriptions of AdS spacetime? We see from equation 5.25 that we may treat it as flat spacetime with the usual temporal and spatial components $t, \vec{x}$, along with an extra dimension parameterised by the coordinate z which due to its domain and appearing as an overall factor takes the metric from infinitely small to infinitely large. Further to this we recognise that for constant values of z we are left simply with flat spacetime multiplied by an overall conformal factor, and in this way we can see the AdS space as being built of infinitely many slices of flat spacetime stacked on top of each other; for example in the specific case of AdS_5 we have infinitely many versions of normal 4-dimensional flat Minkowski spacetime built together to form the fifth dimension. We demonstrate an idea of how this would appear in figure 5.2. If we look at the limiting cases of the AdS space we see that as the extra dimension takes the limit $z \to 0^+$ we have a second-order singularity but also this case is conformally equivalent to the Minkowski metric and so we can describe the anti-de Sitter space as having a conformal Minkowski space at infinity. We also see that in metric 5.24 there will be a singularity at $r \to 0^+$, equivalent to $z \to \infty$ for metric 5.25. As this singularity only occurs in the r dependent metric it is obvious that it is a coordinate singularity rather than a true curvature singularity, however we can still glean some interesting information from it. To cover the full spacetime we would also need another Poincaré patch in the region $r \in \{-\infty, 0^-\}$ (equivalent to $z \in \{0^-, -\infty\}$), and so we can deduce that the coordinate singularity present in that limit is actually demonstrating the presence of a Poincaré horizon.

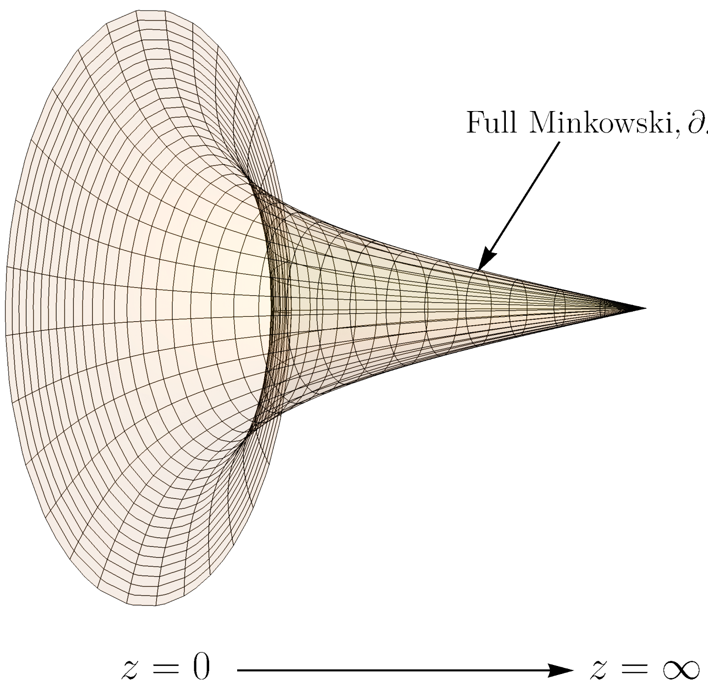

Figure 5.2: A sketch of AdS space. At $z = 0$ we have the coordinate horizon and at $z \to \infty$ we have the Poincaré horizon. Each "plane" that can be seen represents taking a slice of the manifold $\partial\mathcal{M}$ at that $z =$ const and seeing that it is flat Minkowski space; there are infinitely many of these.

At finite temperature, this description also must include a black hole in the spacetime, which will be discussed later.

With basic properties of both conformal field theories and anti-de Sitter spacetimes in hand then we shall move on to one other necessity for the discussion of strings, the idea of supersymmetries.

5.3 Supersymmetry (SUSY)

Another extension to the Standard Model which contains a new class of symmetries and was a major influence on the development of string theory is supersymmetry, also known as SUSY. Similarly to conformal theories this is an extension of Poincaré algebra with extra symmetries which are known as "supersymmetries", and in fact we may state that including supersymmetry enhances the conformal group to a conformal supergroup which extends the conformal algebra to a superconformal algebra. However the similarities end there. In 1967 Coleman and Mandula put forth their "no-go theorem" [134] which effectively states that there is no non-trivial way to combine spacetime and internal symmetries. This can be bypassed by the consideration of "anti"-commuting symmetry generators instead of the ones we are used to, and the main effect of these is that a supersymmetric transformation alters the spin by 1/2, *i.e.* the supersymmetric generators Q act on the quantum states by turning a boson into a fermion and vice versa through

$$Q|\text{boson}\rangle = |\text{fermion}\rangle \quad \text{and} \quad Q|\text{fermion}\rangle = |\text{boson}\rangle \ . \tag{5.29}$$

As supersymmetry is important to string theory as a whole but not integral to our work we shall only go briefly through the most important points. Supersymmetry extends the Poincaré algebra with the addition of anticommuting generators which are spinors in nature that we can denote by Q^a_α for the left-handed spinor and $\bar{Q}_{a\dot{\alpha}}$ for the right-handed spinor. The index α is the spinor index and $a = 1, \ldots, \mathcal{N}$ denotes the number of independent supersymmetries, which for this discussion we shall restrict to $\mathcal{N} = 1$. The algebra (also called the *superalgebra*) for this situation is given by

$$\begin{aligned}
\{Q_\alpha, Q_\beta\} &= \{\bar{Q}_{\dot{\alpha}}, \bar{Q}_{\dot{\beta}}\} = 0 \\
[Q_\alpha, P^\mu] &= [\bar{Q}_{\dot{\alpha}}, P^\mu] = 0 \\
\{Q_\alpha, \bar{Q}_{\dot{\alpha}}\} &= 2\sigma^\mu_{\alpha\dot{\alpha}} P_\mu \\
[Q_\alpha, M^{\mu\nu}] &= (\sigma^{\mu\nu})_\alpha^\beta Q_\beta \\
[\bar{Q}^\alpha, M^{\mu\nu}] &= (\bar{\sigma}^{\mu\nu})^{\dot{\alpha}}_{\dot{\beta}} \bar{Q}^{\dot{\beta}} \ ,
\end{aligned} \tag{5.30}$$

where $\epsilon_{\dot{\alpha}\dot{\beta}}$ and $\epsilon_{\alpha\beta}$ can be used to raise and lower spin indices and we have defined the quantities $\sigma^{\mu\nu} = \frac{1}{4}(\sigma^\mu\bar{\sigma}^\nu - \sigma^\nu\bar{\sigma}^\mu)$ and $\bar{\sigma}^{\mu\nu} = \frac{1}{4}(\bar{\sigma}^\mu\sigma^\nu - \bar{\sigma}^\nu\sigma^\mu)$ which are formed of the Pauli matrices σ^μ and their barred counterparts $\bar{\sigma}^\mu$ defined through $(\bar{\sigma}^\mu)^{\dot{\alpha}\alpha} = \epsilon_{\alpha\beta}\epsilon_{\dot{\alpha}\dot{\beta}}(\sigma^\mu)_{\beta\dot{\beta}}$.

5.4 String Theory

String theory in certain formulations has been a contender for a Grand Unified Theory (and possibly a Theory of Everything) for many years due to its ability to explain links between areas of physics much more elegantly than many other theories that have come before it. However it did not first start like this, and it certainly was not intended as such. String theory began in earnest in the 1960's as an attempt to explain the nature of hadrons through the strong nuclear force such as in references [135, 136]. It was quickly discarded however as even though it had some success explaining desired properties it also predicted the existence of anomalies such as a massless spin-2 particle, something not observed nor expected in experiments. Further to this, the newly formulated quantum chromodynamics (QCD) had proven to be exactly what was needed to explain the strong force, moving focus away from string theory. This property of a massless spin-2 particle was later realised to be the perfect candidate for the graviton, and that along with multiple other characteristics led theorists to study string theory now as a basis for quantum gravity. Let us go through some of the basics that lead us to the enthralling and integral dualities of string theory.

Where string theory differs from the conventional view of particles in the Universe is that "normal" particles were thought to be pointlike, that is have no spatial dimensions (which in itself is one of the reasons for the large number of infinities present); string theory posits that the fundamental constituents are instead formed of one-dimensional "string-like" objects, which can be either open or closed in nature. Whereas a traditional point-like particle will trace out the familiar one-dimensional worldline as it moves through spacetime, a string will instead trace out a two-dimensional "worldsheet". The excitations of these particular objects (like the excitations of a violin string corresponding to a note or overtone) correspond to the spectra of particles.

5.4.1 Bosonic String Theory

This was the first incarnation of string theory, and it is named as such as it can only attempt to explain the bosonic sector. There are two main topologies present in bosonic string theory: open and closed strings. Open strings will have two endpoints whereas closed strings will obviously have no endpoints. A fundamental string is a particular case of a p-brane, which in more familiar language is just a p-dimensional object which moves through spacetime. In particular, a point particle as is usual is identified as being a $p = 0$ brane and a string can be identified as a one-brane (*i.e.* with $p = 1$). These strings or one-branes are especially important as their quantum theories are renormalisable.

There are two equivalent ways of writing the string theory action at a classical level in terms of the spacetime embedding of the string worldsheet $X(\sigma, \tau)$, where σ and τ are the two parameters necessary to specify a point on a two-dimensional worldsheet. These are the Nambu-Goto action (using the convention $d^2\tilde{\sigma} = d\sigma d\tau$)

$$S_{\text{NG}} = -\frac{1}{2\pi\alpha'} \int_{\Sigma} d^2\tilde{\sigma} \sqrt{-\det(g_{MN}\partial_\alpha X^M \partial_\beta X^N)}\ , \tag{5.31}$$

which has a more readily distinguishable physical interpretation but is difficult to quantise due to its square-root form (where here g_{MN} is the metric on the $(d+1)$-dimensional spacetime), and the Polyakov action

$$S_{\mathrm{P}} = -\frac{1}{4\pi\alpha'}\int_{\Sigma} d^2\tilde{\sigma}\sqrt{-h}h^{\alpha\beta}g_{MN}\partial_\alpha X^M\partial_\beta X^N \tag{5.32}$$

which is more predisposed to quantisation. The Polyakov action is built upon an auxiliary worldsheet metric $h_{\alpha\beta}$, and both actions contain as an overall factor the inverse string tension or "Regge slope" α' which is related to the string tension T through $T = 1/(2\pi\alpha')$. Through dimensional analysis we can also associate the Regge slope to the natural length scale of the model as

$$\alpha' = l_s^2 \ , \tag{5.33}$$

where l_s is the string length. In many ways this string length can be thought of as the only meaningful scale and parameter in string theory.

As previously mentioned, this type of theory permits open and closed strings. These are subject to certain boundary conditions, namely Dirichlet and Neumann conditions. In a closed string the embedding functions are periodic *i.e.* $X^\mu(\sigma,\tau) = X^\mu(\sigma+\pi,\tau)$ (where we choose that the coordinate σ has bounds $-\pi \leq \sigma \leq \pi$), but for an open string we can have either Neumann conditions at the end of the string (which corresponds to $X'_\mu[\sigma = -\pi,\pi] = 0$) or Dirichlet conditions (which corresponds to $X_\mu[\sigma = -\pi] = a$, $X_\mu[\sigma = \pi] = b$ where a, b are constants).

It does not make sense for the open strings to have free endpoints on nothing and just end anywhere, and so this allows us to introduce new dynamical objects called "D-branes" which are named after the requirement for Dirichlet boundary conditions (also called Dp-branes where p is the spatial dimension) which these endpoints live on. These branes have tension and so are affected by gravity and interactions with other objects; they are meaningful stringy objects in their own right.

For any sort of theory which attempts to describe the Universe we expect to be able to quantise it, and so we do the same with this theory. Under this procedure, the quantum operators form what is known as the "Virasoro algebra" [137]. Introducing light-cone coordinates on the worldsheet of

$$\sigma^\pm = \tau \pm \sigma \ , \tag{5.34}$$

we may decompose the worldsheet solution X^μ into left-moving ($X_L^\mu(\sigma^+)$) and right-moving ($X_R^\mu(\sigma^-)$) waves. The Virasoro generators L_m and $\tilde{L}_m$ are formed from the modes of the *left-movers* and *right-movers* of the string α_{-n}^μ and $\tilde{\alpha}_{-n}^\mu$ which are each described by a conformal field theory, and the quantum version of this algebra satisfies

$$[L_m, L_n] = (m-n)L_{m+n} + \frac{c}{12}m(m^2-1)\delta_{m+n,0} \ , \tag{5.35}$$

where c is the central charge, also equal to the spacetime dimension $c = D$. Only with the choice of spacetime dimension $D = 26$ does the string spectrum under this algebra not contain the non-physical negative norm states, and so this is known as the critical dimension.

This is not the only way to find the dimension necessary for bosonic string theory. Another way is to consider that under a scale transformation on the curved worldsheet we find that the trace of the energy-momentum tensor goes as

$$T^\mu_\mu \propto (D-26)R \ , \tag{5.36}$$

which leads us to the conclusion that to remove the trace anomaly and maintain the symmetries found classically then bosonic string theory can only be quantised if we make the choice $D = d + 1 = 26$.

In the end though it was found that bosonic string theory is obviously unsuitable for a realistic description of nature: not only can it not account for fermions, it has a severe problem with tachyonic states. Although thought to be a theory killer for a long time, string theory eventually underwent another revolution as we shall see next.

5.4.2 Superstring Theory

The next step in the evolution is superstring theory, which attempts to solve some of the difficulties on bosonic string theory. The discovery of supersymmetry in 1971 and its properties mentioned in section 5.3 led to the incorporation of SUSY into string theory as superstring theory initially by Ramond [138] and also by Neveu and Schwarz [139]. There are two main ways to accomplish this, either by the Ramond-Neveu-Schwarz (RNS) formalism or the Green-Schwarz (GS) formalism, which are equivalent in certain circumstances. We shall explore the RNS formalism. The key difference between the bosonic string and the superstring is the addition of fermionic modes on its worldsheet, and so we include the fermionic fields $\Psi^\mu(\tau,\sigma)$ which are two-component spinors $\Psi^\mu(\tau,\sigma)^{\mathrm{T}} = (\psi^\mu_-(\tau,\sigma), \psi^\mu_+(\tau,\sigma))$. We do so by slightly modifying the previous string action into

$$S = -\frac{1}{2\pi}\int d^2\sigma \left(\partial_\alpha X^\mu \partial^\alpha X_\mu + \overline{\Psi}^\mu \rho^\alpha \partial_\alpha \Psi_\mu\right) \ , \tag{5.37}$$

where we have set the string tension to $T = 1/\pi$ (or equivalently $\alpha' = 1/2$), and the quantity ρ^α is the two-dimensional equivalent of the Dirac matrix satisfying $\{\rho^\alpha, \rho^\beta\} =$

$2\eta^{\alpha\beta}$ (see appendix I). Similarly to as is usual, the conjugate field is defined through $\overline{\Psi}^{\mu} = \Psi^{\mu\dagger} i\rho^0$ with $(\Psi^{\mu})^{\dagger}$ being the Hermitian conjugate of the fermionic field. Under the transformations

$$\begin{aligned} \delta X^{\mu} &= \epsilon^{\dagger} i\rho^0 \Psi^{\mu} \equiv \bar{\epsilon}\Psi^{\mu} \ , \\ \delta\Psi^{\mu} &= \rho^{\alpha}\partial_{\alpha}X^{\mu}\epsilon \ , \end{aligned} \tag{5.38}$$

where ϵ is an infinitesimal Majorana spinor formed of two real Grassmann numbers ϵ_-, ϵ_+ through

$$\epsilon = \begin{pmatrix} \epsilon_- \\ \epsilon_+ \end{pmatrix} \tag{5.39}$$

we find that the action is invariant (up to boundary terms which can be dropped with suitable boundary conditions), and so we see that these transformations mix bosons and fermions and therefore the action is inherently supersymmetric.

Once again there are various types of boundary conditions possible in the model, however in this case the choice of boundary conditions will split the theory into two sectors. For open strings, the Ramond (R) sector consists of choosing boundary conditions at one end of the string that specify

$$\psi_+^{\mu}(\sigma = \pi) = \psi_-^{\mu}(\sigma = \pi) \ , \tag{5.40}$$

and this will give rise to fermions. The Neveu-Schwarz (NS) sector instead consists of choosing the boundary conditions

$$\psi_+^{\mu}(\sigma = \pi) = -\psi_-^{\mu}(\sigma = \pi) \ , \tag{5.41}$$

and this will give rise to bosons. Thus the open string allows for four distinct sectors corresponding to the choice of boundary conditions on each end of the string: R-R, R-NS, NS-R, and NS-NS. For closed strings the boundary conditions are instead given by

$$\psi_{\pm}(\sigma) = \pm\psi_{\pm}(\sigma + \pi) \ , \tag{5.42}$$

with the difference in signs leading to periodic or antiperiodic boundary conditions for the $+$ or $-$ case respectively.

Performing a similar analysis as for the bosonic case we can again try and quantise the theory. In this case we now instead can form the "super-Virasoro algebra", and we obtain two different versions of the algebra for the two different sectors caused by the boundary conditions. There is a supercurrent associated with the symmetries of the superstring action 5.37 given by

$$J_A^{\alpha} = -\frac{1}{2}(\rho^{\beta}\rho^{\alpha}\Psi_{\mu})_A \partial_{\beta}X^{\mu} \ , \tag{5.43}$$

which is formed by two independent components J_- and J_+. We will generate two sets of modes associated with this supercurrent depending on which sector we are in: the modes F_m are associated with the Ramond sector and the modes G_r are associated with the Neveu-Schwarz sector. In the Ramond sector therefore we can construct the super-Virasoro algebra as [138]

$$\begin{aligned}
[L_m, L_n] &= (m-n)L_{m+n} + \frac{D}{8}m^3\delta_{m+n,0} \ , \\
[L_m, F_n] &= \left(\frac{m}{2} - n\right) F_{m+n} \ , \\
\{F_m, F_n\} &= 2L_{m+n} + \frac{D}{2}m^2\delta_{m+n,0} \ ,
\end{aligned} \tag{5.44}$$

and in the Neveu-Schwarz sector we can construct the super-Virasoro algebra as [140]

$$\begin{aligned}
[L_m, L_n] &= (m-n)L_{m+n} + \frac{D}{8}(m^3 - m)\delta_{m+n,0} \ , \\
[L_m, G_r] &= \left(\frac{m}{2} - r\right) G_{m+r} \ , \\
\{G_r, G_s\} &= 2L_{r+s} + \frac{D}{2}\left(r^2 - \frac{1}{4}\right)\delta_{r+s,0} \ ,
\end{aligned} \tag{5.45}$$

where the central charge in this situation is related to the spacetime dimension through $c = D + D/2$. The indices m, n refer to integers $m, n \in \mathbb{Z}$ and the indices r, s refer to half integers $r, s \in \mathbb{Z} + \frac{1}{2}$.

Once again there is a particular choice of spacetime dimension in which the string spectrum does not contain the negative norm states, and so for superstring theory the critical spacetime dimension is $D = 10$.

With the significantly more realistic string theory consisting of bosons and fermions now produced we are in a much more solid place theoretically, however the tachyonic mode still persists and the spectrum is not properly spacetime supersymmetric. Fortunately, it was discovered in 1977 by Gliozzi, Scherk and Olive that further conditions through the GSO projection should be imposed on the spectrum of the RNS string which leads to the removal of tachyon and further to a truly supersymmetric theory in ten-dimensional spacetime [141, 142]. This discovery lead to the first superstring revolution as it is named, which began in 1984.

In this treatment quantities are constructed called “G-parity operators”, which are defined through a number operator counting fermions F (specifically F_{NS} in the NS sector and F_R in the R sector) as

$$G = (-1)^{F_{NS}+1} = (-1)^{\sum_{r=1/2}^{\infty} b^i_{-r} b^i_r + 1} \tag{5.46}$$

in the NS sector and

$$G = \Gamma_{11}(-1)^{F_R} = \Gamma_{11}(-1)^{\sum_{n=1}^{\infty} d^i_{-n} d^i_n} \tag{5.47}$$

in the R sector, where Γ_{11} is the ten dimensional analogue of the Dirac matrix γ_5 in four dimensions (see appendix I for properties and details) and d_n, b_r are Grassmann-valued Fourier modes found when Fourier expanding the superstrings. When applying Γ_{11} to a spinor, the values

$$\Gamma_{11}\Psi = \pm\Psi \tag{5.48}$$

are defined as having either a positive $(+\Psi)$ or negative $(-\Psi)$ chirality. With this projection we must make some choices, namely that we have both the left- and right-moving sectors in which we must choose which G eigenstate to project out independently, and this must be done in both the R and NS sectors. In making this choice we actually separate our theory out into *two distinct types* of string theory, named type IIA and IIB. The distinctions are as such: in type IIA string theory the left- and right-moving R-sector ground states have the chirality chosen to be opposite, whereas in type IIB string theory the left- and right-moving R-sector ground states have the chirality chosen to be the same. There is a rich structure for each of these types of string theory which is beyond the scope of this thesis, so with the basics definitions covered we shall move onto what other possible types of string theory there are.

5.4.3 Further String Theories

As we have just seen, we have already found two consistent but distinct types of string theory. This at first glance seems unfortunate, surely if the purpose of string theory is to try and construct the one overarching "theory of everything" there should not be ambiguity about the fundamental properties. In fact, this may not even be the worst part of it; there actually turns out to be even more types of string theory which are completely consistent and one cannot say that one type is "more fundamental" than any other. The possible ten-dimensional theories are:

- Type I
- Type IIA
- Type IIB
- Heterotic $SO(32)$
- Heterotic $E_8 \times E_8$.

We saw where the type IIA and IIB theories came from, but what about the others? There is in fact a close relationship between type I and type II string theory, specifically type IIB string theory. An *orientifold projection* in string theory requires physical states be invariant under a mirror symmetry. If we orientifold type IIB string theory we arrive at type I string theory [143, 144] by considering that type IIB orientifolds are generalised orbifolds that involve world-sheet parity reversal along with geometric symmetries of the theory. The orientifold procedure results in an unoriented closed string theory. Consistency then generically requires introducing open strings that can be viewed as starting and ending on D-branes [145]. In particular, Type I compactifications on toroidal orbifolds can be viewed as Type IIB orientifolds with a certain choice of the orientifold projection [146].

The other two types of string theories mentioned, $SO(32)$ and $E_8 \times E_8$, are closed string theories and are known as *heterotic string theories.* They are called this due to their composition: they are assumed to be the combination of a supersymmetric chiral piece and a non-supersymmetric piece *i.e.* made up of both bosonic strings and superstrings, and were first proposed in ref. [147]. In these types of models the left-moving degrees of freedom of the 26-dimensional bosonic string theory are combined with the right-moving degrees of freedom of the 10-dimensional superstring theory.

5.4.4 Dualities of String Theory and M-Theory

We now know that there are five distinct types of string theory possible. How do we reconcile this and decide which one should describe the Universe? Whilst exploring string theory and how the observable dimensions will be reduced down to the usual four, the idea of compactification popularised by Kaluza and Klein was investigated. Following this procedure then, a spatial dimension in the theory (which we choose to be X^d) is compactified on a circle, meaning that it is periodic. For superstring theory this will mean our spacetime shall be topologically equivalent to the product of 9-dimensional Minkowski spacetime and a circle of radius R, that is $\mathbb{R}^{8,1} \times S^1_R$. What will this mean for our boundary conditions? The non-compactified boundary conditions shall stay the same as

$$X^\mu(\sigma = 0, \tau) = X^\mu(\sigma = 2\pi, \tau) \ , \tag{5.49}$$

but the S^1 compactified dimension will now have condition

$$X^9(\sigma = 2\pi, \tau) = X^9(\sigma = 0, \tau) + 2\pi R W \ , \quad W \in \mathbb{Z} \ , \tag{5.50}$$

where W is known as the winding number. The winding number describes how many times a string has wound around the compactified dimension, and in what direction. This allows the winding number to take any positive or negative integer value, as demonstrated in figure 5.3.

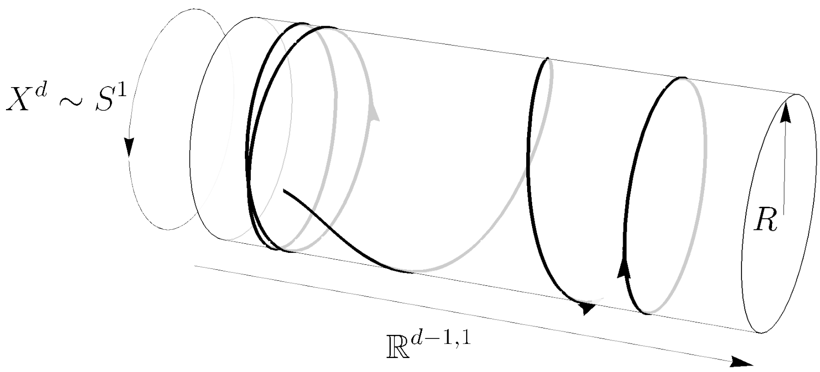

Figure 5.3: $d+1$-dimensional spacetime with the spatial dimension d compactified on a circle S^1 with radius R. The dark black curves show strings living on the spacetime winding around the compactified dimension. The closed string on the left has winding number $W=2$, the open string in the middle has a positive non-integer winding number, and the closed string on the right has winding number $W=-1$.

In this type of compactification the momentum will be quantised for X^9 as

$$p^9 = \frac{n}{R} \ , \tag{5.51}$$

and what we will find then is that a string with n units of momentum, a winding number of W, and N_L, N_R total number of oscillators on the left and on the right has a total mass given by

$$M^2 = \frac{n^2}{R^2} + \frac{W^2R^2}{\alpha'^2} + \frac{2}{\alpha'}(N_L + N_R - 2) \ , \tag{5.52}$$

and a level matching condition of

$$N_R - N_L = nW \ . \tag{5.53}$$

What we can see from equation 5.53 is that under the exchange of meaning of the momentum n and the winding number W it is invariant. What about equation 5.52? Under the same exchange the mass is not equivalent, however if we also simultaneously make the exchange $R \to \alpha'/\tilde{R}$ we recover the same form as we had previously, and this secondary substitution does not alter the level matching condition. We call this duality the “T-duality” (for target-space duality), and it is described through the exchanges

$$\begin{aligned} T &: \mathbb{R}^{d-1,1} \times S^1_R \longleftrightarrow \mathbb{R}^{d-1,1} \times S^1_{\tilde{R}} \ , \\ T &: W \longleftrightarrow n \ . \end{aligned} \tag{5.54}$$

What this means is that the winding-mode excitations in the description compactified on a circle of radius R correspond to momentum levels in the dual description compactified on a circle of radius $\tilde{R}$. Exchanging the winding and momentum amounts to exchanging the bosonic field $X^\mu_L + X^\mu_R$ with $X^\mu_L - X^\mu_R$ and the superstring field Ψ^μ with $\overline{\Psi}^\mu$ which will reverse the GSO projections, meaning that under the T-duality one type of type II string theory gets converted into the other as:

Type IIB compactified on S^1 with radius $R \longleftrightarrow$ Type IIA compactified on S^1 with radius $\tilde{R}$.

This remarkable duality led to the *second superstring revolution* and to to the realisation of other dualities. Shortly after it was found that the distinction between the $E_8 \times E_8$ and $SO(32)$ heterotic theories only exists in ten dimensions, and after toroidal compactification there is a single moduli space demonstrating that the $E_8 \times E_8$ and $SO(32)$ heterotic theories are also related by a T-duality [25].

In 1994 a further duality was proposed in ref. [148] named "S-duality" in reference to its relating strong couplings and weak couplings. In string theory, this relates the string coupling g_s (which is the genus of the string worldsheet or equivalently the expansion in string loop number) to $1/g_s$. A special case is one of a string theory model which exhibits both T- and S- type dualities, and is dual to $\mathcal{N} = 4$ SYM; we shall study shortly. For the type I superstring and $SO(32)$ heterotic string the low-energy effective actions can actually be related by a transformation $\Phi \to -\Phi$ (where Φ is the dilaton), along with a rescaling of the metric as [149]

$$g_{\mu\nu} \to e^{-\Phi} g_{\mu\nu} \ . \tag{5.55}$$

From this it can be seen that the SO(32) heterotic and type I string theories in ten dimensions are dual to each other as descriptions of the same quantum theory in different regions of parameter space. Also, due to the relation

$$g_s = \langle e^{\Phi} \rangle \ , \tag{5.56}$$

where $\langle e^{\Phi} \rangle$ is the vacuum expectation value of the dilation field, we see that the exchanging of the sign of the dilaton implies that the string coupling of the type I superstring is the reciprocal of the string coupling of the heterotic $SO(32)$. This provides the duality that a strong-coupling region of one theory can be described by dynamics of solitonic states which is equivalent to the weak-coupling dynamics of elementary states of the other [150].

The S-duality also appears in a surprising way, in that it was found that type IIB string theory with the string coupling constant g_s is actually equivalent to the very same theory with the coupling $1/g_s$.

Finally, one may ask whether there is any sort of description of the other two superstring theories under this S-duality. What is found is that they (the type IIA superstring and the $E_8 \times E_8$ heterotic string) exhibit an eleventh dimension at strong coupling which grows as $g_s l_s$ (shaped as a circle for type IIA and a line for $E_8 \times E_8$) and thus approach a common eleven-dimensional limit. The theory that emerges is known as M-theory (for magic or mystery), and although it is not hugely well-understood it has garnered much interest and study as its possibility of being the all-encompassing theory which we seek. Explorations of it are plentiful and could fill many pages, but as interesting as it is we do not need details of it for this work. All else we shall say on this topic is that the low energy effective theory for M-theory is 11-dimensional supergravity (also called SUGRA, however other dimensions do also have SUGRA also), which is somewhat special since it is the highest possible dimension if one requires that there be no massless state with spin higher than two [151]. We direct the interested reader to reviews [152, 153, 154] for more details.

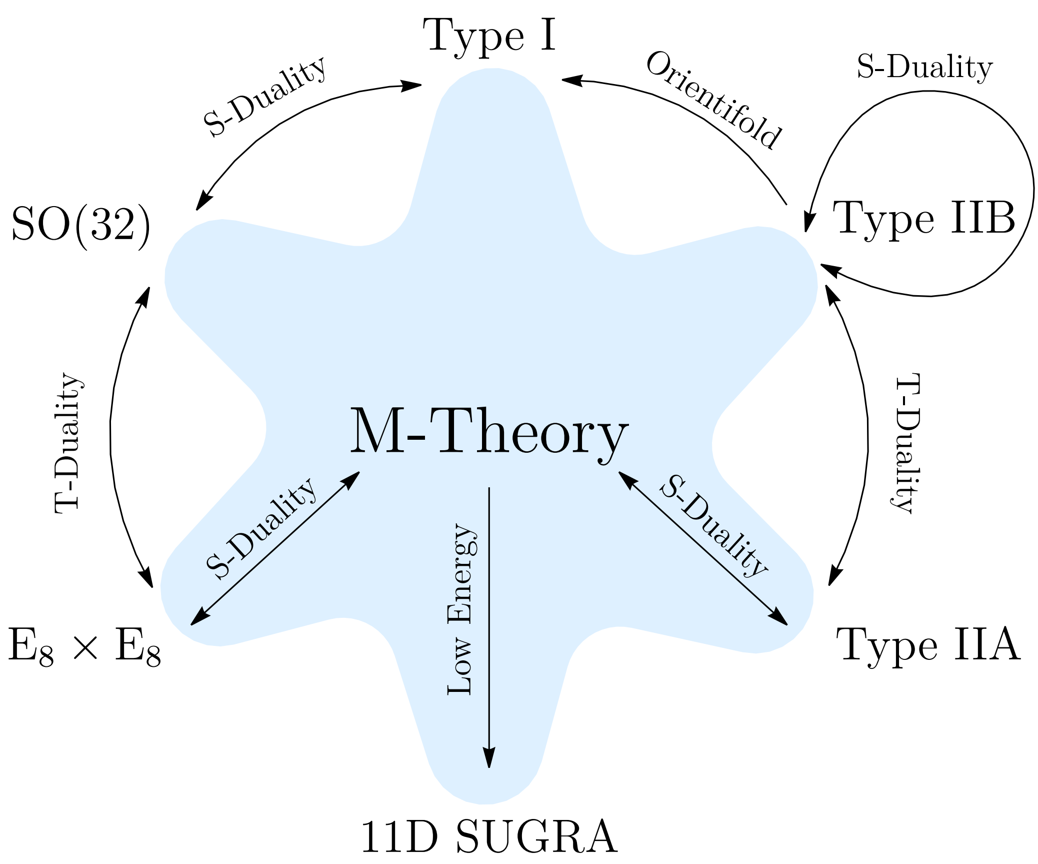

Figure 5.4: The consistent types of string theory as branches of M-theory with the dualities relating them.

So we have found that all consistent string theories are related in what is known as the “web of dualities” (which is depicted in figure 5.4) and we no longer have to make a choice of which is the correct one to describe the Universe. That this is the case is remarkable, as many of these theories appear to have totally different properties and explain very different effects yet are related by “simple” dualities. Of particular interest to us is the S-duality. Many areas of physics are limited in their ability to explain physical phenomena due to relying upon perturbation theory which is only valid in the weak coupling regime, despite numerous very important physical aspects existing only at strong coupling. A duality therefore which could translate easily calculable perturbation results into the strongly coupled regime would be very useful if we could formulate the situation in a “stringy” context, and this is what we shall explore in the form of the AdS/CFT correspondence.

Chapter 6

AdS/CFT Correspondence *a.k.a.* Holography

We may wonder: "*If string theory is truly meant to describe the Universe, surely we should experience some of these dualities in the physics we know now such as in quantum field theory, which string theory should reduce to in the low-energy limit.*" This is indeed the case. The S-duality, for instance, is present in a non-stringy context in electromagnetism under the exchange of $\mathbf{E} \to \mathbf{B}$ and $\mathbf{B} \to -\frac{1}{c^2}\mathbf{E}$ which shows that under the exchange of the electric and magnetic fields the theory is invariant (in vacuum, magnetic monopoles are required for the non-vacuum case). The Lagrangian coupling in this instance goes from $\mathcal{L} \propto \frac{1}{g^2}$ to $\mathcal{L} \propto g^2$, and so we see that this is precisely an S-duality due to the relation of strong to weak coupling.

This line of reasoning also led to the AdS/CFT correspondence being formulated in 1997-98 in Refs. [133, 155, 156], which at the heart of it is built upon the properties of D-branes. If we recall the D-branes we mentioned earlier which we defined as p-brane objects on which open strings could end with Dirichlet boundary conditions we can explore a few of their important properties. One such property is that the massless spectrum of open strings on a Dp-brane for type II string theory is maximally supersymmetric $U(1)$ gauge theory in $p+1$ dimensions; the internal excitations of the Dp-branes sources a gauge field described by the Dirac-Born-Infield action (an action describing electromagnetism with a limiting field strength). If we consider instead when N of them are in coincidence we enjoy a $U(N)$ gauge theory on their world-volume [157]. This is due to the fact that we have N^2 open string subsectors linking one D-brane to another as they can start and end on any combination of the D-branes, which in the limit when they are stacked on top of each other will all have massless modes and we thus obtain the reduction of $U(N) \simeq \frac{SU(N)\times U(1)}{\mathbb{Z}_N}$

gauge theory from ten dimensions to $d = p + 1$. Further to this, as the $U(1)$ subgroup decouples, then due to the composition of $U(N)$ we actually identify the our duality as being (supersymmetric) Yang-Mills theory with gauge group $SU(N)$ (see Polchinski's lectures [158] for much greater detail on D-branes, or reviews such as [159, 160, 161]).

Obviously, as we have begun this analysis considering string-based objects there must be a fully string theory description of these interacting D-branes too which may lead to some other way of viewing the system. As we have said previously these D-branes are fully dynamic objects, and for a large amount of these D-branes (corresponding to large N) this stack is a heavy object embedded into a theory of closed strings existing in the entire spacetime which contains gravity. In fact it is deeper than that; as strings can split and join freely two open strings which reside on the same D-brane can come together, merge into a closed string, and therefore are no longer bound to the brane and can travel unhindered in the spacetime bulk. These p-branes therefore emit Hawking radiation [162] which corresponds to all closed string fields that can move in the bulk, and therefore permit a gravitational description through supergravity coupled to massive modes of these strings, which in the limit of low energy would simply be a supergravity description.

This is the crux of the field theory/gravity correspondence. There are multiple equally valid descriptions of the theory which link very different concepts springing from a string theory setup, both describing a gravitational theory and a gauge theory. We shall now proceed to a specific example to get a feel of this correspondence. For overall reviews of the AdS/CFT correspondence see *e.g.* [163, 164, 165, 166, 167].

6.1 $\mathcal{N}$=4 Supersymmetric Yang-Mills Theory

Let us look at this correspondence in the concrete and famous example of $\mathcal{N}$=4 Supersymmetric Yang-Mills (SYM) theory. For N coincident Dp-branes the metric and dilaton backgrounds may be expressed in the following simple string frame form [132]:

$$ds^2 = H^{-1/2}(r)\left[-dt^2 + \sum_{i=1}^{p}(dx^i)^2\right] + H^{1/2}(r)\left[dr^2 + r^2 d\Omega_{8-p}^2\right] \ , \tag{6.1}$$

where $d\Omega_{8-p}^2$ is the $(8-p)$-dimensional sphere metric and $H(r)$ is the warp-factor defined through

$$H(r) = 1 + \frac{L^{7-p}}{r^{7-p}} \ . \tag{6.2}$$

The warp factor is related to the dilaton through the relation

$$e^{\Phi} = H^{(3-p)/4}(r) \ . \tag{6.3}$$

Let us specify to the $p = 3$ case, meaning that we are now considering a stack of D3-branes in type IIB string theory (type IIB as type IIA describes even integer p-branes and IIB describes odd integer p-branes due to consistency of boundary conditions[1]) which as a consequence of the reduction lives in $d = p + 1 = 4$. This stack of D3-branes give rise in particular to $\mathcal{N}$=4 SYM. The quantity $\mathcal{N}$ describes the number of supersymmetries present, and the gauge group of this theory is $SU(N)$, with N being the rank of the gauge group and the number of D-branes.

Exploring the various limits of the bulk we see that as $r \to \infty$ we have $H \to 1$, and so the metric reduces to flat 10-dimensional Minkowski. In the opposite limit as $r \to 0$ however the warp factor goes as $H(r) \approx L^4/r^4$, and so the metric becomes

$$ds^2 = \frac{r^2}{L^2}\eta_{\mu\nu}dx^\mu dx^\nu + \frac{L^2}{r^2}dr^2 + L^2 d\Omega_5^2 \ . \tag{6.4}$$

If we then make the familiar substitution $r = L^2/z$ we transform the metric to the form

$$ds^2 = \frac{L^2}{z^2}(dz^2 + \eta_{\mu\nu}dx^\mu dx^\nu) + L^2 d\Omega_5^2 \ , \tag{6.5}$$

which if we compare with the metric 5.25 we see that the first term is simply AdS_5 and so the metric is the product space of $\mathrm{AdS}_5 \times \mathbb{S}^5$.

From the point of view of the supergravity background solution, the gauge theory lives in the original metric (before taking the $r \to 0$ limit). Therefore in the new $\mathrm{AdS}_5 \times \mathbb{S}^5$ limit space we can say that the gauge theory lives at $r \to \infty$, or $z \to 0$, which as we have proven when analysing AdS space, is part of the real boundary of global AdS space, and in Poincaré coordinates $z \to 0$ is a Minkowski space. Therefore the gravity theory lives in $\mathrm{AdS}_5 \times \mathbb{S}^5$, whereas the Super Yang-Mills theory lives on the 4 dimensional Minkowski boundary of AdS_5 parametrised by t and $\vec{x}$.

This is the reason as to why this correspondence is known as the *holographic principle* [168, 169, 170, 171, 172]; the entire information content of a quantum supergravity theory in a given volume can be encoded in an effective field theory at the boundary surface of this volume, and therefore just like a hologram a $d + 1$-dimensional picture can be built solely out of d-dimensional information.

We need to explore the limits of this space and the couplings present also. We have a relation of the radius of the space compared to the string length as

$$\left(\frac{L}{\ell_s}\right)^{7-p} = (2\sqrt{\pi})^{5-p}\,\Gamma\left(\frac{7-p}{2}\right) g_s N \ , \tag{6.6}$$

[1]Technically all integer branes are possible in both type IIA and type IIB, however only odd branes are stable for type IIB and only even branes are stable for type IIA due to being BPS objects.

which for our D3 brane case simplifies to

$$\left(\frac{L}{\ell_s}\right)^4 = 4\pi g_s N \ . \tag{6.7}$$

However we can also remember that the string coupling and Yang-Mills coupling can be related through $g_{\rm YM}^2 = 4\pi g_s$, and further that the 't Hooft coupling of the dual gauge theory is simply $\lambda = g_{\rm YM}^2 N$, allowing the string length and radius to be related through

$$\left(\frac{\ell_s}{L}\right)^2 = \frac{1}{\sqrt{\lambda}} \ . \tag{6.8}$$

What can we glean from this relation? When the field theory is described by weak coupling, the radius of curvature L must be small compared to ℓ_s, and therefore the gravitational geometry is strongly curved. However when the gravitational background is weakly curved (and therefore more easily tractable) the radius of curvature is large, and therefore the field theory is strongly coupled, which is something we shall discuss in the following section.

This is the heart of why the AdS/CFT correspondence is so useful: when usual perturbation methods break down for field theories in the strong coupling regime, the problem can be translated into a weakly curved gravitational theory which is easily solved so long as the right identifications are made for dual quantities.

One further consideration we need to make is the limits of validity of this analysis. Depending on our regime, there could be possible corrections from either quantum gravity effects or from string effects that we wish to avoid. We can think about the quantum gravity effects in terms of the (ten-dimensional) Planck length and how our radius compares to it. We find the relation between the two as

$$\left(\frac{l_P}{L}\right)^8 = \frac{\pi^4}{2N^2} \ , \tag{6.9}$$

which is gained from examining the coefficient of the ten-dimensional Einstein-Hilbert action. If we are to avoid having quantum gravity corrections we must require then that $l_P/L \to 0$, and complementing this to avoid "stringy" corrections we must require that $\ell_s/L \to 0$ at the same time. From these restrictions then we see that this discussion is only valid in the limits where

$$N \gg 1 \ , \quad \text{and} \quad \lambda \gg 1 \tag{6.10}$$

if we do not compute corrections from these effects.

An interesting limit to work in is the 't Hooft limit, which consists of taking $N \to \infty$ whilst also keeping the 't Hooft coupling fixed at a constant value. This corresponds to considering only planar diagrams (Feynman diagrams which can be drawn on a sphere with zero handles *i.e.* $h = 0$ when considering topological surfaces) whilst non-planar diagrams will be subleading effects categorised by $1/N^2$ behaviour. This is due to the fact that there are fewer colour index contractions (or "loops") for non-planar diagrams which have the same momentum structure as their planar counterparts, and as these index contractions provide factors of N this leads to the non-planar diagrams being suppressed in comparison.

6.2 Holographic Dictionary

From the dualities we have explored we can now form a "holographic dictionary" which translates quantities from one limit of the duality to the other and is necessary if we wish to correctly identify what processes in field theory look like in their gravitational description.

It is useful to first look at the symmetry groups of the two separate theories. The isometry group of AdS_{d+1} is given by $SO(2,d)$, the same as the conformal group in $(d-1,1)$ dimensions, and the symmetry group for the sphere $\mathbb{S}^5$ is the usual $SO(6)$. The 32 supersymmetries present are inherently halved with the inclusion of the D3 branes which break 16 Poincaré supersymmetries, however near the horizon these are joined by 16 conformal supersymmetries enhancing the overall symmetry group to $SU(2,2|4)$.

For the $\mathcal{N} = 4$ SYM theory we find a global symmetry group which is described by the superconformal group $SU(2,2|4)$, and also for this supergroup the bosonic subgroup is found through the product of the R-symmetry group and conformal group as $SO(2,4) \times SO(6)_R$ [173], and so for our case with $d = 4$ the symmetry groups coincide.

This is a large piece of evidence in the AdS/CFT correspondence's favour; completely identical group structures would already innately suggest an isomorphism between two theories without the arguments we have just put forward. With this structure we can feel justified in relating quantities and operators on both sides.

We begin the dictionary by stating the famous Witten-GKP relation [155, 156] (GKP here referring to Gubser, Klebanov, and Polyakov)

$$Z_{\mathcal{O}}[\phi_0]_{\mathrm{CFT}} = Z_\phi[\phi_0]_{\mathrm{string}} \,, \tag{6.11}$$

which allows us to relate the partition function of type IIB string theory with the generating functional of CFT correlation functions. This is the strongest version of this relation, however more frequently the weaker version is considered which relates solutions of type IIB supergravity containing leading asymptotic behaviour near the conformal boundary as acting as the generating functional for connected correlation functions with an operator $\mathcal{O}$. This uncovered equivalence between the fundamental quantities of both theories is once again a large piece of supporting evidence for the AdS/CFT correspondence.

For this duality to be useful, we wish to relate the observables on both sides, which will be *e.g.* the matter fields on the supergravity side and the operators on the field theory side. We can try and explore this in the simplest case, that of the scalar field. If we again recollect the AdS metric 5.25 and remember the equation of motion for a scalar as

$$\left(\frac{1}{\sqrt{-g}}\partial_\mu\sqrt{-g}g^{\mu\nu}\partial_\nu - m^2\right)\phi(z,x) = 0 \ , \tag{6.12}$$

and Fourier transform to a plane wave decomposition $\phi(z,x) = e^{ip^\mu x_\mu}\phi_p(z)$ we find a relation for the scalar field of

$$z^2\partial_z^2\phi_p(z) - (d-1)z\partial_z\phi_p(z) - (\eta_{\mu\nu}p^\mu p^\nu z^2 + m^2L^2)\phi_p(z) = 0 \ . \tag{6.13}$$

As we care mostly about the case at $z \to 0$, we consider this limit and see that the field behaves as $\phi_p(z) \sim z^\Delta$, which when inputted into 6.13 and then taking the limit $z \to 0$ leads to the condition

$$\Delta_\pm = \frac{d}{2} \pm \sqrt{\frac{d^2}{4} + m^2L^2} \ , \tag{6.14}$$

where $\Delta_\pm$ correspond to the two distinct solutions possible as roots from the condition

$$\Delta(\Delta - d) = m^2L^2 \ , \tag{6.15}$$

and are related through $\Delta_- = d - \Delta_+$. We can therefore expand the boundary behaviour of the field as

$$\phi(z,x) = \phi_1(x)z^{\Delta_-} + \phi_2(x)z^{\Delta_+} + \dots \ , \tag{6.16}$$

where ϕ_1 and ϕ_2 are as yet undetermined general quantities. We see from the metric 5.25 that AdS should have a dilatation invariance under the simultaneous transformations $x \to \lambda x$ and $z \to \lambda z$, and so for the scalar field to be invariant we must require that ϕ_1 and ϕ_2 transform as

$$\begin{aligned} &\phi_1(x) \to \lambda^{-\Delta_-}\phi_1(x) \ , \\ &\phi_2(x) \to \lambda^{-\Delta_+}\phi_2(x) = \lambda^{\Delta_- - d}\phi_2(x) \ , \end{aligned} \tag{6.17}$$

and thus recalling eq. 5.7 we see that this is simply telling us that ϕ_1 has conformal dimension Δ_-, whereas ϕ_2 has a different but related dimension. As we can see then, there seems to be an exact linkage between the group representations as well as the conformal dimension and mass, and so from this we can make the identification that a scalar field of mass m^2 in AdS is dual to a conformal scalar operator $\mathcal{O}$ of dimension Δ on the field theory side. Further to this, by dimensional analysis we may identify ϕ_2 as the vacuum expectation value for this dual scalar field theory operator $\mathcal{O}$, and ϕ_1 as the source for this operator.

An important point to note is that in AdS space scalar fields can be stable even for negative masses due to the shape of the potential. This leads to what is known as the *Breitenlohner-Freedman bound* [174, 175], which states that stable solutions can exist for

$$m^2L^2 \geq -\frac{d^2}{4} \ . \tag{6.18}$$

In addition, the unitarity bound for scalars $\Delta \geq (d-2)/2$ which requires all states in a representation have positive norm limits the solution to only the one we have previously presented, however in the range

$$-\frac{d^2}{4} \leq m^2L^2 \leq -\frac{d^2}{4} + 1 \tag{6.19}$$

both types of solution are permissible, meaning that the how we identified the source and the vacuum expectation value of the field theory operator can be interchanged. This will be especially important for our work later.

Although the arguments we have put forth are specifically for the scalar field, this type of reasoning can be generalised for fields of higher spin. From this we can find meanings for the fermionic fields, gauge fields, and metric tensor living on the gravitational side for the field theory dual.

If we put all of these duality relations together then we can form the "holographic dictionary" which relates important quantities from both dual theories, and these dualities are summarised in Table. 6.1.

Field Theory on Boundary	Gravity in Bulk
Generating Functional $\mathcal{Z}[\phi_0(x)] =$ $\langle \exp \int_{\partial\mathcal{M}} d^dx \phi_0(x)\mathcal{O}(x)\rangle$	Partition Function $\mathcal{Z}[\phi_0(x)] =$ $\int_{\phi_0} \mathcal{D}\phi \exp(-S[\phi(x), g_{\mu\nu}])$
Scalar Operator $\mathcal{O}$	Scalar Field ϕ
Fermionic Operator $\mathcal{O}_\psi$	Dirac Field ψ
Symmetry Current J_μ	Maxwell Field A_μ
Energy-Momentum Tensor $T_{\mu\nu}$	Metric Tensor $g_{\mu\nu}$
Scalar Operator Dimension Δ	Mass of Field m^2

Table 6.1: The holographic dictionary, relating field theory and gravity quantities.

6.3 Holographic Renormalisation

In quantum field theories, divergences of multiple types are commonplace. There are two main divergence types, namely infrared (IR) divergences and ultraviolet (UV) divergences. The IR divergences appear from theories containing massless particles such as photons where arbitrary amounts can be present, whereas UV divergences come from the fact that undetermined momenta can be as large as possible, or the distance between any two positions in spacetime can be made as small as possible. Studying CFTs means that we will inherently have to figure out how to deal with these divergences also.

Some in-depth treatments of the particularities of holographic renormalisation are found in Refs. [176, 177, 178, 179, 180, 181], and we shall utilise these in our explanations. As they are used frequently for this section they shall not be referenced every time they are necessary, so we direct the reader to these for all more in-depth explanations necessary. Due to the correspondence we have just studied, we recognise that when we speak of UV divergences on the field theory side, this will actually translate over to IR divergences on the gravitational side, and similarly QFT IR divergences relate to gravitational UV divergences. Mainly we shall be interested in correlation functions on the field theory side which suffer from UV divergences, and so this shall translate to finding ways to deal with IR or near boundary divergences gravitationally. Further to this, renormalisation and the renormalisation group through the dictionary can be related to the idea that the radial coordinate of a spacetime with asymptotically AdS geometry can be identified with the RG flow parameter of the boundary field theory [182].

To renormalise our theory we effectively need to find a way to rid ourselves of the divergences which plague the action due to our choice in Lagrangian. To do this we employ the use of subtracting “counterterms” which are of the same form as the terms already considered in the non-renormalised Lagrangian. We can consider this type of process as a type of “reparameterisation”, but really the idea behind why this sort of procedure is fine to do is that we are not adding terms in the *ad hoc* sense that we have just decided they are necessary and we pluck them from nowhere. Instead, we realise that the way we have formulated the theory is in a non-ideal way, and therefore because of this we receive divergences which tell us we must find a way to reparameterise the theory which removes these. Ergo, to obtain physically meaningful quantities we cancel these divergent terms by related counterterms which are strictly dictated by our theory.

As we shall only be considering the use of scalar operators and the energy-momentum tensor (corresponding to scalar fields coupled to gravity) in our papers I shall stick to discussion of these elements in terms of holographic renormalisation, which means considering how to renormalise massive scalars and the metric.

To calculate well-behaved quantities therefore we need to regularise and then renormalise the action, through

$$S_{\mathrm{ren}} = S_{\mathrm{reg}} + S_{\mathrm{ct}} \ . \tag{6.20}$$

We construct the regularised action S_{reg} by simply choosing a cutoff point for the bulk coordinate in the theory labelled $\epsilon > 0$, which if we took to its true limit of $\epsilon = 0$ would lead to divergences. After regularisation we work through the machinery of holographic renormalisation to locate the divergences fully, then apply constrained counterterms to remove these divergences. Once removed, we finally take the limit $\epsilon \to 0$ and obtain a renormalised, finite result.

For a scalar field ϕ coupled to gravity, we shall be considering a base action of the form

$$S[G,\phi] = \frac{1}{8\pi G_{d+1}}\left(\int_{\mathcal{M}} d^{d+1}x\sqrt{-G}\left[\frac{R_G}{2} + G^{\mu\nu}\partial_\mu\phi\partial_\nu\phi + 2V(\phi)\right] - \int_{\partial\mathcal{M}} d^dx\sqrt{-\gamma}K\right) \ , \tag{6.21}$$

where the cosmological constant is absorbed into the definition of the potential $V(\phi)$, $G_{\mu\nu}$ is the $d+1$-dimensional metric with determinant $G = \det G_{\mu\nu}$ and related Ricci scalar R_G, and the second term is the GHY term explained previously. This will be recast in terms of the boundary fields and their leading falloffs which are of most importance (in our case $g_{(0),ab}$ and $\phi_{(0)}$), and then regularised with the cutoff ϵ, leaving a regularised action as

$$S_{\mathrm{reg}}[g_{(0)}, \phi_{(0)}; \epsilon] = S_{\text{non-ren}}[g_{(0)}, \phi_{(0)}]\Bigg|_{x_5=\epsilon} \ . \tag{6.22}$$

This action will contain the express divergences which must be dealt with, along with the finite terms which dictate the theory and terms of higher order in ϵ which will be irrelevant after renormalisation. With the divergent terms located we can construct the action containing the counterterms S_{ct}, which will be fashioned as

$$S_{\mathrm{ct}}[g(x,\epsilon), \phi(x,\epsilon); \epsilon] = -S_{\mathrm{reg}}[g_{(0)}, \phi_{(0)}; \epsilon]_{\mathcal{O}(\epsilon)<\epsilon^0} \ , \tag{6.23}$$

i.e. it is formed of the negative of terms with a factor of epsilon of order less than ϵ^0. Whilst the regularised action is expressed in terms of the leading boundary expansion coefficient, the counterterm must be expressed in terms of the full fields living on the boundary (which are dependent upon these coefficients and simplify to them in the full limit) to satisfy covariance. Finally with the counterterms removing any possible divergences we combine the regularised action with the counterterms and take the full limit of $\epsilon \to 0$ to determine the renormalised action

$$S_{\mathrm{ren}}[g_{(0)}, \phi_{(0)}] = \lim_{\epsilon\to 0}\left(S_{\mathrm{reg}}[g_{(0)}, \phi_{(0)}; \epsilon] + S_{\mathrm{ct}}[g(x,\epsilon), \phi(x,\epsilon); \epsilon]\right) \ . \tag{6.24}$$

This renormalised action therefore defines for us a generating functional for renormalised correlation functions. After this renormalisation process, we can vary the renormalised action with respect to the fields to find

$$\delta S_{ren}[g_{(0)ab}, \phi_{(0)}] = \int d^4x \sqrt{g_{(0)}} \left(\frac{1}{2} \langle T_{ab} \rangle \delta g^{ab}_{(0)} + \langle \mathcal{O} \rangle \delta \phi_{(0)} \right) , \tag{6.25}$$

which now allows us to determine the one-point operators through the relations

$$\langle \mathcal{O} \rangle = \frac{1}{\sqrt{g_{(0)}}} \frac{\delta S_{\text{ren}}}{\delta \phi_{(0)}(x)} \tag{6.26}$$

and

$$\langle T_{ab} \rangle = \frac{2}{\sqrt{g_{(0)}}} \frac{\delta S_{\text{ren}}}{\delta g^{ab}_{(0)}(x)} . \tag{6.27}$$

It will also be useful to express these relations in terms of the full fields on the boundary, which we shall detail later. We now turn to some concrete examples. Although we will require the full action of Einstein-Hilbert gravity coupled to scalars, we will study each piece of the action individually and will then combine in a later section.

6.3.1 Einstein-Hilbert Gravity

As gravitation makes up a large area of our study, we must determine how to deal with the metric in terms of renormalisation. For holography we shall be dealing with Einstein-Hilbert gravity, which will take the action introduced earlier in eq. 5.17 with cosmological constant Λ giving

$$S_{\text{EH}} = \frac{1}{16\pi G_{d+1}} \left(\int_{\mathcal{M}} d^{d+1}x \sqrt{-g} \left(R_G - 2\Lambda \right) - 2 \int_{\partial \mathcal{M}} d^d x \sqrt{-\gamma} K \right) , \tag{6.28}$$

where again R_G is the Ricci scalar of the full $d+1$-dimensional metric $G_{\mu\nu}$, which has a related Ricci tensor $R^G_{\mu\nu}$. The variation of this action produces the Einstein equations

$$R^G_{\mu\nu} - \frac{1}{2} R_G G_{\mu\nu} - \Lambda G_{\mu\nu} = 0 , \tag{6.29}$$

which we wish to solve to be able to determine information about our operators and boundary falloffs. For the AdS metric we have been considering with a generalised d-dimensional sector appearing as

$$ds^2 = \frac{L^2}{z^2} \left(dz^2 + g_{ab}(x,z) dx^a dx^b \right) , \tag{6.30}$$

we may expand g_{ab} as

$$g_{ab}(x,z) = g_{(0),ab}(x) + z^2 g_{(2),ab}(x) + \ldots + z^d g_{(d),ab}(x) + z^d h_{(d),ab}(x) \log z^2 + \ldots , \tag{6.31}$$

with the logarithmic piece appearing only in even dimensions for d. This metric and expansion are useful and will be the metric we employ for holographic renormalisation in one of our papers, however it is conventional to switch to another metric for the renormalisation arguments, which we shall follow. All results found are transferable between metrics. For this we make the substitution $\rho = z^2$, which transforms the metric to the Fefferman-Graham form [183]

$$ds^2 = G_{\mu\nu}dx^\mu dx^\nu = \frac{L^2}{4\rho^2}d\rho^2 + \frac{L^2}{\rho}g_{ab}(x,\rho)dx^a dx^b \ , \tag{6.32}$$

where now the d-dimensional part is given by

$$g_{ab}(x,\rho) = g_{(0),ab}(x) + \ldots + \rho^{d/2}g_{(d),ab}(x) + \rho^{d/2}h_{(d),ab}\log\rho + \ldots \ . \tag{6.33}$$

This metric and expansion lead to the following Einstein equations

$$\begin{aligned}\rho[2g''_{ab} - 2(g'g^{-1}g')_{ab} + \operatorname{Tr}(g^{-1}g')g'_{ab}] + L^2R_{ab}(g) - (d-2)g'_{ab} - \operatorname{Tr}(g^{-1}g')g_{ab} &= 0\\ \nabla_a \operatorname{Tr}(g^{-1}g') - \nabla^b g'_{ab} &= 0\\ \operatorname{Tr}(g^{-1}g'') - \frac{1}{2}\operatorname{Tr}(g^{-1}g'g^{-1}g') &= 0 \ ,\end{aligned} \tag{6.34}$$

where a prime denotes a derivative with respect to ρ and ∇_a is the covariant derivative with respect to g_{ab}. If we consider these equations order by order in ρ we may find the coefficients in the expansion of 6.33. At leading order we may set $\rho = 0$ in the first equation of 6.34 to retrieve

$$g_{(2),ab} = \frac{1}{d-2}\left(R_{ab} - \frac{1}{2(d-1)}Rg_{(0),ab}\right) \ , \tag{6.35}$$

and this can be repeated further for higher orders. Using what we have found so far then, we can regularise the action by setting a cutoff $\epsilon > 0$, entering our metric expansion, and integrating. This gives a regularised action of

$$\begin{aligned}S_{\text{EH,reg}} &= \frac{1}{16\pi G_{d+1}}\left(\int_{\rho\geq\epsilon} d^{d+1}x\sqrt{G}\,(R_G + 2\Lambda) - 2\int_{\rho=\epsilon} d^dx\sqrt{\gamma}K\right)\\ &= \frac{1}{16\pi G_{d+1}}\int d^dx\left[\int_{\rho=\epsilon} d\rho\frac{d}{\rho^{d/2+1}}\sqrt{g} + \frac{1}{\rho^{d/2}}\left(4\rho\partial_\rho\sqrt{g} - 2d\sqrt{g}\right)\right] \ ,\end{aligned} \tag{6.36}$$

which can be shown in its divergent form as [177]

$$S_{\text{EH,reg}} = \frac{1}{16\pi G_{d+1}}\int d^dx\sqrt{g_0}\left(\epsilon^{-d/2}a_{(0)} + \epsilon^{-d/2+1}a_{(2)} + \ldots - \log\epsilon\, a_{(d)}\right) + \mathcal{O}(\epsilon^0) \ , \tag{6.37}$$

where the functions $a_{(n)}$ are conventional and in terms of constants or curvature quantities, such as

$$a_{(0)} = \frac{2(d-1)}{L^2}, \quad a_{(2)} = \frac{R}{2(d-1)}, \quad a_{(4)} = \frac{L^2}{2(d-2)^2}\left(R_{ab}R^{ab} - \frac{1}{d-1}R^2\right) \ . \tag{6.38}$$

By eq. 6.23 we see that our counterterms must be the negative of these divergent terms living at the boundary, and so we induce a metric at the boundary $\rho = \epsilon$ through $\gamma_{ab} = (L^2/\epsilon)g_{ab}$, which has determinant $\gamma = (L^{2d}/\epsilon^d)g$. As we have actions in terms of $g_{(0)}$, we will need to invert eq. 6.33 to find them in terms of γ. Inverting as a perturbative series, we find

$$\sqrt{g_{(0)}} = \sqrt{\gamma}\epsilon^{d/2}\left(1 - \frac{1}{2}\epsilon\,\mathrm{Tr}(g_{(0)}^{-1}g_{(2)}) + \frac{1}{8}\epsilon^2[(\mathrm{Tr}(g_{(0)}^{-1}g_{(2)}))^2 + \mathrm{Tr}(g_{(0)}^{-1}g_{(2)})^2] + \dots\right) . \tag{6.39}$$

This allows us to now write our counterterms at the boundary, which is given by (after a lot of calculation)

$$\begin{aligned} S_{\mathrm{ct}} = \frac{1}{16\pi G_{d+1}} \int_{\rho=\epsilon} \sqrt{\gamma}\Bigg[&2(d-1) + \frac{1}{2-d}R[\gamma] \\ &+ \frac{1}{(d-4)(d-2)^2}(R^{(\gamma)}_{ab}R^{(\gamma),ab} - \frac{d}{4(d-1)}R[\gamma]^2) - \log\epsilon\, a_{(d)} + \dots\Bigg] , \end{aligned} \tag{6.40}$$

where $R^{(\gamma)}_{ab}$ and $R[\gamma]$ are the Ricci tensor and scalar based on γ_{ab} respectively. When restricting to a particular dimension, the number of applicable terms changes. For even dimensions, only the first $d/2$ terms must be kept along with the logarithmic term; for odd dimensions, only the first $(d+1)/2$ terms are to be kept. With our actions now in terms of the induced metric, we can look to the form of the energy-momentum tensor. The form presented earlier can be modified to be in terms of the full field through

$$\langle T_{ab}\rangle = \frac{2}{\sqrt{g_{(0)}}}\frac{\delta S_{\mathrm{ren}}}{\delta g^{ab}_{(0)}(x)} = \lim_{\epsilon\to 0}\frac{2}{\sqrt{g}}\frac{\delta(S_{\mathrm{reg}} + S_{\mathrm{ct}})}{\delta g^{ab}(x,\epsilon)} . \tag{6.41}$$

From this we can recast this in terms of the induced metric on the boundary $\rho = \epsilon$ by the relations presented earlier,

$$\langle T_{ab}\rangle = \lim_{\epsilon\to 0}\left(\frac{L^{d-2}}{\epsilon^{d/2-1}}\frac{2}{\sqrt{\gamma}}\frac{\delta(S_{\mathrm{reg}} + S_{\mathrm{ct}})}{\delta\gamma^{ab}(x)}\right) = \lim_{\epsilon\to 0}\left(\frac{L^{d-2}}{\epsilon^{d/2-1}}T^{\gamma}_{ab}\right) , \tag{6.42}$$

where T^{γ}_{ab} is the energy-momentum tensor at the boundary $\rho = \epsilon$. This boundary tensor can be split into its two constituent parts as $T^{\gamma}_{ab} = T^{\mathrm{reg}}_{ab} + T^{\mathrm{ct}}_{ab}$, arising from S_{reg} and S_{ct} respectively. We can find general forms for both of these energy-momentum tensor pieces so as to be able to find the full tensor. The first piece, T^{reg}, is the much simpler of the two. From the definition in eq. 6.37 we can write it as being comprised of the extrinsic curvature tensor K_{ab} and its trace as

$$\begin{aligned} T^{\mathrm{reg}}_{ab} &= \frac{1}{8\pi G_{d+1}}(K_{ab} - K\gamma_{ab}) \\ &= \frac{1}{8\pi G_{d+1}}\left(\frac{1-d}{\epsilon}g_{ab}(x,\epsilon) - \partial_\epsilon g_{ab}(x,\epsilon) + g_{ab}(x,\epsilon)\,\mathrm{Tr}[g^{-1}(x,\epsilon)\partial_\epsilon g_{ab}(x,\epsilon)]\right) . \end{aligned} \tag{6.43}$$

Moving on to the counterterm piece, we can now make use of the counterterm action we found earlier in eq. 6.40 and therefore take the functional derivative with respect to the induced metric to find

$$\begin{aligned}T^{\text{ct}}_{ab} = \frac{1}{8\pi G_{d+1}} \Bigg(&(d-1)\gamma_{ab} + \frac{1}{(d-2)}\left(R_{ab} - \frac{1}{2}R\gamma_{ab}\right) \\ &- \frac{1}{(d-4)(d-2)^2}\Bigg[-\nabla^2 R_{ab} + 2R_{abcd}R^{cd} + \frac{d-2}{2(d-1)}\nabla_a\nabla_b R \\ &- \frac{d}{2(d-1)}RR_{ab} - \frac{1}{2}\gamma_{ab}\left(R_{cd}R^{cd} - \frac{d}{4(d-1)}R^2 - \frac{1}{d-1}\nabla^2 R\right)\Bigg] - T^{a_{(d)}}_{ab}\log\epsilon\Bigg) \ ,\end{aligned} \tag{6.44}$$

where the term $T^{a_{(d)}}_{ab}$ corresponds to the energy-momentum produced when considering the term proportional to $a_{(d)}$ in eq. 6.40. It can be shown that for even dimensions this term is related to the term appearing in the expansion of the metric of $h_{(d)}$ through

$$T^{a_{(d)}}_{ab} = -\frac{d}{2}h_{(d)ab} \ . \tag{6.45}$$

Finally with these relations for T^{reg}_{ab} and T^{ct}_{ab} we can move on to calculating $\langle T_{ab}\rangle$. For this part we shall specify $d = 4$, as that is the case we shall actually want to consider in the papers (to replicate the realistic 4D world) and each dimension has very different results. To do so we shall also need to rewrite both expressions in terms of $g_{(0)}$, which will require inverting the Ricci tensor. This is found through

$$\begin{aligned}R_{ab}[\gamma] = R_{ab}\left[g_{(0)}\right] + \frac{1}{4}\epsilon\Big(&2R_{ac}\left[g_{(0)}\right]R^c_b\left[g_{(0)}\right] - 2R_{acbd}\left[g_{(0)}\right]R^{cd}\left[g_{(0)}\right] \\ &-\frac{1}{3}\nabla_a\nabla_b R\left[g_{(0)}\right] + \nabla^2 R_{ab}\left[g_{(0)}\right] - \frac{1}{6}\nabla^2 R\left[g_{(0)}\right]g_{(0)ab}\Big) + \mathcal{O}\left(\epsilon^2\right) \ .\end{aligned} \tag{6.46}$$

Combining our results and taking the functional derivative, we arrive at the result (where we have now dropped all arguments in the curvature tensors, which are to be understood as all calculated from $g_{(0)}$)

$$\begin{aligned}\left\langle T_{ab}\left[g_{(0)}\right]\right\rangle = \frac{1}{8\pi G_{d+1}}\lim_{\epsilon\to 0}\Bigg[&\frac{1}{\epsilon}\left(-g_{(2)ab} + g_{(0)ab}\,\mathrm{Tr}(g^{-1}_{(0)}g_{(2)}) + \frac{1}{2}R_{ab} - \frac{1}{4}g_{(0)ab}R\right) \\ &+\log\epsilon\left(-2h_{(4)ab} - T^{a_{(d)}}_{ab}\right) \\ &-2g_{(4)ab} - h_{(4)ab} - g_{(2)ab}\,\mathrm{Tr}(g^{-1}_{(0)}g_{(2)}) - \frac{1}{2}g_{(0)ab}\,\mathrm{Tr}(g^{-1}_{(0)}g_{(2)})^2 \\ &\frac{1}{8}\left(R_{ac}R^c_b - 2R_{abcd}R^{cd} - \frac{1}{3}\nabla_a\nabla_b R + \nabla^2 R_{ab} - \frac{1}{6}\nabla^2 R_{(0)ab}\right) \\ &-\frac{1}{4}g_{(2)ab}R + \frac{1}{8}g_{(0)ab}\left(R_{cd}R^{cd} - \frac{1}{6}R^2\right)\Bigg] \ .\end{aligned} \tag{6.47}$$

We can see that straight away our formula for $T^{a_{(d)}}_{ab}$ in eq. 6.45 specified for $d = 4$ will remove the logarithmic divergence. Employing another result we have found, we can input the value of $g_{(2)ab}$ we found in eq. 6.35 to see that the $1/\epsilon$ divergence is removed. Finally using the first Einstein equation in 6.34 we can calculate $h_{(4)ab}$, and from this we find

$$\begin{aligned} h_{(4)ab} &= \frac{1}{2}(g_{(0)}^{-1}g_{(2)})^2_{ab} - \frac{1}{8}g_{(0)ab}\,\mathrm{Tr}(g_{(0)}^{-1}g_{(2)})^2 \\ &+ \frac{1}{8}\left(\nabla^c\nabla_a g_{(2)bc} + \nabla^c\nabla_b g_{(2)ac} - \nabla^2 g_{(2)ab} - \nabla_a\nabla_b\,\mathrm{Tr}(g_{(0)}^{-1}g_{(2)})\right) \\ &= \frac{1}{8}R_{abcd}R^{cd} + \frac{1}{48}\nabla_a\nabla_b R - \frac{1}{16}\nabla^2 R_{ab} - \frac{1}{24}RR_{ab} + \left(\frac{1}{96}\nabla^2 R + \frac{1}{96}R^2 - \frac{1}{32}R_{cd}R^{cd}\right)g_{(0)ab}\ . \end{aligned} \tag{6.48}$$

Entering this expression as well, all divergences have now been removed and we can take the limit of $\epsilon \to 0$ to calculate the fully renormalised energy-momentum tensor of

$$\begin{aligned} \langle T_{ab}\rangle = \frac{2}{8\pi G_{d+1}}\Bigg(& g_{(4)ab} - \frac{1}{8}\left[(\mathrm{Tr}(g_{(0)}^{-1}g_{(2)}))^2 - \mathrm{Tr}(g_{(0)}^{-1}g_{(2)})^2\right] - \frac{1}{2}(g_{(0)}^{-1}g_{(2)})^2_{ab} \\ & + \frac{1}{4}g_{(2),ab}\,\mathrm{Tr}(g_{(0)}^{-1}g_{(2)}) + (\text{scheme dep. } h_{(4)})\Bigg)\ . \end{aligned} \tag{6.49}$$

As we can see, in the $d = 4$ case we have retained an undetermined tensor $g_{(4)ab}$ which is exactly as expected. Scheme dependent terms can also enter through local finite counterterms.

6.3.2 Massive Scalar Field

One of the major components we will need to renormalise is a scalar field. We can consider the action of a massive scalar field

$$S_\phi = \frac{1}{2}\int d^{d+1}x\sqrt{-G}\left(G^{\mu\nu}\partial_\mu\phi\partial_\nu\phi + m^2\phi^2\right)\ , \tag{6.50}$$

where m is the scalar mass and $G = \det G_{\mu\nu}$. As we will later be examining scalars in potentials we may think of this case as a scalar with potential $V(\phi) = -m^2\phi^2$. Obviously when more complex potentials are explored there will be extra terms to be renormalised. For the AdS metric we have been reviewing of

$$ds^2 = \frac{L^2}{z^2}\left(dz^2 + g_{ab}dx^a dx^b\right) \tag{6.51}$$

we shall take the ansatz of the scalar field to be

$$\phi(x,z) = z^{d-\Delta}\tilde{\phi}(x,z)\ , \tag{6.52}$$

where we expand the field $\tilde{\phi}(x,z)$ around the AdS boundary at $z = 0$ as

$$\tilde{\phi}(x,z) = \phi_{(0)}(x) + z^2\phi_{(2)}(x) + \ldots + z^d\phi_{(d)}(x)\ . \tag{6.53}$$

Once again however we switch to the Fefferman-Graham form, which causes the expansion of the field to change to

$$\phi(x,\rho) = \rho^{(d-\Delta)/2}\tilde{\phi}(x,\rho)\ , \tag{6.54}$$

and

$$\tilde{\phi}(x,\rho) = \phi_{(0)}(x) + \rho\phi_{(2)}(x) + \ldots + \rho^{d/2}\phi_{(d)}(x) \ . \tag{6.55}$$

A massive scalar field must obey the related Klein-Gordon equation

$$(\Box_G - m^2)\phi = 0 \ , \tag{6.56}$$

where $\Box_G$ is the Laplacian

$$\Box_G \phi = \frac{1}{\sqrt{G}}\partial_\mu(\sqrt{G}G^{\mu\nu}\partial_\nu\phi) \ . \tag{6.57}$$

Entering the definition for ϕ in eq. 6.54 with expansion eq. 6.55, we therefore find that the scalar field must satisfy the relation

$$\begin{aligned} 0 = &(m^2L^2 - \Delta(\Delta - d))\tilde{\phi}(x,\rho) + 2(2\Delta - d - 2)\rho\partial_\rho\tilde{\phi}(x,\rho) - \rho\Box_g\tilde{\phi}(x,\rho) \\ &- (d-\Delta)\rho\tilde{\phi}(x,\rho)\partial_\rho \log g - 2\rho^2\partial_\rho\tilde{\phi}(x,\rho)\partial_\rho \log g - 4\rho^2\partial_\rho^2\tilde{\phi}(x,\rho) \ , \end{aligned} \tag{6.58}$$

where $\Box_g\phi = \frac{1}{\sqrt{g}}\partial_a(\sqrt{g}g^{ab}\partial_b\phi)$, $g = \det g_{ab}$. We can explore this relation order by order to find out more. In the limit $\rho \to 0$ we see that we find

$$(m^2L^2 - \Delta(\Delta - d))\tilde{\phi}(x,\rho) = 0 \ , \tag{6.59}$$

which corresponds to the scalar mass condition found previously in eq. 6.15; this must be satisfied even when $\rho \neq 0$. Applying this condition we can continue examining eq. 6.58, and so inputting the expansion in eq. 6.55 gives

$$\phi_{(2)}(x,\rho) = \frac{1}{2(2\Delta - d - 2)}\left(\Box_{g_0}\phi_{(0)}(x) + (d-\Lambda)\phi_{(0)}(x)\,\mathrm{Tr}(g_{(0)}^{-1}g_{(2)})\right) \ , \tag{6.60}$$

where $\Box_{g_0}$ is the Laplacian with respect to $g_{(0)}$ and Jacobi's formula of $\frac{d}{dt}\det A(t) = (\det A(t)) \cdot \mathrm{Tr}\left(A(t)^{-1} \cdot \frac{dA(t)}{dt}\right)$ has been utilised. This analysis may be recursively applied by differentiating eq. 6.58 and entering the form found for each expansion coefficient.

As an aside let us quickly look at the limit $g_{ab} \to \delta_{ab}$, such as is the case for locally regular AdS. In this limit eq. 6.60 simplifies to

$$\phi_{(2)}(x,\rho) = \frac{1}{2(2\Delta - d - 2)}\Box_\delta\phi_{(0)}(x) \ , \tag{6.61}$$

where $\Box_\delta = \delta^{ab}\partial_a\partial_b$. If we compute the recursion as mentioned in this case, we see that there is a general formula of

$$\phi_{(2n)}(x,\rho) = \frac{1}{2n(2\Delta - d - 2n)}\Box_\delta\phi_{(2n-2)}(x,\rho) \ . \tag{6.62}$$

Evidently, there is a problem with the general form at a particular terminating point satisfying $2\Delta - d - 2n = 0$ which will also appear in the specific forms at $2\Delta - d -$

$2 = 0$ due to the denominator becoming zero. This will only occur in even dimensions when the conformal dimension is an integer or in odd dimensions when the conformal dimension takes a half-integer value. In these situations the expansion must be modified by introducing a logarithmic term at the $\rho^{(2\Delta-d)/2}$ order as

$$\tilde{\phi}(x,\rho) = \phi_{(0)}(x) + \rho\phi_{(2)}(x) + \ldots + \rho^{(2\Delta-d)/2}(\phi_{(2\Delta-d)}(x) + \log(\rho)\psi_{(2\Delta-d)}(x)) + \ldots \ . \tag{6.63}$$

However, when we enter this expression back into the scalar field equation we find this means that $\phi_{(2\Delta-d)}$ is no longer determined by the equations of motion, but $\psi_{(2\Delta-d)}$ is through the relation

$$\psi_{(2\Delta-d)}(x) = -\frac{1}{2^{2\Delta-d}\Gamma(\Delta-d/2)\Gamma(\Delta-d/2+1)}\Box_\delta^{\Delta-d/2}\phi_{(0)}(x) \ . \tag{6.64}$$

Reverting back to the general form of the metric the situation is similar and $\phi_{(2\Delta-d)}$ will not be determined, however we can find $\psi_{(2\Delta-d)}$ such as in the case $2\Delta - d = 2$, which is given by

$$\psi_{(2)} = -\frac{1}{4}\left(\Box_{g_0}\phi_{(0)}(x) + \frac{1}{2}\,(d-2)\,\phi_{(0)}(x)\,\mathrm{Tr}(g_{(0)}^{-1}g_{(2)})\right) \ . \tag{6.65}$$

We can now move on to regulating and renormalising the scalar case. Integrating over the bulk past the finite cutoff $\rho \geq \epsilon$, we find (using integration by parts and the Klein-Gordon equation 6.56)

$$\begin{aligned} S_{\phi,\mathrm{reg}} &= \frac{1}{2}\int_{\rho\geq\epsilon} d^{d+1}x\sqrt{G}\left(G^{\mu\nu}\partial_\mu\phi\partial_\nu\phi + m^2\phi^2\right) \\ &= \frac{1}{2}\int_{\rho\geq\epsilon} d^{d+1}x\sqrt{G}\ \phi(x,\epsilon)\left(-\Box_G + m^2\right)\phi(x,\epsilon) - \frac{1}{2}\int_{\rho=\epsilon} d^dx\sqrt{G}g^{\rho\rho}\phi(x,\epsilon)\partial_\epsilon\phi(x,\epsilon) \\ &= -L^{d-1}\int_{\rho=\epsilon} d^dx\sqrt{g(x,\epsilon)}\epsilon^{d/2-\Delta}\left[\frac{1}{2}(d-\Delta)\tilde{\phi}^2(x,\epsilon) + \epsilon\tilde{\phi}(x,\epsilon)\partial_\epsilon\tilde{\phi}(x,\epsilon)\right] \ . \end{aligned} \tag{6.66}$$

We may now write this in a way that exemplifies the divergent terms by expanding out the fields, giving the regularised action as

$$S_{\phi,\mathrm{reg}} = L^{d-1}\int d^dx\sqrt{g_{(0)}}\left(\epsilon^{d/2-\Delta}a_{(0)} + \epsilon^{d/2-\Delta+1}a_{(2)} + \ldots - \log\epsilon\, a_{(2\Delta-d)}\right) + \mathcal{O}(\epsilon^0) \ , \tag{6.67}$$

where the functions $a_{(n)}$ are again conventional and in terms of the leading boundary fall-off $\phi_{(0)}$, *e.g.*

$$a_{(0)} = -\frac{1}{2}(d-\Delta)\phi_{(0)}^2, \quad a_{(2)} = -\frac{1}{4}\,\mathrm{Tr}\, g_{(2)}\phi_{(0)}^2 + (d-\Lambda+1)\phi_{(0)}\phi_{(2)} \ . \tag{6.68}$$

As we have that $\Delta > d/2$ there will be only a finite number of divergent terms that need renormalisable treatments when we finally take the limit $\epsilon \to 0$; if there were to be infinitely many that needed counterterms we would call the theory *non-renormalisable*. At this point we know exactly which terms will cause our divergences, and so we know that our counterterms must be exactly those which cancel them out. As we stated previously, our counterterms need to be constructed with the fields living at the boundary for covariance, and so we require $\phi_{(0)}, \phi_{(2)}$, *etc.* in terms of $\phi(x, \epsilon)$. To calculate these we invert eq. 6.54 with expansion 6.63, giving (with some caveats depending upon the value of $2\Delta - d$)

$$\phi_{(0)}(x) = \epsilon^{-(d-\Delta)/2} \left(\phi(x,\epsilon) - \frac{1}{2(2\Delta - d - 2)} \Box_\gamma \phi(x,\epsilon) + \dots \right) . \tag{6.69}$$

With these inversions, we can write the counterterms as[2]

$$\begin{aligned} S_{\text{ct}} = \int d^d x \sqrt{\gamma} \Bigg[& \frac{d-\Delta}{2} \phi^2(x,\epsilon) \\ & + \frac{1}{2(2\Delta - d - 2)} \left(\phi(x,\epsilon) \Box_\gamma \phi(x,\epsilon) + \frac{d-\Delta}{2(d-1)} R[\gamma] \phi^2(x,\epsilon) \right) + \dots \Bigg] . \end{aligned} \tag{6.70}$$

Similarly to the pure gravity case, we can write the one-point function as

$$\langle \mathcal{O} \rangle = \frac{1}{\sqrt{g_{(0)}}} \frac{\delta S_{\text{ren}}}{\delta \phi_{(0)}(x)} = \lim_{\epsilon \to 0} \frac{1}{\sqrt{g}} \frac{\delta (S_{\text{reg}} + S_{\text{ct}})}{\delta \phi(x,\epsilon)} , \tag{6.71}$$

which can then be put in terms of the boundary γ_{ab} as

$$\langle \mathcal{O} \rangle = \lim_{\epsilon \to 0} \left(\frac{L^d}{\epsilon^{d/2}} \frac{1}{\sqrt{\gamma}} \frac{\delta (S_{\text{reg}} + S_{\text{ct}})}{\delta \phi(x,\epsilon)} \right) . \tag{6.72}$$

6.3.3 Scalar-Gravity System

With both sectors understood in terms of holographic renormalisation we can move on to the situation where we include a coupled scalar+gravity system through

$$S_{\text{tot}} = S_{\text{EH}} + S_\phi , \tag{6.73}$$

which allows for a backreaction of the scalar field satisfying the Einstein equations

$$R_{\mu\nu} - \frac{1}{2} G_{\mu\nu} R - \Lambda G_{\mu\nu} = 8\pi G T_{\mu\nu} . \tag{6.74}$$

[2] This is valid when we have the condition $\Delta < d/2 + 2$, except when the condition $2\Delta - d = 1$. In this case, the coefficient of the term in parentheses is modified from $1/[2(2\Delta - d - 2)]$ to $-1/4 \log \epsilon$.

If we take eq. 6.32 to be the metric we consider again, along with eq. 6.33 to be the expansion of the d-dimensional part, we find the Einstein equations

$$\begin{aligned}
\rho\left[2g''_{ab} - 2\left(g'g^{-1}g'\right)_{ab} + \mathrm{Tr}\left(g^{-1}g'\right)g'_{ab}\right] + R_{ab}(g) - (d-2)g'_{ab} - \mathrm{Tr}\left(g^{-1}g'\right)g_{ab}& \\
= 8\pi G_{d+1}\rho^{d-\Delta-1}\left[\frac{(\Delta-d)\Delta}{d-1}\phi^2 g_{ab} + \rho\partial_a\phi\partial_b\phi\right]& \\
\nabla_a \mathrm{Tr}\left(g^{-1}g'\right) - \nabla^b g'_{ab} = 16\pi G_{d+1}\rho^{d-\Delta-1}\left[\frac{d-\Delta}{2}\phi\partial_a\phi + \rho\partial_\rho\phi\partial_a\phi\right]& \\
\mathrm{Tr}\left(g^{-1}g''\right) - \frac{1}{2}\mathrm{Tr}\left(g^{-1}g'g^{-1}g'\right) = 16\pi G_{d+1}\rho^{d-\Delta-2}\left[\frac{d(\Delta-d)(\Delta-d+1)}{4(d-1)}\phi^2\right.& \\
\left. +(d-\Delta)\rho\phi\partial_\rho\phi + \rho^2\left(\partial_\rho\phi\right)^2\right]\,,&
\end{aligned} \tag{6.75}$$

which obviously reduce to equations 6.34 in the limit $\phi = 0$ as it should do. In this system, much of the machinery we have presented is still applicable, except now we must contend with backreaction. We therefore will have to solve the coupled equations 6.75 and 6.58 which will involve inserting both sets of expansions, for the scalar field and the metric. Although the exact details will be very case specific, generally the formulae we have derived do apply except with certain extensions to take into consideration the role of the scalar field. Specifically for example, when working through the Einstein equations 6.75 we will now find that the falloffs of the metric expansion will depend upon the boundary coefficients of the field which relate to the source and vacuum expectation value of the field.

Field Theory on Boundary	Gravity in Bulk
Generating Functional $W[J]$	Regularised Action $S_{\text{reg}}[\phi]$
Renormalised Generating Functional $W_{\text{ren}}[J]$	Renormalised Action $S_{\text{ren}}[\phi]$
RG Flow	Bulk radial geometry evolution

Table 6.2: The additions to the holographic dictionary from holographic renormalisation.

Finally, we note a few of the dictionary discoveries we have made along the journey during holographic renormalisation in table 6.2; remembering these will help with understanding how quantities have been related during the research later in the thesis.

6.4 Fluid/Gravity Correspondence

A caveat that we have so far left out is that all of our considerations for the duality so far have necessarily been at zero temperature; an energy scale drops out of the discussion due to conformality ensuring physics is the same at any energy scale. Naturally for physical problems we expect to be able to describe things in terms of a temperature, and so we need to find a way to incorporate this. Fortunately, we have already come across the constituent ideas necessary for this type of discussion. In subsection 3.2.1, we discussed that to translate QFT from zero temperature to finite temperature we needed to Wick rotate the time direction, and therefore the temporal dimension becomes compactified on a circle. We find that for string theory, this takes our stack of D-branes to a stack of black D-branes, the string theory description of black holes in extended dimensions.

This promotes the supergravity background metric 6.1 to (specifying to $d = 4, p = 3$)

$$ds^2 = H^{-1/2}(r)\left[-f(r)dt^2 + \sum_{i=1}^{3}(dx^i)^2\right] + H^{1/2}(r)\left[f^{-1}(r)dr^2 + r^2 d\Omega_5^2\right] \ , \tag{6.76}$$

where $d\Omega_5^2$ is the 5-dimensional sphere metric, $H(r)$ is the warp-factor defined the same as in 6.2 with $p = 3$, and $f(r)$ is the blackening factor defined through

$$f(r) = 1 - \frac{r_h^{7-p}}{r^{7-p}} \ , \tag{6.77}$$

which is specified at $p = 3$ for our case. Taking similar limits as for the zero-temperature case, as $r \to \infty$ we again recover exactly the same situation with flat Minkowksi at the boundary. In the other limit at $r/L \ll 1$, we can again take $H(r) \approx L^4/r^4$ and rewrite the metric as

$$ds^2 = \frac{L^2}{z^2}\left[-\left(1 - \frac{z^4}{z_h^4}\right)dt^2 + \sum_{i=1}^{3}(dx^i)^2 + \left(1 - \frac{z^4}{z_h^4}\right)^{-1} dz^2\right] + L^2 d\Omega_5^2 \ , \tag{6.78}$$

where we have used the substitution $z = L^2/r$ and $z_h = L^2/r_h$. As we can see, the metric is almost identical to what we found previously, with all sectors sharing the same radius L. In fact, if we remember at the very beginning of our discussion the form of eq. 2.30 with $D = 5$, we see that the anti-de Sitter portion of the metric has simply been modified to also contain a Schwarzschild black hole. Our space has therefore been modified to AdS$_5$-Schwarzschild$\times\mathbb{S}^5$ when considering the inclusion of temperature effects.

We may even check that our usual determination of temperature is still valid. As we said previously, to find a temperature we must Wick rotate and so we take $\tau = it$ and also define a new coordinate

$$\frac{z}{z_h} = 1 - \frac{\rho}{L^2} \ . \tag{6.79}$$

This leaves our metric looking like

$$ds^2 = \frac{4\rho^2}{z_h^2}d\tau^2 + \frac{L^2}{z_h^2}\sum_{i=1}^{3}(dx^i)^2 + d\rho^2 + \dots \ , \tag{6.80}$$

to lowest order in ρ, where ... signifies the higher order terms and also the 5-sphere metric which is unaffected. We may make a further identification of the time coordinate as

$$d\phi = \frac{2}{z_h} d\tau \ , \tag{6.81}$$

which is a direct comparison of eq. 2.40 and near the horizon this leaves us with

$$ds^2 = d\rho^2 + \rho^2 d\phi^2 \ . \tag{6.82}$$

Again periodicity must be imposed to avoid a conical singularity, and so integrating eq. 6.81 exactly like eq. 2.41 as

$$\int_0^{2\pi} d\phi = \int_0^{1/T} \frac{2}{z_h} d\tau \tag{6.83}$$

means we find a Hawking temperature for this setup of

$$T_H = \frac{1}{\pi z_h} \ , \tag{6.84}$$

which is plainly just 2.42 with a particular choice of $f(r)$ and $g(r)$. With the temperature of the system in hand, all other thermodynamic quantities can follow from it, and so we can form a complete thermodynamic picture of a QFT from the thermal description of the black hole on the gravitational side. This leads to questions such as what phase transitions in a field theory translate to for a black hole system. This is obviously dependent upon the type of phase transition the system is experiencing, but generically what it indicates on the gravitational side is an instability of the black hole system [184, 185].

Overall then we have found that at finite temperature the AdS/CFT correspondence must contain a black hole in its interior which provides thermodynamics through the usual black hole thermodynamic relations. We list these additions to the holographic dictionary in Table 6.3.

Field Theory on Boundary	Gravity in Bulk
Finite-Temperature Field Theory	AdS-Schwarzschild
Temperature T	Hawking Temperature T_H
Phase Transition	Black Hole Instability

Table 6.3: Extended holographic dictionary at non-zero temperature.

Evidently this case we have studied is specific to $\mathcal{N} = 4$ SYM theory and we have found a thermodynamic theory from it; this is known as the *top-down approach*. There are in fact two ways to go about studying the AdS/CFT correspondence:

- Top-down: In this approach one starts with a superstring theory and tries to find a field theory similar to their real-world problem.

- Bottom-up: In this approach one starts with the field theory they want to study and attempts to construct a string theory which approximates the situation.

In our papers we shall always be using the bottom-up approach.

Chapter 7

Paper I: Gravitational Waves from a Holographic Phase Transition

Abstract

We investigate first order phase transitions in a holographic setting of five-dimensional Einstein gravity coupled to a scalar field, constructing phase diagrams of the dual field theory at finite temperature. We scan over the two-dimensional parameter space of a simple bottom-up model and map out important quantities for the phase transition: the region where first order phase transitions take place; the latent heat, the transition strength parameter α, and the stiffness. We find that α is generically in the range 0.1 to 0.3, and is strongly correlated with the stiffness (the square of the sound speed in a barotropic fluid). Using the LISA Cosmology Working Group gravitational wave power spectrum model corrected for kinetic energy suppression at large α and non-conformal stiffness, we outline the observational prospects at the future space-based detectors LISA and TianQin. A TeV-scale hidden sector with a phase transition described by the model could be observable at both detectors.

7.1 Introduction

Spontaneous symmetry breaking of gauge theories is a fundamental ingredient of nature, which can manifest itself in the early Universe as a phase transition [186, 187]. In particular, when temperatures were in the range 100-1000 GeV, there may have been a phase transition associated with the breaking of the electroweak symmetry. If this was a first order transition, gravitational waves would have been produced through bubble nucleation, collision and counter-propagating sound waves (see e.g. [188]). There is a strong possibility that they would be of the right frequency to be observed by a space-based gravitational wave detector such as LISA (Laser Interferometer Space Antenna) [189]. LISA will be sensitive to gravitational waves in the frequency range 1 to 10 mHz with characteristic strains of order 10^{-21}, and hence to phase transitions occurring at around 10^{-12} seconds after the big bang (see e.g. [2]).

The standard model electroweak transition is known to be a crossover [10, 11, 12], however, even minimal extensions may allow a first-order transition [190, 191, 192, 193, 194, 195, 196, 197, 198, 199]. One class of extensions invokes strong dynamics just above the electroweak scale, which triggers electroweak symmetry-breaking, while addressing the hierarchy problem (see e.g. [200, 201]). Strongly-coupled field theories are notoriously difficult to study quantitatively. Holography is a technique for simplifying calculation by translating these complex strongly-coupled field theories into more tractable weakly-coupled gravitational theories [202, 167, 203].

Cosmological phase transitions in holographic models have been studied mostly in the context of Randall-Sundrum models [87, 88, 89, 91, 204, 205, 206, 207, 208, 209, 210, 211, 212], where there is a first order phase transition between a black brane geometry and a horizonless geometry. From the field theory dual point of view this is interpreted as a confinement transition [156]. More recently in [213], this approach has been extended to the confinement transition in a model based on a string theory construction, the Sakai-Sugimoto model [214]. In addition [213] also studied chiral phase transitions in the same model. The chiral transition is realised through probe branes in a fixed black brane background entering the horizon [215, 216].

Gravitational wave production has been studied in Randall-Sundrum models [88, 206, 207, 208, 210, 211, 212], and recently in the context of the above-mentioned Sakai-Sugimoto model [217]. It should be noted that all these studies are based on static configurations. Dynamical evolution of strongly coupled theories close to a phase transition has been studied in the context of applications to heavy ion collisions and condensed matter [218, 219, 220, 221], including dynamical phase separation in three-dimensional [222, 223, 224] and four-dimensional [225, 226, 227] theories.

In this paper we study a phase transition in a simple bottom-up holographic model, calculating the equilibrium parameters which are most important in determining gravitational wave signals. We scan over the two parameters of the model, showing that the transitions are generically "intermediate" in strength in the classification of Ref. [118], meaning that the transition strength parameter at the critical temperature (the fraction of the energy available for conversion to kinetic energy and thereby gravitational wave production) is $\alpha = \mathrm{O}(10^{-1})$. Strong transitions ($\alpha = \mathrm{O}(1)$) are also possible with supercooling. We find a strong correlation between α and the stiffness at the critical temperature, meaning that the speed of sound can be quite different from $1/\sqrt{3}$.

We then study the implications for gravitational wave production and observation, using the LISA Cosmology Working Group model [228] as a starting point. We take into account recent work on kinetic energy conversion at strong transitions [118] and when the stiffness is different from 1/3 [116], and include an improved treatment of the effect of the finite lifetime of the source [112].

We find that the transitions in the holographic model are strong enough to be easily seen at LISA (and the similarly configured Taiji [7]), and possibly even TianQin [122], if the peak frequency is in the range of the maximum sensitivity. The condition of observability constrains a combination of the transition temperature, the transition rate parameter, and the wall speed.

The rest of this paper is organized as follows. In Section 7.2 we review the putative first order phase transitions and their relation to properties of expanding bubbles in a cosmological context. In Section 7.3 we will describe the holographic model [229] and its black brane solutions. In Section 7.4 we compute the thermodynamic quantities of interest from the holographic model. Equipped with the equation of state across the phase transition, in Section 7.5 we make a scan over the free parameters of the holographic model and find the regions of the parameter space in which a strongly first order phase transition exists, and the relevant thermodynamic parameters for gravitational wave production. In Section 7.6 we will determine if the signal as extracted from the holographic model is in the sensitivity window of future gravitational wave detectors. We conclude in Section 5 with a discussion of our findings and some thoughts on future developments of our work. Appendices A and B contain details of the holographic renormalisation and the numerical procedures we implement, respectively, and Appendix C contains details of the power

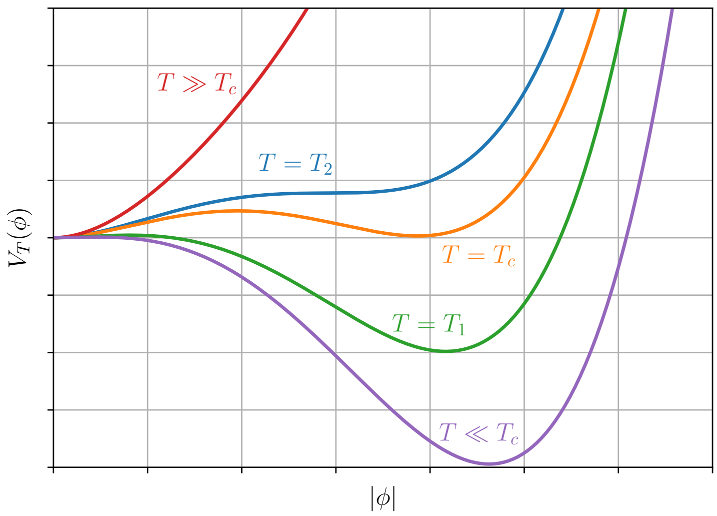

Figure 7.1: The thermal potential for varying temperatures. $T \gg T_c$ is the limit in which the potential is symmetric around $\phi = 0$, $T = T_2$ is the temperature below which a second minimum appears, T_c is the critical temperature at which there are degenerate minima, and $T = T_1$ is where the first minimum at the origin disappears and the second minimum becomes the only equilibrium state.

spectrum model, describing the modifications to that of Ref. [228] we have introduced.

7.2 First order phase transitions

First-order transitions from an 'old' to a 'new' phase proceed through the nucleation of bubbles in the old phase, with an order parameter jumping discontinuously at the transition temperature. Coleman [96, 97] was the first to analyse how a metastable phase could decay through vacuum quantum fluctuations via bubbles nucleating containing a stable phase at zero-temperature in a cosmological setting. Later on Linde [94, 95] generalised Coleman's work to bubbles nucleating at a non-zero temperature. Collision of these bubbles would be an extremely energetic process, leading to gravitational waves being produced in a possibly observable way [230]. Accurately estimating the power spectra of the signal is of great import as detection of cosmological gravitational waves would be strong evidence for physics beyond the Standard Model (see [228] for a review).

Fluctuations in the old phase trigger the nucleation of bubbles of the new phase. These bubbles would then collide and merge until the Universe would saturate with the new phase, at which time the phase transition would be complete. The generation of bubbles and whether conditions are right for them to proliferate is described by four main parameters: transition strength α, transition rate β, nucleation temperature T_N, and the wall speed v_w. Recently, it has also been pointed out that the sound speed, controlled by the stiffness $\partial p/\partial e$ is also important [231, 116].

The important temperatures in a phase transition are as follows. First, the critical temperature T_c, where the free energy of two competing phases first becomes equal, as shown in Fig. 7.1. Bubble nucleation takes place at a lower temperature $T_N < T_c$, where the phase transition actually takes place. Between these two temperatures the system is in a supercooled state. The supercooled state can persist to a minimum temperature T_1, which may be zero.

Another important quantity of a first-order phase transition is the difference in the trace of the energy-momentum tensor between phases, which is the energy available for conversion to shear stress and so dictates the power of the gravitational wave signal. This is quantified in a dimensionless transition strength parameter α, which we define below. We first note that the plasma enthalpy w, pressure p, and energy density e are all related by $w = e + p$. We also introduce a useful quantity θ that is proportional the trace of the energy-momentum tensor:

$$\theta_{s,b} = \frac{1}{4}\left(e_{s,b} - 3p_{s,b}\right) \ , \tag{7.1}$$

where the s/b subscripts represent quantities in the symmetric and broken phase, respectively.[1] The transition strength parameter is then defined as

$$\alpha = \frac{4}{3}\frac{(\theta_s - \theta_b)}{w_s} \ . \tag{7.2}$$

Another quantity which is closely related is the latent heat, found at T_c by

$$L = e_s(T_c) - e_b(T_c) = 4(\theta_s(T_c) - \theta_b(T_c)), \tag{7.3}$$

with the second equality following from the definition of the critical temperature, $p_b(T_c) = p_s(T_c)$. If the latent heat is comparable to the radiation energy density of the universe, we call the transition strongly first order. In terms of the transition strength, this happens when $\alpha \sim 1$. We also call $\alpha \sim 0.1$ intermediate, and $\alpha \gg 1$ very strong, following [232, 114, 118]. The parameter α is a primary focus in this paper, as it can be directly accessed through a holographic calculation, and we will expand on it later.

[1] We use the terms "symmetric" and "broken" for the two phases, following the convention in gauge theories. As we are considering cooling through the transition, the symmetric phase is the 'old' phase and the broken phase is the 'new' phase.

Bubble walls are assumed to expand at a constant speed v_w [233], which is determined by how the wall interacts with the surrounding plasma in the interplay between bubble expansion and frictional forces [234, 125]. Fluid friction is thought to prevent runaway acceleration in phase transitions in gauge theories, although the details of the interactions between the particles of the plasma and the wall are under debate [235, 236, 237]. Ref. [238] recently showed that in confining transitions, the LO "leading order" pressure (the pressure from the partial conversion of the quark's momenta before entering the bubbles into hadron masses [239]) is in principle enough to ensure bubble walls do not runaway asymptotically. The wall speed is of particular importance as it impacts the kinetic energy production, and hence the gravitational wave power.

Another important parameter is the transition rate

$$\beta \equiv \frac{\mathrm{d}}{\mathrm{d}t} \log \left(\frac{\Gamma(t)}{\mathcal{V}} \right) \Bigg|_{t=t_f} , \tag{7.4}$$

where $\Gamma(t)/\mathcal{V}$ is the nucleation rate per unit volume in the symmetric phase. This is evaluated at a time t_f which is at the temperature where the nucleation rate averaged over the whole universe peaks, and can be used to define the nucleation temperature [188]. From these quantities the scale of the theory in the form of the typical bubble separation is set by

$$R_* \propto \frac{v_w}{\beta} . \tag{7.5}$$

The proportionality factor is an O(1) number, which specifically for weak transitions is $(8\pi)^{1/3}$. As it is not known what the factor is for all transition strengths, we will use this number as a first approximation.

Finding β involves a calculation of the effective action for non-constant fields, which is a straightforward procedure in a weakly coupled theory, but in a holographic set-up is challenging enough to merit a separate treatment. Holographic methods for calculating v_w in this theory do not yet exist. When studying gravitational wave production we will therefore treat them as free parameters.[2] For studying gravitational wave power spectra the more useful scale-setting combination is R_*.

7.3 Holographic setup

The gauge/gravity duality is a powerful tool to deal with strongly coupled gauge systems and their phase structure, as strongly coupled systems on one side can be translated into weakly coupled systems on the other. The duality provides a "holographic dictionary"

[2] In weakly coupled theories, there are interesting correlations between β and α [240, 241].

which describes an exact linkage between quantities on the d-dimensional field theory side to quantities on the $(d+1)$-dimensional gravitational side, with surprising success in areas such as heavy ion collisions [202, 167, 203]. Using the duality we are able to calculate quantities relevant for gravitational wave production in phase transitions, which would otherwise be very hard to compute.

The model consists of gravity coupled to a bulk scalar field, with the following action

$$S_{\text{non-reg}} = \frac{2}{\kappa_5^2}\int \mathrm{d}^5x\sqrt{-g}\left(\frac{\mathcal{R}}{4} - \frac{1}{2}\partial_\mu\phi\partial^\mu\phi - V(\phi)\right) + \frac{1}{\kappa_5^2}\int_{\partial\mathcal{M}} \mathrm{d}^4x\sqrt{-\gamma}K \ , \tag{7.6}$$

where the first term is the (4+1)-dimensional Einstein-Hilbert action and the last term is the Gibbons-Hawking-York boundary term [242, 243], with γ representing the determinant of the induced metric on the boundary and K giving the trace of the extrinsic curvature. The potential for the scalar field $V(\phi)$ is defined in terms of a superpotential $W(\phi)$ which was introduced in this holographic setting by [244]. It is worth pointing out that the system is not expected to be supersymmetric and invoking the superpotential is merely a mathematical trick which allows to find solutions by solving a simpler set of first order equations [245]. By analogy with supersymmetric systems we we will dub the solutions to the first order system as "BPS" (Bogomol'nyi-Prasad-Sommerfield).

The general formula for the potential is as follows

$$V(\phi) = -\frac{4}{3}W(\phi)^2 + \frac{1}{2}W'(\phi)^2 \ . \tag{7.7}$$

The superpotential is chosen as in [229], so as to provide the system with a first-order phase transition. It is dependent upon two parameters that we will specify in the numerical calculation (namely ϕ_M and ϕ_Q), and has the form

$$LW(\phi) = -\frac{3}{2} - \frac{\phi^2}{2} - \frac{\phi^4}{4\phi_M^2} + \frac{\phi^6}{\phi_Q} \ . \tag{7.8}$$

When W is inserted into the equation for the potential (7.7), one obtains

$$\begin{aligned} L^2V(\phi) = -3 - \frac{3\phi^2}{2} - \frac{\phi^4}{3} - \left(\frac{1}{3\phi_M^2} - \frac{1}{2\phi_M^4} + \frac{2}{\phi_Q}\right)\phi^6 \\ - \left(\frac{1}{12\phi_M^4} + \frac{6}{\phi_M^2\phi_Q} - \frac{4}{3\phi_Q}\right)\phi^8 + \left(\frac{2}{3\phi_M^2\phi_Q} + \frac{18}{\phi_Q^2}\right)\phi^{10} - \frac{4\phi^{12}}{3\phi_Q^2}. \end{aligned} \tag{7.9}$$

It is evident that both the potential and superpotential have a maximum at $\phi = 0$. At the maximum the second derivative of the potential (which determines mass) takes the value $m^2 = -3/L^2$. Following the usual holographic dictionary [246] for a massive scalar in AdS_5, the field ϕ is dual to a scalar operator $\mathcal{O}$ with a scaling dimension determined by

$$\Delta(\Delta - 4) = m^2L^2 \ . \tag{7.10}$$

The larger solution determines the scaling dimension of the dual operator $\Delta_+ = 3$. The smaller solution corresponds to a coupling with dimension $\Delta_- = 1$. We have deferred details of the holographic renormalisation to Appendix A and hence speed forward to discussing the solutions of the model instead.

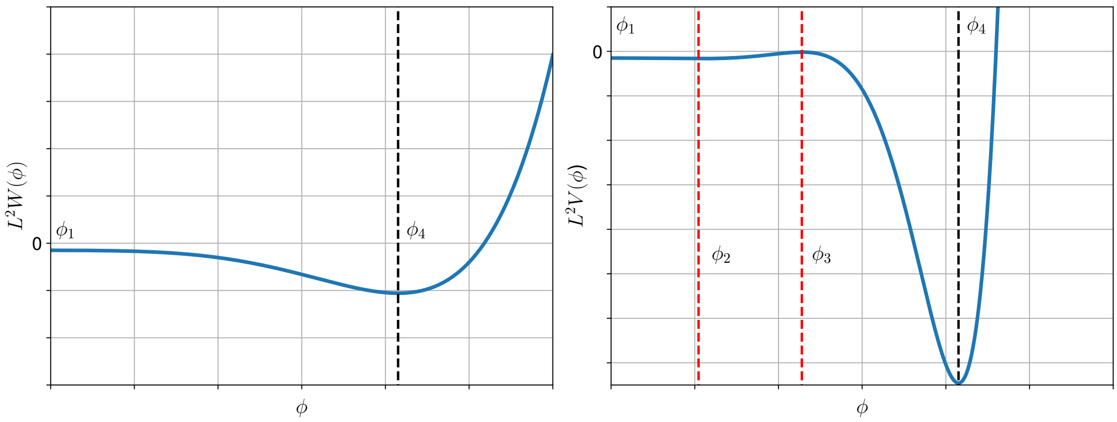

Figure 7.2: Graphs of the superpotential $W(\phi)$ and potential $V(\phi)$ of the theory, with interesting points shown. The superpotential and potential share the BPS extrema ϕ_1 and ϕ_4, whilst only the potential has the non-BPS extrema ϕ_2 and ϕ_3. In this plot the values used are $\phi_M = 0.5$ and $\phi_Q = 5.0$.

The potential and superpotential share a minimum and a maximum, with the minimum known as the BPS vacuum, but for some values of the parameters the potential also contains two “non-BPS” extrema in between these points not present in the superpotential, as seen in Fig. 7.2. The non-BPS minimum corresponds to a vacuum which persists to zero temperature. Some values that realise this situation are the ones used in [229], $\phi_M \simeq 0.5797$ and $\phi_Q = 10.0$; see also related study in [247]. At zero temperature there can be solutions interpolating between the $\phi = 0$ maximum close to the boundary and either the BPS or the non-BPS minimum in the deep interior of the geometry. Each of them correspond to different vacua of the dual field theory. At finite temperature there is a competition between the phases associated to each of these vacua, but even for values of the parameters where the non-BPS extrema are absent from the potential and there is a unique vacuum at zero temperature, a new phase appears at large enough temperatures.

We will be interested in this last situation, so we only look at potentials for which there are no extrema at ϕ_2, ϕ_3 (implying that at $T = 0$ there are less solutions) and with values of $\phi_h < \phi_4$. Branches on the thermodynamic phase diagrams will arise from heating up these vacua, with more discussion on the branch structure found in [229]. We are interested in solutions interpolating between two AdS solutions, which is dual to RG flows from the UV fixed point at $\phi = 0$ to the IR fixed point and so we are looking for solutions where ϕ approaches the conformal vacuum $\phi = 0$ at infinity due to this being where the holographic duality is best understood. The reason for the IR fixed point is that this guarantees that the zero-temperature solution is smooth in the deep IR.

7.3.1 Black brane solutions

In order to determine the thermodynamic properties of this system, we need to find a family of black brane solutions. They can be parametrised by the horizon value of ϕ (denoted ϕ_h), with ϕ_h approaching the value where the potential has a minimum at lower temperatures and zero at higher temperatures. The zero temperature solutions for ϕ indicate that the field is monotonic with respect to the radial coordinate meaning we can use the scalar field as a coordinate, and so we employ the same metric choice as [248], which can be expressed in the Eddington-Finkelstein form as

$$ds^2 = e^{2A(\phi)}\left(-h(\phi)d\tau^2 + d\mathbf{x}^2\right) - 2e^{A(\phi)+B(\phi)}Ld\tau d\phi \ . \tag{7.11}$$

The Einstein equations for this metric Ansatz are

$$\begin{aligned}
A''(\phi) - A'(\phi)B'(\phi) + \frac{2}{3} &= 0 \\
h''(\phi) + (4A'(\phi) - B'(\phi))h'(\phi) &= 0 \\
\frac{3}{2}A'(\phi)h'(\phi) + (6A'(\phi)^2 - 1)h(\phi) + 2e^{2B(\phi)}L^2V(\phi) &= 0 \\
4A'(\phi) - B'(\phi) + \frac{1}{h(\phi)}\left(h'(\phi) - e^{2B(\phi)}L^2V'(\phi)\right) &= 0 \ .
\end{aligned} \tag{7.12}$$

We observe that our scalar field is bounded by $0 \leq \phi \leq \phi_h$, with the requirement that the blackening factor goes to zero at the horizon $h(\phi_h) = 0$.

We emulate the master function procedure first introduced in [249], where by combining the Einstein equations and derivatives thereof we can reduce the problem to only depend on the "master function" and the potential. We consider a smooth "generating function" which will be related to our metric components by

$$G(\phi) = \frac{dA(\phi)}{d\phi} \ . \tag{7.13}$$

Replacing this in the field equations and manipulating them we find

$$\frac{G'(\phi)}{G(\phi) + \frac{4V(\phi)}{3V'(\phi)}} = \frac{d}{d\phi}\log\left(\frac{G'(\phi)}{G(\phi)} + \frac{1}{6G(\phi)} - 4G(\phi) - \frac{G'(\phi)}{\left(G(\phi) + \frac{4V(\phi)}{3V'(\phi)}\right)}\right) \ , \tag{7.14}$$

leaving us with a second order non-linear differential equation to solve. To reduce this to first order equations more suitable for numerical integration, we introduce a new variable defined as

$$H(\phi) = \frac{G'(\phi)}{G(\phi)} \ , \tag{7.15}$$

which when entered into the master equation, and after some further manipulation, yields two differential equations to be solved:

$$G'(\phi) = G(\phi)H(\phi) \tag{7.16}$$

and

$$H'(\phi) = \frac{H(\phi)}{\left(1 + \frac{4\gamma_1(\phi)}{3G(\phi)}\right)} \left[2H(\phi) + \frac{2}{G(\phi)} + \frac{8\gamma_1(\phi)}{9G^2(\phi)} + \frac{1}{\gamma_2(\phi)} + 4G(\phi)\left(1 + \frac{4\gamma_1(\phi)}{3G(\phi)}\right)\right] \ . \tag{7.17}$$

Here we have set

$$\gamma_1(\phi) = \frac{V(\phi)}{V'(\phi)}, \qquad \gamma_2(\phi) = \frac{V'(\phi)}{V''(\phi)}, \qquad \gamma_3 = \frac{V''(\phi)}{V'''(\phi)}, \tag{7.18}$$

for brevity, with the last definition preemptively added. Further following the procedure of [249], the next step is to find the series solution of the master equation around the horizon ϕ_h, which translates to finding series solutions for both $G(\phi)$ and $H(\phi)$. By requiring that the blackening factor goes to zero at the horizon, *i.e.*, $h(\phi_h) = 0$, we can find an expression for $G(\phi_h)$ by combining the last two of the Einstein equations in (7.12) and evaluating them at the horizon. Derivatives of the expression before horizon evaluation can give an expansion up to any desired order. Taylor expanding around ϕ_h therefore gives (denoting $\gamma(\phi_h) = \gamma^h$)

$$G(\phi) = -\frac{4}{3}\gamma_1^h \left[1 + \frac{1}{2}(\phi - \phi_h)\left(\frac{\gamma_2^h - \gamma_1^h}{\gamma_1^h\gamma_2^h}\right)\right] + \mathrm{O}(\phi - \phi_h)^2 \tag{7.19}$$

and

$$H(\phi) = \frac{\gamma_2^h - \gamma_1^h}{2\gamma_1^h\gamma_2^h}\left[1 + \frac{2}{3}(\phi - \phi_h)\left(1 + \frac{\gamma_1^h}{\gamma_2^h\gamma_3^h}\frac{(\gamma_3^h - \gamma_2^h)}{(\gamma_2^h - \gamma_1^h)} - \frac{8}{3}\gamma_1^h\right)\right] + \mathrm{O}(\phi - \phi_h)^2 \ , \tag{7.20}$$

with the condition for H at the horizon

$$\left.\frac{dH}{d\phi}\right|_{\phi_h} = H(\phi_h)\left(\frac{2}{3}\frac{\gamma_1^h}{\gamma_2^h\gamma_3^h}\frac{(\gamma_3^h - \gamma_2^h)}{(\gamma_2^h - \gamma_1^h)} - \frac{16\gamma_1^h}{9} - \frac{3}{2\gamma_1^h} - \frac{4}{3}\right) \ . \tag{7.21}$$

We also wish to know what is happening for these quantities at the other boundary in our model, where $\phi \to 0$. Expansion for small ϕ of (7.19) and (7.20) gives a simple leading behaviour

$$G(\phi) = \frac{dA(\phi)}{d\phi} = -\frac{1}{\phi} + \dots \ , \tag{7.22}$$

and

$$H(\phi) = -\frac{1}{\phi} + \dots \ . \tag{7.23}$$

Once the master function is determined, the other metric quantities have a simple dependence on it.

The first relation comes immediately from the definition of $G(\phi)$ (7.13), that we integrate to obtain $A(\phi)$

$$A(\phi) = -\log\left(\frac{\phi}{\Lambda L}\right) + \int_0^\phi \left(G(\varphi) + \frac{1}{\varphi}\right) d\varphi \ , \tag{7.24}$$

where Λ is an arbitrary constant which overall simply acts as a rescaling through the magnitude of the scalar field non-normalisable mode. Rearranging the first of our field equations (7.12) for $B'(\phi)$ and integrating gives us

$$B(\phi) = \log(|G(\phi)|) + \int_0^\phi \frac{2d\varphi}{3G(\varphi)} \ . \tag{7.25}$$

Finally, eliminating $h'(\phi)/h(\phi)$ from the last two field equations in (7.12) leaves $h(\phi)$ in terms of known quantities, taking the form

$$h(\phi) = -\frac{e^{2B(\phi)}L^2(4V(\phi)) + 3G(\phi)V'(\phi)}{3G'(\phi)} \ . \tag{7.26}$$

With our differential equations and metric functions specified and our boundary conditions established in the form of horizon quantities (7.19) and (7.20), we now show how this master function can be solved.

Analytic solutions to our system of equations are rare, only occurring for specially selected master functions/potentials (see Ref. [250] where $G(\phi) = -1/(3\gamma)$). Therefore, as we are searching for specific solutions of a relatively complicated potential, we will need to resort to numerical methods (see Appendix B).

7.4 Thermodynamics

The entropy and temperature in the dual field theory are determined by the Bekenstein-Hawking entropy and Hawking temperature of the black brane. The entropy is proportional to the area of the horizon while the temperature is proportional to the surface gravity. These can be expressed in terms of metric components as

$$s = \lim_{\phi\to\phi_h} \frac{2\pi}{\kappa_5^2}\sqrt{(g_{xx})^3}, \qquad T = \lim_{\phi\to\phi_h} \frac{1}{2\pi}\frac{\partial_\phi\sqrt{g_{\tau\tau}}}{\sqrt{g_{\phi\phi}}} \ . \tag{7.27}$$

Using the metric (7.11), we can read off the entropy density and temperature as follows

$$s = \frac{2\pi}{\kappa_5^2}e^{3A(\phi_h)}, \qquad LT = \frac{e^{A(\phi_h)-B(\phi_h)}}{4\pi}|h'(\phi_h)| \ . \tag{7.28}$$

All of these functions are now readily evaluated at the horizon using the formulae (7.24)-(7.26) found in Section 7.3. Evaluating $h'(\phi)$ at the horizon simply requires the use of either of the last two field equations in (7.12). Combining everything together, we find the entropy density and temperature in terms of the master function

$$s = \frac{2\pi}{\kappa_5^2}\left(\frac{\Lambda L}{\phi_h}\right)^3 \exp\left\{3\int_0^{\phi_h}\left(G(\phi)+\frac{1}{\phi}\right)d\phi\right\} \tag{7.29}$$

and

$$T = -\Lambda\frac{L^2V(\phi_h)}{3\pi\phi_h}\exp\left\{\int_0^{\phi_h}\left(G(\phi)+\frac{1}{\phi}+\frac{2}{3G(\phi)}\right)\right\} \ . \tag{7.30}$$

At zero temperature the theory becomes conformal at the fixed points (UV and IR), such as the BPS-minimum ϕ_4, due to the zero temperature solutions being the vacuum solutions which have $\langle\mathcal{O}\rangle = 0$,and therefore $\langle T^\mu_\mu\rangle = 0$ which satisfies the condition for conformality. It can be seen that the temperature must go to zero at this minimum by considering the last Einstein equation in (7.12) and noting that for $\phi \to \phi_h = \phi_4$ we find $h(\phi_h = \phi_4) = 0$ and $V'(\phi_h = \phi_4) = 0$. This readily leads to $h'(\phi_h = \phi_4) = 0$ which sets $T = 0$ through equation (7.28). We then expect the entropy density to tend to $\frac{2\pi^2}{45}g_* T^3$ close to those fixed points, where g_* is the effective number of relativistic degrees of freedom of the corresponding CFT. Defining a dimensionless and rescaled measure of the entropy

$$\left(\frac{s}{T^3}\right)_R = \frac{\kappa_5^2}{2\pi^4L^3}\frac{s}{T^3} = -\left(\frac{3}{L^2V(\phi_h)}\right)^3\exp\left(-\int_0^{\phi_h}\frac{2d\phi}{G(\phi)}\right) \ , \tag{7.31}$$

we now have an expression purely depending on the master function and the potential. We compare our calculation of s/T^3 with that obtained in [229] for particular values of the parameters in the potential ($\phi_M \simeq 0.5797, \phi_Q = 10.0$) in Appendix B. Conformal symmetry is achieved at high temperature, when the coupling to the scalar operator is negligible compared with the temperature, and we approach the solution $\phi \sim 0$ in the gravity dual. Here our rescaled quantity tends to 1, and so this implies that our number of degrees of freedom on the gravity side is

$$\frac{s}{T^3} = \frac{2\pi^4L^3}{\kappa_5^2} \ , \tag{7.32}$$

which depends on the radius of curvature L and the five dimensional Newton's constant $\kappa_5^2 = 8\pi G_5$.

For the study of the phase transition, we will also need the energy density and pressure, e and p. The pressure can be obtained directly from s and T using the thermodynamic derivative

$$s = \frac{dp}{dT}, \tag{7.33}$$

which is easily integrable (numerically) to give

$$p = \int_0^T s(\tilde{T})d\tilde{T} \ . \tag{7.34}$$

This is consistent with the holographic renormalisation analysis of Appendix A, in that the vacuum contribution vanishes. The energy density is obtained through the thermodynamic relation

$$e = Ts - p \; . \tag{7.35}$$

Integrating numerically in this way introduces errors, which we checked by comparing to the correct T^4 behaviour at high temperature and found matches well.

Another quantity we are interested in is the expectation value of the scalar operator. As the energy-momentum tensor can be written as $T_{\mu\nu} = \text{diag}(e, p, p, p)$, we may take the trace and use the Ward identity[3]

$$\langle T^{\mu}_{\mu} \rangle = -\Lambda \langle \mathcal{O} \rangle \tag{7.36}$$

to write

$$-\langle T^{\mu}_{\mu} \rangle = e - 3p = \Lambda \langle \mathcal{O} \rangle \; . \tag{7.37}$$

We will fix units to $\kappa_5^2/L^3 = 1$, so implicitly we are computing rescaled quantities such as

$$\langle \tilde{\mathcal{O}} \rangle = \frac{\kappa_5^2}{L^3} \langle \mathcal{O} \rangle \; , \tag{7.38}$$

and similarly for the thermodynamic potentials. We plot the expectation value of the scalar operator, as well as the free energy ($f = -p$) and the rescaled effective degrees of freedom $\tilde{g}_* = g_* \kappa_5^2/L^3$ for various values of ϕ_Q at fixed ϕ_M in Fig. 7.3. These curves are generated by varying the horizon value ϕ_h, which produces a different temperature for each ϕ_h point. The phase transition occurs between solutions where the order parameter is $\langle \mathcal{O} \rangle = 0$ to solutions where $\langle \mathcal{O} \rangle \neq 0$. We first see that, as ϕ_Q increases, f moves away from its usual "swallow tail" first-order transition shape and the energy density and free energy tend to the case with non-BPS extrema, *i.e.* with both phases persisting down to zero temperature. The "kinks" in the swallow tail shape are a consequence of the positivity of the entropy of solutions merging in configuration space. In the IR, the scalar field is non-zero and will be most relevant to all physics considerations. In the UV region, however, all operators tend to $\propto \Lambda T^2$ and to very similar numeric values as well (no difference up to the 13th decimal place for these examples). This is explained by noticing that in the UV region we are considering the vicinity of $\phi \to 0$, which results in the potential acting as

$$V(\phi) \approx -3 + \mathrm{O}(\phi^2) \; , \tag{7.39}$$

[3] For this particular model a possible contribution to the trace anomaly $\sim \Lambda^4$ vanishes, see, *e.g.*, [251, 252] and Appendix A.

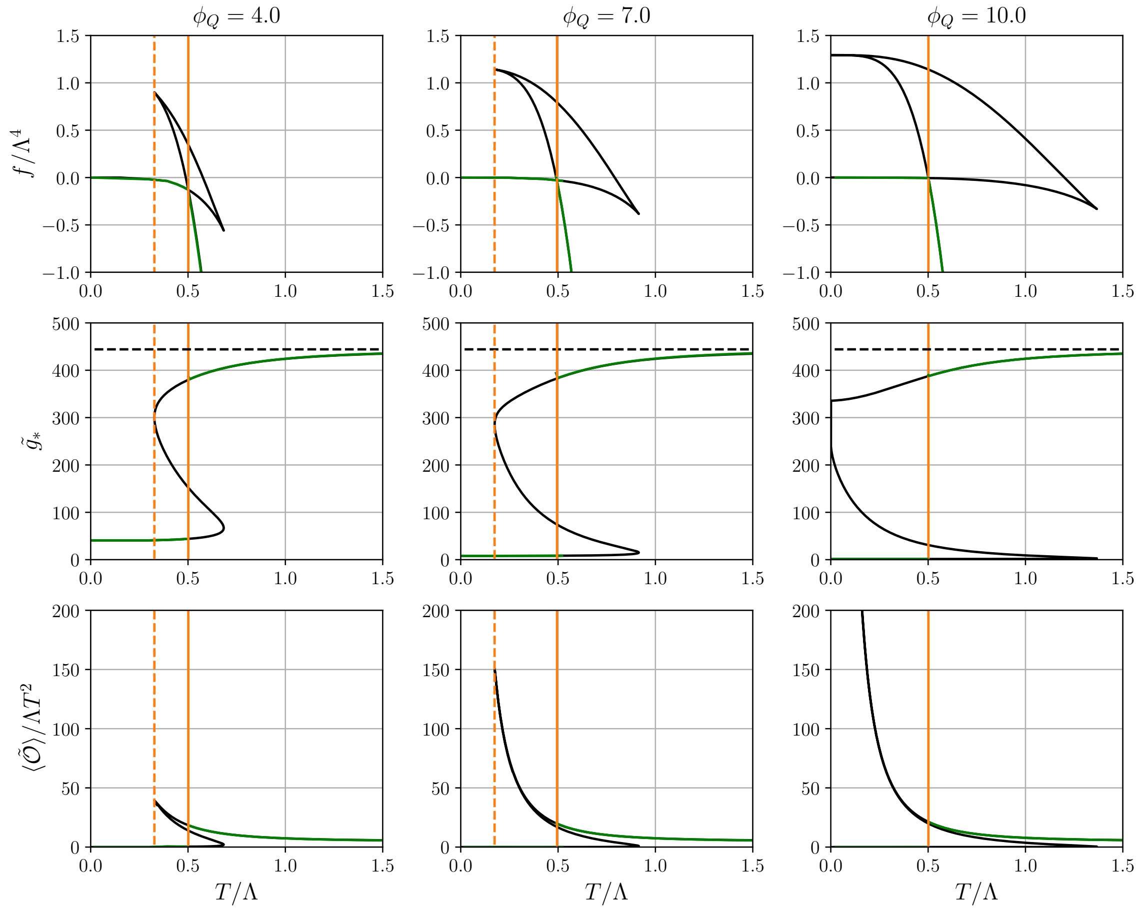

Figure 7.3: Free energy density f, rescaled degrees of freedom $\tilde{g}_*$, and dimensionless scalar condensate $\langle\tilde{\mathcal{O}}\rangle$ over temperature for varying ϕ_Q at constant $\phi_M \approx 0.58$. The solid yellow line on each plot shows the critical temperature T_c, the dashed yellow line on each plot shows the last temperature at which the metastable phase exists T_1, the green line shows the stable phase, and the black dashed line on the middle row plots shows the asymptotic value of $\tilde{g}_*$.

independent of ϕ_M or ϕ_Q values.

Recalling our definition for α (7.2) we now see that we have everything necessary for its calculation, except for knowing how to split the energy density and the free energy into their broken and unbroken phase sections. To do so we remember that the two different branches of the free energy that cross each other on the free energy plot correlate to the two different phases in question, and so the quantities we need are the sections of these branches which exist simultaneously before the critical temperature T_c as shown in Fig. 7.4. The critical temperature is defined as the temperature at which this crossing happens, in which it becomes energetically favourable to transition from one phase to the other.

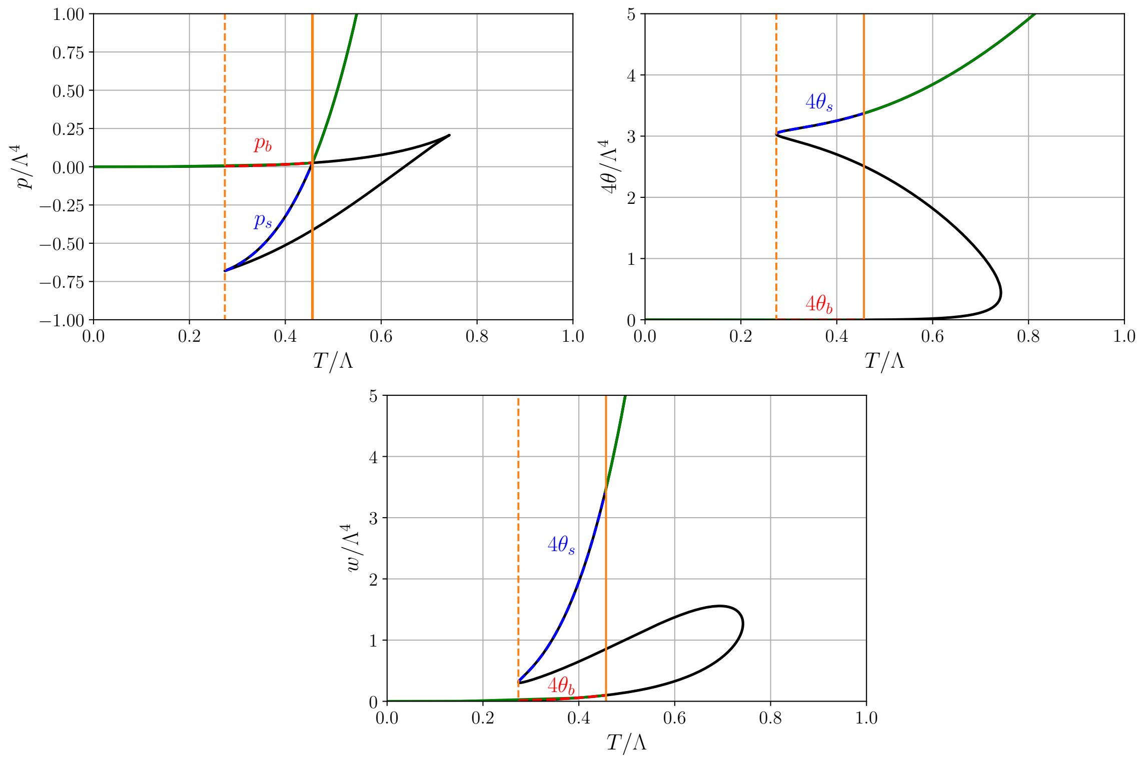

Figure 7.4: Pressure, trace of the energy-momentum tensor, and enthalpy density for $\phi_Q = 10.0$ and $\phi_M = 0.7$, with the different branches labeled. The green line shows the stable phase, the solid yellow line shows T_c, and the dashed yellow line shows T_1.

7.5 Parameter scanning

With all definitions and calculation techniques set in place we can finally move to scanning over the holographic parameters to see how varying these will change the quantities relevant for gravitational wave spectra. The two "dials" we can turn in this theory are the parameters in the potential, ϕ_M and ϕ_Q; varying these changes the shape of the potential and therefore the black brane solutions and thermodynamic quantities derived from them. Increasing ϕ_M effectively means bringing the two non-BPS extrema in the potential $V(\phi)$ closer together, until at a certain value for each ϕ_Q these merge as an inflection point and then disappear completely. The approximate equation of the region with non-BPS extrema is

$$\phi_Q \gtrsim 150\phi_M^5, \tag{7.40}$$

which was found by a fit to the numerical solution of the equations $V'(\phi) = 0$ and $V''(\phi) = 0$.

We have chosen to explore parameter ranges without these non-BPS extrema, as they produce a theory with a metastable minimum at $T = 0$. These are unattractive for cosmological model-building, as the Universe could instead be trapped in an eternally inflating phase.

Fig. 7.5 shows the latent heat and the critical temperature of the phase transition over a region in the (ϕ_M, ϕ_Q) plane. The boundary of the region with non-BPS extrema is marked with a dashed line. Where there is a first-order transition, T_c it is defined as the temperature at which the free energy in both phases is equal. In the cross-over region T_c is defined as the temperature in which the ratio of the trace of the stress energy tensor to the enthalpy (also known as the interaction measure I) peaks, where

$$I = \frac{e - 3p}{e + p}. \tag{7.41}$$

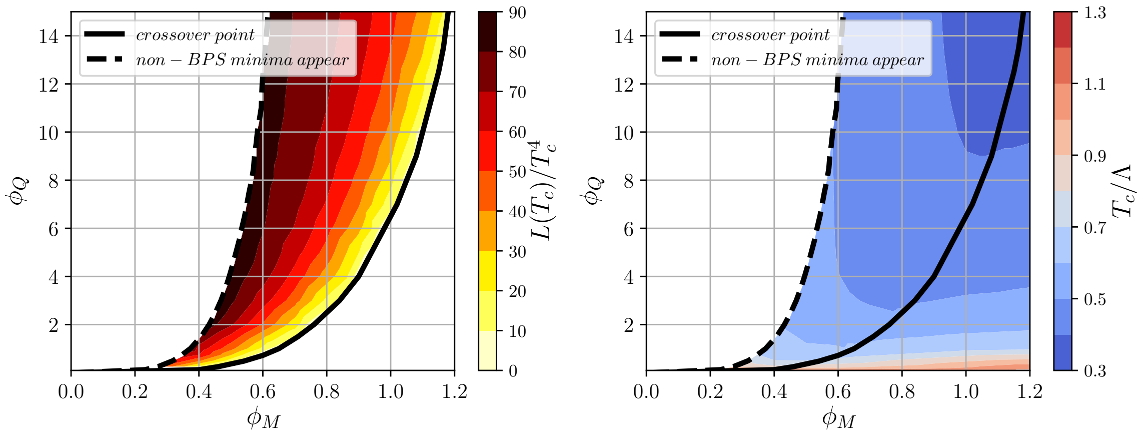

Figure 7.5: Filled contours of latent heat L in units of the critical temperature T_c for different values of the two scalar potential parameters on the left, and of the critical temperature T_c in units of the coupling for different values of the scalar potential parameters on the right. The contours found past the crossover line on the critical temperature plot are from the peak of the interaction measure.

Increasing ϕ_M away from the region (7.40), the latent heat of the first-order transition decreases until it vanishes, as seen in Fig. 7.5, at which point the theory presumably undergoes a second-order phase transition. The region of cross-overs has the approximate formula

$$\phi_Q \lesssim 6.5\phi_M^5, \tag{7.42}$$

obtained by a numerical fit. The boundary is marked with a solid line in Fig. 7.5. Increasing ϕ_Q however has the opposite effect, but much more slowly. As ϕ_Q grows the system is pushed into a stronger first-order phase transition with higher latent heat.

The measure of the strength of the phase transition relevant for gravitational production is α, defined around Eq. 7.2. In Fig. 7.6 we show the value of $\alpha(T_c)$, the value at

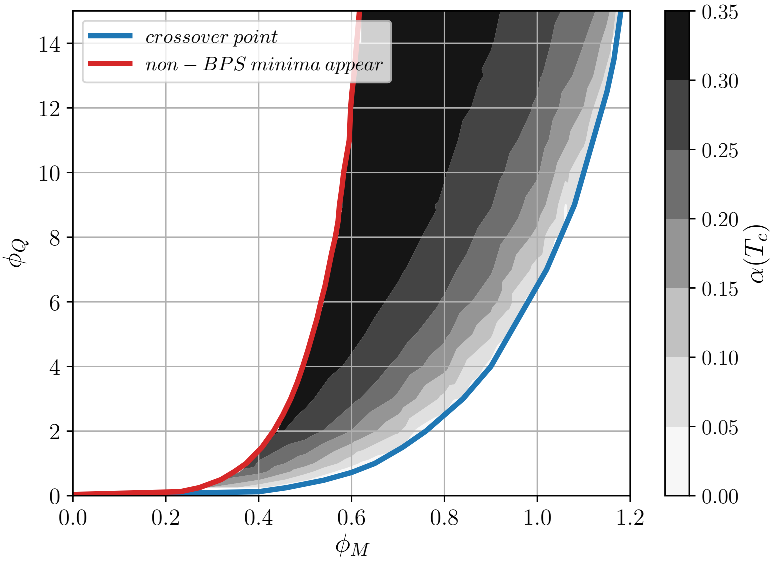

Figure 7.6: Scan of the transition strength parameter α at the critical temperature for different values of the scalar potential parameters.

the critical temperature, in the (ϕ_M, ϕ_Q) plane. It is very promising that there are systems accessible with intermediate transition strengths, as it is thought that, for $\alpha \sim 0.1$ or greater, a signal will be observable at space-based detectors, as we will discuss in the following section.

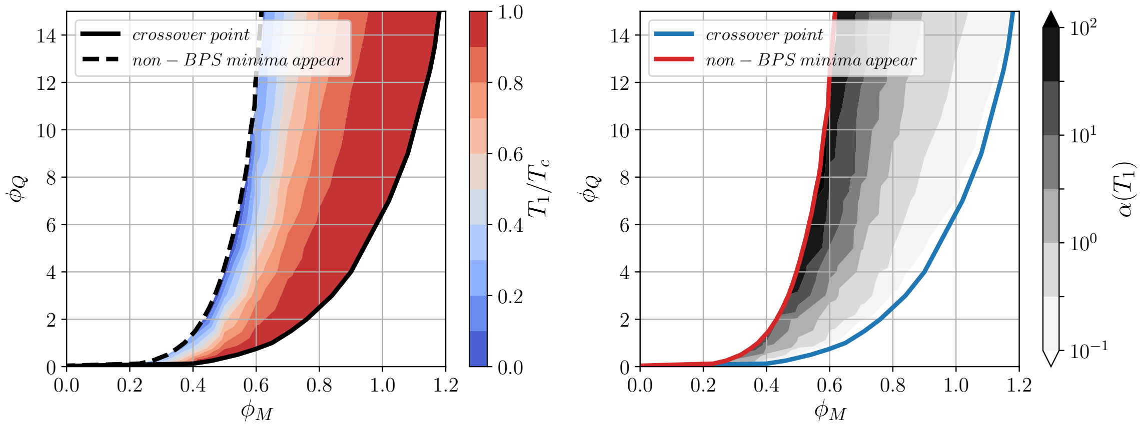

Figure 7.7: Left: contours of T_1/T_c in the (ϕ_M, ϕ_Q) plane, where T_1 is the lowest temperature at which the metastable phase exists. Right: transition strength parameter α at temperature T_1.

The most relevant quantity for the strength of the phase transition is α at the nucleation temperature $\alpha(T_N)$. We have not established the nucleation temperature of the transition, but we do know that the lowest nucleation temperature is the lowest temperature at which the metastable phase exists, which we denote T_1. In Fig. 7.7 we show the ratio T_1/T_c, showing the maximum possible supercooling, as well as $\alpha(T_1)$. As α increases below the critical temperature, as shown in Fig. 7.8, $\alpha(T_1)$ represents the maximum value of the transition strength parameter achievable by supercooling. At the boundary where the non-BPS minima appear $T_1 \to 0$, and the enthalpy of the metastable phase can reach arbitrarily low values. We therefore see diverging values of $\alpha(T_1)$ near that boundary, which can also be seen in the curve for $\phi_M \simeq 0.5797$ in Fig. 7.8.

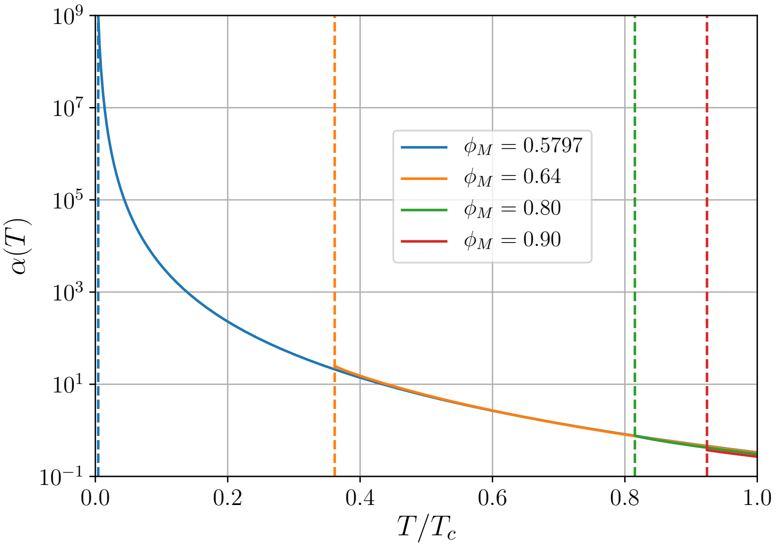

Figure 7.8: Temperature dependence of the transition strength parameter α in terms of T/T_c for $\phi_Q = 10.0$. The dashed lines represent at which value the original, high-temperature minimum is no longer separated by a potential barrier and so disappears, as seen in Fig. 7.1.

The final parameter scans in Fig. 7.9 are that of the stiffness of the equation of state $\partial p/\partial e$ in both phases, a quantity which for barotropic fluids can be identified as the square of the sound speed c_s^2. We have not properly established with a fluctuation analysis that the speed of sound is indeed the square root of the stiffness, but we will nevertheless denote $\partial p/\partial e = c_s^2$ in the following and use both interchangeably. As can be seen in the figure, the conformal value of $3 \times \partial p/\partial e = 1$ is reached in the region where the transition strength is strongest and in fact goes above the conformal value in phase two for the strongest transitions, however, the stiffness steadily declines to relatively small values as we journey towards a crossover transition. The effect this could have on the signal is has been recently discussed in [116, 117] and is described in Appendix C.

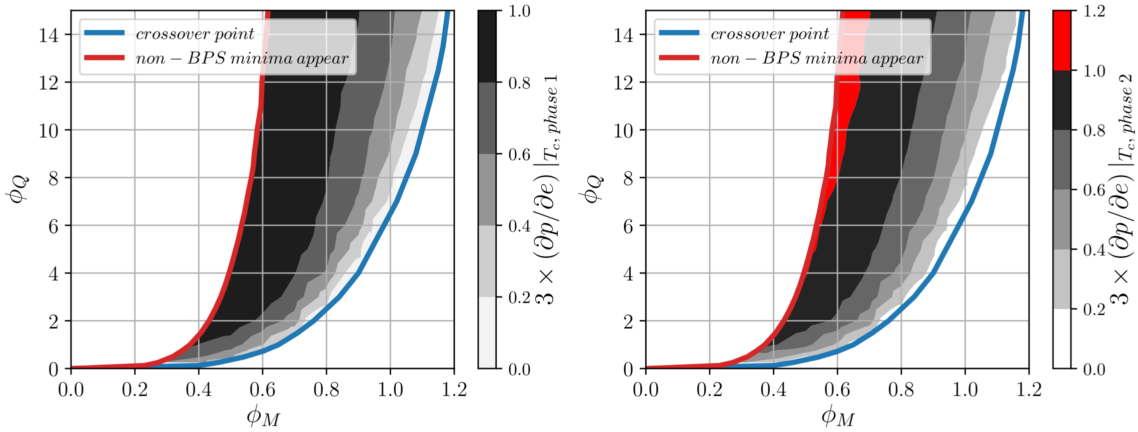

Figure 7.9: Scan of $3 \times \partial p/\partial e$ at the critical temperature in both phases, with phase one (the symmetric phase) on the left and phase two (the broken phase) on the right. Values that fall above the conformal stiffness value $\partial p/\partial e = 1/3$ are shown as a red filled contour.

7.6 Gravitational waves

To see what the results from the holographic model imply for the detectability of gravitational waves by the LISA mission, we turn to the gravitational wave spectra calculations. The quantity of interest is $h^2\Omega_{\rm gw}(f)$, the energy density contained in gravitational waves relative to the total per log frequency interval, sometimes called just the power spectrum. This is to be compared to the detector noise, which is quoted in terms of a sensitivity $h^2\Omega_{\rm Sens}(f)$, which is the gravitational wave power spectrum producing the same amplitude signal as the detector noise at frequency f. The comparison is through the signal-to-noise ratio (SNR) defined below.

The base model for these spectra is summarised in [2], based on numerical simulations [114] and a physical understanding in terms of sound waves [253, 254]. There have been developments in understanding since the appearance of [2], concerning the finite lifetime of the source [112], and kinetic energy production in strong phase transitions [118], and those with stiffness away from 1/3 [116].

With these improvements (see Appendix C), the power spectrum can be written

$$h^2\Omega_{\rm gw} = 2.061 h^2 F_{\rm gw,0}\left(H_{\rm N}R_*\right) K^2 \tilde{\Omega}_{\rm gw} C\left(\frac{f}{f_{\rm p,0}}\right)\left(1 - \frac{1}{\sqrt{1+2x}}\right)\Sigma\,, \tag{7.43}$$

where h is the Hubble parameter today with value 0.678 ± 0.009 [255], H_N is the Hubble rate at nucleation, $F_{\rm gw,0}$ is an attenuation factor

$$F_{\rm gw,0} = (3.57 \pm 0.05) \times 10^{-5}\left(\frac{100}{g_*}\right)^{\frac{1}{3}}\,, \tag{7.44}$$

K is the kinetic energy fraction of the fluid around the expanding bubbles of the stable phase, and $x = H_{\rm N}R_*/\sqrt{K}$, where R_* is the mean bubble separation. The final factor Σ takes into account the effect of kinetic energy suppression recently observed in strong phase transitions [118].

We use $R_* = (8\pi)^{1/3}v_w/\beta$ though the relation is accurate only for weak transitions ($\alpha \lesssim \mathrm{O}(10^{-2})$). We do not yet have a good theory of the function $R_*(v_w,\beta)$; replacing $(8\pi)^{1/3}$ by the sound speed as advocated in [228] is likely to lead to overestimating the power.

The constant $\tilde{\Omega}_{\rm gw}$ has a numerically-determined value of order 10^{-2} [114]. We take it to be 1×10^{-2}, which replicates the correct peak amplitude for an intermediate strength transition with $v_w = 0.92$ but under-predicts the power spectrum for other transitions, so is a conservative estimate. Lastly, $C(s)$ is the spectral shape function

$$C(s) = s^3\left(\frac{7}{4+3s^2}\right)^{7/2} \tag{7.45}$$

with peak frequency

$$f_{p,0} \simeq 26.2\left(\frac{1}{H_N R_*}\right)\left(\frac{T_N}{100\text{GeV}}\right)\left(\frac{g_*}{100}\right)^{1/6}\mu\text{Hz} \tag{7.46}$$

which comes from fits around the peak of the numerically-determined GW power spectrum.

As can be seen, the peak frequency of the power spectrum depends on the nucleation temperature T_N, and also on the wall velocity v_w and transition rate β through R_* (equation 7.5). The peak power is controlled by R_* and the kinetic energy fraction, which in turn is sensitive to the transition strength parameter α and the wall speed v_w, and the stiffness. Hence the power spectrum is controlled by all four crucial parameters mentioned in Section 7.3 as well as the sound speed c_s [116, 117].

We take α to be equal to its holographic value and therefore neglect the Standard Model degrees of freedom, which is discussed in more detail at the end of this section. To properly calculate the nucleation temperature would require a full derivation of the nucleation rate through the effective action, which is beyond the scope of this paper. To circumvent this we realise that the nucleation temperature will always be lower than the critical temperature, and by Fig. 7.7 we see that lowering the temperature will in fact increase the transition strength, thereby increasing the gravitational wave signal. We therefore take a conservative estimate of the nucleation temperature as being at the critical temperature, $T_N = T_c$.

This now allows us to translate the temperatures we found in previous sections which are in units of the coupling to physical temperatures in units of GeV. The lack of new physics up to the TeV scale motivates placing a lower bound of 1 TeV on the coupling Λ.

From Fig. 7.5 we can estimate that this will limit our nucleation temperature to a range from 300 GeV to 1.3 TeV. The vast majority of parameter values (approximately three quarters) fall within the range of temperatures 400 − 600 GeV, which in turn motivates the choice of a nucleation temperature of $T_N = 500$ GeV when plotting spectra from here on.

The only parameter in the gravitational wave power spectrum which depends on this choice is the peak frequency $f_{p,0}$. By inspecting (7.46) we note that an increase of T_N will result in a shift to higher frequencies of the gravitational wave power spectral curves, without a change in shape. For parameter values of $g_* = 100, \alpha = 0.25, \beta/H_\mathrm{n} = 50, v_w = 0.5$ used in Fig. 7.10 values of T_N up to around ~ 750 GeV will keep the peak within the LISA sensitivity window.

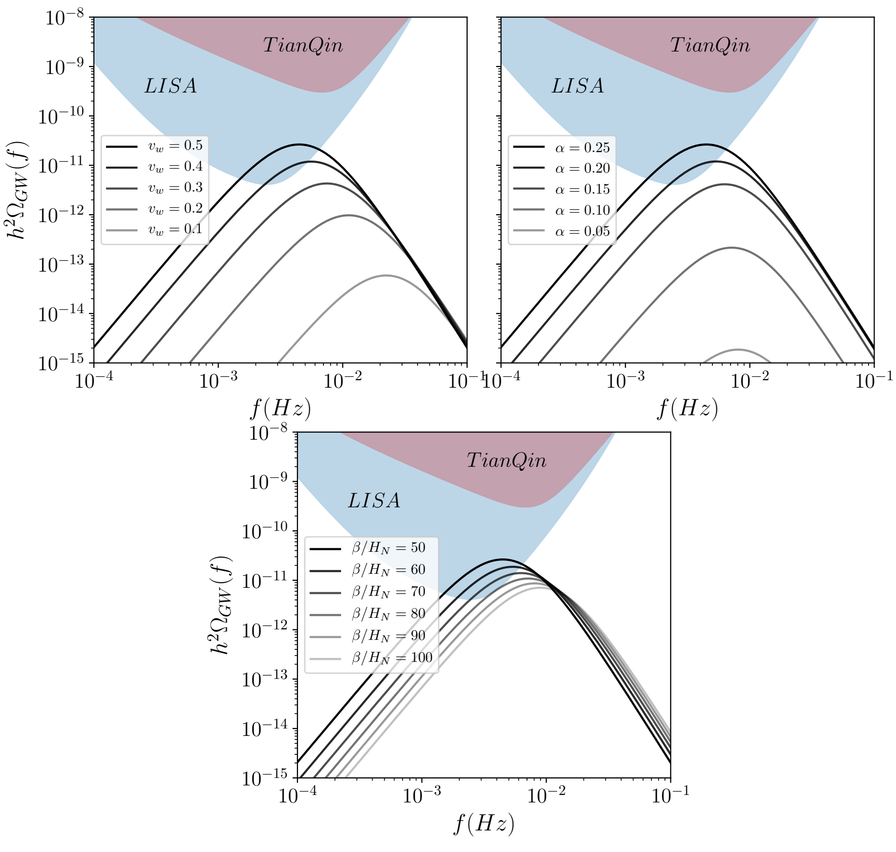

Figure 7.10: Power spectra for varying v_w, α, and β/H_n respectively. The baseline takes values $g_* = 100$, $\alpha = 0.25$, $\partial p/\partial e = \alpha$, $\beta/H_\mathrm{n} = 50$, $v_w = 0.5$, and $T_\mathrm{n} = 500$GeV, and is depicted as the darkest line on every plot.

A gravitational wave detector's sensitivity to cosmological sources is determined from the instrumental noise, converted into an equivalent gravitational wave signal

$$h^2\Omega_{\mathrm{Sens}}(f) = \frac{2\pi^2}{3H_0^2} f^3 S_n(f) \ , \tag{7.47}$$

where $S_n(f)$ is the noise power spectral density and H_0 is the Hubble rate today.

LISA's expected noise power spectral density is fully described in [121]. Another mission Taiji is also planned with very similar parameters to LISA [7]. A third planned space-based mission is TianQin, with a substantially different configuration [8, 256]. In Fig. 7.10 we display the model gravitational wave power spectra for varying $\beta/H_{\rm n}$, v_w, and $T_{\rm n}$ to demonstrate the strength of the signals from phase transitions relative to the sensitivity curves of LISA (taken to also apply to Taiji) and TianQin. We have chosen $g_* = 100$ and $T_{\rm n} = 500$ GeV for all graphs. The darkest line on every plot takes values of $\beta/H_{\rm n} = 50$, $v_w = 0.5$, and $\alpha = 0.25$, with one variable shifting for each plot. We take the stiffness equal to α, in view of the correlation shown in the next section.

Significant quantities determining whether the signal will be in the detectable range are the wall speed and transition strength parameter. As it is evident from the figures, most of the signals we show are strong enough to be detected by LISA, if the peak frequency falls into its range of sensitivity, although all fall short of TianQin's direct detection level. Despite this, particular choices of higher wall speeds and stronger transitions than what we chose could quickly push the signal into the range that allows signal detection from both detectors.

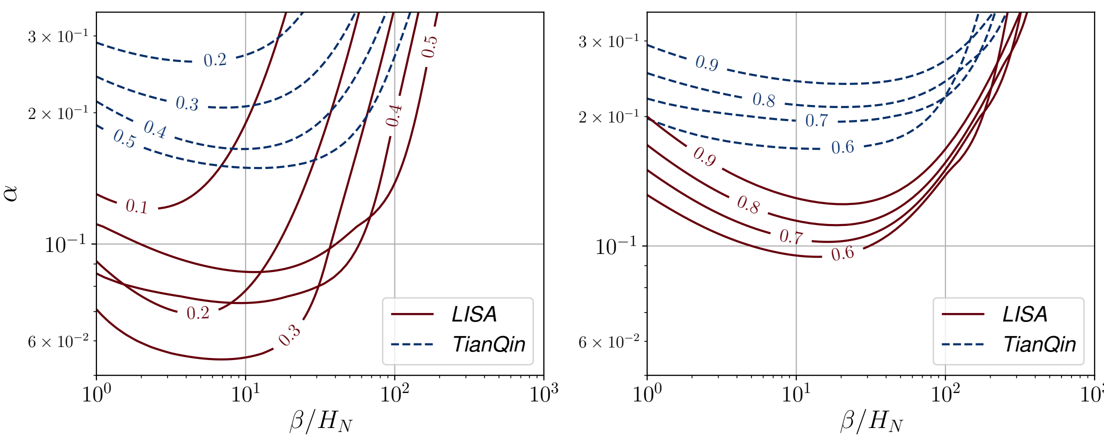

Figure 7.11: Curves of constant wall speed v_w in the $\alpha - \beta$ plane for LISA and TianQin $\Omega_{\rm gw,exp}$, with dark red and dark blue lines representing the detectable signal-to-noise ratio limit of 10 for each wall velocity. The left plot displays wall speeds of $v_w = 0.5$ and below, and the right plot displays wall speeds of $v_w = 0.6$ and above, with the area contained above each line being theoretically detectable for that wall velocity, which is labeled on the line itself. The curve for wall velocity $v_w = 0.1$ for TianQin is not detectable in the range of transition strengths shown, and the temperature used for this plot is $T_{\rm n} = 500$GeV.

To more reliably indicate whether a signal will be seen by a mission we turn to the signal-to-noise ratio SNR. The SNR allows comparison of a gravitational wave signal with the detector's base noise level and whether the signals produced will be discernible from it. Once the power spectrum and detector sensitivity is known, the SNR follows from

$$\mathrm{SNR} = \sqrt{\mathcal{T} \int_{f_{\min}}^{f_{\max}} \mathrm{d}f \left[\frac{h^2 \Omega_{\mathrm{gw}}(f)}{h^2 \Omega_{\mathrm{Sens}}(f)} \right]^2} \,, \tag{7.48}$$

where $\mathcal{T}$ is the mission duration time.

For the LISA mission the duration is taken to be four years in orbit and a duty cycle of usable science data of 75% making $t_{obs} = 3\mathrm{yr}$. Displayed in Fig. 7.11 is a plot combining both the SNR and three of the important parameters (α, β/H_{n}, v_w) for both LISA and TianQin. We take that the stiffness $\partial p/\partial e$ for each point equal to the value of α, a correlation which will be seen later in Fig. 7.14. We note, however, that we have not yet formally calculated the speed of sound in our model, though we expect it to lie close to the square root of the stiffness, at least for high temperatures. A proper calculation requires an analysis of the dispersion relations of the quasi-normal mode spectra of the coupled scalar field and metric components fluctuations, which we hope to perform elsewhere.

It is usually considered that a SNR above 10-20 is highly likely to be detectable [257], and so we produce contours of 10 and above for nine different wall speeds for each detector, which we split into two plots for clarity.

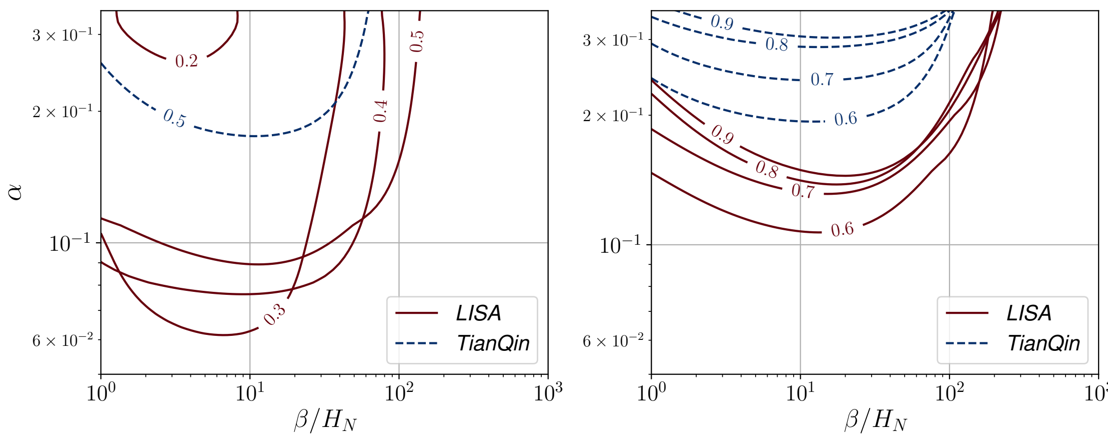

Figure 7.12: Curves of constant wall speed v_w in the $\alpha - \beta$ plane for LISA and TianQin matching Fig. 7.11, now with the suppression Σ applied giving Ω_{gw}, with dark red and dark blue lines representing the detectable signal-to-noise ratio limit of 10 for each wall velocity. Once again the left plot displays wall speeds of $v_w = 0.5$ and below, and the right plot displays wall speeds of $v_w = 0.6$ and above with the temperature used for this plot being $T_{\mathrm{n}} = 500\mathrm{GeV}$.

In Fig. 7.11 we produce these signal-to-noise ratios incorporating the majority of the most recent discoveries including the finite lifetime of the source and the effect of varying sound speeds. In Fig. 7.12 we also incorporate the recently discovered suppression of kinetic energy production in strong phase transitions $\Sigma(v_w, \alpha)$, which as can be seen has a large effect on slower wall speeds, removing most contours for TianQin with slow wall speeds in our parameter range. We show with and without this modification as the data on this effect is sparse and therefore possibly not as illuminating, with some new points having not been analysed in great detail such as not being checked for lattice convergence.

Finally, we discuss the effect of the Standard Model degrees of freedom on the system. First, suppose the Standard Model and holographic degrees of freedom are at the same temperature. If so, there will be no change to the difference in vacuum energy, however there will be a contribution to the enthalpy, as $w_{tot} = w_{holo} + w_{SM}$. Including this into our definition for α modifies the value found as

$$\alpha_{tot} = \alpha_{holo} \left(1 + \frac{\kappa_5^2}{L^3} \frac{g_*^{SM}}{g_{*,holo}^{sym}}\right)^{-1} , \tag{7.49}$$

which depends only on the ratio of degrees of freedom and the constants from the holographic model.

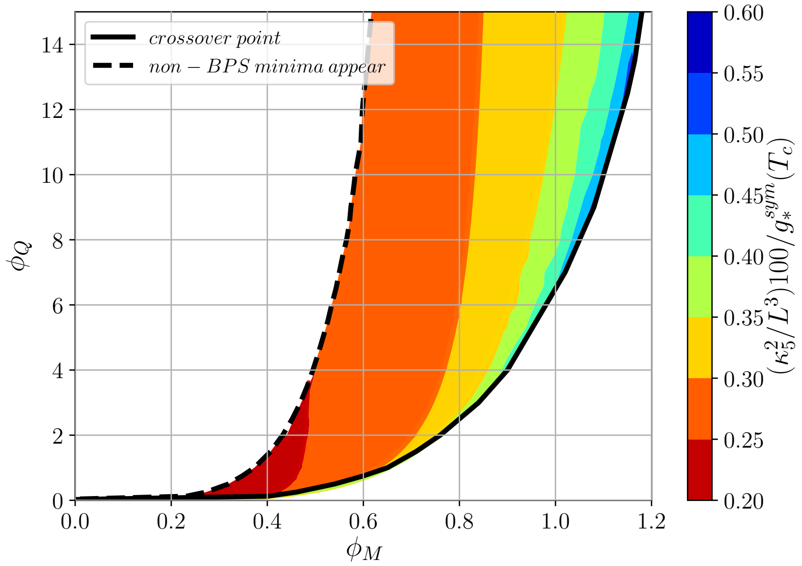

Figure 7.13: Contour plot of the ratio of a reference effective number of relativistic degrees of freedom (100) with the holographic degrees of freedom, scaled by the holographic parameters κ_5^2/L^3, in the symmetric phase at the critical temperature.

We see from Fig. 7.13 that the degrees of freedom ratio is small (always less than unity in units of κ_5^2/L^3), but it is greatly influenced by the gravity dual parameters. This in turn indicates that the ratio is contingent on the gauge group of the dual field theory N^2, which when large will render the standard model contributions negligible. The figure therefore informs how close to a large N limit the theory is required to be in order to neglect standard model corrections. As holography is best formulated in a large N limit however, neglecting this contribution is justified.

7.7 Discussion

In this paper we studied a particular model for phase transitions in a field theory, stemming from a putative strongly coupled sector described by holography. We adopted the so-called bottom-up gauge/gravity approach, using a 5-dimensional model with a single scalar field, whose bulk potential (7.9) has two free parameters, the coefficients of the quartic and sextic terms of a superpotential [229]. From a model builder's perspective this allows us the freedom to explore generic features without the greater complexity of a proper string theory construction.

We focused on the thermodynamic parameters relevant for gravitational wave production: the critical temperature, the latent heat, the transition strength parameter α, the minimum temperature for metastability, and the stiffness $\partial p/\partial e$. We then explored the implications for gravitational wave production in the early universe, if the strongly coupled sector described by the model belonged to an extension of the Standard Model.

The theory has one dimensionful parameter Λ, which can be viewed as the coupling of a dimension-3 scalar operator $\mathcal{O}$ in the effective action of the field theory, and the scale of new physics. We find that the theory has a first order phase transition in the approximate region given in Eq. (7.42). Outside this region is a cross-over.

The critical temperature of the transition T_c is $\mathrm{O}(\Lambda)$, and generally $T_\mathrm{c} < \Lambda$. We found the minimum temperature to which the metastable phase persisted T_1, finding that in the region given in Eq. (7.40) the metastable state persisted to zero temperature. The transition strength parameter at T_c is generally in the range $0.1 \lesssim \alpha \lesssim 0.3$, although it drops to zero at the boundary with the cross-over region, as does the stiffness. The stiffness can be larger than $1/3$, but is also generally in the range $0.1 \lesssim \partial p/\partial e \lesssim 0.3$. It is strongly correlated with the transition strength (see Fig. 7.14).

Our study of gravitational waves was necessarily restricted by the lack of a prediction for the scale Λ, and the equilibrium nature of the calculation, which gave access only to the transition strength parameter and the stiffness. It is therefore illustrative in nature. To gain insight into observational prospects, we assumed a critical temperature of $T_\mathrm{c} = 500$ GeV, with negligible supercooling, and that the number of degrees of freedom of the Standard Model was small in comparison with that of the dual field theory.

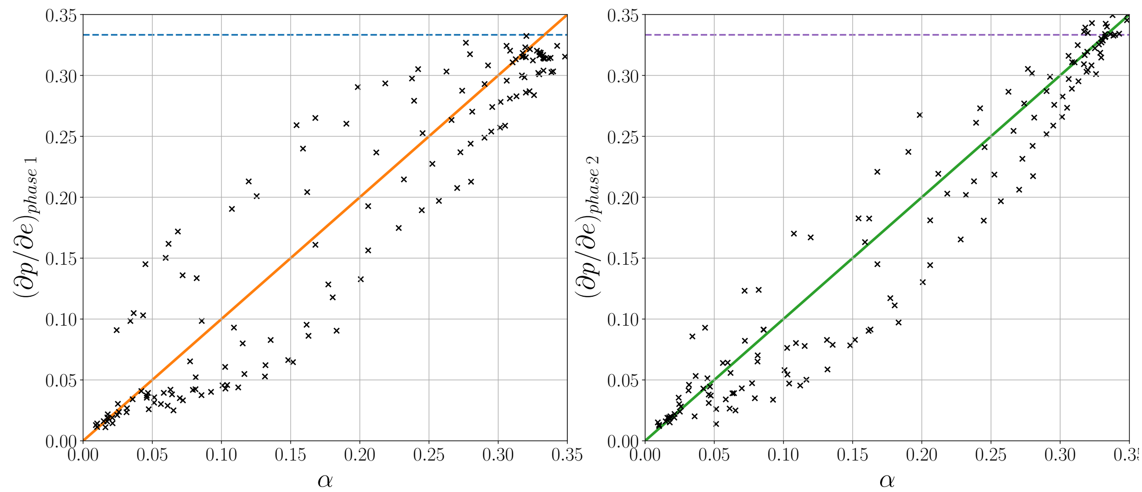

Figure 7.14: Scatter plots for the stiffness of the equation of state for phase one (the symmetric phase) on the left and phase two (the broken phase) on the right. The dashed line represents the conformal value $\partial p/\partial e = 1/3$. Density of points is not significant in this plot and is due to how the values of ϕ_M and ϕ_Q were sampled.

To calculate the gravitational wave power spectrum, we used the LISA Cosmology Working Group recipe [228], augmented by the kinetic energy suppression factor of Ref. [118] (see Appendix C). We explored the consequences of stiffness away from the conformal value of 1/3 using the kinetic energy fraction algorithm recently presented in [117].

With this set of choices, we found that the transitions are strong enough to be observable at LISA over a wide range of parameter space, and there is also a smaller range detectable by TianQin. In order to be more definitive, it is important to calculate the speed of the phase boundary v_{w}, and the amount of supercooling, which is fixed by the rate of change of the tunnelling probability β. These are harder calculations, to which we will return in future.

It is interesting to speculate about which features we have found are generic in a strongly coupled transition. That the critical temperature is below the masses of new states (unless there are also approximate symmetries broken at the transition) is a feature of QCD, in the generalised sense of the temperature of peak interaction measure, which is well below the nucleon and glueball masses. This is in contrast to weakly-coupled theories, where the masses of new states are generally down by a power of a coupling constant from transition temperature. One can also argue that the transition strength parameter is generally intermediate in strength ($\alpha \sim 0.1$). For example, in a confinement transition in a large N theory, as $\mathrm{O}(N^2)$ degrees of freedom become massive and are removed from the effective number of relativistic degrees of freedom, also $\mathrm{O}(N^2)$. While the phase transition in the bottom-up theory we studied is not obviously a confinement transition in a real field theory, it shares this feature of a large change in the number of degrees of freedom, evident in Fig. 7.3.

The strong departures of the stiffness from the conformal value of $1/3$ may also be generic, although its physical origin is difficult to understand. In bottom-up models consisting only of metric and a single bulk scalar field, the scalar potential (7.9) controls all the properties of the dual field theory. For example, the quartic coefficient $-1/3$ can be shown to correspond to attractive interactions in elastic two-to-two scattering events [258, 259] and this coefficient also plays a pivotal role in determining the stiffness. In fact, the value $-1/3$ is precisely the border line case for vanishing trace anomaly and where the equation of state changes from being soft $\partial p/\partial e < 1/3$ to stiff $\partial p/\partial e > 1/3$ [251, 252]. Here we therefore also expect that the equation of state could be stiff if the contributions from the rest of the terms in the scalar potential are negligible and we are in the low temperature regime where the bulk scalar has its most important effect. This effect is partially evidenced in the left plot of Fig. 7.7 for larger values for ϕ_Q. It would be interesting to generalise our study by relaxing fixed quartic coefficient and explore how the stiffness affects the signal-to-noise ratios in the gravitational wave searches.

More generally, the gravitational wave power spectrum contains information about the equation of state of the underlying theory, in this case a strongly coupled one. In order to understand how to access this information, one needs to perform numerical simulations with the correct equation of state and field-fluid coupling. Up to now, these have been performed only with simplified models of weakly-coupled field theories [114, 232, 253]. With holography, one has the exciting prospect of computing the required functions for strongly-coupled theories as well, which will eventually allow gravitational wave detectors to probe the equation of state, and perhaps provide evidence for a phase transition in a strongly-coupled theory. We hope to turn to these computations in future work.

A Holographic renormalisation

Due to the close nature of the relationship between quantum field theory and gravity through the holographic principle, UV divergences on the field theory side from composite operators approaching coincident points in d-dimensions appear as IR divergences on the gravitational side as infinite volumes of AdS_{d+1} geometries. These divergences must be regularised and renormalised, and so the supergravity fields are expanded near the boundary and counterterms must be introduced so as to subtract any divergences that arise. Holographic renormalisation of this type is well known (see e.g. [260]) and it is the procedure we will follow. The initial step is to expand the solutions at the boundary, and for this the Fefferman-Graham metric

$$ds^2 = \frac{L^2}{u^2}\left(g_{ab}\,\mathrm{d}x^a\mathrm{d}x^b + \mathrm{d}u^2\right) \tag{7.50}$$

is used with the boundary at $u \to 0$. Expanding our fields and metric around this point gives

$$g_{ab} = \gamma_{ab} + g^{(2)}_{ab}u^2 + g^{(4)}_{ab}u^4 + \ldots \tag{7.51}$$

for the boundary metric, and

$$\phi = \Lambda u + \Upsilon u^3 + \ldots \tag{7.52}$$

for the scalar field. For these variables Λ has dimension 1 and Υ has dimension 3, causing ϕ to be dimensionless. The leading behaviour of the boundary metric is simply flat Minkowski ($\gamma_{ab} = \eta_{ab}$), and $g^{(2)}_{ab}$ is determined in terms of this and Λ as

$$g^{(2)}_{ab} = -\frac{1}{3}\Lambda^2\gamma_{ab}. \tag{7.53}$$

The u^4 coefficient $g^{(4)}_{ab}$ leads to the energy-momentum tensor. Through the holographic dictionary we can also identify Λ as the coupling to the dual field operator, and Υ as dual to the vacuum expectation value of the $\Delta = 3$ operator. Boundary behaviour in hand, our next job is to tame the divergences by regularising the theory. Denoting the regularised action as S_{reg}, we find the field theory operators through

$$\langle \mathcal{O} \rangle = \frac{\delta S_{\text{reg}}}{\delta\phi}, \qquad \langle T_{ab}\rangle = \frac{\delta S_{\text{reg}}}{\delta\gamma^{ab}} \tag{7.54}$$

where this action is built up of the Einstein-Hilbert with scalar term, Gibbons-Hawking term, and counterterm as

$$S_{\text{reg}} = S_{EH} + S_{GH} + S_{ct}. \tag{7.55}$$

To find this action the extrinsic curvature is needed for the Gibbons-Hawking term, and in these coordinates that is given by

$$K = -\frac{1}{\sqrt{g_{uu}}}\frac{L^4}{u^4}\partial_u \log\left(\frac{L^4}{u^4}\sqrt{-g}\right)\Bigg|_{u\to 0} = -\frac{L^3}{u^3}\partial_u \log\left(\frac{L^4}{u^4}\sqrt{-g}\right)\Bigg|_{u\to 0}. \tag{7.56}$$

We choose the counterterm to regularise the action as a term similar the superpotential, which is usual [261]. Our counterterm therefore is

$$S_{ct} = \frac{2}{\kappa_5^2}\int d^4x\sqrt{-\gamma}\frac{L^3}{u^4}\left(-\frac{3}{2} - \frac{\phi^2}{2} - \frac{\phi^4}{4\phi_M^2}\right)\Bigg|_{u\to 0}, \tag{7.57}$$

which excludes the ϕ_Q term as this will vanish anyway with $(\phi^6/u^4)|_{u\to 0}$ and so would not contribute to the divergences. By choosing this renormalisation scheme we are in effect "preserving supersymmetry" which causes the vacuum energy to vanish. Combining all together and performing the calculations (7.54) generates

$$\langle \mathcal{O} \rangle = -\frac{2L^3}{\kappa_5^2}\left(2\Upsilon + \frac{\Lambda^3}{\phi_M^2}\right) , \tag{7.58}$$

and

$$\langle T_{ab} \rangle = \frac{2L^3}{\kappa_5^2}\left\{ g_{ab}^{(4)} + \gamma_{ab}\left(\Lambda\Upsilon - \frac{\Lambda^4}{18} + \frac{\Lambda^4}{4\phi_M^2}\right)\right\} . \tag{7.59}$$

The tensor which gives rise to the stress-energy tensor, $g_{ab}^{(4)}$, is found to be given by the expression

$$\begin{aligned} g_{ab}^{(4)} = \mathrm{diag}\Big(&-\frac{1}{36}\left(2\Lambda^4 - 18\Lambda\Upsilon + 27h_4\right), \frac{1}{36}\left(2\Lambda^4 - 18\Lambda\Upsilon - 9h_4\right), \\ &\frac{1}{36}\left(2\Lambda^4 - 18\Lambda\Upsilon - 9h_4\right), \frac{1}{36}\left(2\Lambda^4 - 18\Lambda\Upsilon - 9h_4\right)\Big) , \end{aligned} \tag{7.60}$$

where h_4 is the constant associated with the subleading term in the expansion of the blackening factor h in the limit $\phi \to 0$. Recalling that γ_{ab} is simply flat Minkowski, the trace of the stress-energy tensor is therefore

$$\langle T^a_a \rangle = \frac{2L^3}{\kappa_5^2}\left\{ 2\Lambda\Upsilon + \frac{\Lambda^4}{\phi_M^2}\right\} , \tag{7.61}$$

where the constant Λ^4 term has dropped out as well as h_4. It is quickly evident that the Ward identity is satisfied by this, giving the form

$$\langle T^a_a \rangle + \Lambda\langle \mathcal{O} \rangle = 0 . \tag{7.62}$$

B Numerical methods

The numerical integration is performed using scipy's "solve_ivp" function using the "Radau" method, usually with at least 300 points and standard tolerances. It is provided with the system of equations for $G'(\phi)$ and $H'(\phi)$, the Jacobian of the system, and the initial values of $G(\phi_h)$ and $H(\phi_h)$. When numerically integrating, it first must be realised that there is a simple pole at exactly ϕ_h in $H'(\phi)$ as $G(\phi_h) = -\frac{4}{3}\gamma_1^h$. Consequently, the solver must be displaced a small amount, $\phi_h + \varepsilon$, by pushing the initial values slightly away from $G(\phi_h)$ and $H(\phi_h)$. The choice of ε does not seem overly important as long as it is small compared to ϕ_h (i.e. $\varepsilon/\phi_h \lesssim 1\times 10^{-2} - 1\times 10^{-3}$) but large enough to push the solver away from the pole. The "solve_ivp" function is repeated for the desired number of ϕ_h values, with careful consideration being taken for the direction of arrays as the system must be integrated from ϕ_h down to the minimum value.

Once solved, the thermodynamic quantities s and T quickly follow from numerical integration (using scipy's "trapz" function), for each value of ϕ_h. Other thermodynamic quantities in this paper are easily derivable from T and s. Numerical integration and differentiation are subject to errors at large T spacings.

The critical temperature T_c is determined from the self-intersection of the free energy curve in the (f, T) plane. Knowing where T_c is located allows the free energy and energy density curves to be broken up into different branches and found for the symmetric and broken regions, as seen in Fig. 7.4, enabling calculation of α and $L(T_c)$.

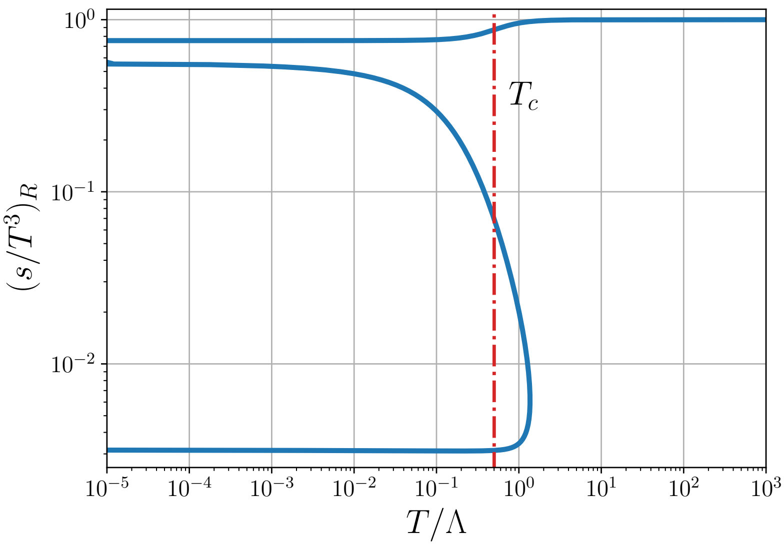

Figure 7.15: Rescaled entropy versus temperature graph for $\phi_M \simeq 0.5797$ and $\phi_Q = 10.0$, with critical temperature $T_c/\Lambda \approx 0.499$.

To ensure our numerics performed well, we checked our results against most graphs in [229]. Fig. 7.15 serves as a comparison with figure 6 in that paper to demonstrate that our numerical solutions are behaving as expected.

C Gravitational wave power spectrum model

The model for the gravitational wave power spectrum from phase transitions has undergone a number of changes as understanding has improved. We may start by considering the form given in the erratum in Ref. [114],

$$\Omega_{\rm gw,0}(f) = 2.061 F_{\rm gw,0} K^2 (H_{\rm n} R_*) \tilde{\Omega}_{\rm gw} C\left(\frac{f}{f_{\rm p,0}}\right). \tag{7.63}$$

The form applies only when the sound wave lifetime $\tau_{\rm sw} = R_*/\sqrt{K}$ is much longer than the Hubble time $H_{\rm n}^{-1}$. Ref. [112] showed that modelling the decay as an abrupt switching off at $\tau_{\rm sw}$ introduces a factor

$$\Upsilon_{\rm sw}(x) = 1 - \frac{1}{\sqrt{1+2x}} \, . \tag{7.64}$$

where $x = \tau_{\rm sw} H_N$. We take the attenuation timescale to be $\tau_{\rm sw} = R_*/\sqrt{K}$. The LISA Cosmology Working Group (LCWG) model takes the function to be $\Upsilon_{\rm sw}(x) = \min(1, x)$. A similar approximation is seen in [240, 262, 263] with further discussion. The lack of understanding of how the power spectrum attenuates and changes in form is the major uncertainty in this model.

The kinetic energy fraction is estimated from an efficiency factor κ, computed for the self-similar flow around a single expanding bubble of the stable phase [264, 119]. It is related to the kinetic energy fraction by

$$K = \frac{\kappa\alpha}{1+\alpha}. \tag{7.65}$$

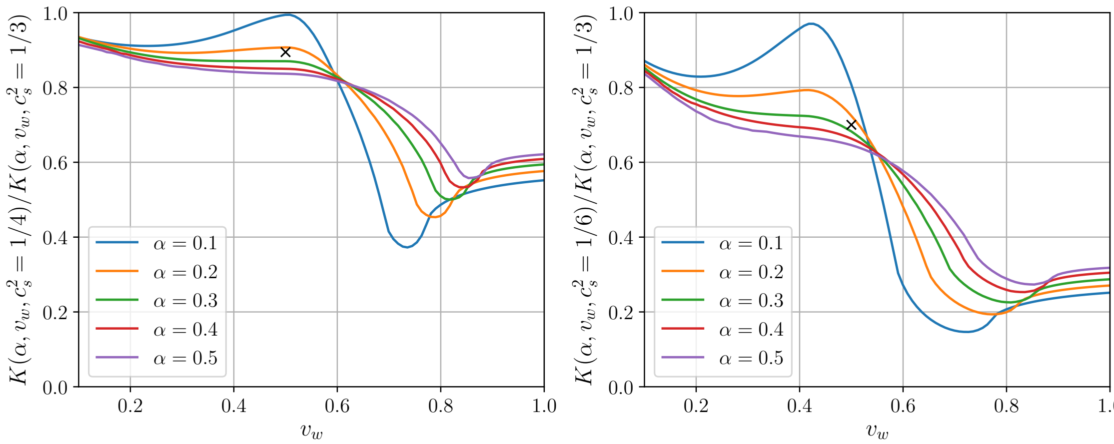

Figure 7.16: Plots of the effect of varying stiffness of the equation of state $\partial p/\partial e$ on the kinetic energy fraction K for $\alpha = 0.1, 0.2, 0.3, 0.4$, and 0.5 as a function of the wall speed v_w. This is displayed as a ratio of the kinetic energy fraction for two different equations of state ($\partial p/\partial e = 1/4, 1/6$) to the kinetic energy fraction of the conformal stiffness $\partial p/\partial e$. Black crosses have been placed on each graph to show a reference point with $v_w = 0.5$ and $\alpha = 0.25$.

The LCWG model uses the fitting formulae for κ in Ref. [119], which are derived in a model with stiffness $\partial p/\partial e = 1/3$. As we find significant departures from 1/3, we use instead the code snippet given in [117], denoting the values obtained as $K_{\rm GKSV}$ Fig. 7.16 shows how the kinetic energy fraction is modified as a function of α and v_w for stiffnesses

1/4 and 1/6. A reference value of $v_w = 0.5$ with $\alpha = 0.25$ has been indicated, for which the maximum reduction in the kinetic energy fraction is about 20%.

Finally, 3-dimensional hydrodynamic simulations of strong first-order thermal phase transitions in [118] showed a deficit in kinetic energy compared to the LCWG value [119], ascribed to slowing of the phase boundary due to reheating of the metastable phase. This will have the effect of reducing the gravitational wave signal, and so must be taken into consideration. We define a suppression function $\Sigma(v_w, \alpha)$, defined as

$$\Sigma(v_w, \alpha) = \Omega_{\mathrm{gw}}/\Omega_{\mathrm{gw,exp}}, \tag{7.66}$$

where Ω_{gw} is the true total gravitational wave power, and $\Omega_{\mathrm{gw,exp}}$ is that predicted by the LCWG model. We take the values of this function by cubic interpolation of the ratio of the last two quantities in Table 1 of [118]. Contours of the suppression function are shown in Fig. 7.17.

The final expression for the gravitational wave power spectrum is

$$\Omega_{\mathrm{gw},0}(f) = 2.061 F_{\mathrm{gw},0} K^2_{\mathrm{GKSV}}(H_{\mathrm{n}} R_*) \tilde{\Omega}_{\mathrm{gw}} C\left(\frac{f}{f_{\mathrm{p},0}}\right) \Upsilon_{\mathrm{sw}}(x) \Sigma(v_w, \alpha)\ . \tag{7.67}$$

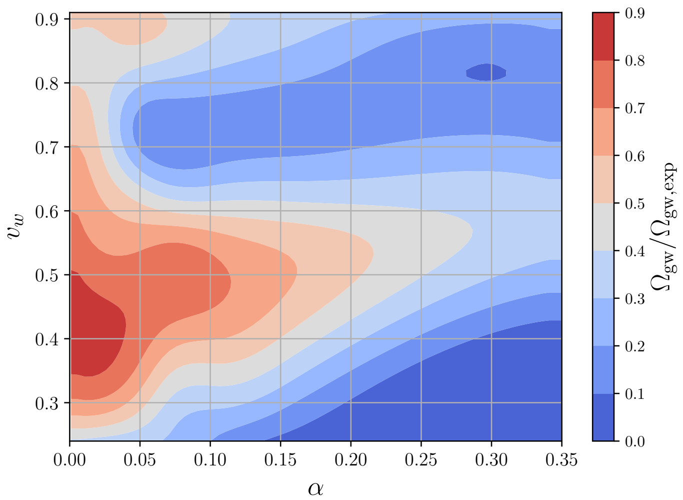

Figure 7.17: Contours of suppression to Ω_{gw} in the form of the ratio Ω_{gw} to $\Omega_{\mathrm{gw,exp}}$, where $\Omega_{\mathrm{gw,exp}}$ is the expected power computed according to the LCWG model.

Chapter 8

Paper II: Effective actions and bubble nucleation from holography

Abstract

We discuss the computation of the quantum effective action of strongly interacting field theories using holographic duality, and its use to determine quasi-equilibrium parameters of first order phase transitions relevant for gravitational wave production. A particularly simple holographic model is introduced, containing only the metric and a free massive scalar field. Despite the simplicity, the model contains a rich phase diagram, including first order phase transitions at non-zero temperature, due to various multi-trace deformations. We obtain the leading terms in the effective action from homogeneous black brane solutions in the gravity dual, and linearised perturbations around them. We then employ the effective action to construct bubble and domain wall solutions in the field theory side and study their properties. In particular, we show how the scaling of the effective action with the effective number of degrees of freedom of the quantum field theory determines the corresponding scaling of gravitational wave parameters.

1 Introduction

First order phase transitions are of great interest especially for early-universe cosmology, where bubble nucleation could result in the production of an observable gravitational wave signal at LISA [5, 2], providing evidence for beyond the Standard Model physics. If this new physics is strongly coupled, computations of the parameters of the phase transition relevant for gravitational wave production with standard techniques (see, *e.g.*, [265, 188] for reviews) fail, and the direct connection between the gravitational wave signature and the masses and couplings of the underlying field theory is lost.

Gravitational waves at strong coupling in SU(N) gauge theories have been investigated using phenomenological models of the free energy density [266, 267, 268]. A complementary approach is through holographic duality [217, 3, 269], but analyses have so far had certain limitations. In [3, 269] only equilibrium properties were computed, with some significant properties such as the bubble nucleation rates left as free parameters. This was not the case in [217], where the transition rate was computed (based on the results in [213]), but some additional assumptions were made, either by working in a quenched sector of the theory or by using a phenomenological approach that does not strictly follow from the holographic dictionary. In this work we will try to partially improve the holographic approach and present a derivation of the transition rate that does not require these assumptions. Although our analysis is motivated by its possible application to cosmological transitions and thus limited to high temperature and zero charge density, it can be straightforwardly generalised to other set-ups.

In quantum field theories the dynamical evolution of the phase transition can start to be addressed by finding the quantum effective action of the theory, which in many aspects is reminiscent of a Ginzburg-Landau effective action. Bubble configurations are obtained from semiclassical solutions to the effective action, and these can be employed to compute key properties of the transition such as the nucleation rate. Bubble production could take place through quantum tunnelling or thermal fluctuations, the probabilities of which can be estimated from the action. However, the dynamical evolution of the bubbles themselves require further analysis, as at nonzero temperature dissipation and drag will enter into play. We will not attempt to describe the dynamical evolution of bubbles, but this has been studied in some models [270, 271, 272].

In a weakly coupled theory, the effective action can be computed by standard perturbative methods (see, however, [273] for a discussion of issues at non-zero temperature). At strong coupling things are as always more difficult. While lattice simulations provide one route of attack (see, *e.g.*, [274]), they are computationally expensive and have great difficulty at non-zero charge density and especially for real time evolution. A possible avenue is to use gauge/gravity duality, or holography, which is well suited both for strong coupling and to study the dynamical evolution of the system at non-zero temperature.

In this paper, we consider the computation of the effective action using holographic duality. This allows us to study a strongly coupled QFT (often a gauge theory in the large-N limit) through the lens of a classical gravitational theory. We will consider only zero charge density, so our focus is on configurations that may be relevant for a cosmological phase transition, and pick a simple model to illustrate our approach. An analysis of the gravitational wave signal extracted in this model will be presented elsewhere [275].

Our approach has some similarities with the effective action approach used to describe the confinement-deconfinement transition from holographic models [213, 276], in that we do not attempt to find gravity solutions dual to bubble configurations, but construct the bubble solutions directly in the field theory. However, we do not make any additional phenomenological assumptions within the holographic model. Our derivation of the effective action follows directly from the usual rules of the duality. We will truncate the effective action by keeping only terms with two derivatives, but we show that higher derivative terms seem to be comparatively suppressed in the bubble configurations we obtain.

The outline of the paper is as follows. In Sec. 2 we warm up with a general discussion of the field theory (quantum) effective action, and show how to extract it from the gravity dual. Then, in Sec. 3, we introduce a particularly simple "bottom-up" gravity theory which nonetheless displays an interesting phase structure upon deforming it by single- and multi-trace operators. By finding a one-parameter family of numerical black brane solutions and applying careful holographic renormalisation, we show how to extract the effective potential, and thereby produce the phase diagram. Furthermore, by solving the linearised equations of motion around the black brane solutions, we show how to derive the (non-canonical) kinetic term as well as a subset of higher derivative terms. In Sec. 4 we then use the effective action to study the first order phase transitions of this theory, by finding the critical bubble solutions and computing their action, which sets the nucleation rate. We discuss implications for early-universe cosmology, including the computations of the nucleation temperature and the transition rate, as well as their dependence on the number of degrees of freedom N. We also briefly discuss domain walls and compute their surface tension for the complete parameter space, allowing us to comment on the applicability of the thin-wall approximation. Our conclusions and the discussion of the extensions of our work appear in Sec. 5. The appendices detail on the holographic renormalisation, exact results at large temperatures, and also the linearised fluctuation equations.

2 The quantum effective action from holography

Consider a theory with a scalar field Ψ whose action we denote $S[\Psi]$. The path integral in the presence of an external source J is

$$\mathcal{Z}[J] = \int \mathcal{D}\Psi \, \exp\left[iS[\Psi] + i\int d^4x J\Psi\right] \ . \tag{8.1}$$

From the path integral one can obtain the closely related generating functional for *connected* correlation functions

$$\mathcal{W}[J] = -i \log \mathcal{Z}[J] \ , \tag{8.2}$$

we define the effective action through a functional Legendre transform,

$$\Gamma[\langle\Psi\rangle_J] = \mathcal{W}[J] - \int d^4x \, \langle\Psi\rangle_J J \ . \tag{8.3}$$

In this definition J should be understood as being a functional of $\langle\Psi\rangle_J$ determined implicitly through the relationship

$$\frac{\delta\mathcal{W}[J]}{\delta J} = \langle\Psi\rangle_J \ . \tag{8.4}$$

This is also the statement that $\langle\Psi\rangle_J$ — sometimes referred to as the classical field — corresponds to the expectation value of Ψ for a given source J. Separating the expectation value of the field in the sourceless and sourced parts

$$\psi = \langle\Psi\rangle_{J=0}, \quad \delta\psi = \langle\Psi\rangle_J - \langle\Psi\rangle_{J=0} \ , \tag{8.5}$$

the effective action can be recast as a functional of $\delta\psi$. The effective action so defined is the generating functional of 1-point irreducible (1PI) connected correlation functions $\Gamma_n(x_1,\ldots,x_n;\psi)$; hence it can be expanded as

$$\Gamma[\psi+\delta\psi] = \sum_{n=0}^{\infty}\frac{1}{n!}\int d^4x_1 \ldots d^4x_n \Gamma_n(x_1,\ldots,x_n;\psi)\delta\psi(x_1)\ldots\delta\psi(x_n) \ . \tag{8.6}$$

The 1PI connected correlators themselves admit in principle an expansion around the trivial vacuum $\psi = 0$

$$\begin{aligned}\Gamma_n(x_1,\ldots,x_n;\psi) = {} & \Gamma_n(x_1,\ldots,x_n;0) \\ & + \sum_{k\geq 1}\frac{1}{k!}\int d^4y_1 \cdots d^4y_k \Gamma_{n+k}(x_1,\ldots,x_n,y_1,\ldots,y_k;0)\psi(y_1)\cdots\psi(y_k) \ .\end{aligned} \tag{8.7}$$

The full effective action is in general highly non-local, as can be seen from this expansion. However, if there are no gapless degrees of freedom, at sufficiently low energies one expects that it can be written as an integral over a local effective Lagrangian, and furthermore, that it can be expanded for small derivatives:

$$\Gamma[\psi+\delta\psi] = \int d^4x \left[-V(\psi+\delta\psi) - \frac{1}{2} Z(\psi+\delta\psi) \partial_\mu \delta\psi\, \partial^\mu \delta\psi + \dots \right] . \tag{8.8}$$

Here $V(\psi+\delta\psi)$ and $Z(\psi+\delta\psi)$ are ordinary functions of $\psi+\delta\psi$, and we have assumed that the sourceless state is static and homogeneous at $J=0$, so that $\partial_\mu\psi = 0$. The function $V(\psi+\delta\psi)$ is known as the effective potential, whose minimum determines the true ground state of the theory.

If ψ coincides with the ground state, further expanding to quadratic order in $\delta\psi$ leads to

$$\Gamma[\psi+\delta\psi] = \int d^4x \left[-V(\psi) - \frac{1}{2} V''(\psi)(\delta\psi)^2 - \frac{1}{2} Z(\psi) \partial_\mu \delta\psi\, \partial^\mu \delta\psi + \dots \right] . \tag{8.9}$$

In order to extract the coefficients in the effective action we compare the expansions in (8.6) and (8.9). Going to momentum space and expanding the correlators Γ_2 around zero frequency and vanishing spatial momenta (we omit the dependence on ψ and factor out a Dirac delta imposing momentum conservation),

$$\widetilde{\Gamma}_2(k) = \widetilde{\Gamma}_2(0) + \frac{1}{2} \frac{\partial^2 \widetilde{\Gamma}_2}{\partial k_i \partial k_j}\Big|_{k=0} k_i k_j + \dots\ , \tag{8.10}$$

one can deduce that

$$V''(\psi) = -\widetilde{\Gamma}_2(0), \quad Z(\psi) = -\frac{1}{6}\delta_{ij} \frac{\partial^2 \widetilde{\Gamma}_2}{\partial k_i \partial k_j}\Big|_{k=0} . \tag{8.11}$$

We will be interested in constructing the effective action up to (at least) second order in the derivative expansion; that is, we want to compute $V(\psi)$ and $Z(\psi)$. We do this in the framework of holographic duality, which lets us study a strongly coupled quantum field theory by solving a classical gravitational one. The essential relationship in the holographic dictionary is the equivalence between the renormalised on-shell gravitational action and the field theory generating functional $\mathcal{W}[J]$. Thus, if one can come by a set of solutions to the gravitational field equations corresponding to different sources J (meaning different near-boundary falloffs for the fields of interest) one can simply evaluate the gravitational action on these solutions to find $\mathcal{W}[J]$, and then Legendre transform to obtain $\Gamma[\langle\Psi\rangle_J]$.

Of course, even the solution of classical field equations for arbitrary boundary conditions can be extremely challenging. However, assuming unbroken translational symmetry in the field theory directions one can typically find such solutions numerically for a large class of theories, including the simple gravity plus scalar theories we focus on later in the paper. This lets us compute $\Gamma[\psi]$ in the limit of uniform fields and sources, *i.e.*, the effective potential.

To access derivative terms in the effective action, we then perturb away from these uniform solutions. The essential insight is that from (8.11), the value of $Z(\psi)$ at some particular value of ψ is just given by the leading terms in the low momentum expansion of the two-point correlators. This is readily done in holography by solving the gravitational field equations linearised around a particular background solution.

Note that since we will be interested in the effective action at some non-zero temperature, the Lorentz invariance displayed in for example (8.9) will be broken. We will mainly be interested in static field configurations, and so limit ourselves to computing the coefficient of the spatial derivatives. Generalizing by including derivatives with respect to time is straightforward.

Previous authors have discussed computing the field theory effective action through holography [277, 278, 279, 280, 281]. Of these, several make use of (fake) superpotential formulations on the gravity side to derive analytical expressions for the effective action. In simplifying limits such as close to conformality these are very useful. In order to describe thermal phase transitions, as our aim is here, further (numerical) work is typically needed. Our approach is in some sense more direct, employing numerics from the outset; the effective potential analysis in references [277, 278] are the closest in spirit.

2.1 Holographic duality

We now give a brief introduction to holographic duality, and argue that the approach we outlined for computing the effective action in a derivative expansion is quite natural and convenient in this setting.

Holographic duality relates a d-dimensional quantum field theory (QFT) with a $D = (d+1)$-dimensional gravitational theory in an (asymptotically) anti-de Sitter (AdS) spacetime of radius L. The AdS behaviour corresponds to a fixed point in the UV of the QFT. If the space is AdS throughout, then the dual is a conformal field theory (CFT), while asymptotically AdS spacetimes correspond to perturbations of the fixed point by some relevant operators. Well-understood examples of this duality originate in string theory, where the QFT is typically a gauge theory with some amount of supersymmetry. To be able to suppress quantum and string effects in the bulk, rendering the gravitational theory classical, one must typically take the limit of many degrees of freedom and strong coupling. If the dual QFT is a gauge theory, the former can be realised as a large-N limit where N is the rank of the group. In CFTs the number of degrees of freedom can be associated with the central charge (in two dimensions), conformal anomaly coefficients (in even dimensions) or other quantities. We will refer to N as the "number of colours", even if the dual field theory is not known.

In slightly more detail, the gravitational constant $\propto \kappa_5^2$ (whose inverse multiplies the 5D gravity action), made dimensionless by dividing by the appropriate power of the radius of curvature L, is related to the number of degrees of freedom. When the dual field theory is a rank-N gauge theory, in particular, we typically have a relation of the form

$$\frac{L^3}{\kappa_5^2} \propto N^2 \ . \tag{8.12}$$

Since we work in a bottom-up setting, the detailed form of this relationship is not known. For simplicity, we will set $L^3/\kappa_5^2 = N^2$, treating N as a free parameter related to the number of degrees of freedom, while keeping in mind it is not necessarily equal to the rank of some gauge group.

The field theory effective action we compute through holography will also have this large pre-factor N^2. This is important for bubble nucleation, since a large bubble action exponentially suppresses the nucleation rate. We will discuss this issue in detail in Sec. 4. For now, we only note that we will explicitly add this factor of N^2 in (8.9), writing it as

$$\Gamma[\psi+\delta\psi] = N^2 \int d^4x \left[-V(\psi) - \frac{1}{2}V''(\psi)(\delta\psi)^2 - \frac{1}{2}Z(\psi)\partial_\mu\delta\psi\,\partial^\mu\delta\psi + \dots \right] \ . \tag{8.13}$$

Thus, in the rest of the paper the quantities $V(\psi)$ and $Z(\psi)$ are $\mathcal{O}(1)$, while the full effective action is $\mathcal{O}(N^2)$.

Through holographic duality, the operator Ψ is associated with a scalar field ϕ in a gravitational theory. The gravitational theory admits classical solutions which are asymptotically anti-de Sitter — near the boundary of these spacetimes, the metric approaches the form

$$ds^2 = \frac{r^2}{L^2}\eta_{\mu\nu}dx^\mu dx^\nu + \frac{L^2}{r^2}dr^2 \quad , \quad r \to \infty \ , \tag{8.14}$$

and the field ϕ will fall off as

$$\phi(r,x) = \frac{\phi_-(x)}{r^{\Delta_-}} + \frac{\phi_+(x)}{r^{\Delta_+}} + \dots \ , \tag{8.15}$$

where $\Delta_\pm = \frac{d}{2} \pm \sqrt{\frac{d^2}{4} + m^2L^2}$.

In a typical realisation of holographic duality, the operators dual to classical fields on the gravity side will be some form of gauge-invariant single-trace operators, meaning they contain a single trace over colour indices. A deformation of the theory consisting of introducing a source for a scalar single-trace operator like Ψ is realised in the gravity dual by imposing a boundary condition such that ϕ_- is non-zero. One can also study deformations by operators with two or more traces; due to large-N factorisation, such operators have a simple description on the gravity side. These will prove useful for us in the next section, as they provide "knobs" to turn in order to make our simple gravity dual exhibit first order phase transitions.

For relevant multi-trace deformations to be possible, the mass of the scalar field must be close to the Breitenlohner-Freedman bound, in the range

$$-\left(\frac{d}{2}\right)^2 \leq m^2L^2 \leq -\left(\frac{d}{2}\right)^2 + 1 \; . \tag{8.16}$$

In this range, the value of the mass allows for alternate quantisation, where the coefficient of the sub-leading falloff ϕ_+ is fixed and identified as the source J of the dual operator. In this case the leading falloff ϕ_- is proportional to the expectation value $\langle\Psi\rangle_J$ of the operator.

Once in alternate quantisation, multi-trace deformations are implemented by generalising the boundary condition on the scalar field [282], allowing ϕ_+ to be given by an arbitrary function of ϕ_-. More specifically, if we want to deform our theory by some general multi-trace deformation $W(\Psi)$, we should impose the boundary condition

$$\phi_+ = \frac{\delta W(\langle\Psi\rangle)}{\delta\langle\Psi\rangle} \; , \tag{8.17}$$

where we recall that $\langle\Psi\rangle$ is proportional to ϕ_-. For example, in the theory we discuss in the next section, we show through careful holographic renormalisation that $\langle\Psi\rangle = -4\phi_-/3$. Then, deforming by say a double trace deformation $W(\Psi) = f\Psi^2/2$ means imposing the boundary condition

$$\phi_+ = f\langle\Psi\rangle = -\frac{4}{3}f\,\phi_- \; . \tag{8.18}$$

The multi-trace deformations we implement have a straightforward effect on the field theory effective action; a deformation by an n-trace operator Ψ^n simply adds a term $\propto \psi^n$ to the effective potential. For single-trace deformations ($n = 1$) this is in fact a general result for all field theories, following from the behaviour of the Legendre transform under a shift. The fact that multi-trace deformations leads to simple polynomial contributions is on the other hand only true in the large-N limit (see, *e.g.*, [279]).

3 Concrete example: CFT with a dimension-4/3 operator

We now apply the general ideas from the previous section to study a remarkably simple gravitational theory whose field theory dual enjoys a first order phase transition at non-zero temperature for a range of parameters. We work in a bottom-up setting, meaning we select a simple gravity theory capturing the features we are interested in. In this case, besides gravity with a negative cosmological constant, all we need is a scalar operator which can act as order parameter for the phase transition. We thus take the gravitational action to be

$$S_{bulk} = \frac{1}{2\kappa_5^2}\int d^5x\sqrt{-g}\left[\mathcal{R} - \partial_\mu\phi\partial^\mu\phi - \mathcal{P}(\phi)\right] \ . \tag{8.19}$$

Here $\mathcal{R}$ is the scalar curvature, g is the metric of the five-dimensional asymptotically anti-de Sitter (AdS) spacetime, ϕ is the scalar field, and $\kappa_5^2 = 8\pi G_5$ is essentially the Newton constant. The potential for the scalar field ϕ is taken to have the minimal form

$$\mathcal{P}(\phi) = -\frac{12}{L^2} + m^2\phi^2 \ , \tag{8.20}$$

with $m^2L^2 = -32/9$ [1]. From this point on we set the radius of curvature $L = 1$. The value of m^2 is within the range of masses allowing two possible quantisations — we will select the alternate quantisation, meaning that the dual operator has dimension $\Delta = 4/3$. Choosing alternate quantisation allows for relevant multi-trace deformations, which provides us with useful "knobs" to turn (in addition to a single-trace deformation and temperature) to arrive at a theory with a first order (thermal) phase transition. We will consider deformations of the original dual CFT, with a scalar operator Ψ and action S_{CFT}, by single-, double-, and triple-trace deformations,

$$S_{CFT} \to S_{CFT} + \int d^4x\left(\Lambda\Psi + \frac{f}{2}\Psi^2 + \frac{g}{3}\Psi^3\right) \ . \tag{8.21}$$

The choice of $\Delta = 4/3$ for the operator is convenient as it means that the triple trace deformation is marginal. Thus, the coupling g is dimensionless, while Λ and f have dimensions 8/3 and 4/3, respectively.

3.1 Finding background solutions

Since we want to study the field theory at non-zero temperature, we search for black brane solutions of the gravitational theory. A convenient ansatz is

$$ds^2 = -e^{-2\chi(r)}h(r)dt^2 + \frac{dr^2}{h(r)} + r^2 d\vec{x}^2 \, , \tag{8.22}$$

[1] The paper [279] discusses a class of potentials, dubbed the '2/3' potential, which has the same mass plus higher order terms; with four instead of five bulk dimensions, this potential can be embedded in $\mathcal{N} = 8$ gauged supergravity.

and $\phi = \phi(r)$. The equations of motion (EoM) for our system can then be written as follows:

$$\chi'(r) + \frac{r}{3}\phi'(r)^2 = 0 \tag{8.23}$$

$$h'(r) + h(r)\left(\frac{2}{r} + \frac{r}{3}\phi'(r)^2\right) + \frac{r}{3}\mathcal{P}(\phi(r)) = 0 \tag{8.24}$$

$$\phi''(r) + \frac{\phi'(r)}{r} - \frac{2r\mathcal{P}(\phi(r))\phi'(r) + 3\mathcal{P}'(\phi(r))}{6h(r)} = 0\ . \tag{8.25}$$

The equations allow for an AdS solution. Near the boundary of *asymptotically* AdS solutions, the fields fall off as

$$\begin{aligned}
\phi &= \frac{\phi_-}{r^{4/3}} + \frac{\phi_+}{r^{8/3}} + \ldots \\
h &= r^2 + \frac{4}{9}\frac{\phi_-^2}{r^{2/3}} + \frac{h_2}{r^2} + \ldots \\
\chi &= \chi_0 + \frac{2}{9}\frac{\phi_-^2}{r^{8/3}} + \ldots\ .
\end{aligned} \tag{8.26}$$

We use standard numerical methods, implemented using *Mathematica*'s **NDSolve** function, to look for hairy black brane solutions. We begin by noting that (8.24) and (8.25) involve only $h(r)$ and $\phi(r)$ (and not $\chi(r)$). We solve these two equations by expanding them in a power series near the black brane horizon at $r = r_H$, imposing that $h(r)$ goes to zero there and that $\phi(r)$ is regular. The resulting near-horizon series solution has two parameters that are not fixed by the equations of motion; the horizon radius r_H and the value of the scalar at the horizon $\phi(r_H) \equiv \phi_H$. For each choice of r_H and ϕ_H, we can numerically integrate the two equations from the horizon to the AdS boundary to obtain a solution for $h(r)$ and $\phi(r)$. We then plug the solution for $\phi(r)$ into (8.23) and solve it for $\chi(r)$, imposing $\chi_0 = 0$ to recover the standard AdS metric near the boundary.

Resulting black brane solutions will be dual to the field theory at non-zero temperature. The temperature and entropy density are set by the Hawking temperature and horizon area of the black brane, given by

$$T = \frac{e^{-\chi(r_H)}h'(r_H)}{4\pi} \qquad \text{and} \qquad s = \frac{r_H^3}{4G_5}\ , \tag{8.27}$$

where we remind that G_5 is related to κ_5 appearing in the pre-factor of the action (8.19) by $2\kappa_5^2 = 16\pi G_5$. We want to construct the field theory effective potential at *fixed temperature*. Using the near-horizon expansion, the above expression for the temperature can be seen to take the form

$$T = -\frac{e^{\chi(r_H)}\mathcal{P}(\phi_H)r_H}{12\pi}\ . \tag{8.28}$$

We see that given one of the free parameters, say ϕ_H, we can tune the other one, r_H, to set the temperature. We use this to set $T = 1$ for all our black brane solutions — all

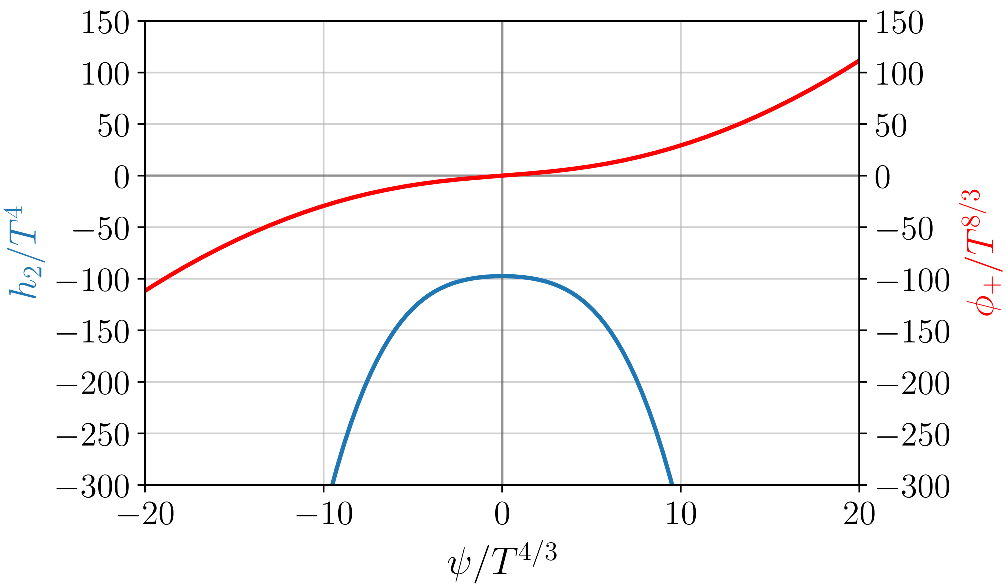

Figure 8.1: The coefficients h_2 (lower blue curve) and ϕ_+ (upper red curve) from (8.26) as functions of $\psi = -\frac{4}{3}\phi_-$, all in units of temperature.

the results we give will thus be in units of temperature. Note that if we had fixed r_H in some other way, say by setting $r_H = 1$ (fixing the entropy), we would have to rescale the solutions such that they all have the same temperature before Legendre transforming to get the effective potential.

Having fixed r_H we are left with a one-parameter family of solutions, one for each ϕ_H. It is useful for our purposes to parameterise the solutions by the quantity $\psi = -\frac{4}{3}\phi_-$, which as we show in Appendix D equals the expectation value of the scalar operator in the dual field theory. We visualise our family of solutions by plotting the coefficients h_2 and ϕ_+ from (8.26) as functions of ψ in Fig. 8.1.

3.2 Effective potential

There are two, essentially equivalent, ways of constructing the field theory effective potential. From (8.3) and (8.13) we see that for uniform fields and sources, the effective potential can be written as

$$V(\psi) = -w(J) + \psi J \ , \tag{8.29}$$

where we defined $w(J) = \mathcal{W}[J]/(\beta V_3 N^2)$ with V_3 being the volume along the spatial directions of the dual field theory, and $\beta = 1/T$ being the extent of the Euclidean time direction. Note that we have also implicitly redefined ψ by a factor of $N^2 = \kappa_5^{-2}$ as compared with section 2, as is also done in the appendix, see (8.78). From the holographic dictionary, we have $\beta V_3 N^2 w(J) = S_{OS}$, where S_{OS} is the full on-shell gravitational action (including all counter-terms). In Appendix D we go through the holographic renormalisation for our theory, which gives us expressions for w, ψ and J in terms of the coefficients in the asymptotic expansion (8.26). The end result is (8.89), which we reproduce here for convenience:

$$V(\psi) = \frac{h_2(\psi)}{2} + \frac{7}{9}\psi\,\phi_+(\psi) + \Lambda\psi + \frac{f}{2}\psi^2 + \frac{g}{3}\psi^3\ . \tag{8.30}$$

From our family of black brane solutions we can extract the functions $h_2(\psi)$ and $\phi_+(\psi)$ (which are plotted in Fig. 8.1), allowing us to evaluate $V(\psi)$. Note that as mentioned in the previous section, the addition of single-, double-, and triple-trace deformations give linear, quadratic, and cubic contributions to the effective potential, respectively; this should be true in general for a holographic theory in the classical gravity limit.

As an alternative road to the effective potential, introduced in [277], we note that (still assuming uniform fields and sources)

$$\frac{dV(\psi)}{d\psi} = J(\psi)\ . \tag{8.31}$$

Since we can easily extract the curve $J(\psi)$ from our family of black brane solutions using the results obtained from holographic renormalisation in Appendix D, we can simply integrate it (numerically) to obtain $V(\psi)$ up to a constant. And this constant can in fact be fixed by noting that the effective potential at small ψ corresponds to the free energy of pure AdS-Schwarzschild, which is easily obtained. We have checked that these two approaches to compute the effective potential agree.

For the $\Lambda = f = g = 0$ theory, which we refer to as the *undeformed* case, this procedure gives us the dashed-dotted blue curve in Fig. 8.2. As one might have expected from such a simple gravity dual there are no exciting features, only a convex potential with a single minimum. Since the gravity theory is symmetric under $\phi \to -\phi$, $V(\psi)$ is an even function. At small field values it goes as

$$V(\psi) = V_0 + \frac{V_2}{2}\psi^2 + \mathcal{O}(\psi^4)\ . \tag{8.32}$$

As small ψ is equivalent to large temperatures, in this limit the background approaches AdS-Schwarzschild. Then, V_0 can be seen to simply equal the free energy density of this solution,

$$V_0 = f_{AdS-Sch} = -\frac{\pi^4}{2} \approx -48.70\ . \tag{8.33}$$

Moreover, as we show in Appendix E, the coefficient V_2 can be found exactly by computing the scalar two-point function in an AdS-Schwarzschild spacetime; the result being

$$V_2 = \frac{9\pi^{17/6}}{\Gamma(1/6)^3} \approx 1.337\ , \tag{8.34}$$

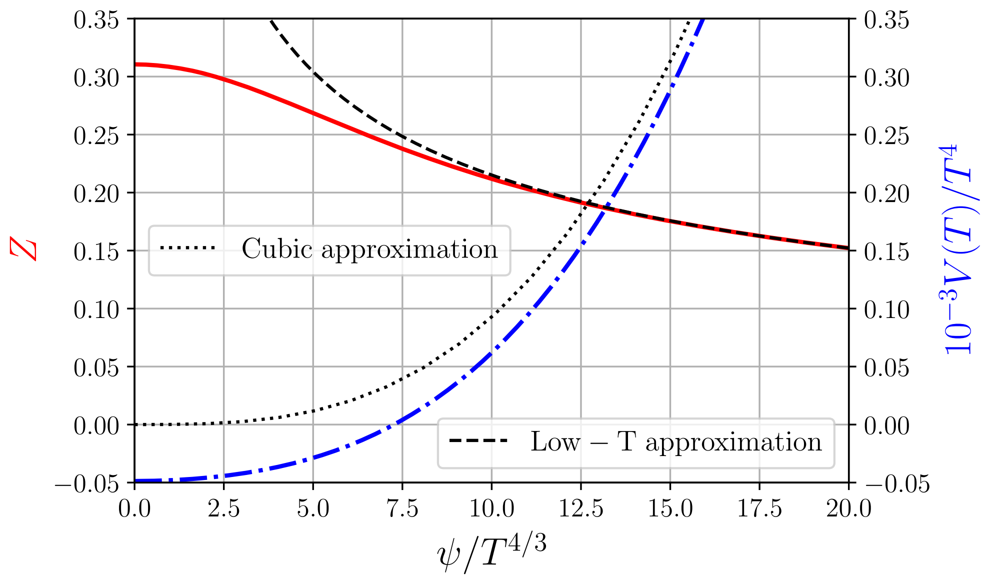

Figure 8.2: The quantum effective potential of the undeformed theory (dashed-dotted blue), and the kinetic term (solid red, discussed in the next subsection).

matching our numerical results well. The explicit temperature dependence of the coefficients in the effective potential follows from simple dimensional analysis: $V_0 \sim T^4$ and $V_2 \sim T^{4/3}$. Since $V_2 > 0$, increasing the temperature will tend to stabilise the trivial vacuum $\psi = 0$. Our strategy will be to introduce additional terms that destabilise the trivial vacuum at zero temperature, in such a way that we can produce a phase transition when V_2 becomes dominant and the trivial vacuum becomes the favoured state at high temperature.

At large field values or small temperatures, the effective potential grows as

$$V(\psi) \sim \frac{\gamma_3}{3}|\psi|^3 \qquad \text{with} \qquad \gamma_3 \approx 0.278 \;, \tag{8.35}$$

as shown by the dotted black line in Fig. 8.2. The cubic behaviour is dictated by the scale invariance of the theory at zero temperature. The full potential cannot be well-fitted by a simple polynomial.

We now consider deforming the theory by single-, double-, and triple-trace deformations. As discussed in Section 2.1, this will add to the "undeformed" effective potential a term linear, quadratic, or cubic in ψ, respectively. We want to consider fixing the theory, *i.e.*, fixing all couplings, and then tuning the temperature in order to look for a thermal phase transition. Of course, by "tuning temperature" we really mean tuning some dimensionless ratio of temperature to some other scale; in our case, it is convenient to define

$$\tilde{T} = \frac{T}{|\Lambda|^{3/8} + |f|^{3/4}} \;, \tag{8.36}$$

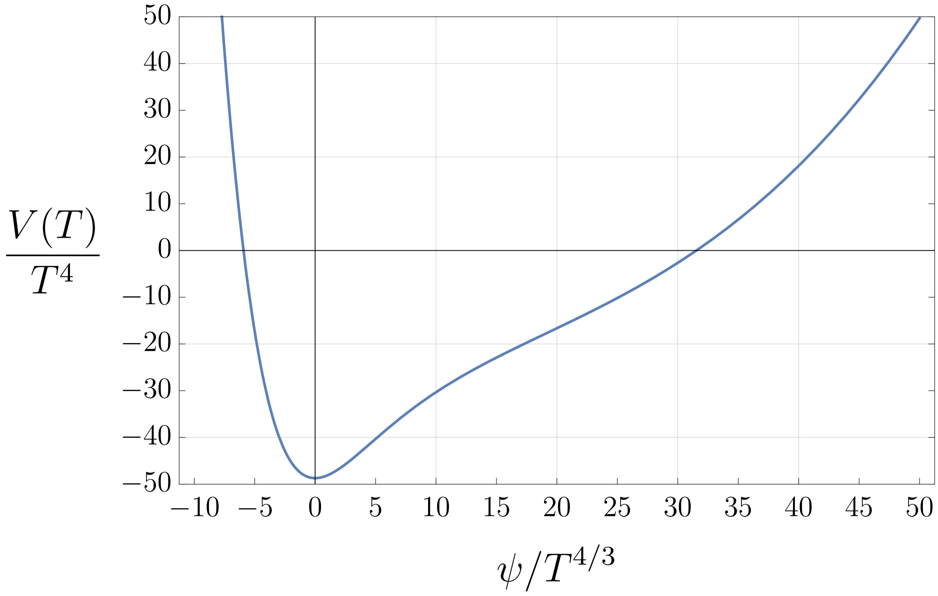

Figure 8.3: The quantum effective potential of the theory with a triple trace deformation, $g = 0.276$.

which remains well-defined when Λ or f (but not both) are zero. In particular, we can just as well tune $\tilde{T}$ by keeping T fixed and tuning Λ and f together (keeping their dimensionless ratio fixed), which is more convenient from a holographic point of view.

Let us emphasise that all the non-trivial strongly coupled physics is in some sense contained in the undeformed effective potential of Fig. 8.2, which is given by the numerically determined functions $h_2(\psi)$ and $\phi_+(\psi)$ in (8.30). The polynomial contributions from single- and multi-trace deformations are on their own reminiscent of a weakly coupled effective description, albeit with the notable difference that the "order parameter" ψ has dimension 4/3, meaning the usual ψ^4-term is irrelevant. We now describe the effective potential and possible phase transitions that result from turning on different combinations of couplings.

Single-trace deformation ($f = g = 0$) Adding a single-trace deformation simply shifts the minimum of the undeformed potential around while still keeping the potential convex, not leading to any phase transition or other interesting features.

Double-trace deformation ($\Lambda = g = 0$) Adding a double-trace deformation is more interesting; for $f < -V_2$, it destabilises the vacuum at $\psi = 0$, leading to a double-well potential. The resulting theory thus has a second order thermal phase transition, breaking the $\psi \leftrightarrow -\psi$ symmetry as $\tilde{T}$ crosses the critical value $V_2^{-3/4}$ from above. This case was studied in [283].

Triple-trace deformation ($\Lambda = f = 0$) Importantly, for large triple-trace deformations $g > \gamma_3$, the potential becomes unbounded from below. Staying below this value, we note that the resulting potential is no longer convex (but still bounded) within the narrow range

$$0.2675 \lesssim g < \gamma_3 \approx 0.278 \ . \tag{8.37}$$

In particular $g = 0.276$ results in Fig. 8.3. But since the triple-trace deformation is marginal this is still a CFT, and thus has no phase transitions as a function of temperature.

Single- and triple-trace deformation ($f = 0$ and $\Lambda, g \neq 0$) Within the interval (8.37), the now non-convex potential displays a first order phase transition. The critical temperature depends on g; for $g = 0.276$, it is $\tilde{T} \approx 0.844$. With this value of g, we also display the potential for a few different $\tilde{T}$ around the transition in Fig. 8.4.

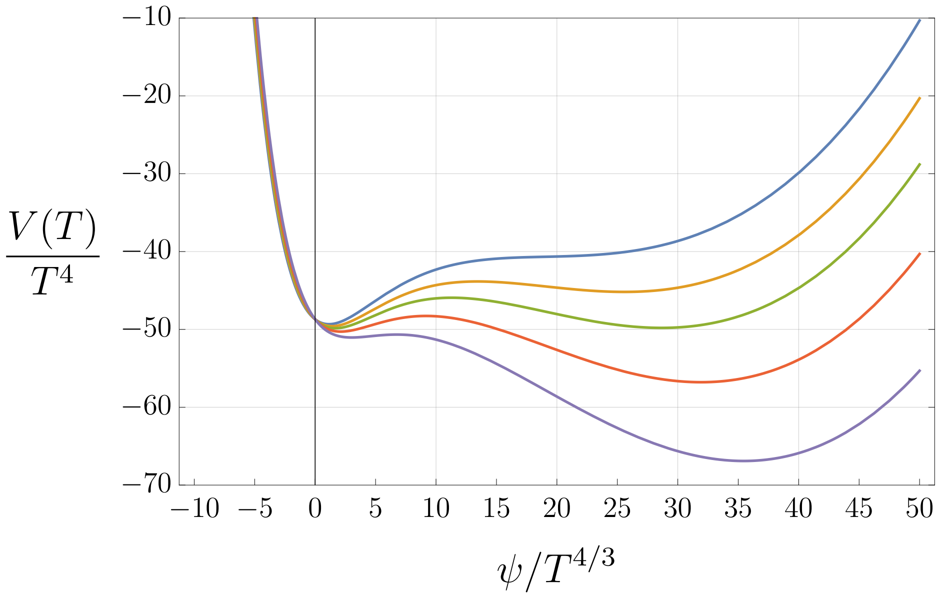

Figure 8.4: The effective potential for the theory with a single- and triple-trace deformation, for a few different values of $\tilde{T}$ around the phase transition (at $\tilde{T}_c \approx 0.844$).The temperature values are $\tilde{T} \approx 0.934$, 0.881, 0.844, 0.802, and 0.757 from the top down.

Double- and triple-trace deformation ($\Lambda = 0$ and $f, g \neq 0$) With $g = 0$, a negative double trace deformation induces a second order phase transition. Any $0 < g < \gamma_3$, however, instead leads to a first order transition. This can be seen by considering the undeformed potential; for small ψ, it can be expanded as in (8.32); adding the quadratic

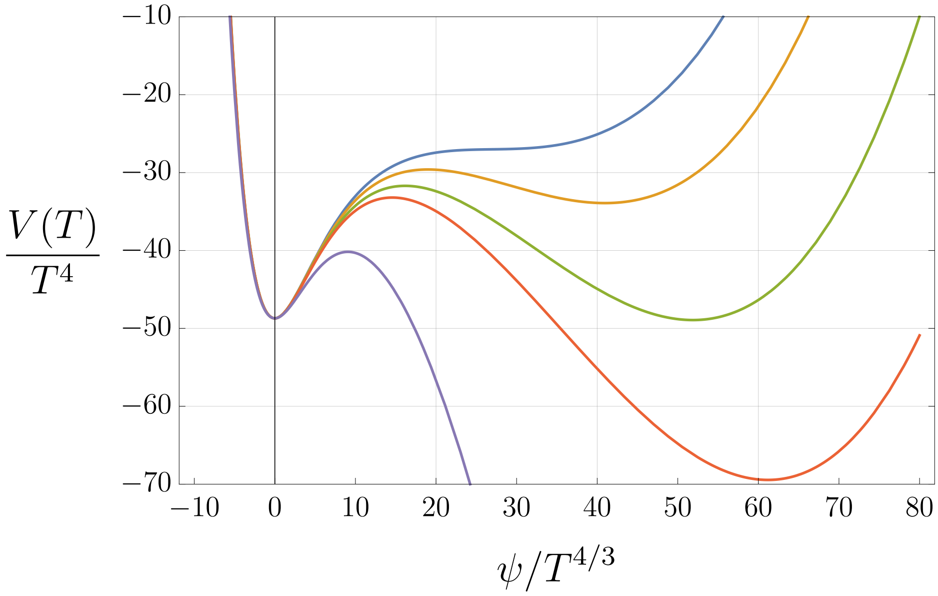

Figure 8.5: The effective potential for the theory with a double- and triple-trace deformation, for a few different values of $\tilde{T}$ around the phase transition (at $\tilde{T}_c \approx 6.72$). The temperature values are $\tilde{T} \approx 8.926$, 7.768, 6.724, 6.006, and 3.344 from the top down.

and cubic contributions from the double- and triple-trace deformations modifies this to be

$$V(\psi) = V_0 + \frac{1}{2}(V_2 + f)\psi^2 + \frac{g}{3}\psi^3 + \mathcal{O}(\psi^4) \ . \tag{8.38}$$

Assuming $f > -V_2$, *i.e.*, above the temperature $\tilde{T}$ where the second order phase transition would set in, this cubic potential has a minimum at $\psi = 0$, a maximum at

$$\psi = -\frac{V_2 + f}{g} \ , \tag{8.39}$$

and then dips below $V(0) = V_0$ at

$$\psi = -\frac{3}{2}\frac{V_2 + f}{g} \ . \tag{8.40}$$

If the small-ψ expansion is valid out to this point, this shows that the minimum at $\psi = 0$ has become metastable leading to a first order phase transition. But for any given $g \neq 0$, the small-ψ expansion will in fact be valid as long as f is close enough to $-V_2$. This guarantees that as we lower the temperature $\tilde{T}$ we will always encounter a first order transition *before* the quadratic term goes negative and causes a second order transition. For $g = 0.276$, Fig. 8.5 shows the effective potential for a few different temperatures around the critical value of $\tilde{T} \approx 6.72$.

Single-, double- and triple-trace deformation In the general case with all couplings non-zero, it is convenient to define a dimensionless coupling

$$\Lambda_f \equiv \frac{\Lambda}{f^2} \tag{8.41}$$

in addition to the already dimensionless g. We then fix the theory by fixing Λ_f and g, and tune $\tilde{T}$ to look for a phase transition. The case $\Lambda_f \to -\infty$ corresponds to the case listed in 3.2 with a first order transition within a narrow region of g. The case $\Lambda_f = 0$ corresponds to the case listed in 3.2 with a first order transition for any g, except for $g = 0$ which gives a second order transition. The full two-dimensional space of couplings interpolates between these cases. Within some extended region the theory will have a first order phase transition.

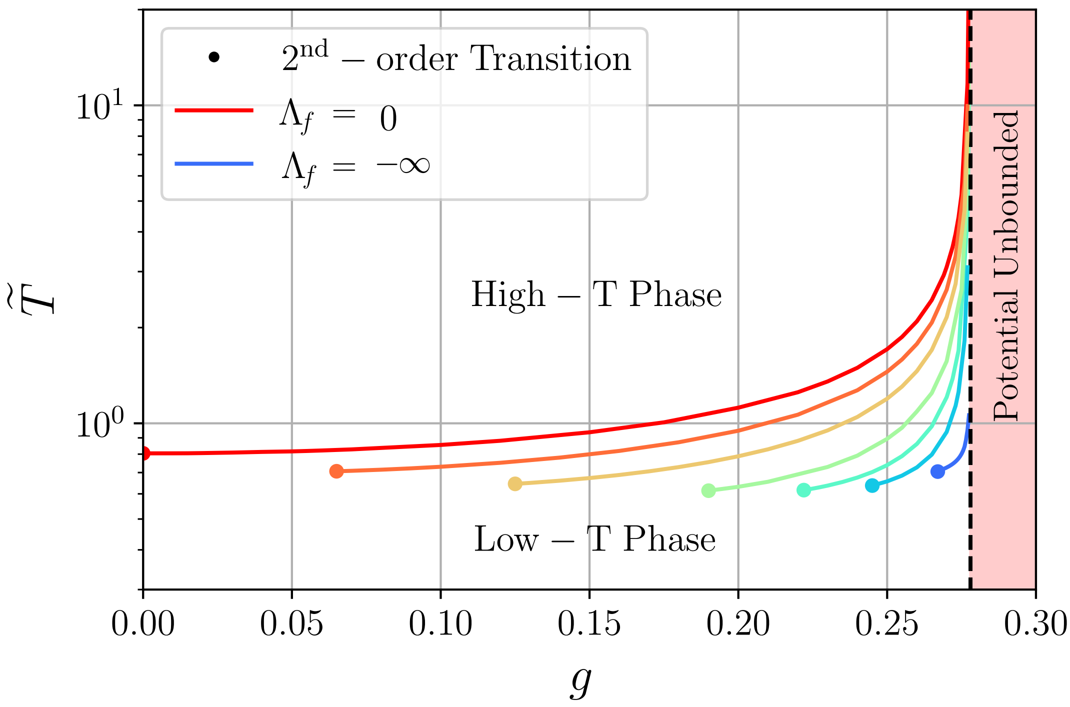

Figure 8.6: Phase diagram of the dual field theory as a function of $\tilde{T}$ and g, for various values of Λ_f ranging from 0 to $-\infty$ and with $N = 1$. The curves take values of $\Lambda_f = 0$, $-\frac{4}{9}$, -1, -4, -16, -100, and $-\infty$ (top-down).

Fig. 8.6 shows a phase diagram of the theory with fixed Λ_f as a function of $\tilde{T}$ and g. Each of the coloured curves corresponds to a line of first order transitions for a certain fixed value of Λ_f; each of these lines terminate in a second order critical point. Note that while we use the label "high-T phase" and "low-T phase", these are not distinct phases in the sense that one can move from one to the other without any sharp transitions by tuning g. The exception is $\Lambda_f = 0$, where the first order line extends over the whole allowed range of g, except for $g = 0$ which corresponds to a second order phase transition.

3.3 Kinetic term

Having discussed the effective potential and the resulting phase structure, we move on to the kinetic term, characterised by the function $Z(\psi)$ in (8.13). Note first of all that the non-zero temperature breaks Lorentz invariance, so time and spatial derivatives will not appear on equal footing. We are mainly interested in studying *static* configurations, and so restrict to finding the coefficient of the spatial derivatives; this is what we mean by $Z(\psi)$ in the following.

As discussed in Sec. 2, we will determine this function by computing the two-point correlator as a function of the expectation value in a low-momentum expansion (at zero frequency). Holographically, this is done by a linearised fluctuation analysis around a given, uniform background solution. We take advantage of the translational symmetry by writing the fluctuations as plane waves, and use the rotational symmetry to align the momentum in the x-direction. Making the common gauge choice $H_{Mr} = 0$, for the metric fluctuation H_{MN} we then have the Ansatz

$$\begin{aligned} ds^2 = & -e^{-2\chi(r)}h(r)\left(1+e^{ikx}H_{tt}(r)\right)dt^2 + \frac{dr^2}{h(r)} + r^2\left(1+e^{ikx}H_{xx}(r)\right)dx^2 \\ & +r^2\left(1+e^{ikx}H_{\perp}(r)\right)\left(dy^2+dz^2\right) + 2r^2 e^{ikx}H_{tx}(r)dt\,dx \\ \phi = & \ \phi(r) + e^{ikx}\varphi(r)\ . \end{aligned}$$

Here we have also used the fact that even in the presence of the fluctuations there is an $SO(2)$ rotational symmetry, which restricts which metric components the scalar mode can couple to.

Plugging in this Ansatz into the equations of motion and expanding to linear order, one quickly notes that H_{tx} decouples from the other modes. With a bit more work, H_{xx} can be eliminated, leaving us with three coupled ordinary differential equations (ODEs), first order in derivatives of H_{tt} and second order in derivatives of $H_{\perp}$ and φ.

Next, one can show that the following linear combinations of modes are invariant under residual gauge transformations,

$$Z_{\phi}(r) = \varphi(r) - \frac{r}{4}\phi'(r)H_{\perp}(r) \tag{8.42}$$

$$Z_H(r) = -e^{-2\chi(r)}h(r)H_{tt}(r) - \frac{r}{4}e^{-2\chi(r)}\left[h'(r) - 2h(r)\chi'(r)\right]H_{\perp}(r)\ , \tag{8.43}$$

and that they satisfy a set of two coupled second order linear ODEs, which we relegate to Appendix F due to their unwieldiness. Near the AdS boundary, these two modes decouple, and the solution asymptotes to

$$\begin{aligned} Z_\phi(r) &= \frac{Z_\phi^-}{r^{4/3}} + \frac{Z_\phi^+}{r^{8/3}} + \dots \\ Z_H(r) &= Z_H^+ r^2 + \frac{Z_H^-}{r^2} + \dots \ . \end{aligned} \tag{8.44}$$

From the holographic renormalisation analysis in Appendix D we see that this small perturbation on the gravity side corresponds to perturbing the source (single-trace coupling) of the dual scalar operator by

$$\delta\Lambda = Z_\phi^+ + \frac{4}{3}W''(\psi)\, Z_\phi^- \ , \tag{8.45}$$

where we pick

$$W(\psi) = \frac{f}{2}\psi^2 + \frac{g}{3}\psi^3 \qquad \text{with} \qquad \psi = -\frac{4}{3}\phi_- \ . \tag{8.46}$$

This perturbation then gives rise to a small change in the scalar expectation value

$$\delta\langle\Psi\rangle = -\frac{4}{3}Z_\phi^- \ . \tag{8.47}$$

A generic solution to the linearised equations will source not only the scalar mode Z_ϕ but also the operator dual to Z_H. To compute the scalar two point function, we must then impose the boundary condition $Z_H^+ = 0$. The two-point function in momentum space is simply the ratio

$$\langle\Psi\Psi\rangle = \frac{\delta\langle\Psi\rangle}{\delta\Lambda} \ . \tag{8.48}$$

Since we are interested in the low momentum limit of the two-point function, we expand the gauge invariant modes as

$$Z_i(r) = Z_i^{(0)}(r) + k^2 Z_i^{(2)}(r) + \dots \qquad \text{with} \quad i \in \{\phi, H\} \ , \tag{8.49}$$

plug this into the fluctuation equations, and solve order by order in k^2. Similarly expanding the coefficients in (8.44) as

$$Z_i^\pm = Z_i^{\pm(0)} + k^2 Z_i^{\pm(2)} + \dots \tag{8.50}$$

we are able to write the two-point function as

$$\langle\Psi\Psi\rangle = -\frac{4}{3}\frac{Z_\phi^{-(0)}}{Z_\phi^{+(0)} + \frac{4}{3}W''(\psi)Z_\phi^{-(0)}} - \frac{4}{3}\frac{Z_\phi^{-(2)}Z_\phi^{+(0)} - Z_\phi^{-(0)}Z_\phi^{+(2)}}{\left(Z_\phi^{+(0)} + \frac{4}{3}W''(\psi)Z_\phi^{-(0)}\right)^2}k^2 + \dots \ . \tag{8.51}$$

Now we use the fact that the part of the effective action quadratic in ϕ — *i.e.*, Γ_2 in the notation of Sec. 2 — equals the inverse of this two point function. This can be used to derive the following expressions

$$\Gamma_2 = -\left(\frac{3}{4}\frac{Z_\phi^{+(0)}}{Z_\phi^{-(0)}} + W''(\psi)\right) + \frac{3}{4}\frac{Z_\phi^{-(2)}Z_\phi^{+(0)} - Z_\phi^{-(0)}Z_\phi^{+(2)}}{\left(Z_\phi^{-(0)}\right)^2}k^2 + \dots \ . \tag{8.52}$$

The first term, of order k^0, should just equal the second derivative of the effective potential. We can compare this with the results from the previous subsection to check our numerics; doing so we find excellent agreement. The second term, at order k^2, is what we are really interested in as it determines $Z(\psi)$:

$$Z(\psi) = \frac{3}{4} \frac{Z_\phi^{-(2)} Z_\phi^{+(0)} - Z_\phi^{-(0)} Z_\phi^{+(2)}}{\left(Z_\phi^{-(0)}\right)^2} \,. \tag{8.53}$$

Note that each $Z_\phi^{\pm(i)}$ here can be regarded as a function of ψ, obtained by solving the fluctuation equations in the gravitational background with $\psi = -\frac{4}{3}\phi_-$. Importantly, we note that $Z(\psi)$ is independent of the multi-trace deformations specified by $W(\psi)$, meaning the kinetic term will be the same for the entire class of theories we study. The resulting $Z(\psi)$ is shown in solid red in Fig. 8.2. It is an even function, admitting an expansion similar to 8.32 for small ψ (large temperatures). At large ψ (small temperatures) it goes as $\psi^{-1/2}$ (see the dashed black curve), which is required by scale invariance to make the kinetic term have dimension four.

3.4 Higher-derivative terms

It is straightforward to continue the work of the previous subsection and compute the two-point function up to higher order in k^2. By the same reasoning as above, this should provide information about higher-derivative terms in the effective action. A complication arises though, since starting at four derivatives, the number of independent terms grows rapidly. Some of these terms involve several external momenta, and require information from higher-order correlation functions to determine. Computing these is beyond the scope of this paper. We have, however, computed the two point function up to order k^4, which lets us extract the four-derivative term $\nabla^2\psi\nabla^2\psi$. This allows us to verify that this term is negligible in the context of bubble nucleation — discussed in the next section — thus providing evidence that the small derivative expansion is applicable there.

4 Bubble nucleation and N dependence

One important motivation for going after the effective action is to understand the phase structure and phase transitions of a field theory. First order phase transitions proceed through bubble nucleation, which in turn is controlled by the effective action previously found. At an arbitrary temperature, the resulting equations of motion should be solved in Euclidean space with the appropriate periodicity imposed in the time-direction, leading in general to a *partial* differential equation. Typically this is simplified into an ordinary differential equation by focussing on the high and low temperature limits, leading to two actions: a zero temperature action with O(4) symmetry arising from purely quantum fluctuation effects causing bubble nucleation [284, 285] and a non-zero temperature, O(3) symmetric action arising from both thermal and quantum fluctuations [123].

Note that while an O(3) symmetric typically exists for any temperature, the O(4) solution only exists at zero temperature, where Lorentz symmetry is unbroken. Nonetheless, it is a good approximation to a true solution as long as the length of the thermal circle is large (and thus the temperature small) compared with the bubble radius. Motivated by this, we study both O(3) and O(4) solutions. We assume that the function multiplying the kinetic term in the O(4) case is the same as in the static O(3) case, which is what was computed in the previous section. This is a reasonable assumption since the O(4) solution is expected to matter more at low temperatures, where Lorentz symmetry is nearly restored.

After integrating along the angular direction in Euclidean spacetime, the $O(4)$ symmetric action is

$$\Gamma_{O(4)} = 2\pi^2 N^2 \int_0^\infty d\rho\, \rho^3 \left(\frac{1}{2} Z(\psi) \left(\frac{d\psi}{d\rho}\right)^2 + V(\psi)\right) \ , \tag{8.54}$$

while for the $O(3)$ symmetric action we integrate along the angular spatial directions and the Euclidean time circle

$$\Gamma_{O(3)} = \frac{4\pi N^2}{T} \int_0^\infty d\rho\, \rho^2 \left(\frac{1}{2} Z(\psi) \left(\frac{d\psi}{d\rho}\right)^2 + V(\psi, T)\right) \ . \tag{8.55}$$

Note that in each case ρ takes a different meaning, in the $O(4)$ symmetric configuration it is the radial direction in full Euclidean four-dimensional spacetime, while in the $O(3)$ symmetric configuration ρ is the radial direction along the three-dimensional space. As earlier, we pull our a factor of N^2, all other quantities then being of order N^0.

To evaluate these integrals we first need to find the field profiles $\psi(\rho)$, by solving the equations of motion derived from the effective action. For the $O(4)$ symmetric bubble, the equation of motion is

$$\frac{d^2\psi}{d\rho^2} + \frac{3}{\rho}\frac{d\psi}{d\rho} + \frac{1}{2}\frac{\partial_\psi Z(\psi)}{Z(\psi)} \left(\frac{d\psi}{d\rho}\right)^2 - \frac{\partial_\psi V(\psi)}{Z(\psi)} = 0 \ , \tag{8.56}$$

while for the $O(3)$ symmetric bubble is

$$\frac{d^2\psi}{d\rho^2} + \frac{2}{\rho}\frac{d\psi}{d\rho} + \frac{1}{2}\frac{\partial_\psi Z(\psi)}{Z(\psi)} \left(\frac{d\psi}{d\rho}\right)^2 - \frac{\partial_\psi V(\psi)}{Z(\psi)} = 0 \ . \tag{8.57}$$

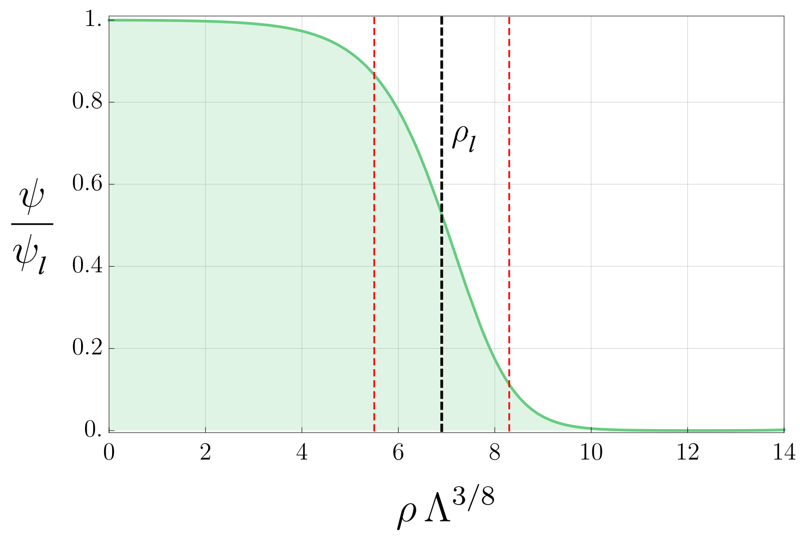

Figure 8.7: Graph of an $O(3)$ bubble solution with $N = 1$ normalised by the low-T phase value ψ_l against the radius. The thick dashed vertical black line in the middle denotes the radius of the bubble ρ_b, and the vertical dashed red lines encompass the bubble thickness. The parameter values are $g = 0.27$, $\Lambda_f = 0$.

These are solved with the well-known "shooting method" with boundary conditions $\psi(\infty) = \psi'(\infty) = 0$ where the initial minimum is shifted to always appear at $V = 0$. An example of a bubble profile is shown in Fig. 8.7 which solves the O(3) equation of motion (8.57).

How steeply the profile transitions from one phase to another details the "thickness" of the bubble wall. Whether the wall is in the thin, thick, or intermediate regime will determine how important quantities will change when considering the number of colours N of the theory, as shown shortly.

In our holographic model, a complete picture of how the bubble action depends upon the temperature is built up by selecting a particular value of the triple trace coupling g and coupling ratio Λ_f, then varying the temperature $\widetilde{T}$. There is therefore one graph of the action for each parameter set g, Λ_f, all of which appear similar in shape to Fig. 8.8.

Another aspect which must be taken into consideration is the fact that we have used a small derivative (or low momentum) expansion for the effective action, truncated at two derivatives. As it is not immediately clear whether the higher order terms will be negligible, we explored what consequence including the term $\partial^2\psi\partial^2\psi$ has on the bubble action. As discussed in subsection 3.4, this term in the effective action can be obtained by computing the scalar two-point function to order k^4. The importance of the effect can be judged by the size of the ratio E_4/E_2, where E_2 is the contribution to the energy from including the k^2 term and E_4 is the contribution to the energy from including the

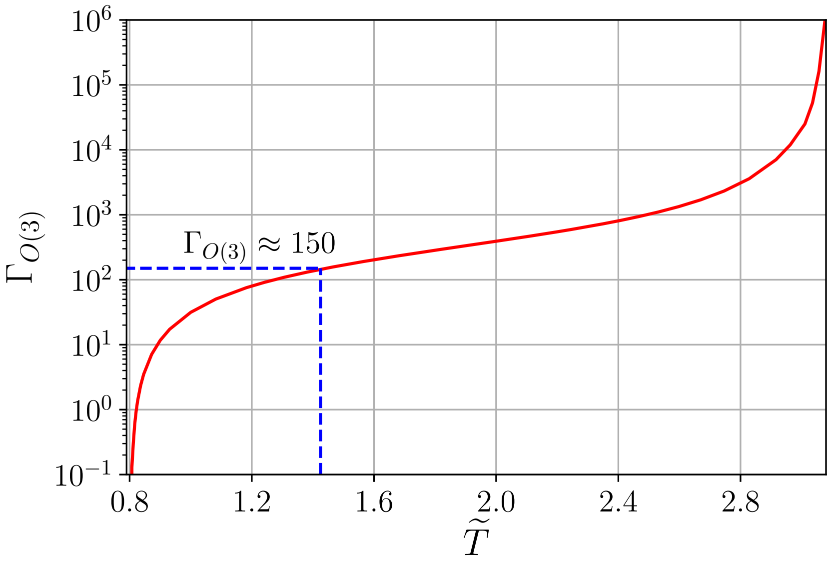

Figure 8.8: Graph of the $O(3)$ bubble action against the temperature $\widetilde{T}$ for triple-trace coupling $g = 0.27$, $\Lambda_f = 0$, and with $N = 1$.

k^4 term, shown in Fig. 8.9. This is plotted against the scaled temperature defined as $(\tilde{T} - \tilde{T}_0)/(\tilde{T}_c - \tilde{T}_0)$, where $\tilde{T}_c$ is the dimensionless critical temperature, and $\tilde{T}_0$ is the dimensionless lower critical temperature at which the metastable minimum disappears.

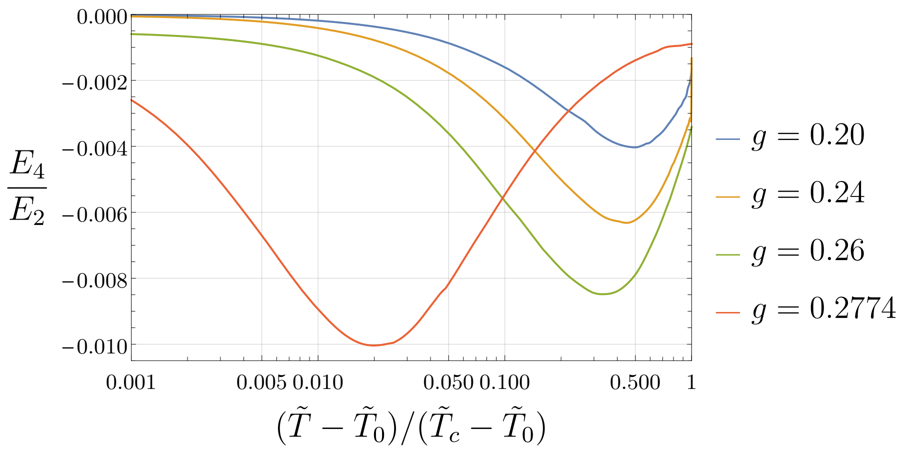

Figure 8.9: Graph of the ratio of k^4 and k^2 energy contributions in the kinetic coefficient $Z(\phi)$ against the temperature $\widetilde{T}$ for triple-trace couplings $g = 0.20$, 0.24, 0.26, and 0.2774 (top-down on the left), with $\Lambda_f = 0$. All curves are for value $N = 1$.

As can be seen in this figure E_4 is a negative contribution with magnitude of less than 1% of the k^2 contribution, and this remains valid in general. We therefore determine that the higher derivative terms can be safely ignored, at least for the correction quadratic in the fields, and that the k^2 term will probably give a very good approximation to the true kinetic function $Z(\psi)$.

The quantities important in the companion paper [275] all rely upon the characteristics of the action curve demonstrated by Fig. 8.8, and in particular which action fulfils the criterion

$$\Gamma(T) = \min[\Gamma_{O(3)}(T), \Gamma_{O(4)}(T)] \ , \tag{8.58}$$

as this could drastically change the temperature at which the bubble nucleates and which region of thickness the bubble is in. We therefore also perform the check of calculating the $O(3)$ and $O(4)$ bubble actions for each temperature value and comparing the sizes, with one illustration of this seen in Fig. 8.10. The action obtained from the $O(3)$ bubble is consistently significantly lower than from the $O(4)$ bubble, and thus will dominate the calculation of the subsequent quantities.

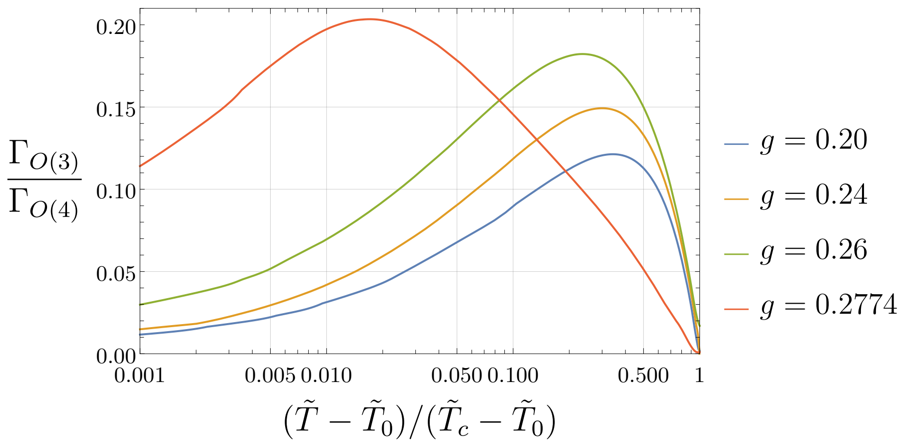

Figure 8.10: Graph of the ratio of $O(3)$ bubble action over $O(4)$ bubble action against the temperature T in units of the source Λ for triple-trace couplings $g = 0.20$, 0.24, 0.26, and 0.2774 (bottom-up on the left), with $\Lambda_f = 0$. All curves are for value $N = 1$.

4.1 Phase transitions in the early universe and large-N scaling

Much recent effort — including that of our companion paper [275] and previous paper [3] — has gone into modelling phase transitions in the early universe using holography, with the hope of finding models that lead to observable gravitational wave signals. In this context, it is important to understand the impact of the large-N limit that holography usually involves. As mentioned in Sec. 2.1, the (effective) action obtained from holography scales as $L^3/\kappa_5^2 \sim N^2$, meaning that in the strict large-N limit bubble nucleation will not occur as the bubble action becomes infinite. In practice we are of course interested in N values which are finite, while still being large enough to ignore finite-N corrections.

In cosmological applications, important quantities which are determined from the effective action include the nucleation temperature T_n, the transition strength α, and the transition rate β/H_n. The nucleation temperature is defined as the temperature at which bubble nucleation will occur (specifically when the nucleation rate per unit volume drops to one bubble per Hubble volume per Hubble time). Through energy considerations (see [275]) this is found to always occur at $\Gamma \approx 150$, and so changing the scale of the action by changing N will invariably alter the temperature at which bubbles are nucleated. We demonstrate this in Fig. 8.11 for various values of N up to $N = 8$, which is the value we take to produce results in the companion paper. ($N \approx 1$ is of course outside the plausible range of the large-N expansion; here we are mainly interested in visualising the impact of changing N on the cosmological parameters.)

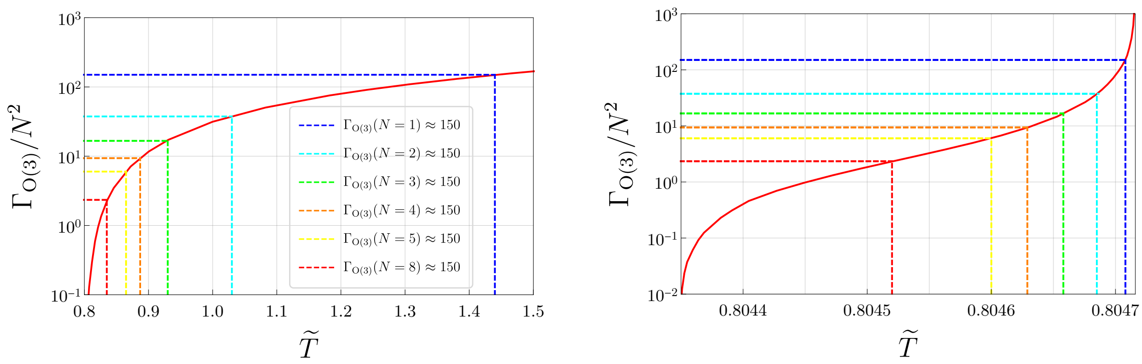

Figure 8.11: The solid red curves show a section of the graph of the $O(3)$ bubble action against the temperature $\widetilde{T}$ for $g = 0.27$ and $\Lambda_f = 0$ (left), and the complete graph for $g = 0.01$ and $\Lambda_f = 0$ (right). As N is increased, the point where the action equals 150, which sets the nucleation temperature, is pushed to the left. The legend applies for both plots.

It is very straightforward to numerically invert the action curve to find out how the nucleation temperature depends upon N. In Fig. 8.12 we show the nucleation temperature dependence upon N for the same two sets of parameters as in Fig. 8.11, demonstrating the change in shape as the N scaling progresses from near the thin-wall limit to the thick-wall limit. We note in particular that as $N \to \infty$, the nucleation temperature always approaches the lower critical temperature T_0, where the barrier between the vacua in the effective potential vanishes and the bubble action goes to zero.

The transition rate β/H_n can be expressed as

$$\frac{\beta}{H_n} = T\frac{d}{dT}\Gamma(\psi, T)\Big|_{T_\mathrm{n}} , \tag{8.59}$$

where H_n is the Hubble parameter evaluated at the nucleation temperature. As the

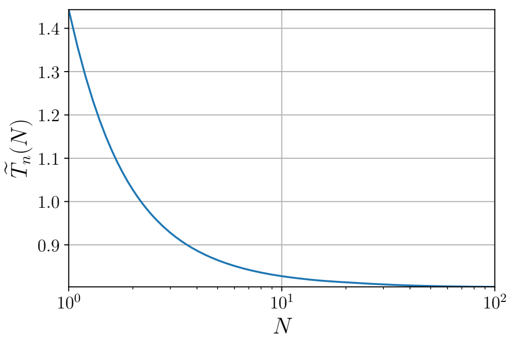

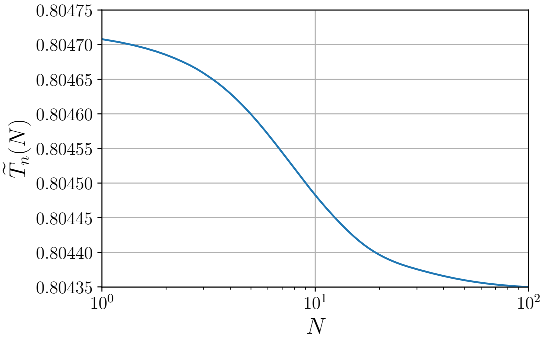

Figure 8.12: Graph of the nucleation temperature $\widetilde{T}_n$ against N for triple-trace coupling $g = 0.27$ and $\Lambda_f = 0$ (left), and $g = 0.01$ and $\Lambda_f = 0$ (right) showing the effect of N scaling.

transition rate actively involves a derivative with respect to Γ, the N^2 scaling of the holographic action has a substantial effect. For sufficiently large N, we have as already mentioned $T_\mathrm{n} \approx T_0$ placing us in the thick wall limit. We observe that the temperature dependence of the action in our model is well fitted by a power law near T_0,

$$\Gamma \sim N^2(T - T_0)^x \tag{8.60}$$

with $x > 0$. Using this and the fact that T_n occurs when $\Gamma \approx 150$, we get

$$N^2(T_\mathrm{n} - T_0)^x \sim 150 \; . \tag{8.61}$$

Then, using this in Eq. (9.6), we find

$$\frac{\beta}{H_n} \sim T_\mathrm{n} N^2 x \left(T_\mathrm{n} - T_0\right)^{x-1} \sim T_\mathrm{n} N^2 x (150 N^{-2})^{\frac{x-1}{x}} \sim 150^{\frac{x-1}{x}} T_\mathrm{n} x N^{2/x} \; , \tag{8.62}$$

implying that $\beta/H_\mathrm{n} \sim N^{2/x}$. Thus, for sufficiently large N, the transition rate diverges rendering the gravitational wave signal unobservable.

However, for more moderate values of N it is possible to instead sit close to the thin wall limit, $T_\mathrm{n} \approx T_\mathrm{c}$. The quadratic divergence in this limit, $\Gamma \sim N^2(T_\mathrm{c} - T)^{-2}$, then leads in a similar way to $\beta/H_\mathrm{n} \sim N^{-1}$, decreasing with N in accordance with lattice results for the surface tension [286].

The above analytic results for the N scaling in the thin and thick wall limit can be confirmed numerically, as shown in Fig. 8.13. On the left, we see that as the action at $\Gamma \approx 150$ for $N = 1$ begins close to the lower critical temperature T_0 for $g = 0.27$, it is dominated by the thick-wall N scaling result, always increasing the transition rate with N. For $g = 0.01$ on the right, however, we see that the action at $\Gamma \approx 150$ for $N = 1$ begins in the thin-wall regime close to T_c, with β/H_n decreasing as N increases slightly, then as

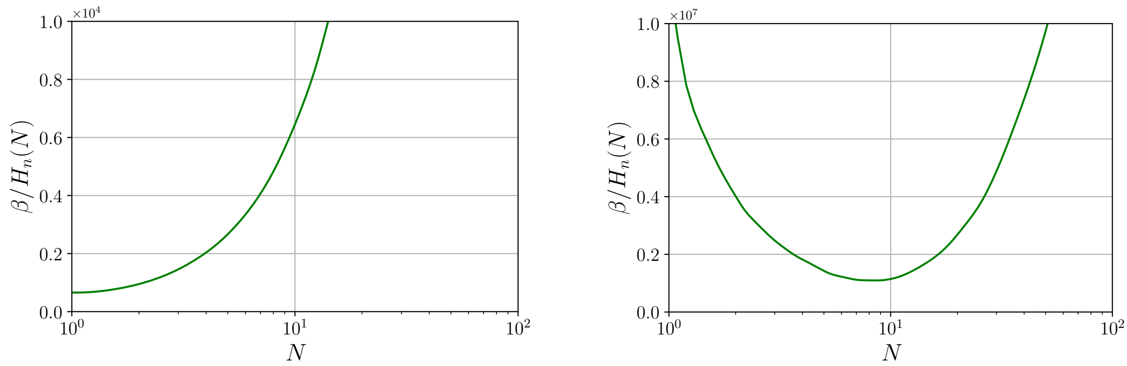

Figure 8.13: Graph of the transition rate β/H_{n} against N for triple-trace coupling $g = 0.27$ and $\Lambda_f = 0$ (left), and $g = 0.01$ and $\Lambda_f = 0$ (right) showing the effect of N scaling.

N increases further it transitions through the intermediate and then into the thick-wall regime where it again ends up dominating and increasing the transition rate. In this case there is an "optimal" $N \approx 8$ which minimises the transition rate (leading to easier to observe gravitational wave signals), while still potentially being large enough to avoid significant finite-N corrections.

4.2 Domain wall solutions

As a special case of the study of bubble nucleation, we can also consider the limit $T \to T_{\mathrm{c}}$, often referred to as the thin-wall limit since the bubble wall here becomes small compared to the overall size of the bubble. Precisely at $T = T_{\mathrm{c}}$ there is no bubble nucleation (as the bubble action diverges) but one can instead have coexistence of the two phases, separated by a domain wall with some particular surface tension. Determining the surface tension is interesting both since it can be related to the nucleation rate near T_{c} and since it determines properties of possible mixed phases. Domain walls in mixed phases have already been studied using dynamical solutions of the Einstein equations [225, 222, 226, 223, 224, 270] and with an effective action phenomenologically derived from a holographic model [276]. Here, we investigate the domain wall solutions using an effective action which is rigorously derived in a gradient expansion using the rules of holography.

The surface tension σ is calculated through the formula

$$\sigma = \int_{-\infty}^{\infty} dx \left(\frac{1}{2} Z(\phi(x)) \left(\nabla\phi(x)\right)^2 + V(\phi(x)) \right) , \tag{8.63}$$

which represents the surface tension of a domain wall extending along the $x = 0$ plane, with the domain wall field profile here being related to the bubble field profile through $\phi = \psi - \psi_h$ at T_{c}, where ψ_h is the value of the field at the high-T phase minimum. This

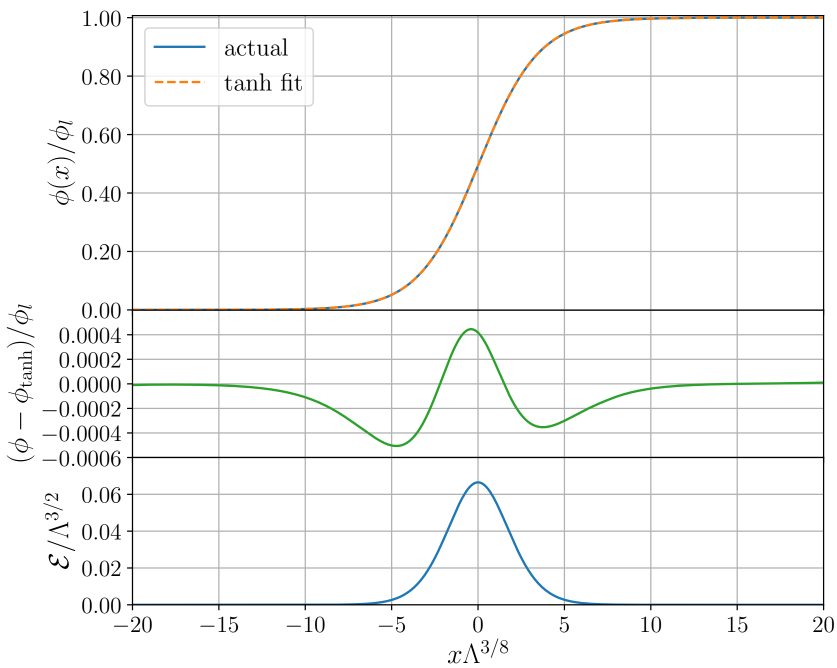

Figure 8.14: Profile of the difference between the field and its high-T phase minimum $\phi = \psi - \psi_h$ normalised by its maximum value ϕ_l, the thin-wall approximation to the profile, the difference between the two, and the energy of the profile for $g = 0.1, \Lambda_f = 0$. All curves are for value $N = 1$.

integral can be performed by finding the profile of the field $\phi(x)$ numerically through the equation of motion

$$\frac{d^2\phi}{dx^2} + \frac{1}{2}\frac{\partial_\phi Z(\phi)}{Z(\phi)}\left(\frac{d\phi}{dx}\right)^2 - \frac{\partial_\phi V(\phi)}{Z(\phi)} = 0\ . \tag{8.64}$$

We utilise $Mathematica's$ **FindRoot** function to first locate the extrema in our effective potential, and then the **NDSolveValue** function with the shooting method. We shoot from the local maximum to each of the minima, providing an initial guess of the derivative of the field at the local maximum and varying it until the solution reaches the minimum and stays there for a sufficient distance.

It is interesting to compare the resulting solution to a simple analytic approximate expression with Lagrangian $\mathcal{L} = \frac{1}{2}\left(\partial_\mu\phi\right)^2 - V(\phi)$, which is exact when the potential is an even quartic function. The domain wall solution to this then takes the form of a hyperbolic tangent [276],

$$\phi_{\mathrm{tanh}}(x) = \frac{\phi_b}{2}\left(1 + \tanh\left(\frac{x}{L_w} + \delta\right)\right)\ . \tag{8.65}$$

Here ϕ_b is the value of the field in the broken minimum, L_w is the thickness of the wall, and δ is a parameter allowing for a shift in the domain wall. Once we have the field profile from the numerical solver, we can use a fitting function such as $Python's$ **curve_fit** to find the values of L_w and δ which best approximate the actual solution.

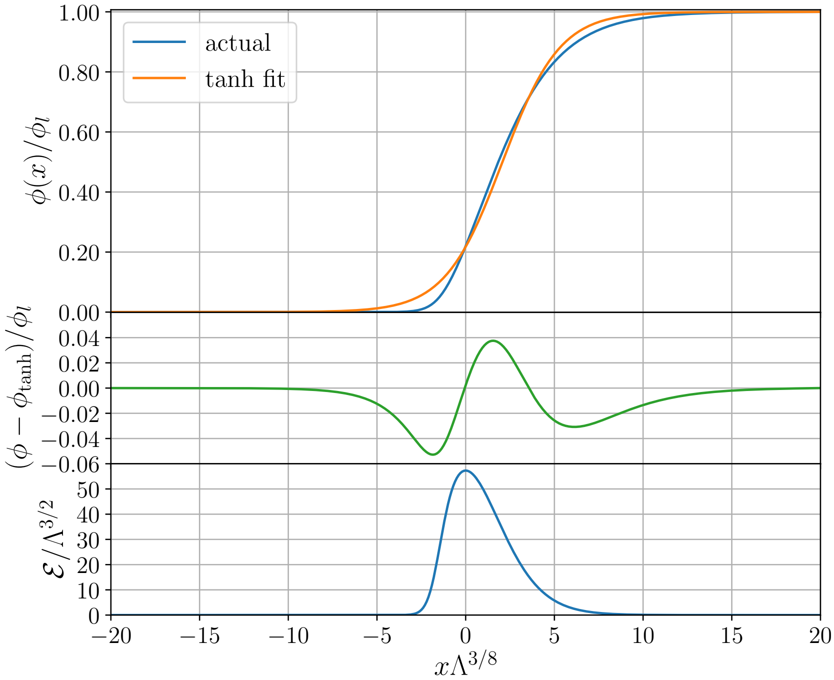

Figure 8.15: Field profile and thin-wall approximation, difference between the two, and energy of the profile for $g = 0.2774, \Lambda_f = 0$. All curves are for value $N = 1$.

In Fig. 8.14 we plot the analytic tanh-solution over the actual solution for parameter set $g = 0.1$, $\Lambda_f = 0$, along with the difference between the two solutions in the form of $(\phi(x) - \phi_{\tanh}(x))/\phi_l$ and the scaled energy density $\mathcal{E}$ in units of the source Λ, where the energy density is given through

$$\mathcal{E} = \frac{1}{2} Z(\phi(x)) \left(\nabla\phi(x)\right)^2 + V(\phi(x)) \ . \tag{8.66}$$

The effective potential for this parameter set has minima which are close together, and the curve between the minima is well-approximated by a quartic function, which is also seen in how closely the tanh approximation overlays the actual field profile. As is evident from the middle plot of Fig. 8.14, the difference between the approximate solution and the actual solution for the scalar field is never greater than 5×10^{-4}. The difference in energy density $\mathcal{E}$ between actual and tanh-fit is similarly good, never increasing past 3×10^{-3} (seen in Fig. 8.16).

In Fig. 8.15 however for parameter set $g = 0.2774$, $\Lambda_f = 0$, the minima of the effective potential are far away from each other, and the curve between the minima is not close to a simple quartic. Thus the tanh-fit performs significantly worse here; the differences between the actual and approximate solution are about 100 times larger than in the previous case.

Another interesting feature for this parameter set in Fig. 8.15 is how skewed the energy density is in the bottom plot. For domain walls taking a tanh-like form we see a nicely symmetric energy distribution like in Fig. 8.14, which again demonstrates how far the departure is from this approximation. This departure is greatly pronounced for $\mathcal{E}$, with the difference in results off by tens of percents (close to 30% difference where the effect is most noticeable). This is again about 100 times larger than in the previous case and is also seen in Fig. 8.16.

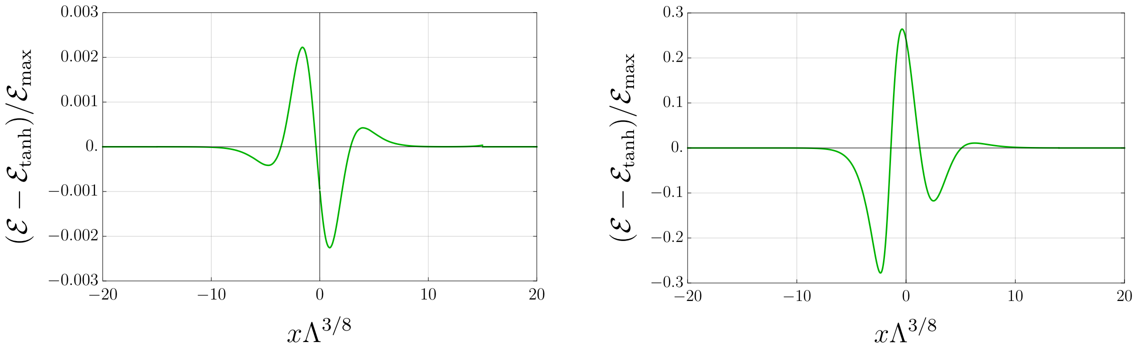

Figure 8.16: Plots of the difference between the actual energy density solution $\mathcal{E}$and the tanh approximation energy density solution $\mathcal{E}_{\text{tanh}}$ scaled by the maximum value of the actual energy density $\mathcal{E}_{\text{max}}$ for the cases $g = 1, \Lambda_f = 0$ on the left and $g = 0.2774, \Lambda_f = 0$ on the right. Both curves are for value $N = 1$.

Once we have found how the field behaves between the two minima, we can input it into eq. 8.63 to be able to calculate the surface tension. We produce a scan of this quantity in Fig. 8.17, with the surface tension in units of the source. Near the left hand boundary where g is small and the minima are close together we see that the surface tension is small, and goes explicitly to zero at the boundary. On the right hand side, however, where g is large and the minima are far away from one another the surface tension reaches values over 100. In this area of parameter sets, the values found effectively drop their dependences on Λ_f as the minima are so far apart that the difference is negligible. A note here is that although the surface tension will scale with N, it scales uniformly and so will not distort different parts of the parameter space in different ways.

5 Discussion and outlook

In this paper we discussed the computation of the quantum effective action in a strongly coupled theory using holographic duality. The effective action was computed in a derivative expansion, and we focused on extracting the effective potential and the (non-canonical)

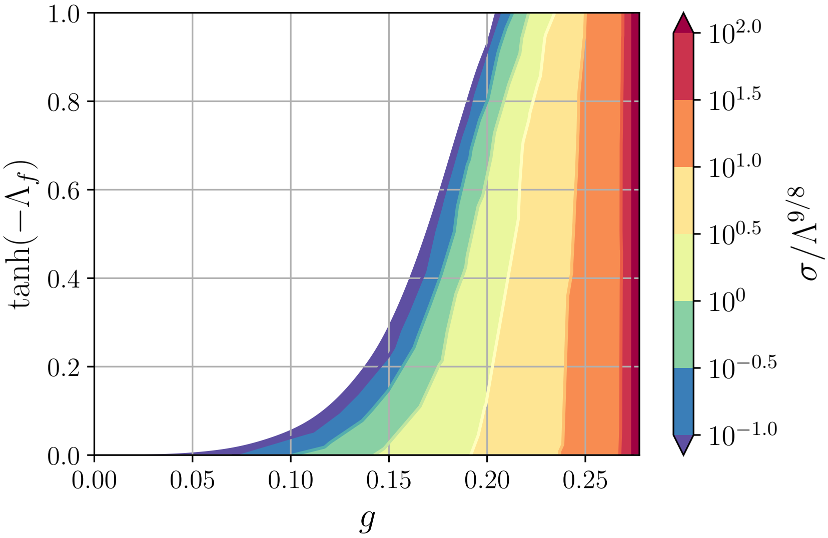

Figure 8.17: Scan of the domain wall surface tension σ in units of the source, with $N = 1$.

two-derivative kinetic term. Higher-derivative terms can in principle be included in a straightforward fashion; however, the number of possible terms grows quickly at higher order, and higher order correlation functions must be computed, requiring considerably more effort.

Our methods for constructing the effective action are general, applying to any holographic model. It is however interesting to note a possible complication. One of the ways to construct the effective potential was to integrate the source J with respect to the field ψ, implying that J should be a single-valued function of ψ. We know that there is a one-parameter family of solutions to the bulk theory, meaning that one can construct a curve in the (ψ, J) plane, but we know of no reason why the function $J(\psi)$ is guaranteed to be single-valued, as it happens to be in the simplified model.

As a concrete example of our approach we studied a simple bottom-up gravity theory, with a scalar field whose mass allows it to be identified with a dimension-4/3 operator in the dual field theory. Turning on a temperature and deforming the putative dual CFT by single-, double-, and triple-trace operators, we mapped out a surprisingly rich phase diagram.

Our main motivation for computing the effective action was to study first order phase transitions mediated by bubble nucleation. Thus we proceeded to find “bounce” solutions to the equations of motion obtained from the effective action, and studied their properties. An interesting application of this technology is to early-universe cosmology, where a first-order phase transition can give rise to potentially observable gravitational waves. Our companion paper [275] will discuss this in more detail, including the computation of all quasi-equilibrium gravitational wave parameters in our simple toy model.

Bubble nucleation is based on the idea of fluctuations, quantum or thermal, which allow the system to overcome the potential barrier between the false and true vacua. In the gravity dual, such fluctuations are suppressed by the large parameter L^3/κ_5^2. For a holographic theory to make an *observable* prediction in the case of gravitational waves signals (for example), it is thus vital to set this parameter (which is roughly dual to the degrees of freedom, or N^2 in a gauge theory) to some finite value. With this in mind, we briefly discussed the N-dependence of our results. The main takeaway is that, while indeed the transition rate always diverges for $L^3/\kappa_5^2 \sim N^2$ large enough, there can in general exist a range of N where the transition rate is somewhat *suppressed* compared with the naive extrapolation to $N = 1$.

As we elaborate on in more detail in the companion paper [275], the simple holographic model studied herein leads, for most of the parameter range, to large transition rates, implying difficult-to-observe gravitational wave signals. It would be interesting to explore more models in this way, and ideally isolate properties of the gravity dual leading to observable signals.

In addition to cosmological applications, the framework outlined here might also find uses in holographic models of nuclear physics at non-zero charge density [287, 288, 289]. Here, one would be concerned with, *e.g.*, the possible first order transition between the nuclear and chirally restored quark matter phases. If no other scalar condensation would occur in this transition, the order parameter would simply be the charge density, jumping from one non-zero value to another. The corresponding source would then be the chemical potential. However, since chiral symmetry will be restored, a careful implementation of holographic renormalisation is crucial when identifying the source and the expectation values of the dual operator, and therefore also in the computation of the effective action.

The chiral transition is particularly interesting in astrophysical contexts. For example, to address the question if the quark matter phase is realisable in stellar processes, one needs to know the relevant time scales of the phase conversion process. In addition to the pressure difference between the phases, a key ingredient setting the time scale is the surface tension [290], the computation of which we have also discussed here. Indeed, the surface tension is relevant for bubble nucleation of quark matter in supernovae [291, 292], neutron star mergers [293, 294, 295], and for a possible quark-hadron mixed phase in the interior of quiescent neutron stars [296, 297].

Ideally, as with the equation of state, the surface tension should be calculated from the underlying fundamental theory, QCD. The density regimes, where two available perturbative approaches, chiral effective theory and perturbative QCD, are valid are far apart such that at a possible first-order transition at least one of them, very likely both, cannot be trusted [298].

Previous estimates of the surface tension were either performed in the framework of chiral models that lack the nuclear matter ingredient or employed two different models for nuclear and quark matter, which are glued together at the phase transition, treating the surface tension as a free parameter [299]. We desire a self-consistent framework where both phases are available at once, (*e.g.*, [288]) and so can determine the surface tension by following standard computations [284, 285, 123] extended to the context of deconfinement phase transitions [300, 301]. One of the major goal of our program is to show how the quantum effective action is obtained using gauge/gravity duality and then predicting the surface tension and all other quasi-stationary parameters [275] at the deconfinement phase transition. This goal is achieved by extending our work to non-zero chemical potential.

D Boundary analysis and holographic renormalisation

It is convenient to define the function

$$k(r) \equiv r^2 e^{-\chi(r)} \left[r h'(r) - 2h(r) - 2rh(r)\chi'(r) \right] \ , \tag{8.67}$$

since it can be shown using the equations of motion that it is constant, $k'(r) = 0$. Evaluating this function on the horizon and on the AdS boundary gives the equality

$$r_H^3 e^{-\chi(r_H)} h'(r_H) = -4h_2 + \frac{128}{27}\phi_-\phi_+ \ , \tag{8.68}$$

where we have used the asymptotic solution (8.26). This can be rewritten in terms of the temperature and entropy density (8.27) as

$$h_2 = -\frac{\kappa_5^2 T s}{2} + \frac{32}{27}\phi_-\phi_+ \ . \tag{8.69}$$

Turning now to the gravity action (8.19), we can use the equations of motion to show that on-shell it can be written as a total derivative in the radial coordinate:

$$S_{bulk} \overset{on-shell}{\longrightarrow} \frac{1}{\kappa_5^2} \int d^4x \, dr \left[-\partial_r \left(\sqrt{g} \frac{h(r)}{r} \right) \right] = -\frac{1}{\kappa_5^2} \int d^4x \left[\sqrt{g} \frac{h(r)}{r} \right]_{r_H}^{r_\infty} \ . \tag{8.70}$$

Here we have integrated from the horizon r_H to some cutoff surface at a radius r_∞. As usual the on-shell action diverges as the cutoff is taken to infinity, requiring renormalisation through the addition of counter-terms defined on the cutoff surface. In the present case, these are

$$S_{CT} = \frac{1}{\kappa_5^2} \int d^4x \sqrt{\gamma} \left[c_0 + c_1 \phi(r) n^\mu \partial_\mu \phi(r) + c_2 \phi(r)^2 + c_3 \phi(r)^3 \right] \ , \tag{8.71}$$

where γ is the determinant of the induced metric γ_{ij} on the cutoff surface, and the c_i's are constants to be fixed shortly. Note that the cubic term only gives a finite contribution as the cutoff is taken to infinity. Terms of even higher order vanish at the boundary and are therefore not necessary to include. We also include a Gibbons-Hawking term

$$S_{GH} = \frac{1}{\kappa_5^2} \int d^4x \sqrt{\gamma} K \ , \tag{8.72}$$

where K is the trace of the extrinsic curvature K_{ij}.

The complete gravity action including boundary terms is then $S_C = S_{bulk} + S_{GH} + S_{CT}$. Requiring that S_C is finite as $r_\infty \to \infty$ imposes constraints on the counter-terms:

$$c_0 = -3 \qquad \text{and} \qquad c_2 = \frac{2}{3}(2c_1 - 1) \ . \tag{8.73}$$

The finite result for the complete action on-shell can then be written in terms of the constants of the near-boundary expansion as

$$S_C \xrightarrow{on-shell} \frac{\beta V_3}{\kappa_5^2} \left(-\frac{h_2}{2} + \left(\frac{28}{27} - \frac{4}{3} c_1 \right) \phi_- \phi_+ + c_3 \phi_-^3 \right) \ . \tag{8.74}$$

Here we have also carried out the integration in the Euclidean time direction, giving a factor of $\beta = 1/T$, and the three spatial directions, giving a formally infinite volume factor which we denote by V_3. If we instead vary our action — including the counter-terms — with respect to the scalar field ϕ, we find the following:

$$\delta_\phi S_C = \frac{1}{\kappa_5^2} \int d^4x \left\{ -\frac{4}{3} c_1 \phi_- \, \delta\phi_+ + \left(\frac{4}{3}(1 - c_1)\phi_+ + 3 c_3 \phi_-^2 \right) \delta\phi_- \right\} \ . \tag{8.75}$$

This variation should vanish on solutions, but there are several possible ways to make that happen.

D.1 Standard quantisation

In the standard case, the leading falloff ϕ_- is fixed. With this choice, the dual CFT has a dimension 8/3 (single trace) operator Ψ. A geometry with boundary condition $\phi_- = 0$ is dual to an undeformed state of this CFT, and a geometry obeying $\phi_- = \Lambda$ is dual to a state of the deformed CFT $S_{CFT} \to S_{CFT} + \Lambda\Psi$.

Fixing ϕ_- means $\delta\phi_- = 0$. To make the variation of the action above vanish on solutions, we are forced to set $c_1 = 0$. The expectation value of the dual operator is then given by

$$\kappa_5^2 \frac{\delta_\phi S_C}{\delta \phi_-} = \frac{4}{3}\phi_+ + 3c_3\phi_-^2 \ . \tag{8.76}$$

Note that the constant c_3 of the finite counter-term is still unfixed, and that the expectation value depends on it. The on-shell action becomes

$$S_C \overset{on-shell}{\longrightarrow} \frac{\beta V_3}{\kappa_5^2}\left(-\frac{h_2}{2} + \frac{28}{27}\phi_-\phi_+ + c_3\phi_-^3\right) \ . \tag{8.77}$$

D.2 Alternate quantisation

In the mass range (8.16), one can instead choose to fix the sub-leading falloff ϕ_+ — this is the choice we are mainly interested in, since it also allows for multitrace deformations. With this choice, the dual CFT has a dimension 4/3 single trace operator Ψ. A geometry with boundary condition $\phi_+ = 0$ is dual to an undeformed state of this CFT, and a geometry obeying $\phi_+ = \Lambda$ is dual to a state of the deformed CFT $S_{CFT} \to S_{CFT} + \Lambda\Psi$.

Fixing ϕ_+ means $\delta\phi_+ = 0$. To make the variation of the action vanish on solutions, we are then forced to set $c_1 = 1$ and $c_3 = 0$. Then the expectation value of the dual operator is given by

$$\psi \equiv \kappa_5^2 \frac{\delta_\phi S_C}{\delta\phi_+} = -\frac{4}{3}\phi_- \ . \tag{8.78}$$

The on-shell action becomes

$$S_C \overset{on-shell}{\longrightarrow} \frac{\beta V_3}{\kappa_5^2}\left(-\frac{h_2}{2} - \frac{8}{27}\phi_-\phi_+\right) \ . \tag{8.79}$$

D.3 Double and triple trace deformation

We now consider deforming the alternate quantisation CFT by a double-trace and a triple-trace deformation. This requires the addition of a new, non-covariant counter-term to the action. We thus define the full action to be $S_C = S_{bulk} + S_{GH} + S_{CT} + S_W$, with

$$S_W = \frac{1}{\kappa_5^2}\int d^4x\sqrt{g}\left[\psi\, W'(\psi) - W(\psi)\right] \ , \tag{8.80}$$

and ψ given by (8.78). As in the previous subsection, we set $c_1 = 1$. The on-shell action becomes

$$S_C \overset{on-shell}{\longrightarrow} \frac{\beta V_3}{\kappa_5^2}\left(-\frac{h_2}{2} - \frac{8}{27}\phi_-\phi_+ + c_3\phi_-^3 + \psi\, W'(\psi) - W(\psi)\right) \ . \tag{8.81}$$

and its variation is

$$\begin{aligned}\delta_\phi S_C &= \frac{1}{\kappa_5^2}\int d^4x \left\{-\frac{4}{3}\phi_-\,\delta\phi_+ + 3c_3\phi_-^2\delta\phi_- + \frac{16}{9}\phi_-\,W''(\psi)\delta\phi_-\right\} \\ &= \frac{1}{\kappa_5^2}\int d^4x \left\{-\frac{4}{3}\phi_-\delta\left(\phi_+ - \frac{9}{8}c_3\phi_-^2 + W'(\psi)\right)\right\}\ .\end{aligned} \tag{8.82}$$

We can see that in this setup, the constant c_3 simply shifts the cubic term in W, so we will set $c_3 = 0$ and instead let

$$W(\psi) = \frac{f}{2}\psi^2 + \frac{g}{3}\psi^3 \tag{8.83}$$

giving

$$S_C \overset{on-shell}{\longrightarrow} \frac{\beta V_3}{\kappa_5^2}\left(-\frac{h_2}{2} - \frac{8}{27}\phi_-\phi_+ + \frac{8}{9}f\phi_-^2 - \frac{128}{81}g\phi_-^3\right) \tag{8.84}$$

and

$$\delta_\phi S_C = \frac{1}{\kappa_5^2}\int d^4x \left\{-\frac{4}{3}\phi_-\delta\left(\phi_+ - \frac{4}{3}f\phi_- + \frac{16}{9}g\phi_-^2\right)\right\}\ . \tag{8.85}$$

The variation now vanishes on solutions with the boundary condition

$$\phi_+ - \frac{4}{3}f\phi_- + \frac{16}{9}g\phi_-^2 = J \tag{8.86}$$

with J a constant. This very general boundary condition allows for a single-, double-, and triple-trace deformation of the original CFT.

The field theory generating functional $\mathcal{W}[J]$ is equal to the gravitational on-shell action. For uniform fields and sources, we define $w(J) \equiv \kappa_5^2\mathcal{W}[J]/(\beta V_3)$; then we can write

$$w(J) = -\frac{h_2(J)}{2} - \frac{8}{27}\phi_-(J)\,J + \frac{40}{81}f\phi_-^2(J) - \frac{256}{243}g\phi_-^3(J)\ . \tag{8.87}$$

Here we have used (8.86), and we emphasize that in this expression, h_2 and ϕ_- should be regarded as functions of J, which we need to solve the full gravitational equations of motion to determine.

To get an expression for the effective potential, we substitute (8.78), (8.86), and (8.87) into (8.29), giving

$$V(\psi) = -w(J) + \psi J = \frac{h_2(\psi)}{2} + \frac{7}{9}\phi_+(\psi)\,\psi + \frac{f}{2}\psi^2 + \frac{g}{3}\psi^3\ . \tag{8.88}$$

Note that all the non-trivial information contained within the coefficients h_2 and ϕ_+, which as we indicate should now be regarded as functions of $\psi = -\frac{4}{3}\phi_-$; these must be extracted from numerical solutions. Meanwhile, the multi-trace deformations give simple polynomial contributions. We can furthermore include also the possibility of a single-trace deformation $\Lambda\Psi$ by shifting $J \to J - \Lambda$ in (8.86) before substituting it into (8.29), giving

$$V(\psi) = \frac{h_2(\psi)}{2} + \frac{7}{9}\phi_+(\psi)\,\psi + \Lambda\psi + \frac{f}{2}\psi^2 + \frac{g}{3}\psi^3\ . \tag{8.89}$$

E Exact result for the effective potential at large temperatures

As explained in Sec. 2, the second derivative of the effective action gives the inverse of the two-point function. In the gravitational bulk, two-point functions can be computed by a fluctuation analysis. For our particular holographic model, we derived (8.52), which we reproduce here:

$$\Gamma_2 = -\left(\frac{3}{4}\frac{Z_\phi^{+(0)}}{Z_\phi^{-(0)}} + W''(v)\right) + \frac{3}{4}\frac{Z_\phi^{-(2)}Z_\phi^{+(0)} - Z_\phi^{-(0)}Z_\phi^{+(2)}}{\left(Z_\phi^{-(0)}\right)^2}k^2 + \dots \, . \tag{8.90}$$

Here, the first term of order k^0 should equal the second derivative of the effective potential.

In general we can only determine these terms numerically. However, in the limit of small field values — or equivalently, large temperatures — the background approaches pure AdS-Schwarzschild, where it is possible to find an analytic solution. In this background, the two gauge invariant modes in (8.42) decouple, and the equation for $Z_\phi(r)$ with $k = 0$ takes the form

$$Z_\phi^{(0)\prime\prime}(z) - \frac{3+z^4}{z-z^5}Z_\phi^{(0)\prime}(z) + \frac{32}{9}\frac{Z_\phi^{(0)}(z)}{z^2-z^6} = 0 \, , \tag{8.91}$$

where we have switched to the radial coordinate $z = r_H/r$. This can be solved in terms of hypergeometric functions as

$$Z_\phi^{(0)}(z) = c_1 z^{4/3}\, {}_2F_1\left[1/3, 1/3, 2/3, z^4\right] + c_2 z^{8/3}\, {}_2F_1\left[2/3, 2/3, 4/3, z^4\right] \, . \tag{8.92}$$

Regularity on the horizon $z = 1$ imposes

$$\frac{c_2}{c_1} = -\frac{\Gamma(2/3)^3}{\Gamma(1/3)^2\,\Gamma(4/3)} \, . \tag{8.93}$$

Expanding the result near the AdS boundary at $z = 0$, we then find

$$\frac{Z_\phi^{+(0)}}{Z_\phi^{-(0)}} = -\frac{\pi^{3/2} r_H^{4/3}}{18\Gamma(7/6)^3} \, . \tag{8.94}$$

Plugging into (8.90) and expressing the result in units of temperature, where for AdS-Schwarzschild $T = r_H/\pi$, this provides the coefficient V_2 in the small-field (or high-T) expansion of the effective potential (8.32). The result is

$$V_2 = \frac{9\pi^{17/6}}{\Gamma(1/6)^3} \, , \tag{8.95}$$

which is what we quote in (8.34). This also agrees with the analysis in [283].

F Gauge invariant fluctuation equations

The gauge invariant modes introduced in (8.42) satisfy the two coupled linear second order differential equations,

$$Z_\phi''(r) + AZ_\phi'(r) + BZ_H'(r) + CZ_\phi(r) + DZ_H(r) = 0 \tag{8.96}$$

$$Z_H''(r) + EZ_H'(r) + FZ_\phi'(r) + GZ_H(r) + HZ_\phi(r) = 0 \; , \tag{8.97}$$

with

$$A = \frac{1}{r} - \frac{r\mathcal{P}(\phi)}{3h(r)} \tag{8.98}$$

$$B = \frac{e^{2\chi(r)} r\left(3\mathcal{P}'(\phi) + 2r\mathcal{P}(\phi)\phi'(r)\right)}{h(r)\theta(r)} \tag{8.99}$$

$$C = -\frac{4r^2\phi'(r)^2\mathcal{P}(\phi)}{\theta(r)} - \frac{6r\phi'(r)\mathcal{P}'(\phi)}{\theta(r)} - \frac{k^2}{r^2h(r)} - \frac{r\phi'(r)\mathcal{P}'(\phi) + 3r^2\mathcal{P}''(\phi)}{3h(r)} \tag{8.100}$$

$$D = \frac{r^2e^{2\chi(r)}\left(3\mathcal{P}'(\phi) + 2r\mathcal{P}(\phi)\phi'(r)\right)\left(\mathcal{P}(\phi) - h(r)\phi'(r)^2\right)}{6h(r)^2\,\theta(r)} \tag{8.101}$$

$$E = \frac{r\mathcal{P}(\phi)}{3}\left(\frac{36}{\theta(r)} - \frac{1}{h(r)}\right) - \frac{2}{3}r\phi'(r)^2 + \frac{5}{r} \tag{8.102}$$

$$F = 0 \tag{8.103}$$

$$G = -\frac{9k^2 + r^4\mathcal{P}(\phi)\phi'(r)^2}{9r^2h(r)} + \frac{12\mathcal{P}(\phi)}{\theta(r)} + \frac{4}{r^2} + \frac{r^2\phi'(r)^4}{9} - \frac{4}{3}\phi'(r)^2 \tag{8.104}$$

$$H = \frac{e^{-2\chi(r)}}{9h(r)\theta(r)}\left(\theta(r) - 18h(r)\right)\left(12rh(r)\mathcal{P}(\phi)\phi'(r) + \theta(r)\mathcal{P}'(\phi)\right) \; , \tag{8.105}$$

and where we defined

$$\theta(r) \equiv h(r)\left(r^2\phi'(r)^2 + 6\right) - r^2\mathcal{P}(\phi) \; . \tag{8.106}$$

Chapter 9

Paper III: Gravitational Waves at Strong Coupling from an Effective Action

Abstract

Using a holographic derivation of a quantum effective action for a scalar operator at strong coupling, we compute quasi-equilibrium parameters relevant for the gravitational wave signal from a first order phase transition in a simple dual model. We discuss how the parameters of the phase transition vary with the effective number of degrees of freedom of the dual field theory. Our model can produce an observable signal at LISA if the critical temperature is around a TeV, in a parameter region where the field theory has an approximate conformal symmetry.

1 Introduction

A first order phase transition in the early Universe [284, 187, 233, 123] would generate gravitational waves (GWs) [230, 104]. If the critical temperature of the transition were around the electroweak scale 0.1 − 1 TeV, the GWs would be potentially observable at future space-based detectors, such as the Laser Interferometer Space Antenna (LISA) [302, 2], while a critical temperature around the scale of confinement of the strong interaction (100 MeV) is of interest for pulsar timing arrays. Recent reports of a possible signal at NANOgrav [303], which if confirmed would likely be from merging supermassive black holes [304], have also prompted an examination of phase transitions as a source [305].

In the Standard Model it is well established that both the confinement and electroweak transitions are crossovers [1, 10, 306, 307]. However, the Standard Model is incomplete: for example, it does not account for the dark matter in the Universe or the baryon asymmetry (see e.g. [308] for a pedagogical review). Numerous extensions have been put forward to solve these and other problems, which would also induce a first order electroweak transition (see e.g. [309, 2] for reviews). Hence a search for GWs from the early Universe is also a search for physics beyond the Standard Model.

A first order phase transition in the early Universe would proceed through the nucleation, expansion and merger of bubbles of the stable phase [310, 233, 311, 107], (see [312, 188] for pedagogical reviews). The consequent disturbances in the cosmic fluid would produce GWs [230, 104]. Much progress has been made recently towards an accurate understanding of the process [2], with the aim of enabling LISA to probe the physics of an era that is difficult to explore otherwise.

However, if the phase transition occurs at strong coupling, we are confronted by the difficulty of computing thermodynamic and transport properties. In this letter, we present a consistent strong-coupling framework for the calculation of the quasi-equilibrium properties most relevant for GW production, and illustrate its use with a simple model.

The GW signal from a first order phase transition depends on four main parameters: the nucleation temperature T_{n}, the transition rate β, the dimensionless transition strength parameter α, and the wall (phase boundary) speed v_{w}. The speed of sound also affects the signal [313, 314]. The critical temperature of the phase transition T_{c} sets the scale. These parameters control the conversion of energy into fluid motion and are directly connected to the detailed shape of the GW power spectrum [114, 315], through which they are accessible at LISA [316]. Hence their calculation is of utmost importance to the drive to use GW detectors to probe high energy physics.

At weak coupling perturbative methods can give good results for the quasi-equilibrium parameters T_n, β, and α (for recent discussion of the calculations and their uncertainties see [317, 318, 273]). In general, v_w is a fully non-equilibrium quantity that has been computed only in various approximations [234, 125, 319, 320, 235, 321, 322, 323]. If, however, the extension to the Standard Model is a strongly coupled field theory the parameters are much more difficult to calculate. Historically, lattice methods have been used for the strictly equilibrium quantities in specific theories, the critical temperature and the latent heat: for example, it is known that SU(N) Yang-Mills theory, where N is the number of colours or independent charges, has a first order confinement transition for $N \geq 3$ (see e.g. [324]). GW production in such theories has been studied in [325, 266]. The functional renormalisation group has recently been used for GW production in a scalar field theory at strong coupling [326].

In recent years, holography has proved a powerful tool to rework the problem, equating field theories with string theories in a larger number of dimensions [133, 156]. Quantities in a field theory with a large number of degrees of freedom at strong coupling are computable from classical solutions in the string theory, which are essentially solutions to Einstein equations with various fields as sources of energy-momentum. Using holography, thermodynamic properties of phase transitions have been studied in so-called “bottom-up” models (where the source fields are not formally derived from a string theory) [327, 247, 229], and GWs have been considered in the context of neutron star mergers [328, 329, 288] and phase transitions in the early Universe [3]. Recently there has also been progress in finding the wall speed [270, 271, 272].

In this letter, we outline a new method for calculating the quasi-equilibrium parameters α, β, and $T_\mathrm{n}/T_\mathrm{c}$. The method uses a quantum effective action, which we show that it can be derived using holography, giving full details in [330]. With it we construct bubble solutions taking the system to the stable phase directly in the field theory, avoiding the need to solve partial differentials in the gravity dual. The computed quantities are then used to determine the corresponding signals using current models of GW production [2]. The scaling of the results with N in the putative gauge theory is discussed and scans for all quantities are shown for $N = 8$, where the holographic assumption of large N should still be valid. Here we define N from $L^3/\kappa_5^2 = N^2$, where κ_5^2 is the 5D gravitational constant and L the radius of curvature.

We find that the large N restriction generically pushes β/H_n (where H_n is the nucleation Hubble rate) to high values; $10^3 - 10^8$ in this particular model for $N = 8$, with the vast majority of values above 10^5. This restricts a detectable GW signal to a corner of parameter space where the minima in the effective potential are far apart and breaking of conformal invariance in the trivial vacuum is $1/N$ suppressed. In this region, a phase transition with critical temperature around 1 TeV would be observable, which is around the scale where one would expect physics beyond the Standard Model to appear.

2 Effective action from holography

We start with a free scalar field ϕ in five dimensions with action

$$S_{\text{bulk}} = \frac{1}{2\kappa_5^2}\int d^5x\sqrt{g}\left(\mathcal{R} + \frac{12}{L^2} - (\partial\phi)^2 - m^2\phi^2\right) \tag{9.1}$$

where $\mathcal{R}$ is the Ricci scalar and m the mass parameter. We will set $L = 1$ hereafter. We are interested in homogeneous, isotropic solutions that are asymptotically AdS$_5$ with a black brane in the interior; a suitable ansatz is

$$ds^2 = -e^{-2\chi(r)}h(r)dt^2 + \frac{dr^2}{h(r)} + r^2 d\vec{x}^2 \ , \quad \phi = \phi(r) \ . \tag{9.2}$$

Such a black brane solution is dual to a field theory state with temperature $T = e^{-\chi(r_H)}h'(r_H)/4\pi$ and entropy density $s = 2\pi r_H^3/\kappa_5^2$, both evaluated at the horizon radius r_H of the black brane, where $h(r_H) = 0$. Fixing T, one finds a one-parameter family of solutions. At the boundary $r \to \infty$, the scalar field falls off as $\phi \sim \phi_-/r^{\Delta_-} + \phi_+/r^{\Delta_+}$, where $\Delta_\pm = 2 \pm \sqrt{4+m^2}$. The one-parameter family of solutions determines ϕ_+ as a function of ϕ_-; this can be related to the generating functional of a conformal field theory (CFT) in Minkowski space, defined on the boundary $r \to \infty$.

We will use here "alternative quantisation" in which ϕ_+ determines the source of a field operator Ψ of the CFT, and ϕ_- is related to the expectation value $\langle\Psi\rangle$ [331]. Choosing this quantisation allows us to deform the CFT by the operators Ψ, Ψ^2, and Ψ^3, with couplings Λ, f, and g, respectively. The deformations, which are implemented through the choice of boundary conditions at $r \to \infty$ [282], result in a theory with first order thermal phase transitions for suitable parameters. We take the cubic term to be exactly marginal (scaling dimension 4) which amounts to choosing $m^2 = -32/9$ in (9.1). Thus the scaling dimensions for Λ and f are $8/3$ and $4/3$, respectively.

We therefore have three scales T, Λ, and f which are assembled into two dimensionless ratios, chosen to be $\Lambda_f = \Lambda/f^2$ and $\widetilde{T} = T/(|\Lambda|^{3/8} + |f|^{3/4})$. The overall scale is a free parameter at this simplified level.

The boundary field theory effective action at T is defined as a functional of field expectation value ψ through

$$\Gamma_T[\psi] = W_T[J] - N^2 \int d^4x\, \psi J \ , \tag{9.3}$$

with $W_T[J]$ being the generating functional in the presence of a source J, and the factor of N^2 appearing due to the definition $\psi = W'_T[J]/N^2$. For static configurations, the first two terms in the derivative expansion are

$$\Gamma_T[\psi] = -N^2 \int d^4x \left(V_T(\psi) + \frac{1}{2} Z_T(\psi)(\nabla\psi)^2 \right) \ , \tag{9.4}$$

where $V_T(\psi)$ is the effective potential. By using the holographic equivalence of the renormalised on-shell gravitational action with the generating functional [277, 283, 280], and assuming homogeneous solutions, one can find the effective potential [330], giving

$$V_T(\psi) = \frac{h_2(\psi,T)}{2} + \frac{7}{9}\psi\,\phi_+(\psi,T) + \Lambda\psi + \frac{f}{2}\psi^2 + \frac{g}{3}\psi^3 \ . \tag{9.5}$$

Here h_2 comes from the boundary fall-off of the metric function $h \sim r^2 + 4\phi_-^2/9r^{2/3} + h_2/r^2$, and $\psi = -\frac{4}{3}\phi_-$.

To extract the coefficient of the kinetic term $Z_T(\psi)$ we note that the full quadratic part of $\Gamma_T[\psi]$ equals the inverse of the two-point function of Ψ. In momentum space, $Z_T(\psi)$ is then given by the coefficient of the k^2 term in a low-momentum expansion of the inverse of the two-point function. On the holographic side this can be computed by a standard fluctuation analysis [332]. For our solutions, the k^4 term is negligible [330], validating the derivative expansion.

Fixing the theory means fixing Λ_f and g; here we restrict to the region $-\infty < \Lambda_f \leq 0$ and $0 \leq g < \gamma_3 \approx 0.278$ ($g > \gamma_3$ renders the potential unbounded from below). In a large part of this, shown in colour in the figures below, the theory displays a first order thermal phase transition.

3 Gravitational wave parameters

We can use the flat-space field theory we have constructed to study phase transitions in the early Universe, as relaxation rates at temperature T are expected to be much faster than the Hubble rate $H(T)$. The phase transition proceeds through localised fluctuations of ψ into the stable phase, just large enough so that the pressure difference overcomes the surface tension. The most probable fluctuation, the critical bubble, is in the form of a bubble with a spatial O(3) symmetry, invariant in the periodic imaginary time coordinate

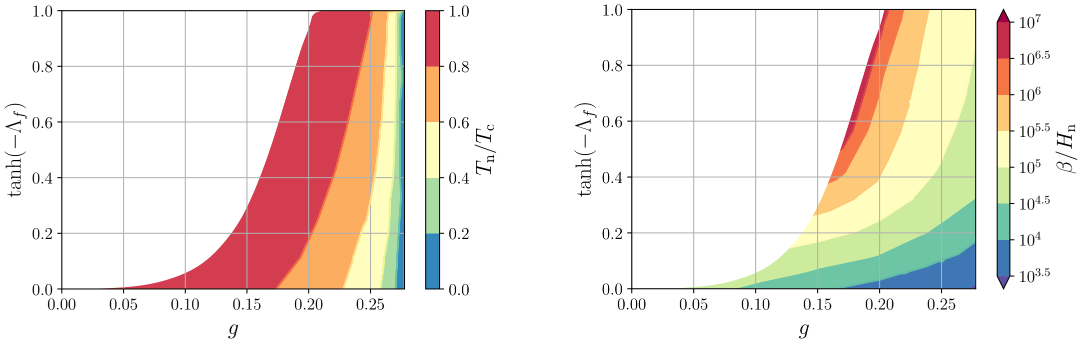

Figure 9.1: Scans of the nucleation temperature $T_{\mathrm{n}}/T_{\mathrm{c}}$ (left) and the transition rate β/H_{n} at T_{n} (right).

[123]. The rate per unit volume of bubble nucleation $p(t)$ increases rapidly from zero below T_{n}, a change quantified by the transition rate parameter $\beta = -d\log(p)/dt$. To a good approximation it can be written $p(t) = p_0 \exp(-\Gamma_b(T))$, where Γ_b is the Euclidean action for the critical bubble, whose time dependence is a consequence of the non-zero cooling rate in the expanding Universe. The transition rate parameter is evaluated at T_{n}, the peak of the globally-averaged bubble nucleation rate per unit volume. Hence, given that the temperature decreases as $dT/dt = -H(T)T$,

$$\beta/H_{\mathrm{n}} = T\frac{d}{dT}\Gamma_b(T)\Big|_{T_{\mathrm{n}}} . \tag{9.6}$$

To find the critical bubble, we extremise the O(3)-symmetric action

$$\Gamma_{\mathrm{O(3)}} = \frac{4\pi N^2}{T}\int d\rho\, \rho^2 \left(\frac{1}{2}Z_T(\psi)\left(\psi'\right)^2 + V_T(\psi)\right) , \tag{9.7}$$

looking for solutions representing a bubble of stable phase surrounded by metastable phase. We solve numerically the resulting Euler-Lagrange equation with boundary conditions $\psi(\infty) = 0 = \psi'(0)$, where the field is defined to vanish at the metastable minimum, and $\psi(0)$ is the shooting parameter. The asymptotic boundary condition is imposed at a suitably large finite radius, which we take to be $20(|\Lambda|^{3/8} + |f|^{3/4})$.

The phase transition can be thought to start when the nucleation rate per unit volume reaches one bubble per Hubble volume per Hubble time, that is, $p = H^4$. The nucleation temperature is reached shortly after, so an approximation to T_{n} can be found through $\Gamma_b(T_{\mathrm{n}}) \sim 4\,\log\left(M_{\mathrm{P}}/T_{\mathrm{c}}\right)$. Hence, for $T_{\mathrm{c}} \approx 100$ GeV, bubble nucleation occurs when the action drops to about 150 [311].

To understand how the results depend on N, note that the bubble action Γ_b is generally a monotonic function of temperature below T_{c}. The action diverges quadratically [311] at T_{c} and goes to zero at some lower temperature T_0 where the effective potential barrier

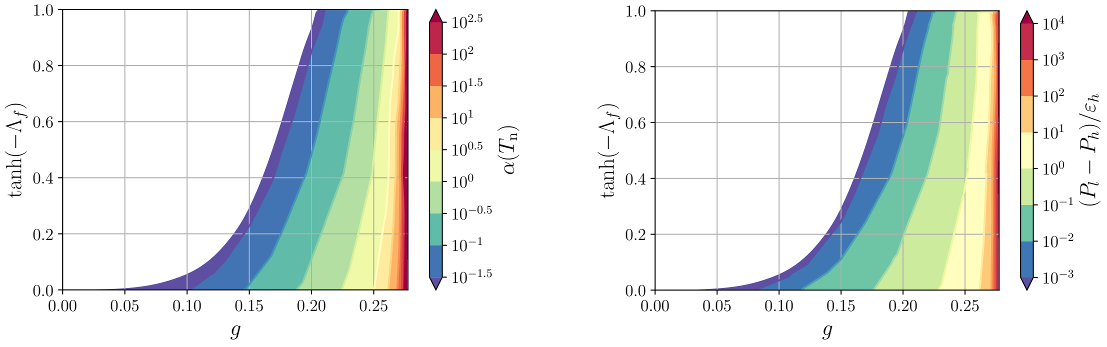

Figure 9.2: Scan of the transition strength α (left) and pressure change over energy density at T_n (right).

between the vacua vanishes. As the pre-factor of the action scales as N^2, sufficiently large N will push T_n down towards T_0. We call this the large supercooling case. We assume that the temperature dependence near T_0 is a power law $\Gamma_b \sim N^2(T - T_0)^x$ with $x > 0$, the form followed by theories with a canonical kinetic term and a quartic potential, where $x = 3/2$ [311]. Fitting a similar power law to our data, we find a value of $x \approx 1.4 - 1.5$. Eq. (9.6) and the definition of T_n then quickly lead to $\beta/H_\mathrm{n} \sim N^{2/x}$. Thus, for large N, β/H_n increases with N.

In practice, we are interested in finite but large N. Then, it is possible that instead $T_\mathrm{n} \approx T_\mathrm{c}$. In this small supercooling case, one can approximate the solution as a so-called "thin wall" bubble, consisting of a large ball of the stable phase surrounded by a spherical phase boundary, thin compared with its radius. In this case $\Gamma_b \sim N^2(T_\mathrm{c} - T)^{-2}$,[1] which leads to $\beta/H_\mathrm{n} \sim N^{-1}$, decreasing with N. Thus there can exist models with an "optimal" value of N which minimises β/H_n while still being large enough for the large-N limit to give accurate results at leading order. In fact, for certain parameter values this is the case for our holographic model; however, despite this the β/H_n values remain large. The full range of β/H_n for our parameter space is displayed in Fig. 9.1 on the right, along with the ratio $T_\mathrm{n}/T_\mathrm{c}$ in the left plot. The small supercooling limit $T_\mathrm{n} \approx T_\mathrm{c}$ is approached at the left-most boundary for both plots.

The energy available for conversion into fluid motion is quantified by the transition strength α, which depends on the enthalpy density $w = Ts$ and the pressure P in the two phases. Writing $\theta = w/4 - P$, the transition strength parameter is then defined as

[1] Note that our considerations imply that the surface tension of the phase boundary is proportional to N^2, consistent with lattice results in SU(N) gauge theories [286, 333, 324]. However, lattice results also permit models with a different N-dependence [266, 267].

[334, 315]

$$\alpha = \frac{4}{3}\frac{\theta_h(T) - \theta_l(T)}{w_h(T)}\bigg|_{T_\mathrm{n}} , \tag{9.8}$$

where subscripts h and l denote the phases stable at high and low temperatures, respectively.

The enthalpy density can be found from the solution to the gravity dual, $\kappa_5^2 Ts = -2h_2 - \frac{16}{9}\phi_+\psi$, and the pressure is available from V_T evaluated at its minima. The values for α are shown in the left plot of Fig. 9.2.

The N dependence of α in cases of small and large supercooling follows from linear expansion of α near a reference temperature T_*, $\alpha(T_\mathrm{n}) = \alpha(T_*) + \alpha'(T_*)(T_\mathrm{n} - T_*)$, where T_* is either T_c or T_0. The values $\alpha(T_*)$, being ratios, are independent of N. However, the next term grows with N in the small supercooling case, and decreases as $N^{-2/x}$ in the large supercooling case.

We do not yet have a simple way to calculate the bubble wall velocity v_w. To estimate the wall speed, we adapt a result from [270, 271, 272] that at small velocities, v_w is proportional to the pressure difference divided by the high-T phase energy density at T_n. To extrapolate to larger velocities, we assume

$$u_\mathrm{w} = \gamma_\mathrm{w} v_\mathrm{w} = C\,\frac{P_l - P_h}{\varepsilon_h}\bigg|_{T_\mathrm{n}} , \tag{9.9}$$

where C is an O(1) constant and γ_w is the Lorentz factor. The pressure difference divided by the energy density is shown in the right plot of Fig. 9.2; to estimate the wall speed we set $C = 1$. It is not important to get a precise value for u_w at high γ_w, as the hydrodynamic solution for the flow set up by the expanding bubble, and hence the GW signal, depends only on v_w. The same argument for N scaling can be made for u_w as can be made for α.

Finally, collating the information gained on α, β/H_n, T_n, and v_w we calculate the maximum of the GW power spectrum $\Omega_{\mathrm{gw},0}$, and the frequency at which it occurs in units of T_c. We use the standard LISA Cosmology Working Group model [2], improved with a numerical kinetic energy suppression factor [335], as described in [3]. We take $c_s^2 = 1/3$, as in the region where there is strong supercooling (and a detectable signal) the sound speed is close to the conformal value. We plot $\max(\Omega_{\mathrm{gw},0})$ as a function of our parameters in Fig. 9.3.

The maximum of the spectrum, which is independent of the temperature of the phase transitions, takes a broad range of values between 10^{-34} and 10^{-10}). A value above about 10^{-13} would be observable at LISA, if the peak frequency was in the range of highest sensitivity $10^{-2} - 10^{-3}$ Hz. We find that T_c would need to be in the range 0.3 to 1.8

TeV for a signal to be detected. This puts the critical temperature in a range relevant for models of strong dynamics leading to electroweak symmetry breaking, such as composite Higgs models (see *e.g.* [80] for a review).

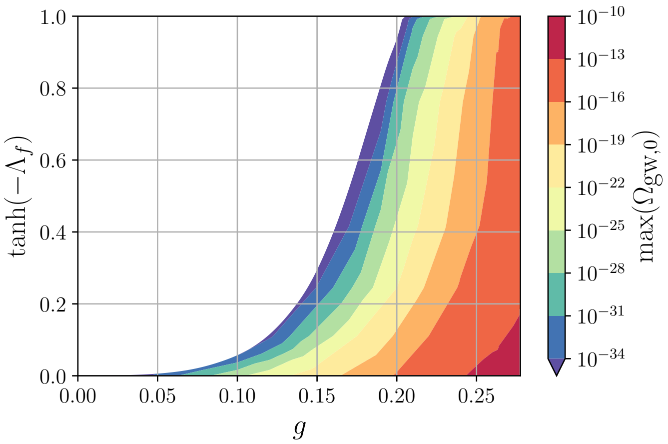

Figure 9.3: Maximum GW power spectrum, combining Fig. 9.1 and 9.2 data, using the model of [2] and [3].

4 Discussion

In this letter we outlined the construction of the effective action for a holographic strongly coupled field theory, and used it to compute the equilibrium and quasi-equilibrium quantities relevant for GW production in a first order phase transition in the early Universe. Details of the construction of this action are presented in [330]. The effective action describes a scalar field at non-zero temperature, computed in a derivative expansion. That such an action is needed to describe a phase transition has already been argued [336, 276]; it is also known that hydrodynamics alone is insufficient to describe the bubble's evolution after nucleation [270].

We illustrated the effective action method with a simple holographic 5D theory with a massive free scalar, which in alternative quantisation is dual to a 4D CFT that can be deformed by simple relevant or marginal operators. The theory has first order transitions over a wide region of dimensionless coupling ratio space.

Using an estimate for the phase boundary speed motivated by numerical simulations of a similar system [270], we computed the GW power according to current state of the art [2, 315, 3]. While the transition is supercooled and strong over a large parameter region, in the sense that a large fraction of the available potential energy is converted into kinetic energy of the fluid, the transition is also generally rapid, completing in less than 10^{-3} of the Hubble time, which reduces the signal strength. In our parameterisation of the model only a relatively small region would be observable at LISA, if the critical temperature is around 1 TeV. The favoured region has relatively small coupling $\Lambda \approx 0$ and a cubic coupling g close to the boundedness limit.

In the parameter range leading to an observable signal, the phenomenology of the holographic model conforms quite well with the nearly-conformal dynamics described in [337], including large supercooling followed by a strong transition and a peaked frequency in the millihertz range with a critical temperature of the order of TeV. The nearly-conformal physics can be understood from the fact that when $\Lambda = 0$, the breaking of conformal invariance by the coupling f in the trivial vacuum $\psi = 0$ is suppressed in the large-N limit. In addition, the large-N limit favours supercooling; since the height of the potential barrier increases with N, the transition is delayed at the metastable trivial vacuum until it is on the verge of becoming unstable.

The model is a very simplified one, intended to demonstrate the effective action method for computing GWs from phase transitions in strongly coupled field theories. The observation that TeV-scale phase transitions lead to observable signals motivates the exploration of more realistic models. The method also gives general predictions for the behaviour of the parameters with N.

The method does not yet allow us to compute v_{w}. It would be very interesting to look for terms in the effective action coupling the scalar to the fluid, similar to those known to appear in weakly-coupled theories [338, 234, 339].

Chapter 10

Conclusion

We may summarise the result of this thesis as follows: holography has proved very successful in its use as a tool to explore phase transitions beyond the perturbative regime. Many complex ideas have had to be brought together to fully understand the role it can play in illuminating strongly-coupled field theories and their possibilities for gravitational wave detection, however it has triumphed where myriad other approaches have failed. We shall now summarise the main points of each chapter.

In chapter 2 the role of general relativity as a base mechanism for exploring curved spacetimes was described, as well as how this was used in the past to derive important properties of the Universe and its expansion. This "Hubble cosmology" was necessary to see how the effects on an expanding Universe would be displayed in gravitational wave signals which have travelled vast distances and are no longer blind to this process. In this beginning commentary the consequence of singularities in general relativity in the form of black holes were noted, with some crucial properties elucidated such as how temperature and entropy were first applied to these unusual objects. These later played a large role in linking either side of the AdS/CFT correspondence at finite temperature.

Moving on, in chapter 3 another foundation of modern physics was highlighted with the description of the Standard Model. The symmetries that form its basis (which are $\mathrm{SU}(3)_c\times\mathrm{SU}(2)_\mathrm{L}\times\mathrm{U}(1)_\mathrm{Y}$) were shown to source group algebras with generators which mediated the different fundamental forces known, except gravity. The particles of the Standard Model were demonstrated to be massless due to no inherent terms quadratic in the fields, however with the inclusion of the Higgs boson it was illustrated how spontaneous symmetry breaking could provide the mechanism for mass terms to appear. The idea of unification of forces were shown to put into context how SSB could be part of how symmetries were restored at earlier, hotter times, and therefore from the need to understand field theories with non-zero temperature the basics of finite-temperature field theories were reviewed. To calculate how this finite temperature would affect the theory, the notion of effective actions and potentials were detailed. Quantum effects already have an effect upon the tree-level Higgs potential, and it is shown that this is in the form of the Coleman-Weinberg potential. Promoting the treatment to one-loop thermal calculations, the CW potential is found as well as temperature dependent terms, which cause a phase transition as the system drops below a critical point in temperature-space. The Standard Model phase transition type is then discussed, and despite being a relatively uninteresting crossover for conventional systems, very plausible motivations are found for considering that it will instead be first-order. Finally, the dynamics of a first-order electroweak phase transition are evaluated.

In the next chapter, chapter 4, a derivation of gravitational waves as perturbations of a flat background metric of general relativity was presented. A very convenient set of gauge choices were described which simplified the situation greatly named the transverse-traceless gauge, and how this is projected out is defined. Extending this to curved backgrounds, a non-linear version of the previous discussion was used to show how there is actually an energy-momentum tensor associated with the gravitational waves and that this curves spacetime. This tensor forms the basis of calculating gravitational wave signals and so lead nicely into describing all components that characterise the spectrum, which turn out to be just five main parameters. The quantity which determines whether a detector will be able to discern a signal (signal-to-noise ratio) is briefly touched upon as well as which missions are to be considered. Lastly, the five main parameters are described in detail to understand their calculation.

The concluding background knowledge is then presented in chapters 5 and 6, which are a treatise on string theory and its application of the AdS/CFT correspondence. To understand this correspondence the properties of conformal field theories were noted such as which transformations are respected, and how this is expressed for renormalisation in quantum field theories through the RG flow was discovered. Anti-de Sitter spacetimes were next explored through how their geometry is expressed as a maximally symmetric manifold, as well as some notes on the meaning of taking slices of this space. As supersymmetry played a large role in the formation of string theory, the base aspects of supersymmetric transformations as well as the algebra were listed before moving on to the main theme of the chapter. The history and incentive for the formulation of string theory was then detailed, with the bosonic theory and its Virasoro algebra expounded.

The critical dimension and then shortcomings of this string type were set out. Superstring theory was then introduced with its ability to include fermions into the spectrum as well, now with the super-Virasoro algebra of the NS and R sectors augmenting the previous algebra. Other shortcomings of bosonic theory such as tachyonic states were shown to be removed with the GSO projection, and the introduction of this with different parities demonstrated there were multiple types of string theory. After this the other types were briefly presented as well as a discussion about how all were actually related by dualities. The idea of a web of dualities was put forth, which led to holography through an s-duality. It was shown that stacks of d-branes allowed for gauge theories, leading to a description in both a field theory and stringy gravitational sense. A specific case of $\mathcal{N} = 4$ SYM theory being dual to these coincident branes was put forth to demonstrate the duality, as well as its limits of applicability. The holographic dictionary was built from relating quantities on both sides allowing the correspondence to be seen clearly. The subject of how to renormalise this type of theory was then covered just as is necessary for a regular QFT, and finally finite temperature was considered again so as to relate the duality to the thermodynamic parameters necessary for gravitational wave production.

With all of the background information necessary to understand the research produced during the doctorate, after this point the thesis turned to my published research. The first paper presented in chapter 7 studied a holographic model of a scalar field coupled to gravity in an attempt to emulate a scalar in the early Universe, with the potential derived from a superpotential for simpler differential equations. The potential was specifically chosen with multiple variable parameters so as to allow a first-order transition in some region of its parameter space generating gravitational waves. Using the knowledge of the holographic principle, we wanted to calculate thermodynamics from this system by considering a black hole at the horizon and through the Bekenstein-Hawking relations describe this with a temperature and entropy. To do this however we needed to solve a set of complicated differential equations, which we performed through the use of the master function technique and numerical solvers. From this technique the free energy and energy density were easily calculated in terms of just the field and master function, and these thermodynamic parameters led immediately to the transition strength and sound speed necessary for calculating GW signals, as well as a few other interesting quantities. The ability to turn the dials in the superpotential also allowed for a large scan over parameter space in the theory to determine generic features, which was performed for all important quantities. It was found that the strength was generally strong *i.e.* at the critical temperature (where the strength would be lowest) the values found are mostly in the intermediate to strong region as per the definitions of section 4.3.1, and as the temperature lowers these values increase dramatically. These were finally combined with the analysis of GW spectra to perform scans over GW signals, and it was determined that it would be quite plausible to detect gravitational waves from this model providing the transition rate fell in the correct range, which was left as a free parameter. An interesting correlation also seemed to suggest that the stiffness (related to sound speed) and transition strength were strongly correlated.

The next paper in chapter 8 expanded on the ideas in the last paper by attempting to find a way to calculate the transition rate holographically. The transition rate required full calculation of the effective action and potential of a model, which was not fully understood in a holographic setting. To calculate these effective quantities we turned to the duality, where we could relate operators to scalar fields. We chose to "alternately quantise", meaning the usual definitions for source and operator from the boundary field terms are reversed. This allowed for deformations on the field theory side by multi-trace operators, which imposed conditions on the boundary of the scalar field. For holography a special property is realised in which the large-N limit allows multi-trace deformations to act just as simple polynomial contributions to the effective potential. Building from this we described a simple holographic model with up to triple-trace deformations; this allowed for a certainty of a first-order phase transition. Proper holographic renormalisation allowed for well-defined effective potentials to be constructed, and from these once again a relation between the model and thermodynamic quantities was found for multiple combinations of deformations. These are formed into a full parameter space with a phase diagram showing the locations of various types of phase transition, and a few bubble solutions are calculated to demonstrate the technique's abilities. Due to the N^2 dependence of the holographic action changing the N-value will have a noticeable effect, and so general arguments were made about how this will affect most of the important quantities for gravitational waves. Finally to show a concrete test of the accuracy we used bubble solutions to calculate the domain wall solutions and from that the surface tension. This was compared to the "tanh" profile and found to fit remarkably well in the limit where we expected congruence, differing by less than 0.1% in these cases. A scan was made of the surface tension for reference.

In the last chapter, chapter 9, we produced a culmination of the results of the first two papers and utilised their techniques to be able to build up a picture of possible gravitational wave signals. The same holographic model as in 8 was used, and from this full brane black solutions were constructed numerically. This allowed calculation of the effective action which required the effective potential as well as the non-canonical kinetic term $Z(\phi)$. Action profiles were found for each point in the parameter space, and from this the nucleation temperature could be deduced. After $T_{\rm n}$ was found it was possible to determine the nucleation rate $\beta/H_{\rm n}$, something not computed holographically without numerous approximations before. Full parameter space scans were produced for both of these. The method used in 7 was then employed to calculate both the transition strength and sound speed. A parameter scan is again performed for the strength but not the sound speed, and the N-dependence for this quantity is explored. For completeness we wished to also have some arguments for the value of the wall speed as it is the last parameter needed to be computed. We adapted the results from refs. [270, 271, 272] which were small velocity arguments to produce a parameter scan for a quantity related to the wall speed, and found that this quantity also seems closely related to the transition speed in agreement with the result found in paper 1. Lastly these scans were fully combined with the spectrum analysis in paper 1 to produce a full scan of the maximum gravitational wave power spectrum. It was found that the detection of gravitational waves would be possible, but only for a small (but technically infinite) region of the parameter space where the model tends towards roughly conformal dynamics.

Overall, we can see that the research produced during this project has provided a significant leap forward in the understanding of how to consider gravitational wave models holographically. A brand new technique has been devised to allow for the computation of effective field theory quantities through the much lesser used alternate quantisation, which opens up a whole new arena in much more than just gravitational wave analysis. Computing all but one of the necessary parameters for the GW spectrum and demonstrating that these sorts of models can actually produce detectable signals is a great boon for motivating further holographic explorations. This however leads us to the shortcomings of the analysis. We have as of yet not been able to determine how to move past near equilibrium quantities in a significant manner. As the wall speed is of this class and has a huge effect on the production of signals, this is crucial knowledge if we wish to say with certainty whether we would find signals or not. Even more than this, all models that we have considered have just been "toy" models, only fit for proof of concept rather than for use as actual justification for searching for signals in detectors like LISA. Much more in-depth work is necessary for any sort of near-reality theory, especially in the realm of moving closer towards either finding these sort of results from a fully-derived string theory or from a fully Standard Model like field theory. Although there is a large amount to do, this thesis with its related published work has hopefully shown that these avenues are very promising and well worth more time and effort to explore them more comprehensively.

Chapter 11

Extra Appendices

G Conventions, Notations, and Formulae

Here we will give a brief, bullet pointed list of the basic but important notations and formulae we use in this work.

- 4D metric tensor in flat space:

$$g_{\mu\nu} = \eta_{\mu\nu} = \mathrm{diag}(-,+,+,+) \tag{11.1}$$

- 4D metric tensor in flat Euclidean space, "Minkowski metric":

$$g_{\mu\nu} = \delta_{\mu\nu} = \mathrm{diag}(+,+,+,+) \tag{11.2}$$

- Einstein summation convention will always be used when possible for repeated indices, so that generally for a quantity x_i with n components

$$x^i x_i = \sum_{i=1}^{n} x^i x_i = x^1 x_1 + x^2 x_2 + \ldots + x^n x_n \ . \tag{11.3}$$

- The use of natural units is employed throughout the thesis, meaning that

$$c = \hbar = G = k_B = 1 \ , \tag{11.4}$$

  except where they are necessary for understanding and are reinserted. This will happen most commonly for the gravitational constant. In this unit style quantities will most frequently be described in units of the meaningful parameter, the electronvolt (eV) or this unit with prefixes (meV, MeV, GeV, *etc.*)

H Poincaré Symmetry and Algebra

The Poincaré group is the group related to Minkowskian spacetime, and its symmetry is the symmetry describing special relativity. It is the group which leaves the metric invariant under translations, rotations, and boosts, and therefore it contains the Lorentz group (which contains the rotations and boosts) as a subgroup. The generators of the two are P^μ for the translations and $M^{\mu\nu}$ for the Lorentz transformations, and therefore the Poincaré algebra is found through the commutation relations as:

$$\begin{aligned} [P^\mu, P^\nu] &= 0 \ , \\ [M^{\mu\nu}, P^\rho] &= i(g^{\nu\rho}P^\mu - g^{\mu\rho}P^\nu) \ , \\ [M^{\mu\nu}, M^{\rho\sigma}] &= i(g^{\mu\sigma}M^{\mu\rho} + g^{\nu\rho}M^{\mu\sigma} - g^{\mu\rho}M^{\nu\sigma} - g^{\nu\sigma}M^{\mu\rho}) \end{aligned} \tag{11.5}$$

I Dirac Algebra in various dimensions

The Dirac algebra, first derived for the use of explaining spin-$\frac{1}{2}$ particles [340], has uses in many forms throughout this work in various dimensions. In four dimensions it is described by the gamma/Dirac matrices γ^μ, $\mu = 0, 1, 2, 3$ which generate a Clifford algebra $Cl_{1,3}$. This is due to their anticommuting property

$$\{\gamma^\mu, \gamma^\nu\} = \gamma^\mu\gamma^\nu + \gamma^\nu\gamma^\mu = -2\eta^{\mu\nu}\mathbb{I}_4 \ , \tag{11.6}$$

where we have used the convention for $\eta^{\mu\nu}$ defined in appendix G. In the Dirac representation these matrices appear as (when formed through the Pauli matrices)

$$\gamma^0 = \begin{pmatrix} \mathbb{I} & 0 \\ 0 & -\mathbb{I} \end{pmatrix}, \quad \gamma^k = \begin{pmatrix} 0 & \sigma_k \\ -\sigma_k & 0 \end{pmatrix} \ . \tag{11.7}$$

which when written out fully are

$$\begin{aligned} \gamma^0 &= \begin{pmatrix} 1 & 0 & 0 & 0 \\ 0 & 1 & 0 & 0 \\ 0 & 0 & -1 & 0 \\ 0 & 0 & 0 & -1 \end{pmatrix}, \quad \gamma^1 = \begin{pmatrix} 0 & 0 & 0 & 1 \\ 0 & 0 & 1 & 0 \\ 0 & -1 & 0 & 0 \\ -1 & 0 & 0 & 0 \end{pmatrix}, \\ \gamma^2 &= \begin{pmatrix} 0 & 0 & 0 & -i \\ 0 & 0 & i & 0 \\ 0 & i & 0 & 0 \\ -i & 0 & 0 & 0 \end{pmatrix}, \quad \gamma^3 = \begin{pmatrix} 0 & 0 & 1 & 0 \\ 0 & 0 & 0 & -1 \\ -1 & 0 & 0 & 0 \\ 0 & 1 & 0 & 0 \end{pmatrix} . \end{aligned} \tag{11.8}$$

From these, a fifth gamma matrix which will be useful in various situations can be generated through

$$\gamma^5 \equiv i\gamma^0\gamma^1\gamma^2\gamma^3 \ , \tag{11.9}$$

which satisfies the conditions

$$(\gamma^5)^2 = 1 \ , \quad (\gamma^5)^\dagger = \gamma^5 \ , \quad \text{and} \quad \{\gamma^5, \gamma^\mu\} = 0 \ . \tag{11.10}$$

Different dimensional versions can be found by generalising this, two more of which we will require are the two-dimensional and ten-dimensional analogues. In two dimensions the Dirac matrices with matrix multiplication forms a Clifford algebra $\mathrm{C}l_{1,1}$ with matrices satisfying

$$\{\rho^\alpha, \rho^\beta\} = 2\eta^{\alpha\beta}\mathbb{I}_2 \ . \tag{11.11}$$

For these we pick a basis which gives the form of the Dirac matrices as

$$\rho^0 = \begin{pmatrix} 0 & -1 \\ 1 & 0 \end{pmatrix} \quad \text{and} \quad \rho^1 = \begin{pmatrix} 0 & 1 \\ 1 & 0 \end{pmatrix} \ . \tag{11.12}$$

Finally the ten dimensional version forms a Clifford algebra $\mathrm{C}l_{1,9}$ through the gamma matrices Γ^μ, $\mu = 0, \ldots, 9$. These matrices satisfy

$$\{\Gamma^\mu, \Gamma^\nu\} = -2\eta^{\mu\nu}\mathbb{I}_{10} \ , \tag{11.13}$$

however we will not write out their full forms (see for instance [341] for more information on the construction of gamma matrices). A quantity can be formed in likeness to the matrix γ^5 in the four-dimensional case as a ten-dimensional analogue through

$$\Gamma^{11} \equiv \Gamma^0\Gamma^1\Gamma^2\Gamma^3\Gamma^4\Gamma^5\Gamma^6\Gamma^7\Gamma^8\Gamma^9\Gamma^{10} \ . \tag{11.14}$$

This satisfies the properties

$$(\Gamma^{11})^2 = 1 \quad \text{and} \quad \{\Gamma^{11}, \Gamma^\mu\} = 0 \ , \tag{11.15}$$

similarly to eq. 11.10.

J Grassmann Algebra

The Grassmann algebra is the set of objects $\mathbb{G}$ that are generated by a basis $\{\theta_i\}, i = 1 \ldots n$, the elements of which we call the Grassmann numbers. The most basic property of these

Grassmann numbers is that they anticommute *i.e.* $\{\theta_i, \theta_j\} = \theta_i\theta_j + \theta_j\theta_i = 0$ and so are useful in their ability to describe fermionic fields. Other basic properties are:

- The Grassmann numbers add commutatively $\theta_i + \theta_j = \theta_j + \theta_i$
- They are able to be multiplied by complex numbers s.t. $a\theta \in \mathbb{G}$ for $a \in \mathbb{C}$, $\theta \in \mathbb{G}$
- $\exists$ a null (zero) element 0 s.t. $\theta_i + 0 = \theta_i$
- As $\theta^2 = 0$ (from sending $\theta_j \to \theta_i$ in anticommuting definition) the most general element of the algebra that can be written for a single field is $g = a + b\theta$ for $a, b \in \mathbb{C}$ and similarly the most general element of the algebra that can be written for two fields is $g = a + b\theta_1 + c\theta_2 + f\theta_1\theta_2$ for $a, b, c, f \in \mathbb{C}$.

J.1 Integration and Differentiation

As useful numbers in quantum field theories we must grasp how this algebra acts under integration and differentiation, which is greatly different than usual. The rule for differentiating the general element of a single field is

$$\frac{d}{d\theta}g = \frac{d}{d\theta}(a + b\theta) = b \ , \tag{11.16}$$

which is similar to usual, however the rule for integration is

$$\int d\theta g = \int d\theta(a + b\theta) = b \ , \tag{11.17}$$

showing that integration acts identically to differentiation, $\frac{d}{d\theta} \equiv \int d\theta$.

These definitions extend to allowing infinite Grassmann numbers as will be necessary for fields, and so

$$\int d\theta_1 d\theta_2 \dots d\theta_{n-1} d\theta_n \equiv \frac{d}{d\theta_1}\frac{d}{d\theta_2} \cdots \frac{d}{d\theta_{n-1}}\frac{d}{d\theta_n} \ . \tag{11.18}$$

Bibliography

[1] S. Borsanyi et al., *Calculation of the axion mass based on high-temperature lattice quantum chromodynamics*, *Nature* **539** (2016) 69 [1606.07494]. xi, 31, 176

[2] C. Caprini et al., *Detecting gravitational waves from cosmological phase transitions with LISA: an update*, *JCAP* **03** (2020) 024 [1910.13125]. xvi, 106, 123, 138, 176, 177, 182, 183

[3] F. R. Ares, M. Hindmarsh, C. Hoyos and N. Jokela, *Gravitational waves from a holographic phase transition*, *JHEP* **21** (2020) 100 [2011.12878]. xvi, 138, 160, 177, 182, 183

[4] LIGO Scientific Collaboration and Virgo collaboration, *Observation of gravitational waves from a binary black hole merger*, *Phys. Rev. Lett.* **116** (2016) 061102. 1

[5] LISA collaboration, *Laser Interferometer Space Antenna*, 1702.00786. 2, 138

[6] P. Amaro-Seoane et al., *Low-frequency gravitational-wave science with eLISA/NGO*, *Class. Quant. Grav.* **29** (2012) 124016 [1202.0839]. 2

[7] W.-H. Ruan, Z.-K. Guo, R.-G. Cai and Y.-Z. Zhang, *Taiji program: Gravitational-wave sources*, *International Journal of Modern Physics A* **35** (2020) 2050075 [1807.09495]. 2, 55, 107, 126

[8] J. Luo, L.-S. Chen, H.-Z. Duan, Y.-G. Gong, S. Hu, J. Ji et al., *Tianqin: a space-borne gravitational wave detector*, *Class. Quantum Gravity* **33** (2016) 035010 [1512.02076]. 2, 126

[9] TianQin collaboration, *The TianQin project: current progress on science and technology*, *PTEP* **2021** (2021) 05A107 [2008.10332]. 2

[10] K. Kajantie, M. Laine, K. Rummukainen and M. E. Shaposhnikov, *Is there a hot electroweak phase transition at $m_H \gtrsim m_W$?*, Phys. Rev. Lett. **77** (1996) 2887 [hep-ph/9605288]. 2, 34, 106, 176

[11] M. Laine and K. Rummukainen, *Strong electroweak phase transition up to $m_H \sim$ 105GeV*, Phys. Rev. Lett. **80** (1998) 5259 [hep-ph/9804255]. 2, 106

[12] M. Laine, G. Nardini and K. Rummukainen, *Lattice study of an electroweak phase transition at $m_H \sim$ 126 GeV*, JCAP **2013** (2013) 011. 2, 106

[13] G. Moore and T. Prokopec, *Bubble wall velocity in a first order electroweak phase transition*, Phys. Rev. Lett. **75** (1995) 777. 2

[14] R.-G. Cai and S.-J. Wang, *Effective picture of bubble expansion*, JCAP **03** (2021) 096 [2011.11451]. 2

[15] A. Friedmann, *Über die Krümmung des Raumes*, Zeitschrift fur Physik **10** (1922) 377. 7

[16] A. Friedmann, *Über die Möglichkeit einer Welt mit konstanter negativer Krümmung des Raumes*, Zeitschrift fur Physik **21** (1924) 326. 7

[17] G. Lemaître, *A Homogeneous Universe of Constant Mass and Growing Radius Accounting for the Radial Velocity of Extragalactic Nebulae*, Annales Soc. Sci. Bruxelles A **47** (1927) 49. 7

[18] G. Lemaître, *L'Univers en expansion*, *Annales de la Société Scientifique de Bruxelles* **53** (1933) 51. 7

[19] H. P. Robertson, *Kinematics and World-Structure*, Astrophysical Journal **82** (1935) 284. 7

[20] H. P. Robertson, *Kinematics and World-Structure II.*, Astrophysical Journal **83** (1936) 187. 7

[21] H. P. Robertson, *Kinematics and World-Structure III.*, Astrophysical Journal **83** (1936) 257. 7

[22] A. G. Walker, *On Milne's Theory of World-Structure*, Proceedings of the London Mathematical Society **42** (1937) 90. 7

[23] S. L. Shapiro and S. A. Teukolsky, *Black holes, naked singularities and cosmic censorship*, *American Scientist* **79** (1991) 330. 9

[24] R. Goswami and P. S. Joshi, *Spherical gravitational collapse inndimensions*, *Physical Review D* **76** (2007) . 9

[25] K. Becker, M. Becker and J. H. Schwarz, *String Theory and M-Theory: A Modern Introduction*. Cambridge University Press, 2006, 10.1017/CBO9780511816086. 10, 81

[26] K. Schwarzschild, *Über das Gravitationsfeld eines Massenpunktes nach der Einsteinschen Theorie*, *Sitzungsberichte der Königlich Preußischen Akademie der Wissenschaften (Berlin)* (1916) 189. 10

[27] R. Penrose, *Asymptotic properties of fields and space-times*, *Phys. Rev. Lett.* **10** (1963) 66. 10

[28] P. J. Davis, *Leonhard euler's integral: A historical profile of the gamma function: In memoriam: Milton abramowitz*, *The American Mathematical Monthly* **66** (1959) 849. 11

[29] W. Israel, *Event Horizons in Static Vacuum Space-Times*, *Physical Review* **164** (1967) 1776. 11

[30] W. Israel, *Event horizons in static electrovac space-times*, *Communications in Mathematical Physics* **8** (1968) 245. 11

[31] B. Carter, *Axisymmetric Black Hole Has Only Two Degrees of Freedom*, *Physical Review Letters* **26** (1971) 331. 11

[32] J. D. Bekenstein, *Black holes and the second law*, *Lett. Nuovo Cim.* **4** (1972) 737. 11

[33] S. W. Hawking, *Black hole explosions?*, *Nature* **248** (1974) 30. 11

[34] S. W. Hawking, *Particle creation by black holes*, *Communications in Mathematical Physics* **43** (1975) 199. 11, 13

[35] J. M. Bardeen, B. Carter and S. W. Hawking, *The Four laws of black hole mechanics*, *Commun. Math. Phys.* **31** (1973) 161. 13

[36] J. D. Bekenstein, *Black holes and entropy*, *Phys. Rev. D* **7** (1973) 2333. 13

[37] H. S. Reall, *Higher dimensional black holes*, *Int. J. Mod. Phys. D* **21** (2012) 1230001 [1210.1402]. 14

[38] O. W. Greenberg, *Spin and unitary-spin independence in a paraquark model of baryons and mesons*, *Phys. Rev. Lett.* **13** (1964) 598. 15

[39] M. Y. Han and Y. Nambu, *Three-triplet model with double* SU(3) *symmetry*, *Phys. Rev.* **139** (1965) B1006. 15

[40] S. L. Glashow, *Partial-symmetries of weak interactions*, *Nuclear Physics* **22** (1961) 579. 15

[41] A. Salam and J. C. Ward, *Electromagnetic and weak interactions*, *Phys. Lett.* **13** (1964) 168. 15

[42] S. Weinberg, *A model of leptons*, *Phys. Rev. Lett.* **19** (1967) 1264. 15

[43] C. N. Yang and R. L. Mills, *Conservation of isotopic spin and isotopic gauge invariance*, *Phys. Rev.* **96** (1954) 191. 15

[44] G. Aad, T. Abajyan, B. Abbott, J. Abdallah, S. Abdel Khalek, A. Abdelalim et al., *Observation of a new particle in the search for the standard model higgs boson with the atlas detector at the lhc*, *Physics Letters B* **716** (2012) 1?29. 18

[45] P. Ramond, *Journeys beyond the standard model*, *Front. Phys.* **101** (1999) . 19

[46] S. L. Glashow, *Partial symmetries of weak interactions*, *Nuclear Physics* **22** (1961) 579. 21

[47] H. Georgi and S. L. Glashow, *Unity of all elementary-particle forces*, *Phys. Rev. Lett.* **32** (1974) 438. 21

[48] D. Kirzhnits, *Weinberg model in the hot universe*, *JETP Lett.* **15** (1972) 529. 24

[49] D. Kirzhnits and A. Linde, *Macroscopic consequences of the weinberg model*, *Physics Letters B* **42** (1972) 471. 24

[50] L. Dolan and R. Jackiw, *Symmetry behavior at finite temperature*, *Phys. Rev. D* **9** (1974) 3320. 24

[51] S. Weinberg, *Gauge and Global Symmetries at High Temperature*, *Phys. Rev. D* **9** (1974) 3357. 24

[52] G. Jona-Lasinio, *Relativistic field theories with symmetry-breaking solutions*, *Il Nuovo Cimento (1955-1965)* **34** (1964) 1790. 25

[53] S. Coleman and E. Weinberg, *Radiative corrections as the origin of spontaneous symmetry breaking*, *Phys. Rev. D* **7** (1973) 1888. 26

[54] J. Iliopoulos, C. Itzykson and A. Martin, *Functional methods and perturbation theory*, *Rev. Mod. Phys.* **47** (1975) 165. 27

[55] L.-H. Chan, *Effective-action expansion in perturbation theory*, *Phys. Rev. Lett.* **54** (1985) 1222. 27

[56] C. M. Fraser, *Calculation of Higher Derivative Terms in the One Loop Effective Lagrangian*, *Z. Phys. C* **28** (1985) 101. 27

[57] T. Matsubara, *A New approach to quantum statistical mechanics*, *Prog. Theor. Phys.* **14** (1955) 351. 29

[58] A. D. Linde, *Infrared Problem in Thermodynamics of the Yang-Mills Gas*, *Phys. Lett. B* **96** (1980) 289. 34

[59] F. Karsch, T. Neuhaus, A. Patkos and J. Rank, *Critical Higgs mass and temperature dependence of gauge boson masses in the SU(2) gauge Higgs model*, *Nucl. Phys. B Proc. Suppl.* **53** (1997) 623 [hep-lat/9608087]. 34

[60] K. Rummukainen, K. Kajantie, M. Laine, M. E. Shaposhnikov and M. Tsypin, *The Universal properties of the electroweak phase transition*, hep-ph/9809435. 34

[61] E.-M. Ilgenfritz, A. Schiller and C. Strecha, *Matter near to the endpoint of the electroweak phase transition*, *Nucl. Phys. B Proc. Suppl.* **73** (1999) 662 [hep-lat/9808023]. 34

[62] F. Csikor, Z. Fodor and J. Heitger, *Where does the hot electroweak phase transition end?*, *Nucl. Phys. B Proc. Suppl.* **73** (1999) 659 [hep-ph/9809293]. 34

[63] G. 't Hooft, *An algorithm for the poles at dimension four in the dimensional regularization procedure*, *Nucl. Phys. B* **62** (1973) 444. 35

[64] G. 't Hooft and M. J. G. Veltman, *One loop divergencies in the theory of gravitation*, *Ann. Inst. H. Poincare Phys. Theor. A* **20** (1974) 69. 35

[65] S. D. M. White, C. S. Frenk and M. Davis, *Clustering in a Neutrino Dominated Universe*, *Astrophys. J. Lett.* **274** (1983) L1. 35

[66] K. Garrett and G. Duda, *Dark matter: A primer*, *Advances in Astronomy* **2011** (2011) 1?22. 35

[67] W. Buchmüller and M. Plümacher, *Matter–antimatter asymmetry and neutrino properties*, *Physics reports* **320** (1999) 329. 36

[68] M. Dine and A. Kusenko, *Origin of the matter-antimatter asymmetry*, *Reviews of Modern Physics* **76** (2003) 1?30. 36

[69] D. E. Morrissey and M. J. Ramsey-Musolf, *Electroweak baryogenesis*, *New Journal of Physics* **14** (2012) 125003. 36

[70] Particle Data Group collaboration, *Review of particle physics*, *Phys. Rev. D* **98** (2018) 030001. 36

[71] M. Pietroni, *The electroweak phase transition in a nonminimal supersymmetric model*, *Nuclear Physics B* **402** (1993) 27. 36

[72] A. Davies, C. Froggatt and R. Moorhouse, *Electroweak baryogenesis in the next to minimal supersymmetric model*, *Physics Letters B* **372** (1996) 88. 36

[73] S. Profumo, M. J. Ramsey-Musolf and G. Shaughnessy, *Singlet higgs phenomenology and the electroweak phase transition*, *Journal of High Energy Physics* **2007** (2007) 010. 36

[74] J. Espinosa, T. Konstandin and F. Riva, *Strong electroweak phase transitions in the standard model with a singlet*, *Nuclear Physics B* **854** (2012) 592. 36

[75] W. Huang, Z. Kang, J. Shu, P. Wu and J. M. Yang, *New insights in the electroweak phase transition in the nmssm*, *Physical Review D* **91** (2015) . 36

[76] J. M. Cline, K. Kainulainen and M. Trott, *Electroweak baryogenesis in two higgs doublet models and b meson anomalies*, *Journal of High Energy Physics* **2011** (2011) . 36

[77] M. Kakizaki, S. Kanemura and T. Matsui, *Gravitational waves as a probe of extended scalar sectors with the first order electroweak phase transition*, *Physical Review D* **92** (2015) . 36

[78] G. Dorsch, S. Huber, T. Konstandin and J. No, *A second higgs doublet in the early universe: baryogenesis and gravitational waves*, *Journal of Cosmology and Astroparticle Physics* **2017** (2017) 052. 36

[79] P. Basler, M. Krause, M. Mühlleitner, J. Wittbrodt and A. Wlotzka, *Strong first order electroweak phase transition in the cp-conserving 2hdm revisited*, *Journal of High Energy Physics* **2017** (2017) . 36

[80] B. Bellazzini, C. Csáki and J. Serra, *Composite Higgses*, *Eur. Phys. J. C* **74** (2014) 2766 [1401.2457]. 36, 183

[81] M. Laine and K. Rummukainen, *The mssm electroweak phase transition on the lattice*, *Nuclear Physics B* **535** (1998) 423. 36

[82] M. Carena, M. Quirós and C. Wagner, *Electroweak baryogenesis and higgs and stop searches at lep and the tevatron*, *Nuclear Physics B* **524** (1998) 3. 36

[83] X. Zhang, *Operator analysis for the higgs potential and cosmological bound on the higgs-boson mass*, *Physical Review D* **47** (1993) 3065. 36

[84] M. Dine, P. Huet, R. L. Singleton, Jr and L. Susskind, *Creating the baryon asymmetry at the electroweak phase transition*, *Phys. Lett. B* **257** (1991) 351. 36

[85] X. Zhang, S. K. Lee, K. Whisnant and B.-L. Young, *Phenomenology of a nonstandard top quark yukawa coupling*, *Physical Review D* **50** (1994) 7042. 36

[86] D. Bodeker, L. Fromme, S. J. Huber and M. Seniuch, *The baryon asymmetry in the standard model with a low cut-off*, *Journal of High Energy Physics* **2005** (2005) 026. 36

[87] P. Creminelli, A. Nicolis and R. Rattazzi, *Holography and the electroweak phase transition*, *JHEP* **03** (2002) 051 [hep-th/0107141]. 36, 106

[88] L. Randall and G. Servant, *Gravitational waves from warped spacetime*, *JHEP* **05** (2007) 054 [hep-ph/0607158]. 36, 106

[89] G. Nardini, M. Quiros and A. Wulzer, *A Confining Strong First-Order Electroweak Phase Transition*, *JHEP* **09** (2007) 077 [0706.3388]. 36, 106

[90] B. Hassanain, J. March-Russell and M. Schvellinger, *Warped Deformed Throats have Faster (Electroweak) Phase Transitions*, *JHEP* **10** (2007) 089 [0708.2060]. 36

[91] T. Konstandin, G. Nardini and M. Quiros, *Gravitational Backreaction Effects on the Holographic Phase Transition*, *Phys. Rev. D* **82** (2010) 083513 [1007.1468]. 36, 106

[92] B. von Harling and G. Servant, *Qcd-induced electroweak phase transition*, *Journal of High Energy Physics* **2018** (2017) 1. 36

[93] L. Randall and R. Sundrum, *Large mass hierarchy from a small extra dimension*, *Phys. Rev. Lett.* **83** (1999) 3370. 36

[94] A. D. Linde, *On the vacuum instability and the Higgs meson mass*, *Phys. Lett. B* **70** (1977) 306. 37, 108

[95] A. Linde, *Fate of the false vacuum at finite temperature: Theory and applications*, *Phys. Lett. B* **100** (1981) 37 . 37, 108

[96] S. Coleman, *Fate of the false vacuum: Semiclassical theory*, *Phys. Rev. D* **15** (1977) 2929. 37, 108

[97] C. G. Callan and S. Coleman, *Fate of the false vacuum. ii. first quantum corrections*, *Phys. Rev. D* **16** (1977) 1762. 37, 57, 108

[98] M. H. Poincaré, *Sur la dynamique de l'électron*, *Rendiconti del Circolo Matematico di Palermo (1884-1940)* **21** (1906) 129. 40

[99] A. Einstein, *Näherungsweise Integration der Feldgleichungen der Gravitation*, *Sitzungsberichte der Königlich Preußischen Akademie der Wissenschaften (Berlin* (1916) 688. 40

[100] S. Khlebnikov and I. Tkachev, *Relic gravitational waves produced after preheating*, *Phys. Rev. D* **56** (1997) 653. 40

[101] R. Easther, J. T. Giblin and E. A. Lim, *Gravitational wave production at the end of inflation*, *Phys. Rev. Lett.* **99** (2007) 221301. 40

[102] J. García-Bellido, D. G. Figueroa and A. Sastre, *Gravitational wave background from reheating after hybrid inflation*, *Phys. Rev. D* **77** (2008) 043517. 40

[103] J.-F. m. c. Dufaux, A. Bergman, G. Felder, L. Kofman and J.-P. Uzan, *Theory and numerics of gravitational waves from preheating after inflation*, *Phys. Rev. D* **76** (2007) 123517. 40

[104] C. J. Hogan, *Gravitational radiation from cosmological phase transitions*, *Mon. Not. Roy. Astron. Soc.* **218** (1986) 629. 40, 176

[105] A. Kosowsky, M. S. Turner and R. Watkins, *Gravitational radiation from colliding vacuum bubbles*, *Phys.Rev.* **D45** (1992) 4514. 40

[106] A. Kosowsky, M. S. Turner and R. Watkins, *Gravitational waves from first order cosmological phase transitions*, *Phys.Rev.Lett.* **69** (1992) 2026. 40

[107] M. S. Turner, E. J. Weinberg and L. M. Widrow, *Bubble nucleation in first order inflation and other cosmological phase transitions*, *Phys.Rev.* **D46** (1992) 2384. 40, 176

[108] A. Kosowsky and M. S. Turner, *Gravitational radiation from colliding vacuum bubbles: envelope approximation to many bubble collisions*, *Phys.Rev.* **D47** (1993) 4372 [astro-ph/9211004]. 40

[109] M. Kamionkowski, A. Kosowsky and M. S. Turner, *Gravitational radiation from first order phase transitions*, *Phys.Rev.* **D49** (1994) 2837 [astro-ph/9310044]. 40

[110] A. Kosowsky, A. Mack and T. Kahniashvili, *Stochastic gravitational radiation from phase transitions*, *AIP Conf. Proc.* **575** (2001) 191 [astro-ph/0102169]. 40

[111] R. Apreda, M. Maggiore, A. Nicolis and A. Riotto, *Gravitational waves from electroweak phase transitions*, *Nucl.Phys.* **B631** (2002) 342 [gr-qc/0107033]. 40

[112] H.-K. Guo, K. Sinha, D. Vagie and G. White, *Phase transitions in an expanding universe: Stochastic gravitational waves in standard and non-standard histories*, 2007.08537. 52, 107, 123, 135

[113] C. Caprini, M. Hindmarsh, S. Huber, T. Konstandin, J. Kozaczuk, G. Nardini et al., *Science with the space-based interferometer elisa. ii: gravitational waves from cosmological phase transitions*, *Journal of Cosmology and Astroparticle Physics* **2016** (2016) 001 [1512.06239]. 53

[114] M. Hindmarsh, S. J. Huber, K. Rummukainen and D. J. Weir, *Shape of the acoustic gravitational wave power spectrum from a first order phase transition*, *Phys. Rev. D* **96** (2017) 103520 [1704.05871]. 53, 109, 123, 124, 131, 134, 176

[115] J. C. Mather, D. J. Fixsen, R. A. Shafer, C. Mosier and D. T. Wilkinson, *Calibrator design for thecobefar?infrared absolute spectrophotometer (firas)*, *The Astrophysical Journal* **512** (1999) 511 [9810373]. 54

[116] F. Giese, T. Konstandin and J. v. de Vis, *Model-independent energy budget of cosmological first-order phase transitions–a sound argument to go beyond the bag model*, *JCAP* **2020** (2020) 057 [2004.06995]. 54, 107, 109, 122, 123, 124

[117] F. Giese, T. Konstandin, K. Schmitz and J. van de Vis, *Model-independent energy budget for lisa*, 2010.09744. 54, 63, 122, 124, 130, 135

[118] D. Cutting, M. Hindmarsh and D. J. Weir, *Vorticity, kinetic energy, and suppressed gravitational-wave production in strong first-order phase transitions*, *Phys. Rev. Lett.* **125** (2020) [1906.00480]. 54, 107, 109, 123, 124, 130, 136

[119] J. R. Espinosa, T. Konstandin, J. M. No and G. Servant, *Energy budget of cosmological first-order phase transitions*, *JCAP* **2010** (2010) 028 [1004.4187]. 54, 61, 135, 136

[120] K. Schmitz, *New Sensitivity Curves for Gravitational-Wave Signals from Cosmological Phase Transitions*, *JHEP* **01** (2021) 097 [2002.04615]. 55

[121] https://www.cosmos.esa.int/web/lisa/lisa-documents. 55, 126

[122] M. Ming, Y. Luo, Y.-R. Liang, J.-Y. Zhang, H.-Z. Duan, H. Yan et al., *Ultraprecision intersatellite laser interferometry*, *International Journal of Extreme Manufacturing* **2** (2020) 022003. 55, 107

[123] A. D. Linde, *Decay of the False Vacuum at Finite Temperature*, *Nucl. Phys. B* **216** (1983) 421. 57, 157, 169, 176, 180

[124] S. Hawking and I. Moss, *Supercooled phase transitions in the very early universe*, *Physics Letters B* **110** (1982) 35. 58

[125] G. D. Moore and T. Prokopec, *How fast can the wall move? A Study of the electroweak phase transition dynamics*, *Phys. Rev. D* **52** (1995) 7182 [hep-ph/9506475]. 61, 110, 177

[126] P. John and M. Schmidt, *Do stops slow down electroweak bubble walls?*, *Nuclear Physics B* **598** (2001) 291?305 [0002050]. 61

[127] L. Leitao and A. Megevand, *Hydrodynamics of phase transition fronts and the speed of sound in the plasma*, *Nucl. Phys. B* **891** (2015) 159 [1410.3875]. 62

[128] E. C. Poggio and H. N. Pendleton, *Vanishing of Charge Renormalization and Anomalies in a Supersymmetric Gauge Theory*, *Phys. Lett. B* **72** (1977) 200. 68

[129] D. R. T. Jones, *Charge Renormalization in a Supersymmetric Yang-Mills Theory*, *Phys. Lett. B* **72** (1977) 199. 68

[130] L. V. Avdeev, O. V. Tarasov and A. A. Vladimirov, *Vanishing of the three loop charge renormalization function in a supersymmetric gauge theory*, *Phys. Lett. B* **96** (1980) 94. 68

[131] M. Grisaru, M. Roček and W. Siegel, *Zero value for the three-loop β function in $n = 4$ supersymmetric yang-mills theory*, *Phys. Rev. Lett.* **45** (1980) 1063. 68

[132] M. Ammon and J. Erdmenger, *Gauge/Gravity Duality: Foundations and Applications*. Cambridge University Press, 2015, 10.1017/CBO9780511846373. 68, 85

[133] J. M. Maldacena, *The Large N limit of superconformal field theories and supergravity*, *Adv. Theor. Math. Phys.* **2** (1998) 231 [hep-th/9711200]. 69, 84, 177

[134] S. Coleman and J. Mandula, *All possible symmetries of the s matrix*, *Phys. Rev.* **159** (1967) 1251. 72

[135] L. Susskind, *Dual symmetric theory of hadrons. 1.*, *Nuovo Cim. A* **69** (1970) 457. 73

[136] B. Andersson, G. Gustafson, G. Ingelman and T. Sjostrand, *Parton Fragmentation and String Dynamics*, *Phys. Rept.* **97** (1983) 31. 73

[137] M. A. Virasoro, *Subsidiary conditions and ghosts in dual-resonance models*, *Phys. Rev. D* **1** (1970) 2933. 74

[138] P. Ramond, *Dual theory for free fermions*, *Phys. Rev. D* **3** (1971) 2415. 75, 77

[139] A. Neveu and J. H. Schwarz, *Factorizable dual model of pions*, *Nucl. Phys. B* **31** (1971) 86. 75

[140] A. Neveu and J. H. Schwarz, *Tachyon-free dual model with a positive-intercept trajectory*, *Phys. Lett. B* **34** (1971) 517. 77

[141] F. Gliozzi, J. Scherk and D. I. Olive, *Supergravity and the Spinor Dual Model*, *Phys. Lett. B* **65** (1976) 282. 77

[142] F. Gliozzi, J. Scherk and D. I. Olive, *Supersymmetry, Supergravity Theories and the Dual Spinor Model*, *Nucl. Phys. B* **122** (1977) 253. 77

[143] M. B. Green and J. H. Schwarz, *Supersymmetrical String Theories*, *Phys. Lett. B* **109** (1982) 444. 79

[144] J. Polchinski, *String theory. Vol. 2: Superstring theory and beyond*, Cambridge Monographs on Mathematical Physics. Cambridge University Press, 12, 2007, 10.1017/CBO9780511618123. 79

[145] J. Polchinski, *Dirichlet branes and ramond-ramond charges*, *Phys. Rev. Lett.* **75** (1995) 4724. 79

[146] Z. Kakushadze, G. Shiu and S.-H. H. Tye, *Type IIB orientifolds, f-theory, type i strings on orbifolds and type i-heterotic duality*, *Nuclear Physics B* **533** (1998) 25. 79

[147] D. J. Gross, J. A. Harvey, E. Martinec and R. Rohm, *Heterotic string*, *Phys. Rev. Lett.* **54** (1985) 502. 79

[148] A. Sen, *Dyon-monopole bound states, self-dual harmonic forms on the multi-monopole moduli space, and sl (2,z) invariance in string theory*, *Physics Letters B* **329** (1994) 217. 81

[149] E. Witten, *String theory dynamics in various dimensions*, *Nucl. Phys. B* **443** (1995) 85 [hep-th/9503124]. 81

[150] A. A. Tseytlin, *On SO(32) heterotic type I superstring duality in ten-dimensions*, *Phys. Lett. B* **367** (1996) 84 [hep-th/9510173]. 81

[151] W. Nahm, *Supersymmetries and their Representations*, *Nucl. Phys. B* **135** (1978) 149. 82

[152] M. Duff, *M-theory (the theory formerly known as strings)*, *International Journal of Modern Physics A* **11** (1996) 5623. 82

[153] N. A. Obers and B. Pioline, *U duality and M theory*, *Phys. Rept.* **318** (1999) 113 [hep-th/9809039]. 82

[154] A. Miemiec and I. Schnakenburg, *Basics of M-theory*, *Fortsch. Phys.* **54** (2006) 5 [hep-th/0509137]. 82

[155] S. S. Gubser, I. R. Klebanov and A. M. Polyakov, *Gauge theory correlators from noncritical string theory*, *Phys. Lett. B* **428** (1998) 105 [hep-th/9802109]. 84, 88

[156] E. Witten, *Anti-de Sitter space and holography*, *Adv. Theor. Math. Phys.* **2** (1998) 253 [hep-th/9802150]. 84, 88, 106, 177

[157] E. Witten, *Bound states of strings and p-branes*, *Nucl. Phys. B* **460** (1996) 335 [hep-th/9510135]. 84

[158] J. Polchinski, *Tasi lectures on d-branes*, hep-th/9611050. 85

[159] C. Bachas, *Half a lecture on d-branes*, in *Gauge Theories, Applied Supersymmetry and Quantum Gravity II*, Imperial College Press, jun, 1997. 85

[160] C. P. Bachas, *Lectures on d-branes*, hep-th/9806199. 85

[161] C. V. Johnson, *D-brane primer*, in *Theoretical Advanced Study Institute in Elementary Particle Physics (TASI 99): Strings, Branes, and Gravity*, pp. 129–350, 7, 2000, DOI [hep-th/0007170]. 85

[162] J. M. Maldacena, *Black holes in string theory*, Ph.D. thesis, Princeton U., 1996. hep-th/9607235. 85

[163] I. R. Klebanov, *TASI lectures: Introduction to the AdS / CFT correspondence*, hep-th/0009139. 85

[164] A. Zaffaroni, *Introduction to the AdS-CFT correspondence*, *Class. Quant. Grav.* **17** (2000) 3571. 85

[165] H. Nastase, *Introduction to AdS-CFT*, 0712.0689. 85

[166] V. E. Hubeny, *The AdS/CFT Correspondence*, *Class. Quant. Grav.* **32** (2015) 124010 [1501.00007]. 85

[167] A. V. Ramallo, *Introduction to the AdS/CFT correspondence*, *Springer Proc. Phys.* **161** (2015) 411 [1310.4319]. 85, 106, 111

[168] G. 't Hooft, *Dimensional reduction in quantum gravity*, *Conf. Proc. C* **930308** (1993) 284 [gr-qc/9310026]. 86

[169] L. Susskind, *The World as a hologram*, *J. Math. Phys.* **36** (1995) 6377 [hep-th/9409089]. 86

[170] C. B. Thorn, *Reformulating string theory with the 1/N expansion*, in *The First International A.D. Sakharov Conference on Physics*, 5, 1991, hep-th/9405069. 86

[171] G. 't Hooft, *The Holographic principle: Opening lecture*, *Subnucl. Ser.* **37** (2001) 72 [hep-th/0003004]. 86

[172] R. Bousso, *The Holographic principle*, *Rev. Mod. Phys.* **74** (2002) 825 [hep-th/0203101]. 86

[173] E. D'Hoker and D. Z. Freedman, *Supersymmetric gauge theories and the ads/cft correspondence*, hep-th/0201253. 88

[174] P. Breitenlohner and D. Z. Freedman, *Positive Energy in anti-De Sitter Backgrounds and Gauged Extended Supergravity*, *Phys. Lett. B* **115** (1982) 197. 90

[175] P. Breitenlohner and D. Z. Freedman, *Stability in Gauged Extended Supergravity*, *Annals Phys.* **144** (1982) 249. 90

[176] M. Henningson and K. Skenderis, *The Holographic Weyl anomaly*, *JHEP* **07** (1998) 023 [hep-th/9806087]. 91

[177] M. Henningson and K. Skenderis, *Holography and the Weyl anomaly*, *Fortsch. Phys.* **48** (2000) 125 [hep-th/9812032]. 91, 94

[178] S. de Haro, S. N. Solodukhin and K. Skenderis, *Holographic reconstruction of space-time and renormalization in the AdS / CFT correspondence*, *Commun. Math. Phys.* **217** (2001) 595 [hep-th/0002230]. 91

[179] M. Bianchi, D. Z. Freedman and K. Skenderis, *Holographic renormalization*, *Nucl. Phys.* **B631** (2002) 159 [hep-th/0112119]. 91

[180] K. Skenderis, *Lecture notes on holographic renormalization*, *Class. Quant. Grav.* **19** (2002) 5849 [hep-th/0209067]. 91

[181] I. Papadimitriou, *Lectures on Holographic Renormalization*, *Springer Proc. Phys.* **176** (2016) 131. 91

[182] M. Fukuma, S. Matsuura and T. Sakai, *Holographic renormalization group*, *Prog. Theor. Phys.* **109** (2003) 489 [hep-th/0212314]. 91

[183] C. Fefferman and C. R. Graham, *Conformal invariants*, no. S131 in Astérisque. Société mathématique de France, 1985. 94

[184] M. Cvetic and S. S. Gubser, *Thermodynamic stability and phases of general spinning branes*, *JHEP* **07** (1999) 010 [hep-th/9903132]. 103

[185] X.-X. Zeng and L.-F. Li, *Holographic Phase Transition Probed by Nonlocal Observables*, *Adv. High Energy Phys.* **2016** (2016) 6153435 [1609.06535]. 103

[186] D. Kirzhnits and A. D. Linde, *Symmetry Behavior in Gauge Theories*, *Annals Phys.* **101** (1976) 195. 106

[187] A. D. Linde, *Phase Transitions in Gauge Theories and Cosmology*, *Rept. Prog. Phys.* **42** (1979) 389. 106, 176

[188] M. B. Hindmarsh, M. Lüben, J. Lumma and M. Pauly, *Phase transitions in the early universe*, 2008.09136. 106, 110, 138, 176

[189] P. Amaro-Seoane, H. Audley, S. Babak, J. Baker, E. Barausse, P. Bender et al., *Laser interferometer space antenna*, 1702.00786. 106

[190] M. Carena, M. Quirós and C. Wagner, *Opening the window for electroweak baryogenesis*, *Phys. Lett. B* **380** (1996) 81 [hep-ph/9603420]. 106

[191] D. Delepine, J.-M. Gérard, R. Gonzalez Felipe and J. Weyers, *A light stop and electroweak baryogenesis*, *Phys. Lett. B* **386** (1996) 183 [hep-ph/9604440]. 106

[192] M. Laine and K. Rummukainen, *The mssm electroweak phase transition on the lattice*, *Nucl. Phys. B* **535** (1998) 423 [hep-lat/9804019]. 106

[193] S. Huber and M. Schmidt, *Electroweak baryogenesis: concrete in a susy model with a gauge singlet*, *Nucl. Phys. B* **606** (2001) 183 [hep-ph/0003122]. 106

[194] C. Grojean, G. Servant and J. D. Wells, *First-order electroweak phase transition in the standard model with a low cutoff*, *Phys. Rev. D* **71** (2005) [hep-ph/0407019]. 106

[195] S. Huber, T. Konstandin, T. Prokopec and M. Schmidt, *Baryogenesis in the mssm, nmssm and nmssm*, *Nuclear Physics A* **785** (2007) 206 [hep-ph/0608017]. 106

[196] S. Profumo, M. J. Ramsey-Musolf and G. Shaughnessy, *Singlet higgs phenomenology and the electroweak phase transition*, *JHEP* **2007** (2007) 010 [0705.2425]. 106

[197] V. Barger, P. Langacker, M. McCaskey, M. J. Ramsey-Musolf and G. Shaughnessy, *Cern lhc phenomenology of an extended standard model with a real scalar singlet*, *Phys. Rev. D* **77** (2008) [0706.4311]. 106

[198] G. Dorsch, S. Huber and J. No, *A strong electroweak phase transition in the 2hdm after lhc8*, *JHEP* **10** (2013) 029 [1305.6610]. 106

[199] P. H. Damgaard, A. Haarr, D. O'Connell and A. Tranberg, *Effective field theory and electroweak baryogenesis in the singlet-extended standard model*, *JHEP* **2016** (2016) [1512.01963]. 106

[200] F. Sannino, *Conformal Dynamics for TeV Physics and Cosmology*, *Acta Phys. Polon. B* **40** (2009) 3533 [0911.0931]. 106

[201] G. Cacciapaglia, C. Pica and F. Sannino, *Fundamental Composite Dynamics: A Review*, *Phys. Rept.* **877** (2020) 1 [2002.04914]. 106

[202] J. Casalderrey-Solana, H. Liu, D. Mateos, K. Rajagopal and U. A. Wiedemann, *Gauge/String Duality, Hot QCD and Heavy Ion Collisions*, 1101.0618. 106, 111

[203] N. Brambilla et al., *QCD and Strongly Coupled Gauge Theories: Challenges and Perspectives*, *Eur. Phys. J.* **C74** (2014) 2981 [1404.3723]. 106, 111

[204] D. Bunk, J. Hubisz and B. Jain, *A Perturbative RS I Cosmological Phase Transition*, *Eur. Phys. J. C* **78** (2018) 78 [1705.00001]. 106

[205] B. M. Dillon, B. K. El-Menoufi, S. J. Huber and J. P. Manuel, *Rapid holographic phase transition with brane-localized curvature*, *Phys. Rev. D* **98** (2018) 086005 [1708.02953]. 106

[206] E. Megías, G. Nardini and M. Quirós, *Cosmological Phase Transitions in Warped Space: Gravitational Waves and Collider Signatures*, *JHEP* **09** (2018) 095 [1806.04877]. 106

[207] P. Baratella, A. Pomarol and F. Rompineve, *The Supercooled Universe*, *JHEP* **03** (2019) 100 [1812.06996]. 106

[208] K. Agashe, P. Du, M. Ekhterachian, S. Kumar and R. Sundrum, *Cosmological Phase Transition of Spontaneous Confinement*, *JHEP* **05** (2020) 086 [1910.06238]. 106

[209] K. Fujikura, Y. Nakai and M. Yamada, *A more attractive scheme for radion stabilization and supercooled phase transition*, *JHEP* **02** (2020) 111 [1910.07546]. 106

[210] L. Delle Rose, G. Panico, M. Redi and A. Tesi, *Gravitational Waves from Supercool Axions*, *JHEP* **04** (2020) 025 [1912.06139]. 106

[211] B. Von Harling, A. Pomarol, O. Pujolás and F. Rompineve, *Peccei-Quinn Phase Transition at LIGO*, *JHEP* **04** (2020) 195 [1912.07587]. 106

[212] E. Megias, G. Nardini and M. Quiros, *Gravitational Imprints from Heavy Kaluza-Klein Resonances*, *Phys. Rev. D* **102** (2020) 055004 [2005.04127]. 106

[213] F. Bigazzi, A. Caddeo, A. L. Cotrone and A. Paredes, *Fate of false vacua in holographic first-order phase transitions*, 2008.02579. 106, 138, 139

[214] T. Sakai and S. Sugimoto, *Low energy hadron physics in holographic QCD*, *Prog. Theor. Phys.* **113** (2005) 843 [hep-th/0412141]. 106

[215] D. Mateos, R. C. Myers and R. M. Thomson, *Holographic phase transitions with fundamental matter*, *Phys. Rev. Lett.* **97** (2006) 091601 [hep-th/0605046]. 106

[216] O. Aharony, J. Sonnenschein and S. Yankielowicz, *A Holographic model of deconfinement and chiral symmetry restoration*, *Annals Phys.* **322** (2007) 1420 [hep-th/0604161]. 106

[217] F. Bigazzi, A. Caddeo, A. L. Cotrone and A. Paredes, *Dark Holograms and Gravitational Waves*, 2011.08757. 106, 138

[218] U. Gürsoy, A. Jansen and W. van der Schee, *New dynamical instability in asymptotically anti–de Sitter spacetime*, *Phys. Rev. D* **94** (2016) 061901 [1603.07724]. 107

[219] R. Critelli, R. Rougemont and J. Noronha, *Holographic Bjorken flow of a hot and dense fluid in the vicinity of a critical point*, *Phys. Rev. D* **99** (2019) 066004 [1805.00882]. 107

[220] M. Attems, Y. Bea, J. Casalderrey-Solana, D. Mateos, M. Triana and M. Zilhão, *Holographic Collisions across a Phase Transition*, *Phys. Rev. Lett.* **121** (2018) 261601 [1807.05175]. 107

[221] H. Bantilan, P. Figueras and D. Mateos, *Real-time Dynamics of Plasma Balls from Holography*, *Phys. Rev. Lett.* **124** (2020) 191601 [2001.05476]. 107

[222] R. A. Janik, J. Jankowski and H. Soltanpanahi, *Real-Time dynamics and phase separation in a holographic first order phase transition*, *Phys. Rev. Lett.* **119** (2017) 261601 [1704.05387]. 107, 163

[223] L. Bellantuono, R. A. Janik, J. Jankowski and H. Soltanpanahi, *Dynamics near a first order phase transition*, *JHEP* **10** (2019) 146 [1906.00061]. 107, 163

[224] X. Li, Z.-Y. Nie and Y. Tian, *Holographic boiling and generalized thermodynamic description beyond local equilibrium*, *JHEP* **20** (2020) 063 [2003.12987]. 107, 163

[225] M. Attems, Y. Bea, J. Casalderrey-Solana, D. Mateos, M. Triana and M. Zilhão, *Phase Transitions, Inhomogeneous Horizons and Second-Order Hydrodynamics*, *JHEP* **06** (2017) 129 [1703.02948]. 107, 163

[226] M. Attems, Y. Bea, J. Casalderrey-Solana, D. Mateos and M. Zilhão, *Dynamics of Phase Separation from Holography*, *JHEP* **01** (2020) 106 [1905.12544]. 107, 163

[227] Y. Bea, O. J. Dias, T. Giannakopoulos, D. Mateos, M. Sanchez-Garitaonandia, J. E. Santos et al., *Crossing a large-N phase transition at finite volume*, 2007.06467. 107

[228] C. Caprini, M. Chala, G. C. Dorsch, M. Hindmarsh, S. J. Huber, T. Konstandin et al., *Detecting gravitational waves from cosmological phase transitions with lisa: an update*, *JCAP* **2020** (2020) 024 [1910.13125]. 107, 108, 124, 130

[229] Y. Bea and D. Mateos, *Heating up Exotic RG Flows with Holography*, *JHEP* **08** (2018) 034 [1805.01806]. 107, 111, 112, 116, 129, 134, 177

[230] E. Witten, *Cosmic Separation of Phases*, *Phys. Rev. D* **30** (1984) 272. 108, 176

[231] M. Garny, T. Konstandin, L. Sagunski and M. Viel, *Neutrino mass bounds from confronting an effective model with BOSS Lyman-alpha data*, 2011.03050. 109

[232] M. Hindmarsh, S. J. Huber, K. Rummukainen and D. J. Weir, *Numerical simulations of acoustically generated gravitational waves at a first order phase transition*, *Phys. Rev. D* **92** (2015) 123009 [1504.03291]. 109, 131

[233] P. J. Steinhardt, *Relativistic Detonation Waves and Bubble Growth in False Vacuum Decay*, *Phys. Rev. D* **25** (1982) 2074. 110, 176

[234] B.-H. Liu, L. D. McLerran and N. Turok, *Bubble nucleation and growth at a baryon number producing electroweak phase transition*, *Phys. Rev. D* **46** (1992) 2668. 110, 177, 184

[235] D. Bödeker and G. D. Moore, *Electroweak Bubble Wall Speed Limit*, *JCAP* **05** (2017) 025 [1703.08215]. 110, 177

[236] S. Höche, J. Kozaczuk, A. J. Long, J. Turner and Y. Wang, *Towards an all-orders calculation of the electroweak bubble wall velocity*, 2007.10343. 110

[237] A. Azatov and M. Vanvlasselaer, *Bubble wall velocity: heavy physics effects*, 2010.02590. 110

[238] I. Baldes, Y. Gouttenoire and F. Sala, *String fragmentation in supercooled confinement and implications for dark matter*, 2007.08440. 110

[239] D. Bödeker and G. D. Moore, *Can electroweak bubble walls run away?*, *JCAP* **2009** (2009) 009 [0903.4099]. 110

[240] J. Ellis, M. Lewicki and J. M. No, *On the Maximal Strength of a First-Order Electroweak Phase Transition and its Gravitational Wave Signal*, *JCAP* **04** (2019) 003 [1809.08242]. 110, 135

[241] A. Eichhorn, J. Lumma, J. M. Pawlowski, M. Reichert and M. Yamada, *Universal gravitational-wave signatures from heavy new physics in the electroweak sector*, 2010.00017. 110

[242] G. W. Gibbons and S. W. Hawking, *Action integrals and partition functions in quantum gravity*, *Phys. Rev. D* **15** (1977) 2752. 111

[243] J. W. York, *Role of conformal three-geometry in the dynamics of gravitation*, *Phys. Rev. Lett.* **28** (1972) 1082. 111

[244] D. Z. Freedman, S. S. Gubser, K. Pilch and N. P. Warner, *Renormalization group flows from holography - supersymmetry and a c-theorem*, *Adv. Theor. Math. Phys.* **3** (1999) 363 [hep-th/9904017]. 111

[245] D. Freedman, C. Nuñez, M. Schnabl and K. Skenderis, *Fake supergravity and domain wall stability*, *Phys. Rev. D* **69** (2004) 104027 [hep-th/0312055]. 111

[246] O. Aharony, S. S. Gubser, J. Maldacena, H. Ooguri and Y. Oz, *Large n field theories, string theory and gravity*, *Physics Reports* **323** (2000) 183–386 [hep-th/9905111]. 111

[247] U. Gürsoy, E. Kiritsis, F. Nitti and L. Silva Pimenta, *Exotic holographic RG flows at finite temperature*, *JHEP* **10** (2018) 173 [1805.01769]. 112, 177

[248] M. Attems, J. Casalderrey-Solana, D. Mateos, I. Papadimitriou, D. Santos-Oliván, C. F. Sopuerta et al., *Thermodynamics, transport and relaxation in non-conformal theories*, *JHEP* **2016** (2016) [1603.01254]. 113

[249] S. S. Gubser and A. Nellore, *Mimicking the QCD equation of state with a dual black hole*, *Phys. Rev. D* **78** (2008) 086007 [0804.0434]. 113, 114

[250] H. Chamblin and H. Reall, *Dynamic dilatonic domain walls*, *Nucl. Phys. B* **562** (1999) 133 [hep-th/9903225]. 115

[251] C. Hoyos, N. Jokela, D. Rodríguez Fernández and A. Vuorinen, *Breaking the sound barrier in AdS/CFT*, *Phys. Rev. D* **94** (2016) 106008 [1609.03480]. 117, 131

[252] C. Ecker, C. Hoyos, N. Jokela, D. Rodríguez Fernández and A. Vuorinen, *Stiff phases in strongly coupled gauge theories with holographic duals*, *JHEP* **11** (2017) 031 [1707.00521]. 117, 131

[253] M. Hindmarsh, S. J. Huber, K. Rummukainen and D. J. Weir, *Gravitational waves from the sound of a first order phase transition*, *Phys. Rev. Lett.* **112** (2014) 041301 [1304.2433]. 123, 131

[254] M. Hindmarsh and M. Hijazi, *Gravitational waves from first order cosmological phase transitions in the sound shell model*, *JCAP* **2019** (2019) 062 [1909.10040]. 123

[255] P. A. R. Ade, N. Aghanim, M. Arnaud, M. Ashdown, J. Aumont, C. Baccigalupi et al., *Planck 2015 results*, *Astronomy & Astrophysics* **594** (2016) A13 [1502.01589]. 123

[256] X. Wang, F. P. Huang and X. Zhang, *Phase transition dynamics and gravitational wave spectra of strong first-order phase transition in supercooled universe*, *JCAP* **2020** (2020) 045 [2003.08892]. 126

[257] M. Tinto, *Enhanced gravitational wave science with LISA and gLISA.*, *Journal of Physics: Conference Series* **840** (2017) 012017. 127

[258] C. Hoyos, N. Jokela and D. Logares, *Scattering length from holographic duality*, *Phys. Rev. D* **101** (2020) 046028 [1910.13929]. 131

[259] C. Hoyos, N. Jokela and D. Logares, *Scattering length in holographic confining theories*, *Phys. Rev. D* **102** (2020) 086006 [2005.06904]. 131

[260] M. Bianchi, D. Z. Freedman and K. Skenderis, *Holographic renormalization*, *Nucl. Phys. B* **631** (2002) 159 [hep-th/0112119]. 132

[261] M. Bianchi, D. Z. Freedman and K. Skenderis, *How to go with an rg flow*, *JHEP* **2001** (2001) 041 [hep-th/0105276]. 132

[262] J. Ellis, M. Lewicki, J. M. No and V. Vaskonen, *Gravitational wave energy budget in strongly supercooled phase transitions*, *Journal of Cosmology and Astroparticle Physics* **2019** (2019) 024–024. 135

[263] J. Ellis, M. Lewicki and J. M. No, *Gravitational waves from first-order cosmological phase transitions: lifetime of the sound wave source*, *Journal of Cosmology and Astroparticle Physics* **2020** (2020) 050–050. 135

[264] M. Kamionkowski, A. Kosowsky and M. S. Turner, *Gravitational radiation from first-order phase transitions*, *Phys. Rev. D* **49** (1994) 2837 [astro-ph/9310044]. 135

[265] A. Mazumdar and G. White, *Review of cosmic phase transitions: their significance and experimental signatures*, *Rept. Prog. Phys.* **82** (2019) 076901 [1811.01948]. 138

[266] J. Halverson, C. Long, A. Maiti, B. Nelson and G. Salinas, *Gravitational waves from dark Yang-Mills sectors*, *JHEP* **05** (2021) 154 [2012.04071]. 138, 177, 181

[267] W.-C. Huang, M. Reichert, F. Sannino and Z.-W. Wang, *Testing the dark SU(N) Yang-Mills theory confined landscape: From the lattice to gravitational waves*, *Phys. Rev. D* **104** (2021) 035005 [2012.11614]. 138, 181

[268] M. Reichert, F. Sannino, Z.-W. Wang and C. Zhang, *Dark Confinement and Chiral Phase Transitions: Gravitational Waves vs Matter Representations*, 2109.11552. 138

[269] Z.-R. Zhu, J. Chen and D. Hou, *Gravitational waves from holographic QCD phase transition with gluon condensate*, 2109.09933. 138

[270] Y. Bea, J. Casalderrey-Solana, T. Giannakopoulos, D. Mateos, M. Sanchez-Garitaonandia and M. Zilhão, *Bubble Wall Velocity from Holography*, 2104.05708. 138, 163, 177, 182, 183, 189

[271] F. Bigazzi, A. Caddeo, T. Canneti and A. L. Cotrone, *Bubble Wall Velocity at Strong Coupling*, 2104.12817. 138, 177, 182, 189

[272] O. Henriksson, *Black brane evaporation through D-brane bubble nucleation*, 2106.13254. 138, 177, 182, 189

[273] O. Gould and T. V. I. Tenkanen, *On the perturbative expansion at high temperature and implications for cosmological phase transitions*, *JHEP* **06** (2021) 069 [2104.04399]. 138, 177

[274] G. D. Moore and K. Rummukainen, *Electroweak bubble nucleation, nonperturbatively*, *Phys. Rev. D* **63** (2001) 045002 [hep-ph/0009132]. 139

[275] F. R. Ares, O. Henriksson, M. Hindmarsh, C. Hoyos and N. Jokela, *Gravitational waves at strong coupling from an effective action*, 2110.14442. 139, 160, 161, 167, 168, 169

[276] R. A. Janik, M. Järvinen and J. Sonnenschein, *A simple description of holographic domain walls in confining theories – extended hydrodynamics*, 2106.02642. 139, 163, 164, 183

[277] T. Hertog and G. T. Horowitz, *Designer gravity and field theory effective potentials*, *Phys. Rev. Lett.* **94** (2005) 221301 [hep-th/0412169]. 142, 148, 179

[278] T. Hertog and G. T. Horowitz, *Holographic description of AdS cosmologies*, *JHEP* **04** (2005) 005 [hep-th/0503071]. 142

[279] I. Papadimitriou, *Multi-Trace Deformations in AdS/CFT: Exploring the Vacuum Structure of the Deformed CFT*, *JHEP* **05** (2007) 075 [hep-th/0703152]. 142, 144, 145

[280] E. Kiritsis and V. Niarchos, *The holographic quantum effective potential at finite temperature and density*, *JHEP* **08** (2012) 164 [1205.6205]. 142, 179

[281] E. Kiritsis, W. Li and F. Nitti, *Holographic RG flow and the Quantum Effective Action*, *Fortsch. Phys.* **62** (2014) 389 [1401.0888]. 142

[282] E. Witten, *Multitrace operators, boundary conditions, and AdS / CFT correspondence*, hep-th/0112258. 144, 178

[283] T. Faulkner, G. T. Horowitz and M. M. Roberts, *Holographic quantum criticality from multi-trace deformations*, *JHEP* **04** (2011) 051 [1008.1581]. 151, 173, 179

[284] S. R. Coleman, *The Fate of the False Vacuum. 1. Semiclassical Theory*, *Phys. Rev. D* **15** (1977) 2929. 157, 169, 176

[285] C. G. Callan, Jr. and S. R. Coleman, *The Fate of the False Vacuum. 2. First Quantum Corrections*, *Phys. Rev. D* **16** (1977) 1762. 157, 169

[286] B. Lucini, M. Teper and U. Wenger, *The High temperature phase transition in SU(N) gauge theories*, *JHEP* **01** (2004) 061 [hep-lat/0307017]. 162, 181

[287] O. Bergman, G. Lifschytz and M. Lippert, *Holographic Nuclear Physics*, *JHEP* **11** (2007) 056 [0708.0326]. 168

[288] N. Jokela, M. Järvinen, G. Nijs and J. Remes, *Unified weak and strong coupling framework for nuclear matter and neutron stars*, *Phys. Rev. D* **103** (2021) 086004 [2006.01141]. 168, 169, 177

[289] N. Kovensky and A. Schmitt, *Holographic quarkyonic matter*, *JHEP* **09** (2020) 112 [2006.13739]. 168

[290] B. W. Mintz, E. S. Fraga, G. Pagliara and J. Schaffner-Bielich, *Nucleation of quark matter in protoneutron star matter*, *Phys. Rev. D* **81** (2010) 123012 [0910.3927]. 168

[291] I. Sagert, T. Fischer, M. Hempel, G. Pagliara, J. Schaffner-Bielich, A. Mezzacappa et al., *Signals of the QCD phase transition in core-collapse supernovae*, *Phys. Rev. Lett.* **102** (2009) 081101 [0809.4225]. 168

[292] D. Logoteta, C. Providencia, I. Vidana and I. Bombaci, *Quark matter nucleation with a microscopic hadronic equation of state*, *Phys. Rev. C* **85** (2012) 055807 [1204.5909]. 168

[293] E. R. Most, L. R. Weih, L. Rezzolla and J. Schaffner-Bielich, *New constraints on radii and tidal deformabilities of neutron stars from GW170817*, *Phys. Rev. Lett.* **120** (2018) 261103 [1803.00549]. 168

[294] A. Bauswein, N.-U. F. Bastian, D. B. Blaschke, K. Chatziioannou, J. A. Clark, T. Fischer et al., *Identifying a first-order phase transition in neutron star mergers through gravitational waves*, *Phys. Rev. Lett.* **122** (2019) 061102 [1809.01116]. 168

[295] P. M. Chesler, N. Jokela, A. Loeb and A. Vuorinen, *Finite-temperature Equations of State for Neutron Star Mergers*, *Phys. Rev. D* **100** (2019) 066027 [1906.08440]. 168

[296] N. K. Glendenning, *First order phase transitions with more than one conserved charge: Consequences for neutron stars*, *Phys. Rev. D* **46** (1992) 1274. 168

[297] H. Heiselberg, C. J. Pethick and E. F. Staubo, *Quark matter droplets in neutron stars*, *Phys. Rev. Lett.* **70** (1993) 1355. 168

[298] A. Kurkela, E. S. Fraga, J. Schaffner-Bielich and A. Vuorinen, *Constraining neutron star matter with Quantum Chromodynamics*, *Astrophys. J.* **789** (2014) 127 [1402.6618]. 169

[299] N. K. Glendenning, *Compact stars: Nuclear physics, particle physics, and general relativity*. 1997. 169

[300] L. F. Palhares and E. S. Fraga, *Droplets in the cold and dense linear sigma model with quarks*, *Phys. Rev. D* **82** (2010) 125018 [1006.2357]. 169

[301] E. S. Fraga, M. Hippert and A. Schmitt, *Surface tension of dense matter at the chiral phase transition*, *Phys. Rev. D* **99** (2019) 014046 [1810.13226]. 169

[302] H. Audley et al., *Laser Interferometer Space Antenna*, 1702.00786. 176

[303] NANOGrav collaboration, *The NANOGrav 12.5 yr Data Set: Search for an Isotropic Stochastic Gravitational-wave Background*, *Astrophys. J. Lett.* **905** (2020) L34 [2009.04496]. 176

[304] H. Middleton, A. Sesana, S. Chen, A. Vecchio, W. Del Pozzo and P. A. Rosado, *Massive black hole binary systems and the NANOGrav 12.5 yr results*, *Mon. Not. Roy. Astron. Soc.* **502** (2021) L99 [2011.01246]. 176

[305] NANOGrav collaboration, *Searching For Gravitational Waves From Cosmological Phase Transitions With The NANOGrav 12.5-year dataset*, 2104.13930. 176

[306] M. Laine and K. Rummukainen, *A Strong electroweak phase transition up to m(H) is about 105-GeV*, *Phys.Rev.Lett.* **80** (1998) 5259 [hep-ph/9804255]. 176

[307] M. Laine, G. Nardini and K. Rummukainen, *Lattice study of an electroweak phase transition at $m_h \simeq 126$ GeV*, *JCAP* **01** (2013) 011 [1211.7344]. 176

[308] J. M. Cline, *TASI Lectures on Early Universe Cosmology: Inflation, Baryogenesis and Dark Matter*, *PoS* **TASI2018** (2019) 001 [1807.08749]. 176

[309] D. J. Weir, *Gravitational waves from a first order electroweak phase transition: a brief review*, *Phil. Trans. Roy. Soc. Lond. A* **376** (2018) 20170126 [1705.01783]. 176

[310] A. H. Guth and E. J. Weinberg, *Cosmological Consequences of a First Order Phase Transition in the SU(5) Grand Unified Model*, *Phys. Rev.* **D23** (1981) 876. 176

[311] K. Enqvist, J. Ignatius, K. Kajantie and K. Rummukainen, *Nucleation and bubble growth in a first order cosmological electroweak phase transition*, *Phys.Rev.* **D45** (1992) 3415. 176, 180, 181

[312] M. Laine and A. Vuorinen, *Basics of Thermal Field Theory*, vol. 925. Springer, 2016, 10.1007/978-3-319-31933-9, [1701.01554]. 176

[313] F. Giese, T. Konstandin and J. van de Vis, *Model-independent energy budget of cosmological first-order phase transitions—A sound argument to go beyond the bag model*, *JCAP* **07** (2020) 057 [2004.06995]. 176

[314] F. Giese, T. Konstandin, K. Schmitz and J. Van De Vis, *Model-independent energy budget for LISA*, *JCAP* **01** (2021) 072 [2010.09744]. 176

[315] M. Hindmarsh and M. Hijazi, *Gravitational waves from first order cosmological phase transitions in the Sound Shell Model*, *JCAP* **12** (2019) 062 [1909.10040]. 176, 182, 183

[316] C. Gowling and M. Hindmarsh, *Observational prospects for phase transitions at LISA: Fisher matrix analysis*, *JCAP* **10** (2021) 039 [2106.05984]. 176

[317] O. Gould, J. Kozaczuk, L. Niemi, M. J. Ramsey-Musolf, T. V. I. Tenkanen and D. J. Weir, *Nonperturbative analysis of the gravitational waves from a first-order electroweak phase transition*, *Phys. Rev. D* **100** (2019) 115024 [1903.11604]. 177

[318] D. Croon, O. Gould, P. Schicho, T. V. I. Tenkanen and G. White, *Theoretical uncertainties for cosmological first-order phase transitions*, *JHEP* **04** (2021) 055 [2009.10080]. 177

[319] P. John and M. G. Schmidt, *Bubble wall velocity in the MSSM*, in *4th International Conference on Strong and Electroweak Matter*, 6, 2000, hep-ph/0012077. 177

[320] S. J. Huber and M. Sopena, *The bubble wall velocity in the minimal supersymmetric light stop scenario*, *Phys. Rev.* **D85** (2012) 103507 [1112.1888]. 177

[321] G. C. Dorsch, S. J. Huber and T. Konstandin, *Bubble wall velocities in the Standard Model and beyond*, *JCAP* **12** (2018) 034 [1809.04907]. 177

[322] A. Azatov and M. Vanvlasselaer, *Bubble wall velocity: heavy physics effects*, *Journal of Cosmology and Astroparticle Physics* **2021** (2021) 058 [2010.02590]. 177

[323] A. Friedlander, I. Banta, J. M. Cline and D. Tucker-Smith, *Wall speed and shape in singlet-assisted strong electroweak phase transitions*, *Phys. Rev. D* **103** (2021) 055020 [2009.14295]. 177

[324] B. Lucini and M. Panero, *SU(N) gauge theories at large N*, *Phys. Rept.* **526** (2013) 93 [1210.4997]. 177, 181

[325] W.-C. Huang, M. Reichert, F. Sannino and Z.-W. Wang*Phys. Rev. D* . 177

[326] D. Croon, E. Hall and H. Murayama, *Non-perturbative methods for false vacuum decay*, 2104.10687. 177

[327] M. Attems, J. Casalderrey-Solana, D. Mateos, I. Papadimitriou, D. Santos-Oliván, C. F. Sopuerta et al., *Thermodynamics, transport and relaxation in non-conformal theories*, *JHEP* **10** (2016) 155 [1603.01254]. 177

[328] N. Jokela, M. Järvinen and J. Remes, *Holographic QCD in the Veneziano limit and neutron stars*, *JHEP* **03** (2019) 041 [1809.07770]. 177

[329] C. Ecker, M. Järvinen, G. Nijs and W. van der Schee, *Gravitational waves from holographic neutron star mergers*, *Phys. Rev. D* **101** (2020) 103006 [1908.03213]. 177

[330] F. R. Ares, O. Henriksson, M. Hindmarsh, C. Hoyos and N. Jokela, *Effective actions and bubble nucleation from holography*, 2109.13784. 177, 179, 183

[331] I. R. Klebanov and E. Witten, *AdS / CFT correspondence and symmetry breaking*, *Nucl. Phys. B* **556** (1999) 89 [hep-th/9905104]. 178

[332] P. K. Kovtun and A. O. Starinets, *Quasinormal modes and holography*, *Phys. Rev. D* **72** (2005) 086009 [hep-th/0506184]. 179

[333] B. Lucini, M. Teper and U. Wenger, *Properties of the deconfining phase transition in SU(N) gauge theories*, *JHEP* **02** (2005) 033 [hep-lat/0502003]. 181

[334] J. R. Espinosa, T. Konstandin, J. M. No and G. Servant, *Energy Budget of Cosmological First-order Phase Transitions*, *JCAP* **1006** (2010) 028 [1004.4187]. 182

[335] D. Cutting, M. Hindmarsh and D. J. Weir, *Vorticity, kinetic energy, and suppressed gravitational wave production in strong first order phase transitions*, 1906.00480. 182

[336] J. K. Ghosh, E. Kiritsis, F. Nitti and L. T. Witkowski, *Revisiting Coleman-de Luccia transitions in the AdS regime using holography*, *JHEP* **09** (2021) 065 [2102.11881]. 183

[337] T. Konstandin and G. Servant, *Cosmological Consequences of Nearly Conformal Dynamics at the TeV scale*, *JCAP* **12** (2011) 009 [1104.4791]. 184

[338] J. Ignatius, K. Kajantie, H. Kurki-Suonio and M. Laine, *The growth of bubbles in cosmological phase transitions*, *Phys.Rev.* **D49** (1994) 3854 [astro-ph/9309059]. 184

[339] G. D. Moore and T. Prokopec, *Bubble wall velocity in a first order electroweak phase transition*, *Phys. Rev. Lett.* **75** (1995) 777 [hep-ph/9503296]. 184

[340] P. A. M. Dirac, *The quantum theory of the electron*, *Proc. Roy. Soc. Lond. A* **117** (1928) 610. 192

[341] M. Petitjean, *Chirality of Dirac Spinors Revisited*, *Symmetry* **12** (2020) 616. 193